

2013

# Cannabinoid CB1R Receptor Mediates Metabolic Syndrome in Models of Circadian and Glucocorticoid Dysregulation

Nicole Bowles

Follow this and additional works at: [http://digitalcommons.rockefeller.edu/student\\_theses\\_and\\_dissertations](http://digitalcommons.rockefeller.edu/student_theses_and_dissertations)

 Part of the [Life Sciences Commons](#)

---

## Recommended Citation

Bowles, Nicole, "Cannabinoid CB1R Receptor Mediates Metabolic Syndrome in Models of Circadian and Glucocorticoid Dysregulation" (2013). *Student Theses and Dissertations*. Paper 232.



CANNABINOID CB<sub>1</sub>R RECEPTOR MEDIATES METABOLIC SYNDROME IN  
MODELS OF CIRCADIAN AND GLUCOCORTICOID DYSREGULATION

A Thesis Presented to the Faculty of  
The Rockefeller University  
in Partial Fulfillment of the Requirements  
for the degree of Doctor of Philosophy

by

Nicole Bowles

June 2013



CANNABINOID CB<sub>1</sub>R RECEPTOR MEDIATES METABOLIC SYNDROME IN  
MODELS OF CIRCADIAN AND GLUCOCORTICOID DYSREGULATION

Nicole Bowles, Ph.D.

The Rockefeller University 2013

The most recent projections in the growing obesity rates across the nation show an increase to 60% by the year 2030. These growing rates of obesity are paralleled by an increased rates of depressive conditions, anxiety, and sleep loss, often with environmental factors at the root of the cause. Stress and the stress response is a dynamic system that reflects one's ability to cope with events, behaviorally or physiologically, as stressors occur over a lifetime. While many key players mediate the effects of stress exposure on disease outcomes including the sympathetic nervous system, parasympathetic, inflammatory cytokines and metabolic hormones, this dissertation focuses on glucocorticoids because of the extensive regulatory role they play in mounting the adaptative response to stress. Additionally, glucocorticoids act to regulate feeding and energy balance, and when not properly regulated, they can lead to increased weight gain, particularly the development of abdominal visceral fat. Independent from their role in the stress response, glucocorticoids are also secreted in a diurnal fashion as regulated by the master circadian (daily) clock in the suprachiasmatic nuclei (*SCN*). Signaling in this regard is at least partially responsible for entraining circadian clocks outside of the *SCN*. Just as shifts in glucocorticoid exposure are associated with metabolic disturbances, disruption of circadian rhythms has also been linked to the development of obesity. However, it remains unclear how the two systems independently and/or collectively regulate energy balance.

The first aim of this dissertation was to determine how disruptions in the environmental photoperiod impacts clock gene expression and if this environmental exposure affects circulating glucocorticoid levels. The second aim was to determine if increased exposure to a rhythmic corticosterone (CORT) disrupted circadian rhythms. Given that CORT imbalances result in circadian disruption and weight gain in both models, the third aim was to determine a mediator in the two systems that regulates CORT synthesis and affects metabolism. Recent studies have demonstrated that glucocorticoids possess the ability to increase the production and release of endocannabinoid molecules. Additionally, endocannabinoids are potent regulators of appetite, energy balance and metabolic processes through both central and peripheral regulation of feeding and metabolism, making the system an ideal candidate.

Mice lacking the cannabinoid CB<sub>1</sub> receptor were protected against all of these changes in metabolic function in both mouse models, indicating that endocannabinoid signaling is required for circadian disruption to promote obesity and metabolic syndrome through glucocorticoid regulation. These alterations are prevented by blocking the CB<sub>1</sub> receptor, not only globally, but also through targeted peripheral inhibition, suggesting that the endocannabinoid system mediates glucocorticoid induced metabolic syndrome through a predominantly peripheral mechanism. These data build upon previous findings that indicate the endocannabinoid system is required for diet-induced obesity. They further suggest that this system plays a much broader role in the regulation of metabolic processes, as well as acting as a mediator of changes in metabolic function in response to an array of stimuli, including environmental exposure, and not just diet composition.

Research presented also aims to highlight the importance of studying different stress-like exposures in mouse models in order to fully characterize the human condition. Chronic environmental stressors, as in chronic disruption of the-light-dark-cycle, provide one such mean to study the impact of stress on a population. The environmental experience has been identified as a potential pathway linking neighborhood disadvantage and poor health, through the dysregulation of stress-related biological pathways.

## **Acknowledgements**

I look back at my first year here at Rockefeller and I realize that I was incredibly naïve. Thankfully, I was driven and had a rather strong interest from day one that kept me motivated even when, emotionally, I was at my limit. I can not give enough thanks to my wonderful advisor who has always been my best advocate. I came into the program as a biochemist who had training in the basics of neuroscience based on prior laboratory experience. My summer internships at Merck pharmaceuticals, where I studied amylin plaque formation in Alzheimer's Disease with Dr. Paul Shugrue, ended up having the largest impact and led me to the laboratory of Dr. Bruce McEwen, upon suggestion from Paul. During the fall semester, Bruce was away in Ireland, so I rotated in the lab of Jan Breslow. However, during my first week at Rockefeller, I also ran into a postdoc of the McEwen lab, who suggested that I work with a new postdoc in the lab, Dr. Ilia Karatsoreos, who had some interesting findings on glucocorticoid hormones and obesity. My stars seemed to be aligning when I met Dr. Matt Hill, another new postdoc to the lab with interest in endocannabinoid regulation of the adaptive stress response. Ilia and Matt became my day-to-day mentors and friends; I miss their daily banter and jokes immensely. Moreover, this dissertation would not have been the same without their guidance and support over the last 5 years.

Outside the lab, I am grateful for the opportunity to have chaired Student Pugwash. As a member of the organization, I had the chance to engage and excite the community about realms outside of pure biology and chemistry. As leader, I was able to not only network, but was also forced to face my nerves and learn how to better cope with public speaking.

Beyond the Rockefeller Community, I have to thank my mom, Michelle DeLoach, my Mom Mom, Theresa Bowles, and my Aunt Tiny for always providing a listening ear. There

were several nights that I would call about my lack of sleep as I ran a time course study, or just the level of stress that I felt mounting as I prepared for my yearly FAC meetings. My best friend and closest confidant throughout graduate school, Ryan, has shared many a conversation with me over the years. I can recall gmail chats with him during conference travels, and bottles of wine shared after my yearly FAC meetings, and most recently glancing up at the purple tulips he bought to motivate my last minute dissertation writing. He keeps me sane, keeps me smiling, and keeps me fed when I would just want to eat some cereal and yogurt. I look forward to continuing my journey knowing that he will be by my side.

While still rather new to my life, I brought home my dog, Mei, in November 2011. She has brought me tremendous joy and reminds me to take a few moments each day to slow down, reflect, and soak in a little vitamin D, granted these are all for her own selfish reasons as she needs a potty break; each day is better with her in my life.

Finally, I go back now to the school and lab and thank all the wonderful techs, postdocs, and administrators I have met through the years. With special shout outs to those in my first year that made the lab such a warm, friendly environment that seemed to welcome me with open arms. Last, but not least, I thank my committee members for their time, listening ear, and words of advice over the last few years.



Table of Contents

ACKNOLEGEMENTS .....v

LIST OF FIGURES..... viii

LIST OF TABLES .....xi

Chapter 1: Introduction..... 1

Chapter 2: Materials and Methods .....26

Chapter 3: Chronic circadian disruption alters body weight, signal regulation, and glucocorticoid signaling .....44

Chapter 4: Chronic glucocorticoid exposure alters metabolism and circadian rhythms ..... 61

Chapter 5: Cannabinoid CB<sub>1</sub> Receptor deficient mice are resistant to metabolic dysregulation following both circadian disruption and chronic glucocorticoid administration .....87

Chapter 6: Characterization of endocannabinoid system signaling in glucocorticoid treated mice..... 124

Chapter 7: Determination of central verses peripheral endocannabinoid regulation ..... 144

Chapter 8: Concluding remarks and future directions..... 177

References:..... 169

## List of Figures

Figure 3.1 Circadian profile in liver and WAT of control and circadian disrupted mice .....	48
Figure 3.2 Clock gene expression in dorsal hippocampus of control and circadian disrupted mice .....	49
Figure 3.3 Transcripts involved in lipid metabolism in white adipose tissue (WAT) of circadian disrupted (LD 10) and control (LD12) mice.....	49
Figure 3.4 Histology of white adipose tissue (WAT) and liver sections in circadian disrupted (LD 10) and control (LD12) mice.....	50
Figure 3.5 Transcripts involved in lipid and glucose metabolism in the livers of circadian disrupted (LD 10) and control (LD12) mice.....	50
Figure 3.6 Chronic circadian disruption results in changes in the diurnal pattern of plasma CORT levels.....	51
Figure 3.7 Diurnal mRNA expression of 11 $\mu$ -hydroxysteroid dehydrogenase type 1 and 2 in white adipose tissue (WAT) and liver .....	54
Figure 3.8 mRNA expression of CRH levels in the PVN and amygdala from circadian disrupted mice .....	55
Figure 4.1 Activity patterns of vehicle and CORT treated mice .....	64
Figure 4.2 Exogenous glucocorticoid (CORT) exposure results in decreased expression in clock genes under the light-dark cycle .....	67
Figure 4.3 Exogenous glucocorticoid (CORT) exposure results in differential expression in clock genes under constant darkness.....	68
Figure 4.4 Exogenous glucocorticoid (CORT) exposure results in decreased expression of clock genes in both the light-dark cycle and under constant darkness.....	69
Figure 4.5 Diurnal mRNA expression in white adipose tissue (WAT) and liver of control and 100 $\mu$ g/mL CORT treated mice .....	79
Figure 4.6 Clamped food intake in CORT treated mice does not prevent weight gain .....	96
Figure Supplementary 4.1 Body temperature rhythms of vehicle and CORT treated mice....	81
Figure 5.1. Circadian disruption causes an increase in body weight gain that is attenuated in CB1 receptor deficient mice .....	91
Figure 5.2. Circadian disruption causes metabolic dysregulation, as evidenced by an increase in circulating triglycerides, insulin and leptin, which is blocked in CB1 receptor deficient mice.....	92

Figure 5.3 CB1 <sup>-/-</sup> mice are resistant to CORT induced weight gain .....	95
Figure 5.4 CORT treated CB1R <sup>-/-</sup> mice do not exhibit increased food and water intake .....	96
Figure 5.5 Spontaneous activity across the day .....	96
Figure 5.6 Metabolic effects of CB1R <sup>-/-</sup> in CORT treated mice.....	98
Figure 5.7 Glucose levels and insulin sensitivity in CORT treated mice.....	99
Figure 5.8 Plasma triglycerides and liver lipid content are greatly reduced in CORT treated CB1R <sup>-/-</sup> mice.....	101
Figure 5.9 Blood chemistry profile .....	102
Figure 5.10 Effect of CB1 R <sup>-/-</sup> hepatic triglycerides and VLDL production.....	102
Figure 5.11 Substrate selection as measured by indirect calorimetry .....	121
Figure 5.12 Effect of global CB1R knockout on liver mRNA expression of genes involved in lipid metabolism .....	113
Figure 5.13 Expression of genes responsible for energy homeostasis and respiration in the liver.....	113
Supplementary Figure 5.1 Global knockout of the CB1R prevents the development of metabolic syndrome in CORT treated mice .....	115
Supplementary Figure 5.2 Time and dose course of SREBP1c expression .....	116
Supplementary Figure 5.3 CB1R <sup>-/-</sup> prevents CORT induced damage to the pancreas and liver .....	117
Figure 6.1 Effect of chronic corticosterone (CORT; 100 µg/mL ) on endocannabinoid parameters in the amygdala .....	128
Figure 6.2. Effect of chronic corticosterone (CORT; 100 µg/mL ) on endocannabinoid parameters in the hippocampus.....	129
Figure 6.3 Effect of chronic corticosterone (CORT; 100 µg/mL ) on endocannabinoids in the hypothalamus .....	131
Figure 6.4 Effect of chronic corticosterone (CORT; 100 µg/mL ) on endocannabinoids in blood circulation.....	131
Figure 6.5 Effect of chronic corticosterone (CORT; 100 µg/mL ) on endocannabinoids in the liver .....	132
Figure 6.6 Effect of chronic corticosterone (CORT; 100 µg/mL on mRNA expression of endocannabinoid parameters in liver.....	132
Figure 6.7 Effect of chronic corticosterone (CORT; 100 µg/mL ) on endocannabinoids in white adipose tissue (WAT) .....	134

Figure 6.8 Effect of chronic corticosterone (CORT; 100 µg/mL on mRNA expression of endocannabinoid parameters in white adipose tissue (WAT) .....	134
Supplementary Figure 6.1 Basal levels in treated mice .....	135
Figure 7.1 Metabolic effects of chronic treatment with AM251 and AM6545 in CORT treated mice concurrently for 4 weeks.....	147
Figure 7.2 Histology of liver and WAT in AM251 treated mice.....	148
Figure 7.3 Histology of liver and WAT in AM6545 CORT treated mice .....	150
Figure 7.4 Metabolic effects of chronic CORT treatment in LCB1R <sup>-/-</sup> mice.....	151
Figure 7.5 Histology of liver and WAT in LCB1R knockout CORT treated mice .....	152
Figure 8.1 Simultaneous CORT treatment and altered light cycle have an additive effect on weight gain and adiposity .....	158
Figure 8.2 Metabolic effect of Simultaneous CORT treatment and altered light cycle.....	158
Figure 8.3 Simultaneous CORT treatment and altered light cycle show a unique interaction in circulating CORT levels and clock gene expression .....	161

## List of Tables

Table 2.1 Forward and reverse primers for qRT-PCR .....	42
Table 4.1 Insulin signaling pathway-related gene expression in gonadal fat pads (white adipose tissue-WAT) .....	70
Table 4.2 Obesity-related gene expression in gonadal fat pads (white adipose tissue-WAT) .....	72
Table 4.3 Obesity related gene expression in in the hypothalamus of corticosterone (CORT) and vehicle treated mice .....	75
Table 5.1 Obesity related gene expression in gonadal fat pads (WAT) .....	104
Table 5.2 Insulin pathway related gene expression in gonadal fat pads (WAT) .....	108
Table 6.1 The effects of chronic corticosterone administration on gene expression of the cannabinoid receptor and fatty acid amide hydrolase .....	130

## **Chapter 1: Introduction**

Obesity is one of the most profound health problems in the United States with more than two-thirds of adults and more than 9 million children aged 6-16 years considered overweight.<sup>1</sup> Although much has been learned about the regulation of body weight and adiposity, the prevalence of obesity continues to rise. Obesity is of particular concern, as not only a disease in and of itself, but also a major risk factor in the metabolic syndrome, which is generally described as a series of physiological markers that put an individual at greater risk of negative cardiovascular outcomes associated with obesity, including diabetes.<sup>2,3</sup> Current explanations of such diseases based on nutritional over consumption, poor diet, and/or lack of physical activity, are inadequate to explain their sudden rise and increased prevalence. Furthermore, most current treatments for the metabolic syndrome have proved unsuccessful, and while some weight can be lost with moderate diet and exercise, the altered hormonal levels after weight gain make it more difficult for weight loss and maintenance of weight once lost.<sup>4</sup> Thus prevention of obesity or diabetes is an essential component of any successful weight loss program.

Obesity is a growing health concern throughout the world, and those with a lower socioeconomic status (SES) are more likely to experience chronic diseases like obesity and high blood pressure, weakened immune system, mental illness and decline of physical strength.<sup>5</sup> When the impact of SES on the development of cardiovascular and metabolic disease is considered, it is crucial to study the social-biological interface, and understand exactly how SES affects the biological factors involved in disease etiology. Lower SES is associated with a range of biological risk factors, including adverse lipoprotein profiles, increased central obesity, impaired glucose tolerance, insulin resistance, raised levels of

fibrogen, abnormalities of cardiac rhythm, and procoagulant blood clotting profiles.<sup>6</sup>

Unfortunately, the pathways through which lower SES causes these changes are still not well understood. While lifestyle and health behaviors such as smoking, lack of physical activity, and alcohol consumption contribute to health outcomes, biological risk persists after social gradient is taken into account. It has, therefore, been argued that low SES may activate psychobiological processes, or neuroendocrine, autonomic and immune responses that in turn promote the development of high-risk profiles.<sup>7</sup>

The role of stress, particularly chronic everyday stressors compared to traumatic but rare events, in the development of negative health outcomes, is often overlooked by health professionals when considering the cause of a disease.<sup>8</sup> This, despite a growing body of research which suggest that it is the inundation of these everyday burdens that strongly affect well-being. These chronic stressors even at a low level may cause an individual to be anxious or depressed, to lose sleep at night, to increase the intake of comfort foods, to smoke and/or drink, and to become more susceptible to infection.

One major issue preventing health professionals from considering a patient's everyday experiences and environment on their health outcome, apart from discrimination and stereotypes (large issues plaguing low SES communities but covered extensively by Williams et al., 2010) is the discrepancy in both human and animal literature describing the effects and possible mechanisms that would link chronic stress and health outcomes.<sup>9</sup> Further, both social and biological scientists think in a specific mindset and see stress to only mean a particular set of effectors. In this introduction, I aim to outline the etiology of the stress response and how many systems of the body including metabolic, cardiovascular, and immune, are directed to mediate this response. In particular, I highlight

the endocannabinoid system, which has gained attention over the last decade for its regulatory role in multiple processes, ranging from feeding to cognition to pain to emotional behavior in response to stressful environments. I further discuss how environmental experiences, sleep and circadian disruption and an individual's behavioral and physiological response whether health-promoting or health-damaging, aid in adaptation but which also can, when overused and out of balance, lead to pathophysiology. Herein I discuss how nontraditional animal models of stress, such as those of sleep and circadian disruption, have attempted to answer these questions, including my own recent studies.

### **Stress, cortisol and HPA dysfunction**

Stress, defined as a state of threatened homeostasis following exposure to extrinsic or intrinsic adverse forces, mobilizes a vast number of physiologic and behavioral responses that constitute the adaptive stress response that aim to restore disturbed equilibrium.<sup>10</sup> Apart from the key systems hypothesized to mediate the effects of stress exposure on disease outcomes: the sympathetic nervous system (SNS), which stimulates release of epinephrine (more commonly known as adrenaline) from the adrenal gland, and the hypothalamic pituitary adrenal (HPA) axis, which produces glucocorticoids (GCs) and several other mediators, including the parasympathetic nervous system, and pro- and anti-inflammatory cytokines, and metabolic hormones, have been described in a dynamic nonlinear network of allostasis.<sup>11,12</sup>

Allostasis refers to the active process by which the body responds to daily events as they vary across the day in response to external and internal demands.<sup>13</sup> Biomediators (HPA, autonomic, metabolic, and immune) act to down- and up-regulate each other depending on



the body's internal concentrations, location, and sequential temporal patterning. Allostasis, unlike homeostasis, which acts to keep physiological parameters in a narrow range, is a dynamic and adaptive process necessitating the need for adjustments of the mentioned biological systems. This adaptive ability comes at a cost termed allostatic load or overload, which refers to the wear and tear that results from either too much stress or from inefficient management of allostasis.<sup>12</sup> Allostatic load can have detrimental effects on health and can manifest in a number of ways, as in repeated hits from multiple stressors, not turning off the stress response when it is no longer needed, not turning on an adequate response at onset, or not habituating to the recurrence of the same stressor, and thus dampening the allostatic response.<sup>12</sup>

The stress hormones, primarily the glucocorticoids (GCs ;*cortisol* in *primates*, *corticosterone* in *rodents*), are of particular interest because of the extensive regulatory role they play in the central nervous system, the metabolic system and the immune system.<sup>14</sup> GCs are the final mediators of the HPA-axis, and play a crucial role in mounting the adaptive response to stress. The central components of the stress system are located in the hypothalamus and the brain stem, and primarily include the parvocellular corticotropin-releasing hormone (CRH) and arginine-vasopressin (AVP) neurons of the paraventricular nuclei of the hypothalamus, and the locus coeruleus-norepinephrine system.<sup>15</sup> The hypothalamus in turn regulates the secretion of adrenocorticotropin hormone (ACTH) from the anterior pituitary via CRH and AVP both of which are secreted in a synchronized mode, which can be disrupted by imposed stressors.<sup>16</sup> Upon ACTH stimulation the adrenal cortex secretes GCs, which act via their widespread receptors to respectively activate or repress numerous genes, many of which are directly related to metabolic pathways.<sup>17</sup> The primary

means of HPA-axis regulation occurs through a well-characterized negative feedback loop where GCs suppress ongoing HPA activity at the hypothalamic and pituitary levels. Despite the clear importance of GCs in feedback regulation, it is important to note that the HPA-axis is also susceptible to GC-independent inhibition as evident from adrenalectomized rats with corticosterone replacement in the form of a pellet, thus maintaining a constant circulating level of corticosterone, but inability to execute a stress response.<sup>18</sup> Nonetheless, these rats maintained the ability to inhibit ACTH responses, arguing for the existence of neuronal inhibitory pathways working in parallel with steroid feedback. Additionally, forebrain and hindbrain regions, which communicate with the PVN, have shown to regulate the HPA-axis under both basal and stress conditions.<sup>19, 20</sup>

GCs have several important functions, such as increasing access to energy stores, increasing protein and fat mobilization, as well as regulating the magnitude and duration of inflammatory responses.<sup>21</sup> Thus, without sensitivity to this feedback system or when the activity of the system becomes dysregulated, excessive or unchecked, secretion of GCs can have deleterious consequences on one's health. The alterations of GC release are a key component of the vital systems that lead to allostatic load, in conjunction with sympathetic activity, proinflammatory cytokines, and a compensatory response in parasympathetic activity. This state leads to increased susceptibility of an organism to an array of disease states, ranging from mood disorders to Type 2 diabetes and cardiovascular disease.

### **Measurement of Glucocorticoids**

Increases in plasma or salivary cortisol levels are used as biochemical markers of stress; however, apart from the observed diurnal pattern (discussed in detail below), GC secretion is

also subject to considerable variation across individuals as well as within individuals across different days.<sup>22</sup> This variation makes measurement of active free GCs difficult. As a result, a number of different approaches to modeling cortisol in humans have been examined, including: slope from highest to lowest point (diurnal slope), size of the cortisol awakening response (CAR), morning or evening levels, and total cortisol concentration over the day measured as area under the curve (AUC) of the diurnal pattern.<sup>23</sup> Waking levels of cortisol and the slope of decline across the day are generally correlated with the CAR and likely capture related features of the diurnal pattern. A flatter or 'blunted' cortisol pattern is thought to indicate HPA-axis dysfunction with a steeper decline believed to indicate a normal rhythm.<sup>24, 25</sup>

To make the story more complicated, cortisol levels can vary depending on the selected assay. Cortisol can be assayed from saliva, plasma, urine, feces and hair. Salivary cortisol is most frequently used at present given the ease of collection over the day. Further, it represents free cortisol that has passively diffused into the salivary glands. Free cortisol represents the fraction of cortisol not bound to binding proteins, including corticosteroid-binding globulin (CBG). While cortisol in the saliva is not bound to CBG, 30-50% has been converted to cortisone (the inactive form of cortisol) by the enzyme 11beta-hydroxysteroid dehydrogenase (11 beta-HSD) type 2, leading to overall lower levels of cortisol in saliva.<sup>26</sup> Urine collections of 12 or 24 h are still often used to provide an integrated measure of HPA activity over a longer period of time. However, it is important to note that urinary free cortisol is a measure of not only cortisol production, but also cortisol metabolism by the liver and clearance by the kidneys. Hair analysis is increasingly more common as they reflect cortisol changes that can occur over weeks and months.<sup>26</sup> While each of these

measurements has advantages and limitations, hair analysis, avoids the requirement of multiple samples taken a specific times of day, making it suitable for population analysis.

### **Hypocortisolism**

The association between stress and increased cortisol has been well documented over the past few decades to the point where stress and increased GC secretion have become synonyms in the literature.<sup>27</sup> Obesity has indeed been associated with increased cortisol excretion that correlated with BMI.<sup>28-30</sup> Anecdotally this comes to no surprise to many who note increased stress is accompanied by increased food intake and weight gain. Further, endocrinologists have noted the striking resemblance between Cushing's syndrome and the metabolic syndrome, thus suggesting a common underlying mechanism.<sup>31</sup> However, while both are characterized by insulin resistance, hypertension, visceral obesity, hyperlipidaemia, and glucose intolerance, circulating GC concentrations are commonly not increased in obesity or Type 2 diabetes, stressing the need to look beyond high circulating GCs.

In addition to global action, GCs also have tissue-specific effects. Visceral adipocytes are particularly responsive to GCs. They not only express higher numbers of GC receptors but are also a key site for the local interconversion of inactive GC precursors into active GCs, a reaction catalyzed by 11 $\beta$ -hydroxysteroid dehydrogenase Type 1 (11 $\beta$ HSD1), which converts cortisone to cortisol.<sup>32</sup>

The role of binding proteins to regulate the availability of free GCs levels is also often overlooked. During the diurnal nadir, only about 5% of GCs circulate unbound in an active thermodynamically "free" form, where they are able to bind to receptors, whereas most are bound to corticosteroid-binding globulin (CBG) or albumin in blood plasma.<sup>33</sup> CBG proteins

are saturated by high-physiological concentrations. For this reason they are subject to large variations of plasma concentrations of free plasma cortisol that occur during diurnal changes. The inactive GCs do not have a pronounced diurnal variation and are rarely protein-bound, which results in a higher inactive GC storage pool in circulating plasma.<sup>34</sup> This inactive storage pool is constantly available to 11 $\beta$ -HSD1 reductase to maintain local active GC concentrations even in periods of low plasma cortisol concentrations, such as during the diurnal nadir. In this way, by expressing 11 $\beta$ HSD1, the target tissue, such as white adipose tissue, is equipped to regulate its own GC concentration and subsequently its GC responsiveness on the receptor level by adjusting the rate of local GC activation.<sup>35</sup>

Use of genetically altered mice further solidified the role of 11 $\beta$ -HSD1 reductase in promoting obesity. 11 $\beta$ -HSD1 knockout mice, show impaired induction of hepatic gluconeogenic enzymes during fasting and a mitigated glycaemic response to stress or induction of obesity.<sup>36</sup> Additionally, they show improved glucose tolerance, increased hepatic insulin sensitivity, and an exaggerated hepatic induction of genes for lipogenic enzymes.<sup>37</sup> In humans, dysregulation of tissue-specific 11 $\beta$ -HSD1 activity also seems to play a role in the development of obesity in that activity in adipose tissue is increased.<sup>38</sup> To this extent, mice over expressing 11 $\beta$ -HSD1 in fat tissue show an increase in enzyme activity to a similar degree to that seen in obese humans, accompanied by visceral obesity with insulin resistance and dyslipidemia;<sup>39</sup> overexpression in hepatic cells of mice produces symptoms of the metabolic syndrome without obesity.<sup>40</sup>

Hypercortisolism has also been linked to depression and it was subsequently proposed that chronic stress causes depression and successive poor health habits that can lead to the metabolic syndrome and ensuing coronary heart disease.<sup>41</sup> Studies examining mood states,

depressive symptoms, and stress levels found that trait anxiety and depression, but not perceived stress, were associated with small but statistically significant cortisol elevation.

However, stressful daily events were associated with increased cortisol secretion, the magnitude of the effect depending on whether the event was still ongoing and on how frequently a similar kind of event had occurred previously.<sup>42</sup> Similarly, Pruessner et al. found higher levels of depressive symptomatology were associated with a greater cortisol response after awakening. In that study, cortisol levels and depressive symptomatology were significantly positively correlated with measures of chronic and acute stress perception.<sup>43</sup>

Biologically, this has been attributed to dysregulation of the HPA axis, particularly hyperactivity.<sup>44</sup> Consistent with this hypothesis, a study looking at 45 postmenopausal women found that hypercortisolemic depression, compared to normocortisolemic depression, was associated with increased visceral fat, suggesting that associations with metabolic abnormalities may be especially powerful for hypercortisolemic depression.<sup>45</sup> A study in an older population confirmed these findings suggesting again that when both depression and high cortisol levels are present, the odds of the metabolic syndrome is increased.<sup>46</sup> Despite convincing evidence that would suggest increased circulation of cortisol leads to weight gain in depressed patients, the mechanism linking the two remains elusive.

In order to obtain a better understanding on how disruption of the HPA-axis function may increase the incidence of the metabolic syndrome, our group recently developed a noninvasive approach to deliver a high dose of corticosterone in the drinking water of mice.

In this way, the adrenal glands remain intact and animals are able to retain some integrity in the diurnal rhythm present in normal animals. This approach has allowed us to avoid confounding variables such as daily injections and surgery for implantation of corticosterone

pellets which could provide additional stress. We are also able to minimize handling with only one weekly cage change and simultaneous weight measurement, procedures that have also been described elsewhere to alter the stress response.<sup>47, 48</sup> A 4-wk exposure to corticosterone (100 µg/ml) in the drinking water resulted in rapid and dramatic increases in weight gain, increased adiposity, elevated plasma leptin, insulin, and triglyceride levels, hyperphagia, glucose intolerance, and decreased home-cage locomotion. A lower dose of corticosterone in the drinking water (25 µg/ml) resulted in an intermediate phenotype in some of these measures with no effect in others. Interestingly, when challenged with a high-fat diet (HFD), mice receiving a high dose of corticosterone gained less weight compared to high dose mice on standard chow (SC), and no significant difference from mice on HFD alone. Whereas low treatment of corticosterone with HFD resulted in significant weight gain compared to both mice on corticosterone or HFD alone. When looking at insulin, leptin, and triglyceride levels the effects of corticosterone in both low and high dose groups are additive, while low corticosterone does not impair glucose tolerance (unpublished). These findings are similar to those from Shpilberg et al. who looked at the impact of a corticosterone pellet implanted in male Sprague-dawley rats and simultaneously placed on a HFD for 16 days. Again animals receiving corticosterone and HFD had a lower body weight, but increased epididymal mass compared to rats given a wax pellet on and placed on a standard diet. These rats also displayed severe fasting hyperglycemia, hyperinsulinemia, insulin resistance, and impaired  $\beta$ -cell response to oral glucose load when compared to control rats.<sup>49</sup> Both models provide suitable means to study the metabolic syndrome and type 2 diabetes and the role that GCs play in mediating these diseases both independently and in conjunction with HFD.

## **Hypocortisolism**

Hypocortisolism, characterized by a hyporesponsiveness on different levels of the HPA-axis, is a phenomenon that occurs in 20-25% of patients suffering from stress-related diseases.<sup>50</sup> Although reports of hypocortisolism in healthy individuals who lived under conditions of ongoing stress go back to the 1960s and 1970s, they were not taken seriously until similar results were seen in sufferers of post-traumatic stress disorder (PTSD).<sup>51-54</sup> More recently, hypocortisolism has also been reported for patients suffering from disorders such as burnout, chronic fatigue syndrome, fibromyalgia, chronic pelvic pain and asthma.<sup>50</sup> Studies over the last few years act as a further indicator that hypocortisolism does not seem to be an exclusive correlate of stress-related pathology, but is also present in healthy subjects living under ongoing stress such as those highlighted by Juster et al. In this study, it was demonstrated that increased allostatic load, the process by which chronic stress causes stress hormones to strain many biological systems, is associated with lower morning and stress reactive cortisol levels in comparison to individuals in the “Low” allostatic load group.<sup>55</sup> In an effort to determine cross-sectional and longitudinal associations between body composition and serum cortisol concentrations in a group of community-dwelling men, a negative association between cortisol concentrations and all body composition parameters was revealed.<sup>56</sup> The impact of neighborhood-level stressors and lack of social support also resulted in an overall decrease in cortisol levels in higher stress, lower support neighborhoods, with a flatter rate of cortisol decline throughout the day.<sup>57, 58</sup> While the presence and specific cause of hypocortisolism is still up for debate, it has been suggested to be a result of a) reduced adrenocortical secretion, at least temporarily during the circadian cycle; b) reduced adrenocortical reactivity; or c) enhanced negative feedback inhibition of the



HPA axis.<sup>27</sup>

Although there is some controversy in clinical studies about the presence and impact of hypocortisolism, research from animal studies provides mechanistic evidence to support its presence under chronic stress. Fries et al. make note of a reported rodent model of hypocortisolism in which rats exposed to 3 wks of restraint stress exhibit a hyperactive HPA-axis with significantly elevated corticosterone levels. However, 2 wks post termination of the stressor the animals show a blunted corticosterone response/hypocortisolism compared to non-stressed control rats.<sup>50</sup> In an alternative model, using morphine withdrawal as a stressor, prolonged elevated levels of ACTH and corticosterone were followed by a continuous drop of corticosterone levels.<sup>59-61</sup> In monkeys, the use of maternal separation as a stressor to mimic early life adversity has been shown to significantly lower basal hair cortisol levels in peer-reared monkeys compared to the mother-reared monkeys 1.5 and 3 years after early separation. Plasma cortisol assessed in the monkeys after 1.5 years of normal social life also indicated that the peak in the peer-reared cortisol response to acute stressors was substantially delayed.<sup>62</sup>

In recent years there have been a growing number of studies looking at the relationship between the impact of obesity and food intake and hypocortisolism. In rodent models this has been studied through the chronic stress response network model, in which rats exposed to repeated chronic restraint stress are then given lard or sucrose and subsequently demonstrate an attenuated stress response compared to those given chow.<sup>63</sup> Similarly, a palatable cafeteria high-fat diet normalized the effects of prolonged maternal separation in rats, reversing increases in anxiety and depressive behaviors, increased corticosterone, increased hypothalamic CRH, and increased hippocampal GC receptor expression.<sup>64</sup> Chronically

stressed rats, over time, develop greater mesenteric fat, which has been shown to inversely correlate with CRH mRNA expression in the paraventricular nucleus.<sup>65</sup> This response is one hypothesized mechanism explaining how, over time, chronically stressed humans appear to have hypocortisolism.

This effect seems to be preserved across species as evident by the chronic stress response network in rhesus monkeys, in which subordinate females consumed more calories, gained more weight, and subsequently showed lower diurnal cortisol responses and dampened cortisol responses to an acute social separation stressor.<sup>66</sup> Findings were analogous in a human study looking at the relation between “comfort food” and HPA-axis response in a group of “highly stressed” women. As with the animal models, it was shown that highly stressed women reported greater emotional eating, greater abdominal fat, and showed blunted output in response to acute stress, as well as signs of a heightened sensitivity to cortisol including lower diurnal cortisol, and an enhanced negative feedback loop as indicated by a dexamethasone response.<sup>67</sup> The biological determinates of decreased circulating GCs, and the link between circulating levels to weight gain, whether dependently through food intake or through an independent mechanism remain to be determined.

### **Circadian rhythm of glucocorticoids**

In addition to being a vital product of the stress response and feedback regulation, GCs follow a normal diurnal rhythm necessary for proper functioning. The vital role of GCs here was highlighted by Mary Dallman’s group, which showed that a diurnal exposure to corticosterone in the drinking water of rats was sufficient to normalize ACTH levels in adrenalectomized rats, perhaps priming neural mechanism subserving a shut-off of the HPA-

axis.<sup>18</sup> This, in contrast to constant but flat GCs in circulation, blunt the turn-on and shut-off of the HPA ACTH response to an acute stressor in ADX rats.<sup>68</sup> Normal cortisol levels have been shown to have a maximum level in the morning, characterized by an acute increase during the first hour after awakening.<sup>69,70</sup> Levels typically drop rapidly for the next couple of hours and then continue to decline slowly throughout the day and night reaching a low point around midnight (rodents as nocturnal animals show the reverse effect with circulating corticosterone).<sup>71</sup>

### **The direct glucocorticoid contribution to obesity**

Persistent exposure to stress, and the concomitant increase in circulating GCs, is accepted as one of the mediators of the ever-growing epidemic of obesity and metabolic syndrome.<sup>72-74</sup> However, until recently, few models were able to recapitulate the weight gain that accompanies stress exposure in many humans. More common, models of chronic stress including certain models of chronic subordination and chronic restraint stress, have repeatedly been associated with a reduction in body weight and a generalized catabolic state.<sup>75-77</sup> While these models are well suited for studying anhedonia and depression that some stressed individuals display, they shed no light on the other side of the coin.

More recently models of chronic psychosocial stress such as social hierarchy disruption and intruder aggression have shown increases in body mass and adiposity in subordinate mice with a negative energy balance in dominant mice<sup>79-81</sup> and increased vulnerability to diet induced obesity.<sup>81,83,47</sup> Although increased food intake is accompanied by stress in many of these studies, weight gain is more often attributable to decreased energy expenditure. Interestingly, increased weight gain and circulating corticosterone in this model is not

accompanied by increased fat pad, the hallmark of GC-induced obesity. Bartolomucci et al. argue that this effect could be attributed to upregulation of the HPA-axis in subordinate mice compared to dominant mice.<sup>84</sup>

In order to model the effects of early life chronic stressors and their potential to dysregulate metabolism, Loizzo et al. developed a paradigm combining psychological and nociceptive manipulations in neonatal life. Neonatal manipulations (10 min of maternal separation plus s.c. sham injection, daily for the first 21 d of life) resulted in increased weight-gain after onset of maturity, showing increased fat tissue and hypertrophic epididymal adipocytes along with increased levels of leptin, triglycerides, and plasma corticosterone. Overweight mice do not present consistent variations in daily spontaneous locomotor activity and show a slight increase in food intake, but only in adulthood. Total life food intake is considered, it accounts for only 20% of the total body weight increase over controls.<sup>85</sup> The above studies all support the concept that stressors early in life can cause obesity in a way that does not involve major increases in food intake.

The effect of chronic GC exposure on obesity is seen predominantly in the visceral area as briefly discussed earlier in this review.<sup>86,87</sup> Additionally, GC exposure leads to increased intake of sweet, fattening, nutrient dense foods<sup>87-89</sup> and when an acute stress is juxtaposed with a chronic stressor, stress eating is increased,<sup>91,92</sup> all of which adds to increased weight gain and obesity. However, as described above, decreases in circulating GCs, whether due to an under-active HPA axis or adjustments in alternative pathways acting to regulate the system and maintain allostasis, can also result in weight gain and the precise role of GCs here needs to be explored. The compensatory role of increased food intake, particularly that of high-calorie, nutrient-sparse foods is clearly a health-damaging behavior, which in the long-

term can lead to allostatic load and, thus not the best coping device for an extended measure of time. Recent work from James Jackson suggests that in certain populations the engagement of such health-damaging behaviors while decreasing life span is able to prevent depression.<sup>93</sup> The latter example provides a great display of the complexity of the stress response and how individuals adapt to and cope with a challenge while also contributing to allostatic load.

In terms of appetite, GCs are noted to have an anorexigenic affect by suppressing hunger centrally through a CRH-mediated mechanism, likely through an acute post-stress inhibition of neuropeptide Y (NPY)-stimulated food intake.<sup>94-96</sup> Long-term GC release acts to stimulate feeding, perhaps as an adaptative response to replenish energy sources lost during the stressful event or to stockpile in the event of a future stressor.<sup>97-99</sup> In the modern world where food, particularly high-energy foods are in abundance and stress can come from more of a psychosocial versus physical form, this adaptation can be particularly harmful.

As stated above, stress and GCs tend to stimulate appetite, particularly for nutrient dense foods, with insulin having a key role in this regard.<sup>63</sup> The preference for calorically dense foods in stressed animals seems to have a beneficial role by dampening HPA-axis response to further stress.<sup>64</sup> The rewarding nature of this cycle led to the research on the role of dopaminergic, opioid and glutamatergic transmission within the nucleus accumbens, given their role in mediating responses to drugs of addiction.<sup>100-102</sup> This reward circuitry has long been known to be activated by eating, and has been shown to be involved with the propensity to ingest highly palatable food.<sup>103</sup>

Beyond appetite, GCs are known to play a vital role in lipid homeostasis, from adipose tissue mobilization to fat deposition and storage. Much evidence here comes from

accumulating visceral fat seen in humans and primates as described above; however, the precise mechanism underlying this relationship is not fully understood. From *in vivo* studies, the general story suggests that infusion of GCs enhances lipolysis by stimulating the release of nonesterified fatty acids from adipocytes through the activation of hormone-sensitive lipase (HSL), an enzyme responsible for enhancing fatty acid mobilization.<sup>104,105</sup> It has been argued that this increase in circulating free fatty acids restricts glucose utilization and encourages insulin resistance.<sup>106</sup> Further it appears that GCs enhance fat storage by increasing LPL activity and in this way affect lipid metabolism by increasing both turnover and uptake of fatty acids in adipose tissue.<sup>107-108</sup>

GCs are also important for the differentiation of preadipocytes into mature adipocytes.<sup>109-110</sup> The role here, in conjunction with their ability to upregulate the NPY Y2 receptor in abdominal fat, subsequently leading to stimulation of proliferation and differentiation of adipocytes, further accentuate the accumulation of fat.<sup>111, 83</sup> Further, GCs seem to play a role in fatty liver through dysregulation of SREBP1c, a transcription factor that regulates lipid-related processes.<sup>112</sup> While it is clear that GCs promote adiposity, a distinct mechanism remains unclear particularly in the case where hypocortisolism may be to blame.

### **Nonclassical mediators between glucocorticoids and obesity: The Endocannabinoid System**

The Endocannabinoid (eCB) System has a well established role in mediating the stress response; inversely, GCs have the ability to increase the production and release of eCB molecules.<sup>113-115</sup> The eCB system was originally characterized as the neuronal system to

which the psychoactive constituent of cannabis  $\Delta$ -9-tetrahydrocannabinol (THC) interacted to exert its effects on physiology and behavior. The endocannabinoids, *N*-arachidonyl ethanolamine (anandamide; AEA) and 2-arachidonoylglycerol (2-AG) are lipid mediators derived from membrane phospholipids or triglycerides. The endocannabinoids are not stored or released vesicularly, but are synthesized and/or released in response to altered activity. The syntheses of AEA and 2-AG occur via separate enzymatic cascades and are evoked by cellular stress, tissue damage, or metabolic challenges.<sup>116,117</sup> 2-AG is degraded by monoacylglycerol lipase (MAGL) and diacylglycerol lipase (DAGL). In contrast, AEA is degraded by an intracellular serine hydrolase, fatty acid amide hydrolase (FAAH).<sup>118</sup> The system is comprised of the cannabinoid CB type 1 and type 2 (CB<sub>1</sub> and CB<sub>2</sub>) receptors. The CB<sub>1</sub> receptor is expressed in the central nervous system as well as metabolically active organs including the liver, adipose tissue, pancreas, and intestine. The CB<sub>2</sub> receptor is predominately expressed in tissue of the immune system.<sup>119</sup>

Accumulating evidence has demonstrated that the eCB system is responsive to modulation by both stress and GCs within the hypothalamus and limbic structures. In vitro work demonstrates that glucocorticoids within the PVN can evoke a rapid induction of eCB synthesis, which in turn acts to suppress incoming excitatory neurotransmission to CRH neurosecretory cells.<sup>114</sup> In vivo work demonstrated that a single administration of CORT increased AEA content within the amygdala, hippocampus and hypothalamus at only 10 min following administration.<sup>120</sup> 2-AG was also found to be elevated 10 min post injection, but only in the hypothalamus. These effects subsided at 1 hour following administration of corticosterone.<sup>113</sup> Functional studies have shown that mice lacking the CB<sub>1</sub> receptor exhibit potentiated secretion of both ACTH and corticosterone following exposure to an array of

psychological stressors. Such data suggest that eCB signaling is engaged by stress to constrain activation of the HPA-axis, when disrupted an exaggerated response occurs.<sup>115</sup>

Overall, studies to date suggest that eCB signaling appears to regulate both the activation and termination of the HPA axis in response to stress through a reduction in AEA and an increase in 2-AG, respectively.<sup>113</sup>

Additionally, eCBs are potent regulators of appetite, energy balance and metabolic processes through both central and peripheral regulation of feeding and metabolism.<sup>121-125</sup>

Research over the last decade showed genetic deletion of the CB1 receptor in mice results in decreased body weight and reduced fat mass. This reduction in weight loss led to the development of a drug for the treatment of obesity: rimonabant (SR141716), a selective CB<sub>1</sub> receptor antagonist.<sup>122</sup>

Given the unique regulatory role of eCBs in stress and energy metabolism, we sought to examine the role of eCB regulation in our hypercortisolism model of metabolic dysregulation. Endocannabinoid mediation also suggested by data presented by Valenzuela, who showed that an overactive liver and epididymal fat CB<sub>1</sub>R due to early life stress may be involved in metabolic alterations in adulthood, which were attenuated by chronic treatment with the CB<sub>1</sub>R antagonist SR141716A.<sup>119</sup>

## **Circadian control**

Daily rhythms in gene expression, physiology, and behavior persist under constant conditions in spite of seasonal changes of light and dark and, therefore, must be driven by self-sustained biological oscillators called circadian clocks.<sup>126</sup> These clocks are adjusted daily



by the light-dark-cycle in order to be in harmony with the outside environment. In mammals, light signals from the outside world are transmitted directly to the suprachiasmatic nuclei (SCN) of the ventral hypothalamus via the retino-hypothalamic tract.<sup>127</sup> Given its ability to synchronize all overt rhythms, the SCN is referred to as the “master clock.”<sup>128</sup> In order to synchronize physiology with external time, the SCN clock emits timed signals through hormonal and neuronal pathways to a series of peripheral circadian clocks found in most organs.<sup>129, 130</sup> Peripheral clocks translate clock time into physiologically meaningful signals through rhythmic activation of clock-controlled genes.<sup>131,132</sup> The clock mechanism in the brain and peripheral tissues consists of two interlocking, regulatory feedback loops. In the first loop, CLOCK and BMAL1 heterodimerize and bind to E-box sequences to mediate transcription of a large number of genes, including Periods (Per1-3) and Cryptochromes (Crys). Pers and Crys constitute part of the negative feedback loop and inhibit CLOCK:BMAL1-mediated transcription.<sup>133</sup> In a second loop, BMAL1 transcription is regulated by reverse erythroblastosis virus a (REV-ERBa), retinoic acid receptor-related orphan receptor a (RORa), and peroxisome proliferator-activated receptor a (PPARa), all of which regulate lipogenesis and lipid metabolism. Subsequently, the CLOCK:BMAL1 heterodimer regulates the expression of Rev-erba, Rora, and PPara.<sup>133-136</sup> Protein expression of the clock genes has been shown to be important for regulation of metabolism as evident by alterations in rhythmic expression in models of high fat feeding and diabetes.<sup>136,137</sup> Additionally, clock gene mutation or knockout has led to not only circadian dysregulation but also metabolic disturbances of lipid and glucose homeostasis.<sup>138-142</sup> Understanding the precise mechanism by which the SCN is able to reset peripheral clocks and how such regulation is able to affect downstream pathways, such as glucose and lipid metabolism, has

been a major focus over the last decade.

GCs have been a particularly attractive candidate in peripheral regulation, because they are secreted in daily cycles and the GC receptor is expressed in most peripheral cell types, but not in the neurons of the SCN.<sup>143,144</sup> In this way, GCs could act as entraining signals as suggested by Balsalobra who demonstrated that adrenal GCs have the ability to reset the clock of subordinated oscillators in the periphery.<sup>145</sup> The adrenal circadian clock was further shown to regulate the rhythmic release of GCs into the blood, which likely controls metabolic rhythms in many other organs, including liver, kidney, and brain.<sup>146-149</sup>

GCs are also interesting as a regulatory signal because of their role in the feeding response. Again, work by Mary Dallman and others has given light to the role of GCs in feeding driven behavior, particularly in regards to weight gain and the desire to eat “comfort foods”, such as sweet and high-fat foods. Studies looking at the relationships between acute and chronic stressors, the brain and the HPA axis show that stress and GCs, in the presence of insulin, increase the relative intake of “comfort foods” and reduce HPA activity. Further, apart from the direct role in the brain to both excite and inhibit CRH and ACTH secretion, GCs act in the periphery to provide an indirect secondary inhibitory feedback signal that limits the degree of chronic stress perceived by an organism.<sup>87</sup>

In the case of circadian rhythms, recent studies have shown that a high-fat diet leads to rapid alterations in both the period of locomotor activity in constant darkness and to increased food intake during the normal rest period under light-dark conditions.<sup>151</sup> These behavioral changes to rhythmicity are accompanied by disrupted circadian gene expression within hypothalamus, liver, and adipose tissue and with altered cycling of hormones and nuclear hormone receptors involved in fuel utilization, such as leptin, thyroid-stimulating

hormone, and testosterone in mice, rats, and humans.<sup>152-155</sup> Similarly a decrease in calorie intake through daytime restricted feeding, results in an uncoupling of circadian clocks in peripheral tissues, such as liver, kidney, heart, and pancreas from the central pacemaker in the SCN.<sup>156,157</sup> Long-term daytime restricted feeding (18 wk) is sufficient to increase the amplitude of clock gene expression and catabolic factors and in this way reduce levels of disease markers.<sup>158-160</sup> When determining the impact of restricted feeding on the harmful effects of high fat feeding, studies found that compared to mice fed an *ad lib* high-fat diet, restricted mice on a high-fat diet were able to restore the expression phase of the clock genes and a reduction in weight and improved insulin sensitivity despite equivalent food consumption.<sup>161</sup> Further, mice on a restricted high-fat diet had decreased circulating corticosterone compared to the restricted low fat chow group.<sup>162</sup> Work here hints to the complex regulatory role of GCs with increases from restricted feeding having beneficial metabolic effects even in the face of inhibition through high-fat feeding, suggesting the role of an alternative upstream mediator.

Work showing that rhythmicity of GCs influences photic entrainment of locomotor activity, led to the elegant studies by Kiessling, who demonstrated that genetic ablation of the adrenal clock accelerated the rate of re-entrainment.<sup>164,165</sup> Further, timed application of metyrapone, an inhibitor of adrenal GC synthesis, elicited a shift in GC rhythmicity, either prolonging or shortening jet lag, depending on the time of administration. Jet lag, is best described in this review as a set of physiological and psychological perturbations experienced when internal circadian rhythms and external times are out of synchrony. This work suggests that the adrenal clock coordinates circadian entrainment during jet lag by gradually adjusting GC rhythm.<sup>165</sup> Studies originally looking at the impact of jet lag, on salivary cortisol found

higher levels in cabin crew versus ground crew across the working day. This increase in cortisol was higher for international transmeridian flying and observed across four different career cohorts suggesting that employees are unable to adapt to the effect of transmeridian flight.<sup>165</sup>

## **Thesis Rationale and objectives**

### **Rationale**

Incidence of the metabolic syndrome, the presence of a range of metabolic dysregularities that lead to type 2 diabetes or cardiovascular disease, is increasing not only in the United States, but also around the world. Several recent studies suggest that metabolic abnormalities are associated with the settings of the circadian clock system,<sup>147,148</sup> and, moreover, that alterations in these settings are among the possible causes of metabolic syndrome. Organisms have developed behavioral and physiological adaptations to not only strong diurnal cues, but also to unforeseen, random stress stimuli such as predator attack or severe weather changes. Moreover, these responses communicate with one another at different signaling levels, resulting in interrelated regulatory networks, and dysregulation of either system can lead to the development of metabolic disorders.<sup>149,150</sup> Indeed, glucocorticoids, which are well known to affect metabolic conditions, entrain the circadian rhythm by phase-shifting the expressions of several core clock genes in peripheral organs, including the liver, kidneys, and heart.<sup>146</sup> Recently, two mouse models were developed in the lab that would allow further investigation into the interaction between glucocorticoid signaling and the core clock and how both may lead to the development of obesity through a common pathway-one a chronic disruption in normal light cues,<sup>166</sup> the other an exogenous administration of corticosterone (CORT) in the drinking water.<sup>47</sup> In addition, the

endocannabinoid system emerged as a possible variable here given its recent and thorough characterization as a moderator of the adaptive stress response<sup>113,114,124,151</sup> as well as its role in regulating energy homeostasis.<sup>121</sup> Therefore, the central goal of the studies presented in this dissertation is to elucidate a novel pathway that can integrate altered glucocorticoid signals and metabolic functions.

## **Hypothesis**

Both increases and decreases in GCs in circulation lead to alterations in clock gene expression and subsequent disturbances in metabolic pathways. These alterations are prevented by blocking the CB<sub>1</sub> receptor not only globally but also through targeted peripheral inhibition suggesting that the endocannabinoid system mediates GC induced metabolic syndrome through a predominantly peripheral mechanism.

## **Objectives**

1. To determine whether exposure to alterations in external light cues result in changed clock gene expression in the white adipose tissue, liver, and hippocampus of wild-type male mice, and if so determine the role glucocorticoid signaling may have on adjusted patterns of expression and subsequent weight gain (Chapter 3).
2. To demonstrate whether chronically increased circulating levels of glucocorticoids result in impaired circadian (daily) rhythms and altered clock and metabolic gene expression in the white adipose tissue and liver of wild-type male mice (Chapter 4).
3. To establish the endocannabinoid system as a mediator in glucocorticoid mediated metabolic abnormalities with the use of CB<sub>1</sub> receptor knockout mice (Chapter 5).

4. To determine the primary source of endocannabinoid and glucocorticoid interaction through characterization of system parameters (Chapter 6) and by specifically targeting the peripheral signaling pathway using pharmacological and genetic approaches (Chapter 7).

## Chapter 2: Materials and Methods

### Animals and protocols

#### *General procedure for corticosterone treated mice*

All animal procedures were undertaken with approval of The Rockefeller University IACUC. Adult male mice (C57/BL6; 19–21 g at receiving) from Charles River Laboratories (Kingston, NY) were group housed (n=5/cage) in standard cages (28.5 x 17 x 13 cm), on a 12-h light, 12-h dark cycle (lights off at 1800 h). A 2 lux red light allowed for animal maintenance in the dark phase. Temperature in the room was maintained at  $21 \pm 2$  C. Mice were allowed to acclimate to the facility for 7 days prior to the beginning of all experimentation. After the acclimation phase, water was replaced with a solution containing 25 or 100  $\mu\text{g/ml}$  free corticosterone (CORT; Sigma, St. Louis, MO) or 1% EtOH vehicle alone as described previously.<sup>47</sup> Animals were weighed once a week during cage change, at which time solutions were replaced, and otherwise left undisturbed.

#### *General procedure for shifted mice*

Male C57BL/6 mice (Charles River, Inc.) were group housed ( $n = 5$  per cage) and allowed 1 week to acclimate to the facility. Food and water were available *ad libitum* for the duration of the experiment. For circadian manipulation, one group of animals was maintained in a 20-h LD cycle, with 10 h of light and 10 h of dark. The control group remained in a 12:12 LD cycle. Animals were weighed weekly during cage change and otherwise left undisturbed for 8 weeks. For the time course shift study mice were euthanized at ZT 0, 6, 12, 18 (n=8-10/group).

### *CORT time course study*

This study was conducted at Washington State University's College of Veterinary Medicine in Pullman, WA. All procedures with animals were undertaken with the approval of the WSU Institutional Animal Care and Use Committee. In this study one cohort of animals was group housed (n=4/cage) and placed on either vehicle, 25 or 100 µg/mL as described above. After 4 weeks of treatment animals were euthanized at ZT 6, 12, or 18 (n=4-6/group). Mice from the second cohort were individually housed. Body temperature and activity was continuously recorded using temperature data-loggers implanted into the peritoneal cavity (SubCue, Inc.), programmed to record body temperature every 30 min, with a resolution of 0.0625 °C. Following implant, animals were allowed 1 week to recover. Body temperature and activity levels were collected using MiniMitter battery-less telemeter system (Respironics, Inc). Data were collected using VitalView software (Respironics), and analyzed in ClockLab for MatLab or ActogramJ for Image J. Following recovery mice were placed on vehicle, 25 or 100 µg/mL CORT. Three days before mice were euthanized, the animals were placed in constant darkness to measure free running circadian rhythmicity. Mice were then euthanized at CT 12 or 18, CT time for each animal based on their individual actogram and thus kill times were staggered.

### *Mouse shift with exogenous CORT replacement*

In this experiment mice were placed in circadian disruption chambers of LD10:10 or control chambers of LD12:12 as described above; however, mice were simultaneously placed on either 25 µg/mL of CORT or vehicle solution as described above. After 8 weeks of



circadian disruption and CORT treatment, mice were euthanized at ZT 6, 12, or 18 (n=4-5/group).

### *Genetic manipulations*

The  $CB1R^{-/-}$  global and liver specific mice used in this study were originally generated and backcrossed to a C57/Bl6J background<sup>167</sup> and were provided by the National Institute of Mental Health.  $CB1R^{-/-}$  mice and their wild-type littermates were bred from heterozygote mother and  $CB1R^{-/-}$  father and wild type breeding pairs, respectively.  $LCB1^{-/-}$  mice were generated by crossing mice homozygous for the  $CB_1$ -floxed allele ( $CB_1^{f/f}$ ), which were on a predominantly C57BL/6N background (7-8 crossings), with mice expressing the bacterial Cre recombinase driven by the mouse albumin promoter (TG[Alb-cre]21 Mgn) that had been backcrossed 7 times to a C57BL/6J background, from Jackson Laboratory,<sup>168</sup> to obtain  $CB_1^{f/f} \times CB_1^{f/fAlbCre}$  breeding pairs. The littermates obtained were on a mixed C57BL/6JxN background. In each experimental paradigm, littermates were used as controls. In each studying knockout mice were euthanized at ZT 4-6, unless otherwise stated. Genotyping of  $CB1^{-/-}$  mice was carried out using Transnetyx, Inc.  $LCB1^{-/-}$  mice were genotyped by PCR for the *Cre* transgene, Cre3- 5' cactcatggaaaatagcgatc 3', Cre4- 5' atctccggtattgaaactccagcgc 3'. Briefly, genomic DNA was obtained from ear punches using Viagen DirectPCR® DNA Extraction System (Los Angeles, CA). 1-2  $\mu$ L of genomic DNA was run with .2 $\mu$ M of Cre3 and Cre4, .2 $\mu$ M dNTPs, 1.5 mM  $MgCl_2$ , 1xPCR buffer, 2u Taq DNA polymerase, and water to a volume of 25 $\mu$ L. PCR cycle was as follows 95°C 2 minutes, 34 cycles of 95°C for 45 seconds, 60°C for 1 minute, 72°C for 1 minute, and a final stage of 72° for 7 minutes.

### *Tissue Collection*

After treatment animals were euthanized by rapid decapitation. Trunk blood was collected in BD Vacutainer K3 EDTA coated glass tubes (VWR, West Chester, PA), placed on ice, and centrifuged at 1500 rpm for 15 min at 4 C. Plasma was removed and stored at -80 C until used for analyses. Spleen, adrenals, liver, and gonadal fat pads from each animal were collected and weighed. A portion of the liver and fat pad along with the entire brain were flash frozen for further analysis. Remaining fat pad, liver, and pancreas were fixed with 4% PFA/PBS overnight for histology.

### **Pharmacological Manipulations**

#### *AM251*

Adult male mice (C57/BL6) were group housed (n=5/cage) and placed on a solution containing 100µg/ml free CORT (Sigma, St. Louis, MO) dissolved in 100% ethanol, and then diluted in regular tap water to a final EtOH concentration of 1%. Control mice received a 1% EtOH solution alone. Mice were given free access to drinking water and fed *ad libitum*, for 4 weeks, at the end of which markers of obesity and metabolic markers were examined (see below). Chronic treatment with AM251 (Tocris) commenced concurrently with CORT in drinking water. AM251 was dissolved in 2% DMSO and >1% Tween 80. 1 h prior to lights off, mice were injected intraperitoneally with vehicle (2% DMSO and >1% Tween 80) or AM251 at 2 mg/kg body. All mice were allowed chow *ad libitum*. Animals and chow were weighed daily, at the time of injection. Animals were otherwise left undisturbed. Tissues were collected and processed as described below.

*AM6545*

CORT and animal treatment followed as above. In tandem with CORT mice received chronic intraperitoneal injections of vehicle or AM6545, a generous gift from Dr. Alex Makriyannis' group at Northeastern, (2% DMSO and >1% Tween 80 with gentle heating) at 10mg/kg 1 h prior to lights off.

## **Histology**

### *Oil Red O*

Frozen sections of the liver (10  $\mu$ m) were stained with Oil Red O and counterstained with hematoxylin for histology. Staining was done on five samples per experimental group.

### *H&E*

Paraffin embedded samples were sectioned at 8  $\mu$ m thickness with a microtome (Microtom). Sections were floated in a water bath at 42 °C, placed on poly-L-lysine-coated Polysine microscope slides (Erie Scientific Company) and allowed to air dry. For hematoxylin and eosin (H&E) staining, sections were dewaxed in xylenes and rehydrated in ethanol baths. Nuclei were stained with Gill no. 2 hematoxylin stain for 8 min and eosin for 10 dips. Sections were then covered with permount and cover slipped. H&E staining was done on five samples per experimental group. Adipocyte length was determined from images at a 10X magnification. 20 randomly selected droplets were measured using Nis-Elements AR software, and averaged per animal.

#### *Immunohistochemistry of F4/80 in WAT*

Paraffin embedded samples, cut at 8 $\mu$ M and dried on slides, rehydrated through changes of xylenes and dilutions of ethanol. Slides were pretreated with a citrate buffer for antigen retrieval (10 mM Citric Acid, 0.05% Tween 20, pH 6.0). Sections were incubated in blocking solution (2% BSA, 50mM glycine, 0.1% Triton X-100, 10% normal goat serum) for 1 h at room temperature and then incubated in a rat antibody solution (1:100; abcam, Cambridge, MA) overnight at 4C. F4/80-immunopositive macrophage cells were detected by biotinylated goat antirat secondary antibody (1:300; Vector Laboratories, Burlingmae, CA) and avidin-biotin-peroxidase (ABC, 1:300; Vector), followed by diaminobenzidine staining. Digital images were captured using a bright-field light microscope and camera (Nikon) and analyzed using Nis-Elements AR software.

#### *Immunohistochemistry of CBG in the liver*

Fresh frozen liver samples, cut at 14 $\mu$ M in the cryostat were fixed in 10% formide for 10 minutes. Slides were then dried and rinses in 2 changes of PBS (5 minutes each). Slides were incubated in 0.3% H<sub>2</sub>O<sub>2</sub> solution in PBS at room temperature for 10 minutes, followed by 2 additional PBS rinses. Sections were incubated in blocking solution (2% BSA, 50mM glycine, 0.1% Triton X-100, 10% normal goat serum) for 1 h at room temperature and then incubated in a rabbit antihuman CBG primary antibody solution (1:300; Affiland) for 72h at 4C. CBG-immunopostivite liver cells were detected by biotinylated goat antirabbit secondary antibody (1:300; Vector Laboratories, Burlingmae, CA) and avidin-biotin-peroxidase (ABC, 1:300; Vector), followed by diaminobenzidine staining. Digital images

were captured using a bright-field light microscope and camera (Nikon) and analyzed using Nis-Elements AR software.

#### *Measurements of blood hormones*

Plasma leptin, adiponectin and insulin levels were assayed using ELISAs (Millipore, Billerica, MA), as was plasma CBG (USCN Life Science, Houston, TX) and plasma glucose and triglyceride levels were assayed using colormetric assays (Cayman Chemicals, Ann Arbor, MI), all using manufacturer's instructions. (Plasma CORT concentrations were measured using a commercially available radioimmunoassay (MP Biomedicals, Inc., Solon, OH). Samples were analyzed in duplicate and results are reported as ng/ml. The assay provided an intra-assay coefficient of variation of 8%, with a lower limit of detectability of 15.9 ng/ml.

#### **Pair Feeding**

The amount of food eaten and body weight were recorded daily. For pair feeding, mice receiving CORT were fed the same amount of regular chow as age matched vehicle group.

#### **Quantitative reverse transcription (RT)-PCR**

In initial studies, looking gene transcription large PCR arrays were used to look at numerous genes known to affect the pathways of obesity and insulin resistance. For these initial studies, mRNA from WAT and brain punches was isolated using the Rneasy Lipid Tissue Mini Kit (Qiagen) and the RT2 First Strand Kit (SABiosciences) was used to create cDNA. Resultant cDNA was used to perform qPCR on RT2Obesity Pathway and insulin

resistant PCR Arrays (SABiosciences). Plates were read on the Roche LightCycler 480 with 1 cycle of 10 min at 95°C followed by 45 cycles of 15s at 95°C and 1 min at 60°C. SYBER Green fluorescence was monitored at the annealing step of each cycle and analyzed with LightCycler Software.

In subsequent studies looking at gene expression, mRNA from liver was extracted using Qiagen's RNeasy Mini kit, and mRNA from WAT and brain punches (in Chapter 4) or dissected hippocampus and amygdala brain regions (from vehicle and CORT treated mice in Chapter 6) were separately homogenized in 1 mL of QIAzol® (Qiagen). For the latter, total RNA was extracted using a RNeasy Mini Kit (Qiagen, Valencia, CA, USA) according to manufacturer's recommendations. For all samples, DNase digestion, to remove contaminating genomic DNA, was also completed using the kit and manufacturer's protocol. Following extraction and digestion, the purity and concentration of RNA were determined by NanoDrop 260/280 ratios (NanoDrop Technologies, Wilmington, DE). All samples tested had a purity of 1.7-2.0. Two micrograms of total RNA, as evaluated by NanoDrop, was reverse transcribed using High Capacity cDNA Reverse Transcription Kits (Applied Biosystems, Foster City, CA) using the manufacturer's recommendations. Target gene expression was quantified with gene-specific primers and Power SYBR Green master mix (ABI) using Applied Biosystems 7900HT Sequence Detection System at 95°C for 10 min, followed by 35 cycles of 95°C for 15 sec, 60°C for 15 sec, and 72°C for 30 sec. Each sample was done in triplicate, and each reaction was repeated at least once to ensure reproducibility. Raw threshold-cycle (Ct) values were obtained from the Sequence Detection Systems 2.0 software (Applied Biosystems). An average cycle threshold value (Ct) was calculated from triplicate results for each gene. Threshold values were normalized to the housekeeping gene

GAPDH or  $\beta$ -actin, to provide  $\Delta$ Ct values. Fold change for each gene was then calculated using the formula  $2^{-\Delta\text{Ct}}$ . Forward and reverse primers were as described in Table 1.

### **In Situ**

To determine CRH mRNA containing cells, fresh frozen brains were cut at 20 $\mu$ M in the cryostat. We constructed a CRH riboprobe, a pBluescript SK vector containing a 1.2-kb fragment of the rat CRH cDNA was linearized with *XhoI* and *SacI* to make antisense and sense cRNA probes, respectively. Labeled RNA probes were synthesized by in vitro transcription of linearized, gel-purified DNA templates using the appropriate T3 and T7 polymerases with S<sup>35</sup>-labeled UTP. Full-length probes were separated from labeling reactions via size-exclusion columns before being mixed with hybridization buffer and measured for specific activity.

Only a random subset of animals (n = 4-5 per group) were processed for *in situ* hybridization histochemistry; remaining brains were punched for qRT-PCR. In brief, slide-mounted sections were thawed and fixed in 3.8% formaldehyde for 10 min. Sections were then processed with proteinase K [1 mg/ml, 0.1 m Tris buffer (pH 8.0); 50 mm EDTA; 10 min] at 37 C and 0.25% acetic anhydride in 0.1 m triethanolamine for 10 min. Before hybridization, slides were rapidly dehydrated in a graded series of ethanols (70, 95, and 100%). Sections were incubated in hybridization buffer [60% formamide; 10% dextran sulfate; 10 mm Tris-HCl (pH 8.0); 1 mm EDTA (pH 8.0); 0.6 m NaCl; 0.2% *N*-laurylsarcosine, 500 mg/ml; 200 mg/ml tRNA; 1 $\times$  Denhardt's; 0.25% sodium dodecyl sulfate (SDS); and 10 mm dithiothreitol] containing DIG-labeled CRH antisense cRNA probes for 16 h at 60 C. After a high-stringency posthybridization wash, sections were treated with

RNase A and were then further processed for immunodetection with a nucleic acid detection kit (Roche Molecular Biochemicals, Indianapolis, IN). Sections were incubated in 1.0% blocking reagent in buffer 1 [100 mm Tris-HCl buffer, 150 mm NaCl (pH 7.5)] for 1 h at room temperature and then incubated at 4°C in an alkaline phosphatase-conjugated DIG antibody (Roche Applied Science, Indianapolis, IN) diluted 1:3500 in buffer 1 for 3 d. On the following day, sections were washed in buffer 1 twice (5 min each) and incubated in buffer 3 [100 mm Tris-HCl buffer (pH 9.5), containing 100 mm NaCl and 50 mm MgCl<sub>2</sub>] for 5 min. They were then incubated in a solution containing nitroblue tetrazolium salt (0.34 mg/ml) and 5-bromo-4-chloro-3-indolyl phosphate toluidinium salt (0.18 mg/ml; Roche Applied Science) for 8 h. The colorimetric reaction was halted by immersing the sections in buffer 4 [10 mm Tris-HCl containing 1 mm EDTA (pH 8.0)]. Tissue hybridized with the sense probe resulted in no specific labeling.

### **Metabolic Phenotyping of CB1<sup>-/-</sup> mice on chronic CORT**

Body composition was determined using NMR technology (EchoMRI, Waco, TX), which reports fat, lean tissue, and water content of the animal. To determine energy expenditure, mice were adapted to individual metabolic chambers. Metabolic measurements (oxygen consumption, carbon dioxide production, food intake, and locomotor activity) were obtained continuously using a CLAMS (Columbus Instruments) open-circuit indirect calorimetry system for 5 consecutive days. RQ was calculated as CO<sub>2</sub> (VCO<sub>2</sub>) production/O<sub>2</sub>(VO<sub>2</sub>) consumption, with the values of 1 or 0.7 indicating 100% CHO or 100% fat oxidation (FO), respectively. FO and CHO were calculated as  $FO = 1.69 * VO_2 - 1.69 * VCO_2$  and  $CHO = 4.57 * VCO_2 - 3.23 * VO_2$  and expresses as ml/kg/hr. <sup>169</sup>



Insulin sensitivity was assessed using a .75 U intraperitoneal insulin challenge after a 6 h dark (feeding period) fast with tail blood sampling before and after injection. Blood glucose was analyzed using the OneTouch Ultra Blood Glucose Monitoring System (LifeScan, Inc, Milpitas, CA). Circulating leptin, insulin, triglycerides, and adiponectin were measured as described above. Additional blood parameters including cholesterol and ALT levels were measured and carried out by the Tri-Institutional core facility.

#### *Measurement of hepatic lipids and VLDL secretion*

In both wild type and CB1<sup>-/-</sup> mice on chronic CORT, total liver lipids were extracted with Folch extractions. Briefly, snap-frozen liver tissues (~100 mg) were homogenized and extracted twice with chloroform/methanol (v/v = 2:1) solution. The organic layer was dried under nitrogen gas and resolubilized in chloroform containing 2% Triton X-100. This extract was dried again and resuspended in water and then assayed for triglyceride concentration using commercial kits as described above.

VLDL-TG secretion rates were determined in mice fasted for 4h and intraperitoneally injected with 400µl of Pluronic-407 (1mg/g body weight) resuspended in PBS. Blood was collected in silastic tubes pretreated with heparin prior to injection and at indicated timepoints (1h, 2h, 4h after injection). Plasma triglyceride levels were measured enzymatically, as described above. The TG production rate (µmol/kg/h) was calculated from the difference in plasma TG levels over a given interval following detergent injection. TG production rates were then expressed as relative changes compared to respective controls.

## Characterization of Endocannabinoid System in CORT treated mice

### *Membrane Preparation*

Brains were removed and the hippocampus, amygdala, and hypothalamus were dissected over dry ice and stored at  $-80^{\circ}\text{C}$  until analysis. Liver samples were also collected in this manner. Membranes were collected from isolated brain regions and liver samples by homogenization of frozen tissue in 10 volumes of TME buffer (50 mM Tris HCl, pH 7.4; 1 mM EDTA and 3 mM  $\text{MgCl}_2$ ). Homogenates were centrifuged at  $18,000 \times g$  for 20 min and the resulting pellet, which contains a crude membrane fraction, was re-suspended in 10 volumes of TME buffer. Protein concentrations were determined by the Bradford method (Bio-Rad, Hercules, CA, USA).

### *CB<sub>1</sub> Receptor Radioligand Binding Assay*

CB<sub>1</sub> receptor agonist binding parameters were determined through radioligand binding using a Multiscreen Filtration System with Durapore 1.2- $\mu\text{M}$  filters (Millipore, Bedford, MA). Incubations (total volume = 0.2 mL) were carried out using TME buffer containing 1 mg/mL bovine serum albumin (TME/BSA). Membranes (10  $\mu\text{g}$  protein per incubate) were added to the wells containing 0.1, 0.25, 0.5, 1.0, 1.5 or 2.5 nM [<sup>3</sup>H]CP 55,940, a cannabinoid CB<sub>1</sub> receptor agonist. Ten  $\mu\text{M}$   $\Delta^9$ -tetrahydrocannabinol was used to determine non-specific binding.  $K_D$  and  $B_{\text{max}}$  values were determined by nonlinear curve fitting of specific binding data to the single site binding equation using GraphPad Prism (San Diego, CA, USA).

### *Fatty Acid Amide Hydrolase (FAAH) Activity Assay*

FAAH activity was measured as the conversion of AEA labeled with [<sup>3</sup>H] in the ethanolamine portion of the molecule ([<sup>3</sup>H]AEA)<sup>7</sup> to [<sup>3</sup>H]ethanolamine as reported previously.<sup>170</sup> Membranes were incubated in a final volume of 0.5 ml of TME buffer (50 mM Tris-HCl, 3.0 mM MgCl<sub>2</sub>, and 1.0 mM EDTA, pH 7.4) containing 1.0 mg/ml fatty acid-free bovine serum albumin and 0.2 nM [<sup>3</sup>H]AEA. Isotherms were constructed using eight concentrations of AEA between 10 nM and 10 μM. Incubations were carried out at 37°C and were stopped with the addition of 2 ml of chloroform/methanol (1:2). After standing at ambient temperature for 30 min, 0.67 ml of chloroform and 0.6 ml of water were added. Aqueous and organic phases were separated by centrifugation at 1,000 rpm for 10 min. The amount of [<sup>3</sup>H] in 1 ml of the aqueous phase was determined by liquid scintillation counting and the conversion of [<sup>3</sup>H]AEA to [<sup>3</sup>H]ethanolamine was calculated. The binding affinity of AEA for FAAH (K<sub>m</sub>) and maximal hydrolytic activity of FAAH (V<sub>max</sub>) values for this conversion were determined by fitting the data to the Michaelis-Menton equation using Prism.

### *Endocannabinoid Extraction and Analysis*

Brain regions and liver samples were subjected to a lipid extraction process as described previously.<sup>171</sup> Briefly, tissue samples were weighed and placed into borosilicate glass culture tubes containing two ml of acetonitrile with 84 pmol of [<sup>2</sup>H<sub>8</sub>]anandamide and 186 pmol of [<sup>2</sup>H<sub>8</sub>]2-AG. Tissue was homogenized with a glass rod and sonicated for 30 min. Samples were incubated overnight at -20°C to precipitate proteins, then centrifuged at 1,500 x g to remove particulates. The supernatants were removed to a new glass tube and evaporated

to dryness under N<sub>2</sub> gas. The samples were resuspended in 300 µl of methanol to recapture any lipids adhering to the glass tube, and dried again under N<sub>2</sub> gas. Final lipid extracts were suspended in 20 µl of methanol, and stored at –80°C until analysis. The contents of the two primary endocannabinoids, AEA and 2-AG within lipid extracts in methanol from brain tissue, were determined using isotope-dilution, liquid chromatography-mass spectrometry as described previously.<sup>173</sup>

#### *Endocannabinoid analysis in blood*

All extractions were performed using Bond Elut C18 solid-phase extraction columns (1 mL; Varian Inc, Lake Forest, CA). Serum samples (0.5mL each) were thawed and made up to 15% ethanol, to which the internal standards (Cayman Chemicals, Ann Arbor, MI) were added. Samples were then vortexed and centrifuged at 1000xg for 4 min. The supernatant was loaded on C18 columns which had been conditioned with 1 mL redistilled ethanol and 3mL of double distilled water (ddH<sub>2</sub>O). The remaining pellet was washed with 100 µL of 15% ethanol and centrifuged again for 3 minutes. The resulting supernatant was also loaded onto the C18 column. Columns were washed with 5mL ddH<sub>2</sub>O and eluted with 1mL of ethyl acetate. The ethyl acetate layer in the resulting elute was removed and dried under N<sub>2</sub>. Lipids in the residual ddH<sub>2</sub>O phase were extracted by mixing with an additional 1 mL of ethyl acetate, which was added to the original ethyl acetate solution. Once dried, samples were resuspended in 20 µL of methanol and stored at -80°C. Endocannabinoids were quantified using isotope-dilution, atmospheric pressure, chemical ionization liquid chromatography/mass spectrometry (LC-APCI-MS) as described elsewhere.<sup>172</sup>

### *Endocannabinoid analysis of adipose tissue*

Extensive method development was needed at Northeastern University to accomplish this task, as a fatty oil results from the liquid-liquid phase extraction of fat. Solid phase extraction created usable samples that did not completely dirty the mass spectrometer. After performing reproducibility studies, the samples sent from Rockefeller University have finally been analyzed.

Mixtures of the dried endocannabinoids and their deuterated analogs that had been stored at -80°C were reconstituted in ethanol for further dilution in a 20 mg/mL solution of fatty acid free bovine serum albumin (BSA) to simulate analyte-free tissue and in ethanol to make the calibration standards, and quality control (QC) samples, as previously described.<sup>174</sup> The calibration curves were constructed from the ratios of the peak areas of the analytes versus the internal standard.

The extraction procedure for the calibration standards, and quality control started with protein precipitation with ice cold PBS, pH 7.4, acetonitrile and the internal standard mixture followed by centrifugation at 14,000 g for 5 minutes at 4°C. Tissue samples were weighed and homogenized in the same solvents prior to centrifugation. The resulting supernatants were diluted in 5% phosphoric acid in water, followed by solid phase extraction. OASIS HLB cartridges (30 mg, 1 mL cartridges) were rinsed with methanol and water prior to loading the diluted samples. The loaded samples were washed with 40% methanol in water, eluted with acetonitrile and evaporated to dryness under nitrogen. Samples were reconstituted in ethanol, vortexed and sonicated briefly and centrifuged prior to immediate analysis for the endocannabinoids.

Chromatographic separation was achieved using an Agilent Zorbax SB-CN column (2.1x50 mm, 5 mm) on a Finnigan TSQ Quantum Ultra triple quad mass spectrometer (Thermo Electron, San Jose CA) with an Agilent 1100 HPLC on the front end (Agilent Technologies, Wilmington DE) as previously described<sup>9</sup>. The mobile phase consisted of 10 mM ammonium acetate, pH 7.3 (A) and methanol (B) in a flow rate of 0.5 ml/min; the autosampler was kept at 4°C to prevent analyte degradation. Eluted peaks were ionized via atmospheric pressure chemical ionization (APCI) in MRM mode. Deuterated internal standards were used for each analyte's standard curves and their levels per gram tissue were determined.

### **Statistical analysis**

Data analyses were accomplished using Prism 5 (GraphPad Software, Inc.). T-test, One-way or Two-way analysis of variance or repeated-measures (RM) ANOVAs were undertaken where appropriate. Our a priori hypothesis is that the *CB1R*<sup>-/-</sup> mice will be resistant to the effects of CD and glucocorticoid administration, so regardless of significance of the interactions, Bonferroni posttests were used to examine differences in all variables among treatment conditions. In all cases, results were considered significant at  $P < 0.05$ . One-way ANOVAs and two-tailed t-tests were conducted to identify significant daily rhythms as indicated with significant levels at  $P < 0.05$ .

**Table 2.1** *Forward and reverse primers for qRT-PCR.*

$\beta$ Actin	Forward	TGTTCCCTTCCACAGGGTGT
$\beta$ Actin	Reverse	TCCCAGTTGGTAACAATGCCA
GAPDH	Forward	ATGACATCAAGAAGGTGGTG
GAPDH	Reverse	CATACCAGGAAATGAGCTTG
CB1R	Forward	GGTTCTGATCCTGGTGGTGTGAT
CB1R	Reverse	CCGATGAGACAACAGACTTCT
FAAH	Forward	TGTGTGGTGGTGCAGGTACT
FAAH	Reverse	CTGCACTGCTGTCTGTCCAT
MAGL	Forward	CCTGTGTGGCGTGCCGATGAC
MAGL	Reverse	GCTGGAGTCAATGCGCCCCAA
DAGL	Forward	TGGAAACCCCCGCCATTGC
DAGL	Reverse	CTGCTTGCCTGCACACCCCA
NAPE-PLD	Forward	GCTGGGACATGCGACGCTGA
NAPE-PLD	Reverse	GCGAAACCGCTTCGGACCCA
SREBP1c	Forward	GGAGCCATGGATTGCACATT
SREBP1c	Reverse	GGCCCGGGAAGTCACTGT
FAS	Forward	CATGACCTCGTGATGAACGTGT
FAS	Reverse	TCGGGTGAGGACGTTTACAAA
ACC-1	Forward	GCGGGAGGAGTTCCTAATTC
ACC-1	Reverse	GGTTGGCATTGTGGATTTTC
PPAR $\alpha$	Forward	GGCTCGGAGGGCTCTGTCATC
PPAR $\alpha$	Reverse	ACATGCACTGGCAGCAGTGGA
PPAR $\gamma$	Forward	CGGGCTGAGAAGTCACGTT
PPAR $\gamma$	Reverse	TGCGAGTGGTCTTCCATCAC
HNF4 $\alpha$	Forward	CCGGTTGACTCTTGATGGCT
HNF4 $\alpha$	Reverse	GCTTGTACTTGGTCCCGTCA
G6P	Forward	CCTCCTCAGCCTATGTCTGC
G6P	Reverse	GAGAGCTCTTGGATGGCTTG

**Table 2.1 Continued**

PCG1 $\alpha$	Forward	GGAGCC GTGACCACTGACA
PCG1 $\alpha$	Reverse	TGGTTTGCTGCATGGTTCTG
TFAM	Forward	GCTTCCAGGAGGCTAAGGAT
TFAM	Reverse	CCCAATCCCAATGACAACCTC
NRF-1	Forward	GGTGCCTAGTGAGAGTGAGTCCCCC
NRF-1	Reverse	TCGGGGCTGAAGAGGGAGAAGTC
Per1	Forward	CAAGTGGCAATGAGTCCAACG
Per1	Reverse	CGAAGTTTGAGCTCCCGAAGT
Per2	Forward	CAGACTCATGATGACAGAGG
Per2	Reverse	GAGATGTACAGGATCTTCCC
Per3	Forward	GTGTACACAGTGTGCAAGCAAACA
Per3	Reverse	ACGGCCGCGAAGGTATCT
Cry1	Forward	CCTCTGTCTGATGACCATGATGA
Cry1	Reverse	CCCAGGCCTTTCTTTCCAA
Cry2	Forward	AGGGCTGCCAAGTGCATCAT
Cry2	Reverse	AGGAAGGGACAGATGCCAATAG
11 $\beta$ HSD1	Forward	AAGGAGCCGCACTTATCTGAAGCCT
11 $\beta$ HSD1	Reverse	GCCCATGAGCTTTCCCGCCTT
11 $\beta$ HSD2	Forward	GGCCTCCTGCCACTCTTGCG
11 $\beta$ HSD2	Reverse	GTGCCGTAGGCTGCCAAGCA



### **Chapter 3: Chronic circadian disruption alters body weight, signal regulation, and glucocorticoid signaling**

#### **Abstract**

Environmental stressors have consistently been linked to increased rates of morbidity and mortality, but the specific mechanisms by which such stressors get “under the skin” remain elusive. Here we look at the impact of disrupted lighting cues as a potential environmental stressor and means to disrupt circadian rhythms. Similar effects can be caused when wakefulness occurs at inappropriate biological times due to environmental pressures (i.e., early school start times, long work hours that include work at night, shift work, jet lag) or the occurrence of circadian rhythm sleep disorders. Previous work from the lab demonstrated that disruption of the light-dark cycle in mice resulted in altered body temperature rhythms (suggesting a disruption in circadian rhythms), changes in neural function, as well as an obese phenotype. Here we looked to extend these findings and determine the consequences of chronic circadian disruption on core clock gene expression, altered hypothalamic-pituitary-adrenal (HPA) axis activity as measured through glucocorticoid, particularly corticosteroid (CORT) signaling, and how the two systems act to induce obesity in this mouse model on the level of white adipose tissue (WAT) and liver metabolism. We report here that male C57BL/6 mice exposed to a 10 h light: 10 h dark circadian cycle (LD10) compared to a normal 12 h light: 12 h dark cycle (LD12) have decreased and blunted diurnal expression of clock genes in WAT and liver tissue associated with a similar pattern in CORT secretion. Decreased signaling acted to increase liver lipid content in the absence of increased food intake, while also decreasing the expression levels and rhythmicity of hepatic gluconeogenic regulatory genes. Adiposity and adipocyte size are increased in LD10 mice,

but we were unable to determine direct clock regulation based on measured end points. Findings in this study provide not only a link between metabolic disorders and environmental light-dark cycles in non-genetically altered animals, but also suggest altered exogenous light, as a chronic stressor. Furthermore, it adds to the growing evidence of hypocortisolism as an outcome of chronic stress and suggests that at least in the case of environment stress hypocortisolism, rather than hypercortisolism as a potential mechanism linking stress to poor health.

## **Rationale**

Disruption of normal circadian cycles is a growing problem in modern society, with shift work and artificial lighting at night being a major contributor.<sup>175</sup> The relationship between circadian disruption (CD) and metabolic dysregulation is becoming appreciated as studies show that shift work, sleep deprivation and circadian misalignment in humans alter insulin sensitivity, increase weight gain and promote obesity.<sup>176-178</sup> Genetic manipulation in mouse models has also demonstrated the vital regulatory role clock genes play in energy balance.<sup>166,179-181</sup> As these factors may be significant contributors to the rise in obesity, understanding the mechanisms' driving changes in metabolic function caused by CD are of immediate concern.

Glucocorticoids (GC) especially the corticosteroids (CORT), which are well known to affect metabolic conditions, entrain circadian rhythms by phase-shifting the expressions of several core clock genes in peripheral organs, including the liver, kidneys, and heart.<sup>145</sup> Therefore, we hypothesized that chronic alterations of the light-dark cycle results in altered circadian rhythms and CORT levels followed by alterations in metabolic function.

## Experimental Design

For long-term effects of circadian disruption, a total of 80 animals were used (40 exposed to a 24-h day-12 h light, 12 h dark (LD12); 40 exposed to shortened 20-h day-10 h light, 10 h dark (LD10)). After 8 weeks in designated light cycle, mice were euthanized at Zeitgeber time (ZT, ZT12=lights OFF) 0, 6, 12, or 18. Blood, brain, gonadal fat pad (white adipose tissue (WAT), and liver were collected and processed from each animal.

## Results

In order to determine if disruptions of environmental light cues affected the rhythm of circadian clocks in peripheral tissues, we investigated clock gene expression in WAT and liver at 4 time points across the circadian cycle. Clock genes showed rhythmic expression in WAT and liver in LD 12 mice; however, the rhythmic expression of clock genes was abolished or extremely blunted in WAT and liver from LD 10 mice, indicating disruption of clock function (Fig 3.1). In WAT of LD12 mice, the rhythmic expression, as determined by one way ANOVA, of Per1 ( $F(4,38)=5.106$ ;  $p=0.003$ ; Fig 3.1A), Per2 ( $F(4,38)=28.22$ ;  $p<0.0001$ ; Fig 3.1B), and Per3 ( $F(4,38)=27.13$ ;  $p<0.0001$ ; Fig 3.1C) all showed peak expression at ZT12 ( $p<0.05$ ) with a nadir of ZT0 in Per1 and Per3, a nadir of ZT6 in Per2. Cry1 ( $F(4,37)=5.85$ ;  $p=0.001$ ; Fig 3.1D) and Cry2 ( $F(4,36)=5.394$ ;  $p=0.002$ ; Fig 3.1E) in WAT showed peaks at ZT18 ( $p<0.05$ ) with a nadir of ZT6 in Cry1 and ZT0 in Cry2. In LD12 mice, Per1 ( $F(4,37)=15.23$ ;  $p<0.0001$ ; Fig 3.1F) and Per3 ( $F(4,38)=18.77$ ;  $p<0.0001$ ; Fig 3.1H) in the liver showed peaks at ZT12 ( $p<0.05$ ) with nadirs at ZT0. Per2 in the liver in LD12 mice was rhythmic ( $F(4,35)=12.15$ ;  $p<0.0001$ ; Fig 3.1G) with an extended peak from ZT12-ZT18 (ZT0 vs. ZT12/18,  $p<0.05$ ) and nadir at ZT0. Cry1 in the liver

( $F(4,39)=4.8;p=0.003$ ; Fig 3.1J) showed a peak at ZT18 ( $p<0.05$ ) and a nadir at ZT6. Clock gene expression measured in the dorsal hippocampus revealed no effect of CD (Fig 3.2).

To better understand the underlying mechanisms of circadian clock disruption in WAT, which may account for weight gain, shown to be significantly higher in LD 10 mice compared to LD 12 mice as early as week 2 as previously shown,<sup>166</sup> we analyzed circadian variations in mRNAs of genes involved in WAT lipid metabolism. PPAR $\gamma$  was selected from literature describing its direct relation to Per2, and for its central role in the control of adipocyte gene expression and differentiation. PPAR $\alpha$  is less adipogenic but is able to induce significant differentiation in response to strong PPAR $\alpha$  activators (Fig 3.3).<sup>182,183</sup> Although somewhat decreased at ZT12, there was no statistical difference in expression of PPAR $\alpha$  between groups; similarly there was no difference in PPAR $\gamma$ , although there appears to be a slight phase advance in LD10 mice. Despite no differences here, there was an increase in adipocyte size in LD10 compared to LD12 mice (t test,  $P=0.0309$ ; Fig 3.4A-C).

To study the effects of shorter light cycles and subsequent decreased clock gene expression on liver tissue, we measured the expression of genes involved in glucose homeostasis. Hepatocyte nuclear factor 4 $\alpha$  (HNF4 $\alpha$ ) and PPAR $\alpha$  were selected from literature which suggest them to be regulated by Per2;<sup>182</sup> they further act as transcriptional factors that regulate glucose-6-phosphatase (G6P), a rate-limiting enzyme in gluconeogenesis. mRNA expression was blunted in LD10 mice with no rhythmicity in HNF4 $\alpha$ , PPAR $\alpha$ , or G6P as determined by one way ANOVA, compared to LD12 mice in which HNF4 $\alpha$  was rhythmic ( $F(4,19)=4.24;p=.017$ ) with peak levels at ZT18 ( $p<.05$ ) and a nadir at ZT0 (Fig 3.5A).

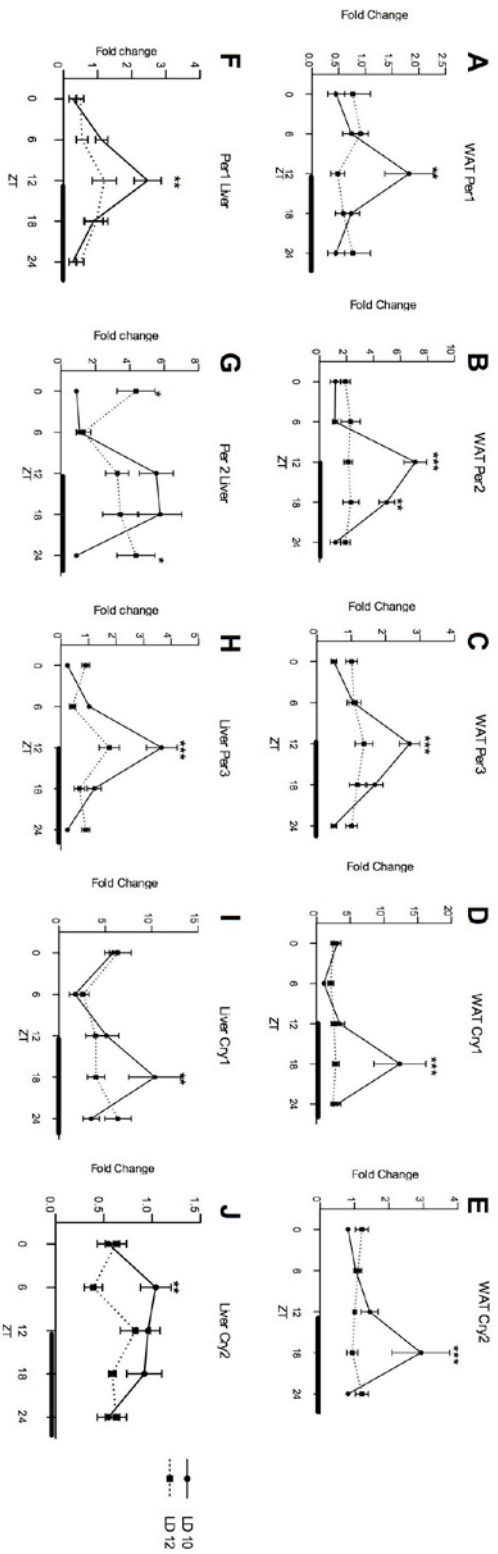


**Figure 3.1** *Circadian profile in liver and WAT of control and circadian disrupted mice.* A shortened light cycle of 10h light: 10 h dark, compared to the regular 12h light: 12 h dark paradigm resulted in blunted circadian rhythms (n=6-8/group and time point). The ZT0 group is re-blotted as ZT24 for continuity. The active period is indicated by the dark bar on the x-axis. Fold changes of gene expression ( $\pm$ SEM) in WAT (A-E) and liver (F-J) in LD12(↓) and LD10(↓) were determined by qRT-PCR. Values represent the level of normalized gene expression relative to the mean, overall normalized gene expression to ZT6. Significant peak levels of expression in LD12 to LD10 \*  $p < 0.05$ , \*\*  $p < 0.01$ , and \*\*\*  $p < 0.001$  by two way ANOVA and Bonferroni posttest.

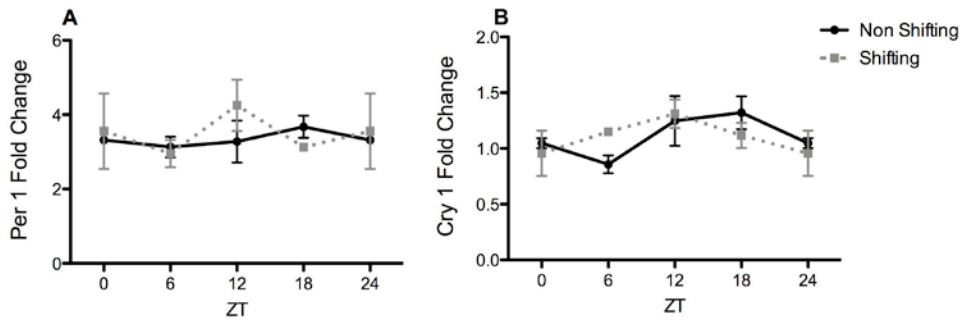


**Figure 3.2** Clock gene expression in dorsal hippocampus of control and circadian disrupted mice. A shortened light cycle of 10h light: 10 h dark, compared to the regular 12h light: 12 h dark paradigm showed no significant difference between groups in either (A)Per1 or (B) Cry1 mRNA expression in the dorsal hippocampus as determined by qRT-PCR, n=4/group and time point. The ZT0 group is re-blotted as ZT24 for continuity. Fold changes of gene expression ( $\pm$ SEM) ,values represent the level of normalized gene expression relative to the mean, overall normalized gene expression to ZT6.

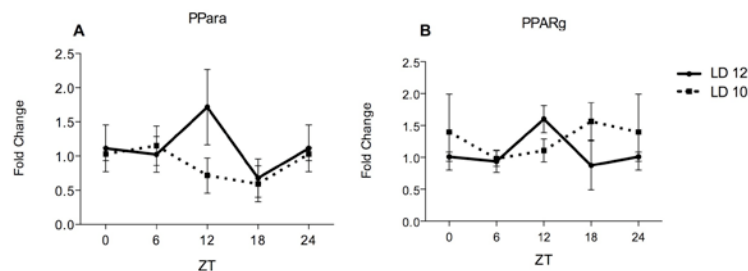


**Figure 3.3** Transcripts involved in lipid metabolism in white adipose tissue (WAT) of circadian disrupted (LD 10) and control (LD12) mice. Expressions of mRNAs encoding (A) PPar $\alpha$  and (B) PPar $\gamma$ . N=4/group for each observed time point. Values represent the level of normalized gene expression relative to the mean, overall normalized gene expression to ZT6. Results are expressed as means  $\pm$  SEM. Two-way ANOVA was used to determine variance with respect to time and groups, followed by Bonferroni's post hoc test.

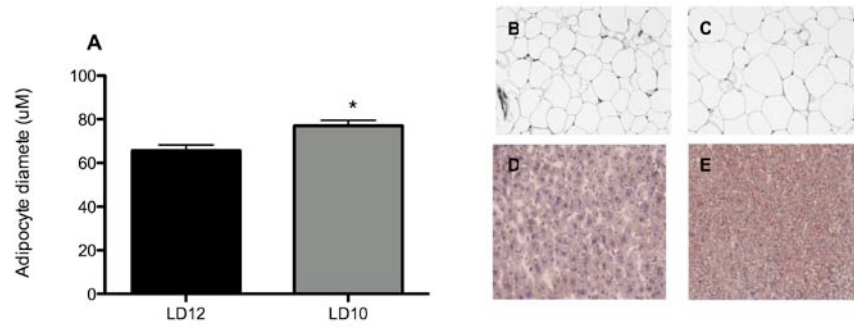


**Figure 3.4** Histology of white adipose tissue (WAT) and liver sections in circadian disrupted (LD 10) and control (LD12) mice. WAT samples embedded in paraffin were sectioned at 8 µm and stained with H&E. Representative samples from (B) LD12 and (C) LD10 mice shown here at 10x. (A) 5 samples from LD 10 and LD 12 mice euthanized at ZT 6 were analyzed for adipocyte length, 20 random droplets were measured per mouse. Fresh frozen liver samples were sections at 14 µm and stained with Oil Red O. (E) LD10 mice have an increased presence of lipid droplets compared to (D) LD12 mice. Representative samples from LD10 and LD12 mice shown here at 10x.

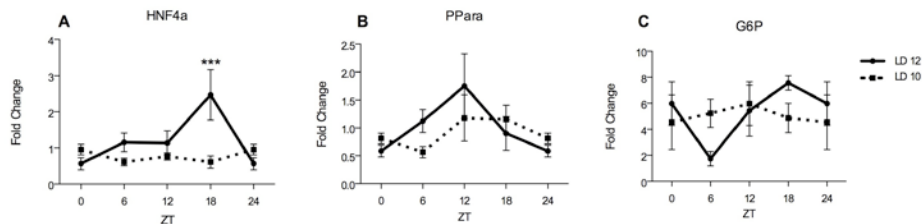


**Figure 3.5** Transcripts involved in lipid and glucose metabolism in the livers of circadian disrupted (LD 10) and control (LD12) mice. (A) HNF4α showed blunted and decreased expression in LD 10 mice. (B) PParα and (C) G6P have a slightly decreased rhythm in LD10 mice but these values did not reach significance. N=4/group for each observed time point. Values represent the level of normalized gene expression relative to the mean, overall normalized gene expression to ZT6. Results are expressed as means ± SEM. Two-way ANOVA was used to determine variance with respect to time and groups, followed by Bonferroni's post hoc test.

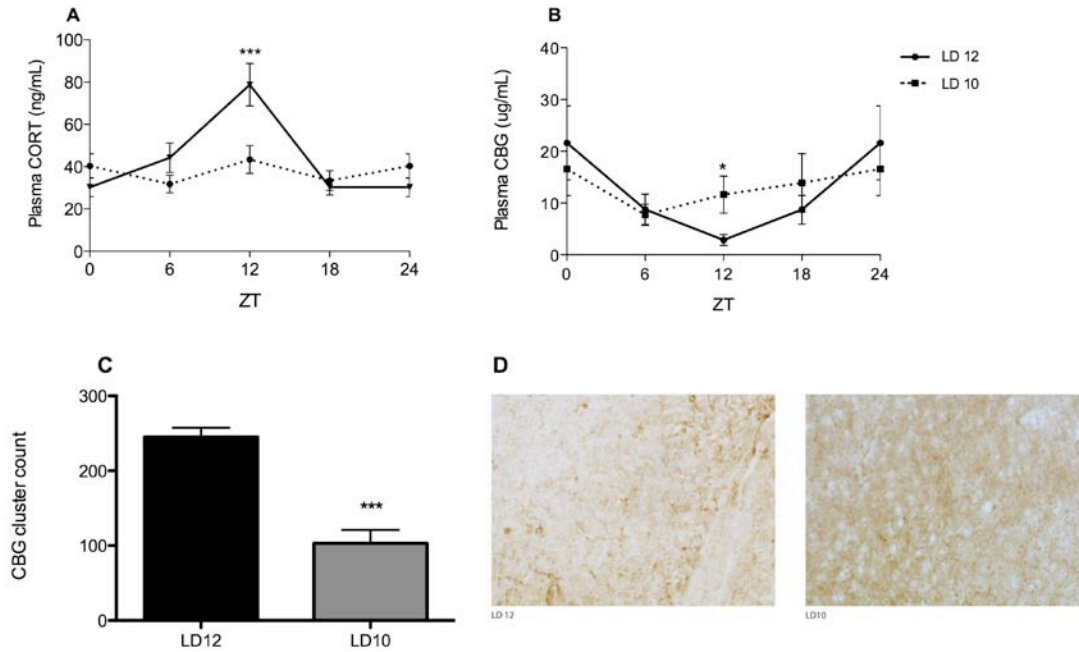


**Figure 3.6** *Chronic circadian disruption results in changes in the diurnal pattern of plasma CORT levels.* (A) Graph depicts total plasma CORT levels taken at 4 time intervals (n=9-10/group/time point). (B) Depicts circulating levels of CBG protein in plasma (n=3-5/group/timepoint). In each graph ZT0 is blotted again as ZT24 for continuity. While circulating levels of CBG are great in LD10 mice, (D) Immunohistochemistry stain for CBG protein and (C) cluster count from stain indicate a decreased presence in the liver, also suggesting increased levels in circulation. \*P<0.05, \*\*\*P<0.001 mark significant in LD12 vs. LD10.



There was also a significant decrease in HNF4 $\alpha$  expression between LD10 and LD12 at ZT18 ( $p < .001$ ). G6P also showed a rhythmic pattern ( $F(3,14)=3.778$ ;  $p=.044$ ) with a peak at ZT18 ( $p < .05$ ) and a nadir at ZT6 (Fig 3.5C). While LD10 levels were blunted, there was no significant difference from LD12 in either G6P nor PPAR $\alpha$  mRNA expression (Fig 3.5B).

In determining the effects of chronic circadian disruption on HPA-axis activity across the day, levels of plasma CORT were measured at 4 time intervals. As expected LD12 mice followed the diurnal pattern of total CORT plasma levels ( $F(4,47)=10.77$ ;  $p < 0.0001$ ) with highest levels at ZT12, corresponding to lights out ( $p < 0.05$ , Fig 3.6A ). LD10 resulted in a blunted rhythm with no clear peak and significantly lower levels at ZT12 ( $p < 0.01$ )

Circulating CBG protein levels also followed a daily pattern ( $F(2,24)=3.006$ ;  $p=0.043$ ) in LD12 mice with a nadir at ZT12 (ZT0 vs. ZT12 t test,  $p=0.0316$ ; Fig 3.6B). This level was significantly higher in LD10 mice at ZT12 (t test  $p=0.0252$ ). CBG levels, measured by immunohistochemistry in livers of LD10 and LD12 mice, revealed a much greater level in control mice (t test  $p < 0.0001$ , Fig 3.6 C-D), suggestive of increased levels in circulation in LD10 mice.

In order to determine the availability of free CORT at the tissue level, we also measured the diurnal mRNA expression of the enzymes 11 $\beta$ HSD1/2 in the WAT and liver, as well as the protein expression of these enzymes at ZT6 (Fig 3.7). In WAT there was no difference in the expression of 11 $\beta$ HSD1 between LD10 and LD12, but 11 $\beta$ HSD2 showed a rhythmic expression in LD12 mice ( $F(4,18)=6.04$ ;  $p=0.005$ ) with a peak at ZT12 ( $p < 0.05$ ) and was significantly greater than LD10 at ZT12 ( $p < 0.01$ ; Fig 3.7B). In the liver mRNA expression of 11 $\beta$ HSD1 showed no rhythmicity in either group but two-way ANOVA pulled out a slight

interaction between LD10 and LD12 mice ( $F(4,65)=2.59;p=0.047$ , Fig 3.7C). In the liver there was a slight rhythmic expression of 11 $\beta$ HSD2 in LD12 mice, but levels did not reach significance ( $F(4,34)=2.465;p=0.065$ ); however, peak expression in LD12 mice at ZT 6 was greater ( $p=0.05$ ) than in the LD10 condition (Fig 3.7D). LD10 mice showed a peak of 11 $\beta$ HSD2 mRNA ( $p<0.05$ ).

To determine the extent of HPA-axis dysregulation, we measured CRH in the PVN and amygdala. Analysis of in situ hybridization in the PVN revealed a main effect of light cycle but no effect in rhythmicity. LD12 mice showed an increased mRNA expression of CRH ( $F(1,74)=7.896;p=0.006$ ) at ZT6 as revealed by posttests analysis ( $p<0.05$ ; Fig 3.8A and C). Analysis in the amygdala found a small interaction between groups ( $F(4,34)=3.314;p=0.0214$ ) and a main effect of time of day ( $F(4,34)=2.851;p=0.039$ ; Fig 3.8B and D), as noted by increased expression at ZT18 in LD12 mice ( $p<0.05$ ).

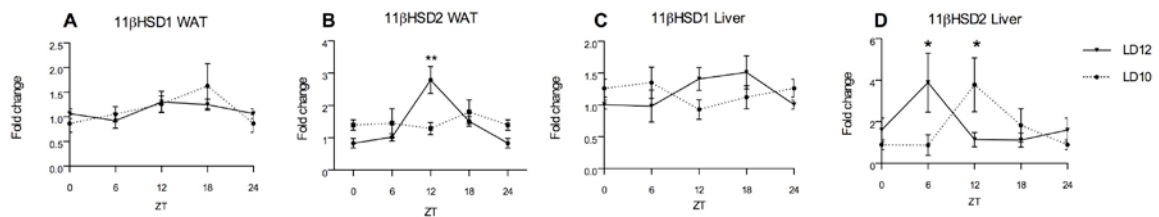


**Figure 3.7** Diurnal mRNA expression of  $11\beta$ -hydroxysteroid dehydrogenase type 1 and 2 in white adipose tissue (WAT) and liver. A shortened light cycle of 10h light: 10 h dark (LD10), compared to the regular 12h light: 12 h dark (LD12) had no effect on (A)  $11\beta$ HSD1 mRNA expression in WAT or (C) liver, but the paradigm resulted in blunted circadian rhythms of  $11\beta$ HSD2 in (B) WAT and a shift in the (D). (n=4-6/group and time point). The ZT0 group is re-blotted as ZT24 for continuity. Fold changes of gene expression ( $\pm$ SEM) were determined by qRT-PCR. Values represent the level of normalized gene expression relative to the mean, overall normalized gene expression to ZT6. Significant peak levels of expression in LD12 to LD10 \*  $p < 0.05$  and \*\* $p < 0.01$  by two way ANOVA and Bonferroni posttest.

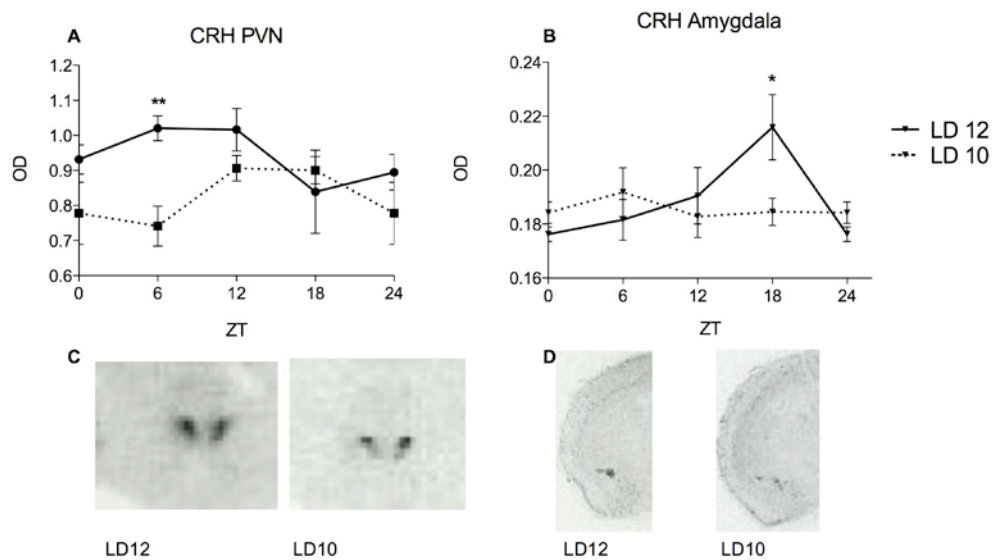


**Figure 3.8** mRNA expression of CRH levels in the PVN and amygdala from circadian disrupted mice. In situ hybridization of CRH revealed a decreased and shifted expression in the (A) PVN and (B) amygdala of LD10 mice. n=6-9/group/time point, as determined by densitometry and plotted as optical density. Representative expression in (C) PVN from ZT6 and (D) amygdala from ZT18. \* denotes  $P < 0.05$ , \*\* $P < 0.01$ .

## Discussion

In the current study we utilized the LD10 model of circadian disruption and showed that beyond increased adiposity and circulating insulin and leptin levels, LD10 mice display increased lipid content in their livers, suggesting the development of fatty liver, and increased size of adipocytes. To reveal the impact of the circadian timing system on this metabolic phenotype, we first looked at clock gene expression in the WAT, liver, and hippocampus. While we showed diurnal variations in WAT and liver, there was no significant effect of circadian disruption in the hippocampus. Data here is consistent with findings in rats where adrenalectomy abolished the *Per2* expression in the central nucleus of the amygdala, but had no effect on rhythms in the basolateral amygdala and dentate gyrus.<sup>184</sup> Changes in expression of peripheral genes as revealed here come as no surprise given the observed metabolic abnormalities in *CLOCK* mutant mice,<sup>179</sup> in a paramount study which linked metabolic function to the molecular clock. In the current study, we went a step further and demonstrated that environmental change can have a similar impact, a concept easily translated into human life. More recent studies have shown the importance of clock alignment in the periphery, particularly in adipose tissue.<sup>180,181</sup>

Given that we saw no difference in the hippocampus but strong effects in the periphery, we turned to see if corticosterone (CORT), the primary corticosteroid in mice were playing a role here. CORT has previously been shown to act as an entrainer for peripheral organs because it is secreted in daily cycles, and its receptor is expressed in most cell types with the exception of neurons in the SCN.<sup>143-144</sup> Corticotropin-releasing hormone (CRH) is also released in a pulsatile manner, and along with arginine vasopressin (AVP) in the hypothalamus, drives the pulsatile release of CORT from the adrenal cortex. Increased

CORT secretion at the circadian peak depends on increased HPA-axis activity and on increased sensitivity of the adrenal cortex to adrenocorticotrophic hormone (ACTH).<sup>185</sup> Decreased or shifted CRH data presented here suggest, in conjunction with decreased circulating CORT in LD10 mice, that the CD model represents some level of HPA-axis dysregulation.

Beyond an arrhythmic and overall decreased level of CORT in disrupted mice, we also noted an increase in corticosteroid-binding globulin (CBG), which is produced in the liver and circulates in the plasma binding CORT with high affinity.<sup>186</sup> CORT bound to CBG is biologically inactive<sup>187,188</sup> and, therefore, is important to measure to get an idea of the free circulating CORT that is able to bind to receptors. Thus, in addition to decreased circulation in total CORT, disrupted mice have significantly reduced free CORT.

CBG levels are known to be affected by season, stress, and time of day<sup>189-195</sup> The time of day finding in CBG was dependent on the diurnal nature of CORT.<sup>195</sup> In this study it may be the case that disruption not only leads to dysregulation of the HPA-axis as exhibited by decreased CORT circulation, and decreased or delayed expression of CRH in the PVN, but an overall misalignment in CORT regulation.

This hypothesis was strengthened by investigation of 11 $\beta$ -hydroxysteroid dehydrogenase (11 $\beta$ HSD) type 1 and 2, the enzymes responsible for reducing cortisone to the active hormone corticosterone and conversely inactivating corticosterone to cortisone, respectively. These enzymes work at the tissue level to activate or deactivate CORT depending on the tissue's needs or in the case of the kidney tubules, where 11 $\beta$ HSD2 is highly expressed, to enable aldosterone to reach the mineralocorticoid receptor by deactivating CORT. In our study presented here, we showed no significant differences in 11 $\beta$ HSD1 in either the WAT

or the liver, while there was a nice rhythmic expression of 11 $\beta$ HSD2 in LD12 mice, with a peak in WAT that corresponded with an increase in circulating CORT levels suggesting that 11 $\beta$ HSD2 was working to decrease CORT availability in WAT at ZT12. This expression was blunted in LD10 mice and while it is possible that we missed a peak in these mice due to our sample times, overall 11 $\beta$ HSD2 levels were decreased. In the liver, 11 $\beta$ HSD2 was shifted in the LD10 mice, while again this could be in relation to a peak that we missed in our times of data collection, it speaks more to our hypothesis that the system of CORT regulation is not in synchrony.

Increased circulating CORT is known to increase adiposity especially in the visceral area through increased lipogenesis,<sup>86,87,104</sup> but the role of blunted CORT on metabolism is less clear. Given that arrhythmic CORT in LD10 mice led to arrhythmic expression of clock genes, we examined Per2 interactions with nuclear receptor PPAR $\alpha$  and PPAR $\gamma$  and nuclear receptor target genes, including Hnf4 $\alpha$ , and G6P, were altered in disrupted mice.<sup>182,196</sup> In WAT there was no significant difference in either PPAR $\alpha$  or PPAR $\gamma$  although mRNA levels showed a flatter rhythm. The same was the case in the liver where Hnf4 $\alpha$ , G6Pc, and PPAR $\gamma$  (the expression of these factors are greater in the liver than WAT)<sup>197</sup> displayed a significantly flatter rhythm in Hnf4 $\alpha$  mRNA levels suggesting impairment of gluconeogenesis in LD10 mice.

It remains to be determined how alterations in gene expression and CORT regulation, which appear to have negative metabolic effects, align with feeding behavior. While we have shown no difference in overall food intake, several studies have demonstrated the importance of daily feeding time,<sup>198,199</sup> which has shown to alter the liver metabolome, as well as nutrient utilization and energy expenditure.<sup>200,201</sup> In CD mice misalignment in

feeding behavior, energy metabolism, and substrate utilization could become worse overtime, as the mice are unable to adjust to the light-cycle. Change in feeding behavior independent of enzyme and receptor regulation could further modify rhythms, as again food availability and food intake alone are sufficient to change rhythms. In this way, weight gain may be a consequence of the body's means to maintain allostasis.

How these findings translate to humans is an important area of research because such effects could put chronically disrupted individuals at risk for developing metabolic and cardiovascular problems. More recently the phenomenon of blunted and decreased daily CORT release, referred here as hypocortisolism, has also been reported for patients suffering from PTSD.<sup>51</sup> More extensive research has also shown the presence of hypocortisolism in body disorders such as burnout, chronic fatigue syndrome, fibromyalgia, chronic pelvic pain and asthma, as well as in healthy individuals living under conditions of ongoing stress.<sup>50, 55</sup> If circadian disruption is able to have a similar effect on CORT circulation, then the phenomena of hypocortisolism may be more common place than once thought, given the number of individuals who operate in conditions where circadian disruption is present (e.g., scientist running circadian experiments, doctors, nurses, and pilots to name a few). As with individuals and animals with chronic stress, chronic circadian disruption could thereby have a markedly altered regulation of the circadian and ultradian rhythms. The circadian rhythm is flattened or lost leading to metabolic abnormalities as we see here, cognitive deficits,<sup>166</sup> impaired inflammatory response as we noted in decreased Il-6 circulation after an LPS challenge (unpublished data), suggesting an overall altered response to acute stressors.

The degree to which the noted metabolic disturbances reflect dysregulation of the clock, dysregulation of CORT, or an interaction between these two systems also remains to be



determined. Studies looking at the effects of chronic mild stress in both BALB/c mice and C57BL/6 mice showed marked differences in terms of end point measurements in terms of corticosterone levels, clock gene expression, and subsequent metabolic parameters. Future work looking into these two mouse strains, which have been shown to have differential responses to HPA-axis perturbations, could shed light on the extent CORT is having an effect in this model of CD.<sup>202,203</sup>

In summary, chronic alterations in environmental lighting cues results in a loss of rhythmicity and dysregulation of CORT secretion. The pattern of CORT activity is associated with the loss of rhythmic clock gene expression in WAT and liver. In WAT the direct relationship to circadian control and lipogenesis remains unclear, but CD appears to alter glucose metabolism in the liver through decreased expression of Hnf4 $\alpha$  and G6P.

## **Chapter 4: Chronic glucocorticoid exposure alters metabolism and circadian rhythms**

### **Abstract**

Chronic glucocorticoid (GC) exposure, as often occurs under conditions of pervasive stress, is accepted as one of the mediators of the obesity and metabolic syndrome epidemic plaguing our nation; however, the molecular mechanisms connecting increased GCs to metabolic dysregulation remains unclear. GC hormones, particularly corticosteroids (CORT) also play a role in the regulation of circadian (daily) rhythms, particularly in some peripheral tissues, as well as in the bed nucleus of the stria terminalis and central nucleus of the amygdala in the brain. CORT effects on rhythms seem to be mediated through direct effects on “clock genes” that regulate intrinsic timing at the cellular level. Given the effect of CORT secretion and signaling on clock gene expression, an imbalance or disruption in CORT signals could affect nutrient metabolism, storage, and feeding related hormone responses. We have recently developed a non-invasive model of CORT administration that delivers CORT through the drinking water of mice. This results in rapid and dramatic increases in weight gain, increased adiposity, elevated plasma leptin, insulin and triglyceride levels, and hyperphagia. In this study, we aimed to determine how chronic high levels of CORT impact circadian rhythms, clock gene expression, and related changes in metabolism. Prolonged treatment with CORT resulted in alteration of circadian rhythms as noted by body temperature, activity levels, and decreased clock gene expression in both white adipose tissue (WAT) and liver. Constant darkness also revealed the ability of increased circulating CORT to decouple clock gene expression in WAT. Additional metabolic analysis in WAT and liver revealed disruptions to lipid and glucose metabolism related pathways. As CORT mice continue to gain weight in the absence of hyperphagia, these effects are likely independent of

food intake. Thus, increased exposure to CORT can interfere with the circadian expression of both core clock genes and metabolism-related genes, offering a mechanism that could contribute to metabolic disorders in our modern 24/7, stressful society.

## **Rationale**

Glucocorticoid (GC) hormones are thought to play a role in the regulation of clock genes involved in the generation of circadian rhythms in peripheral tissues, as well as the bed nucleus of the stria terminalis and central nucleus of the amygdala in the brain.<sup>184,145</sup> Recent studies have also shown circadian rhythmicity in glucocorticoid-related gene expression in human adipose tissue, suggesting that intra-depot cortisol action can be modified in a circadian fashion at the tissue level.<sup>204</sup> Given that increased weight gain and decreased circulation of CORT were associated with decreased expression of clock genes in the periphery (as shown in Chapter 3), we wanted to explore how chronic administration of CORT in the drinking water would affect circadian rhythms as measured through activity, body temperature, clock gene expression and metabolism related genes.

## **Experimental design**

The experiment was carried out with 2 cohorts of mice. In the first group, 48 mice were obtained and placed on vehicle, 25 µg/mL or 100 µg/mL CORT. After 4 weeks of treatment, mice were euthanized at Zeitgeber time (ZT, ZT12=lights OFF) 6, 12, or 18 (n=4-6/group, 2 cages were lost during experiment as the result of aggressive fighting). In the second cohort, 24 mice (n=4/group/time point) were surgically implanted with temperature and activity telemeters. Their daily activity during the light dark cycle was monitored for the duration of

the 4 week CORT treatment, with the last 72 hours in constant darkness (DD). Mice in this cohort were euthanized at circadian time (CT, CT12 = start of daily activity) 12 or CT18 based on their free running period. Blood and tissue were collected at the end of the experiment for processing.

## Results

Mice chronically treated with CORT in the drinking water displayed biphasic activity as suggested by actograms (Fig 4.1A-C) and tempograms (Supplemental Fig 4.1 A-C), where there was a noticeable gap in the middle of the active cycle compared to control mice. Overall activity levels were clearly decreased in CORT treated mice. One way ANOVA and Tukey posthoc revealed decreased daytime activity in 100  $\mu\text{g}/\text{mL}$  CORT treated mice ( $F(2,26)=4.103$ ,  $p=0.0293$ ), and decreased nighttime activity in both 25 and 100  $\mu\text{g}/\text{mL}$  CORT treated mice ( $F(2,26)=105.3$ ,  $p<0.0001$ ; Fig 4.1F). A decreased or flattened amplitude in circadian rhythm in CORT treated mice was also made evident by comparing the magnitude of the change between daytime and nighttime activity levels ( $F(1,40)=25.28$ ;  $p<0.0001$ ; Fig 4.1E). Bonferroni posthoc showed increased effect from days 1-8, to days 9-6 in CORT treated mice only ( $p<0.05$ ). Although there were no change in body temperature amplitudes from week-to-week, actual body temperature was decreased in CORT treated mice ( $F(2,13)=18.78$ ,  $p<0.0001$ ; Supplemental Fig 4.1E), again suggesting a flatter rhythm in CORT mice . Mice were placed in DD (constant darkness) for the final three days of the experiment to determine affects on free running circadian rhythm. DD in the actogram (Fig 4.1A-C) is noted by a decrease in  $Q_p$ , an indicator of circadian robustness.

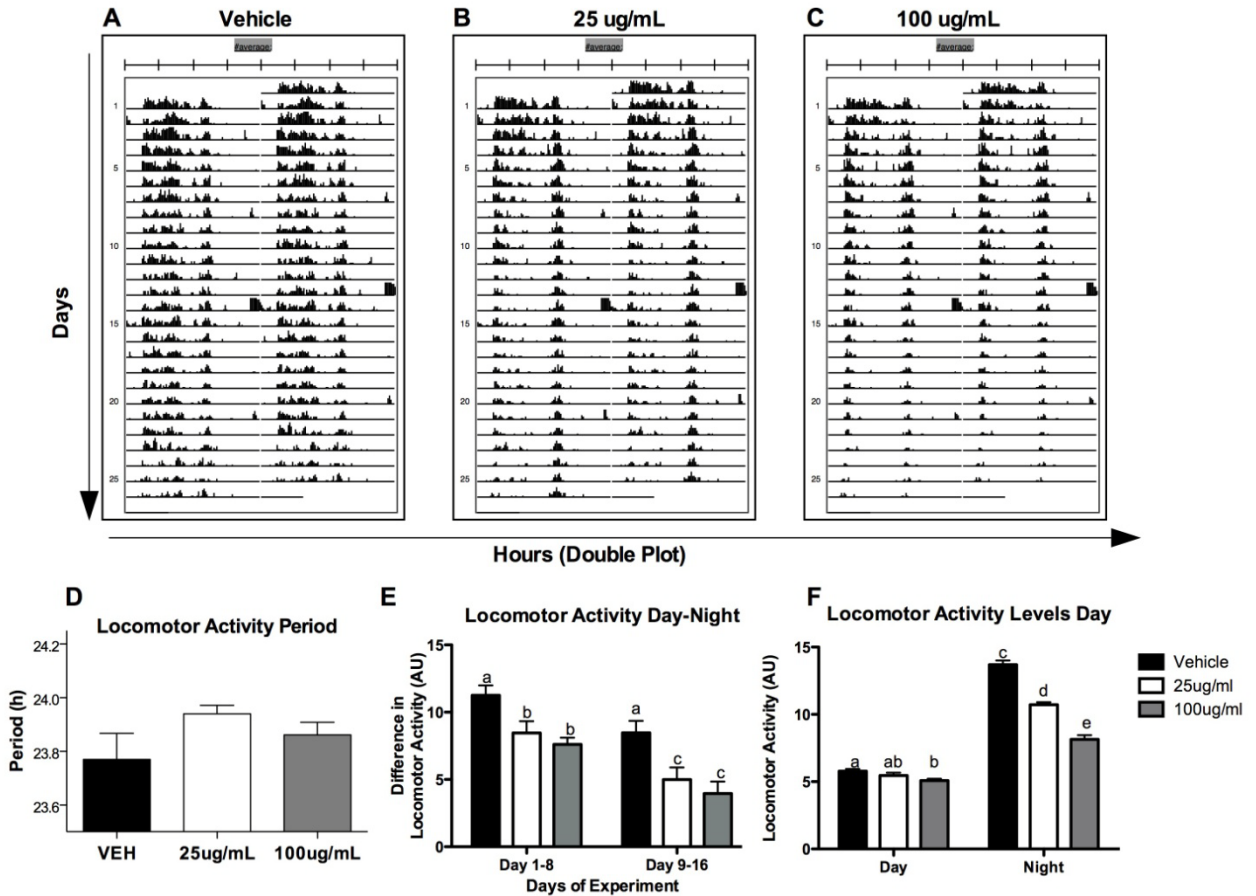


**Figure 4.1** Activity patterns of vehicle and CORT treated mice. Activity levels were recorded in the light-dark cycle through the duration of the 4 week experiment with the use of surgically implanted MiniMitters. (A) Vehicle mice showed normal activity patterns in the light-day cycle while both (B) 25  $\mu\text{g}/\text{mL}$  and (C) 100 $\mu\text{g}/\text{mL}$  doses of CORT treatment resulted in biphasic activity patterns. (E) Altered patterns in activity resulted in a decreased “day-night” locomotor activity in CORT treated mice, indicating a flatter circadian rhythm, as well as an (F) overall decrease in locomotor activity. There was no difference in (D) activity period between groups as determined by free running behavior in constant darkness during the last 3 days of the experiment. Bars with the same letter are non-statistically different from one another as determined by two-way ANOVA and plotted  $\pm\text{SEM}$ .

There was no significant difference in circadian period between groups as measured through activity and body temperature (Fig 4.1D and Supplemental 4.1D respectively).

Changes in activity levels and free running behavior suggested a change in circadian behavior that was confirmed by analysis of clock gene expression in the WAT and liver (Fig 4.2). Specifically, in the WAT rhythmic expression of *Per1* was detected ( $F(2,8)=10.12$ ;  $p=.0064$ ) in vehicle treated mice with a gradual increase from ZT 6 to ZT 12 and a significant decrease in expression at ZT 18 ( $p<.05$ ; Fig 4.2A). Rhythmicity was blunted in 25 $\mu$ g/mL CORT treated mice and severely flattened in the 100  $\mu$ g/mL group. Posthoc tests revealed a significant decrease in *Per1* gene expression between vehicle and 100 $\mu$ g/mL CORT groups at ZT 12 ( $p<.01$ ). Vehicle treated mice showed a stronger circadian pattern of *Per2* mRNA expression ( $F(2,8)=24.43$ ;  $p=.0004$ ), with posthoc tests revealing a significant increase of expression at ZT 12 ( $p<.05$ ; Fig 4.2B). Again the 100  $\mu$ g/mL CORT circadian rhythm was completely blunted and significantly lower at ZT 12 ( $p<.01$ ) compared to vehicle treated mice. Plasma CORT levels were also measured and the typical diurnal pattern was noted in the vehicle treated mice, with a peak at waking (ZT12  $F(2,9)=54.05$ ;  $p<.0001$ ) and decline through the day. In CORT treated mice, this rhythm was no longer determined by endogenous secretion, as adrenal glands in these mice have completely atrophied. As such, the endogenous rhythm in drinking drove plasma CORT levels.<sup>47</sup> In both treated groups, there was a gradual increase from ZT6 to ZT12 (25  $\mu$ g/mL  $p=.014$ ; 100  $\mu$ g/mL  $p=.057$ ); however, unlike vehicle treated mice, CORT plasma levels continued to rise in CORT treated mice through their active period as they drank water (Figure 4.2C). The increase from ZT12 to ZT18 is modest in the 25  $\mu$ g/mL group ( $p=.044$ ), and insignificant in the 100  $\mu$ g/mL group ( $p=.137$ ). The overall levels of plasma CORT were increased in the 100  $\mu$ g/mL group from

ZT6 to ZT18 ( $F(2,11)=6.754$ ;  $p=.012$ ). At ZT18 these levels were significantly higher in 100  $\mu\text{g}/\text{mL}$  mice compared to vehicle treated animals ( $p<.001$ ).

Under DD conditions, increased mRNA expression of Per1 in WAT of 100  $\mu\text{g}/\text{mL}$  CORT animals suggested a possible decoupling from the endogenous rhythm as a result of increased CORT intake (Fig 4.3). Analysis of WAT Per1 revealed a main effect of treatment ( $F(2,16)=13.21$ ;  $p<.001$ ) and subsequent posthoc test showed a significant increase in 100  $\mu\text{g}/\text{mL}$  treated mice compared to vehicle at CT18 ( $p<.001$ ). Analysis of CORT drinking behavior showed an effect of treatment ( $F(2, 17)=8.906$ ;  $p=.002$ ) and time of day ( $F(1,17)=6.709$ ;  $p=.019$ ), and an interaction ( $F(2,17)=3.801$ ;  $p=.0432$ ). Bonferroni posttests showed an increase of CORT in vehicle vs. high CORT mice at CT18 ( $p<.001$ ). These levels were lower in DD than under LD conditions, with a peak of 411  $\text{ng}/\text{mL}$  in constant darkness compared to 600  $\text{ng}/\text{mL}$  in LD for the 100  $\mu\text{g}/\text{mL}$  CORT mice. Similarly, peak levels were around 160  $\text{ng}/\text{mL}$  vs. 250  $\text{ng}/\text{mL}$  for 25  $\mu\text{g}/\text{mL}$  CORT treated mice, and 72  $\text{ng}/\text{mL}$  vs. 151  $\text{ng}/\text{mL}$  in VEH mice in DD vs. LD, respectively. Per2 expression showed a main effect of time a day ( $F(1, 18)=19.15$ ;  $p<.001$ ), as expression increased from CT12 to CT18 in all animals.

In the liver, under LD conditions we again observed rhythmic expression of Per1 mRNA in vehicle treated mice ( $F(2,11)=5.827$ ;  $p=.024$ ), as well as a rhythm in Per2 mRNA ( $F(2,10)=11.85$ ;  $p=.004$ ), with daytime difference between ZT6 and ZT12 ( $P<.05$ ) in both clock genes (Fig 4.4A and 4.4B). Expression was blunted in both CORT treated groups with a decrease in expression of Per1 at ZT 12 (VEH vs. 25  $\mu\text{g}/\text{mL}$   $p<.05$ , VEH vs. 100  $\mu\text{g}/\text{mL}$   $p<.001$ ) and Per2 at ZT 12 (VEH vs. 25  $\mu\text{g}/\text{mL}$   $p<.001$ , VEH vs. 100  $\mu\text{g}/\text{mL}$   $p<.001$ ) and ZT 18 (VEH vs. 100  $\mu\text{g}/\text{mL}$   $p<.05$ ). In DD there was no difference between groups in Per1

expression. Per2 showed a main effect of time of day ( $F(1,17)=25.48$ ;  $p<.0001$ ), and a slight effect of treatment ( $F(2,17)=4.44$ ;  $p=.028$ ).

In order to determine how CORT treatment and altered circadian rhythms impact WAT metabolism, we analyzed several genes known to play active rolls in the development of obesity and insulin resistance in control and the 100  $\mu\text{g}/\text{mL}$  CORT treated mice, by using applied biosciences PCR pathway arrays, results described in Table 4.1 and 4.2. As an active metabolic organ with constant feedback to appetite and food intake regulation to the brain, we also used an array to study the impact in the hypothalamus (Table 4.3). Given a decrease in expression, when comparing to the LD cycle, in all groups with no significant differences between groups. \*indicates  $P<0.05$ , \*\*\* $P<0.001$ .

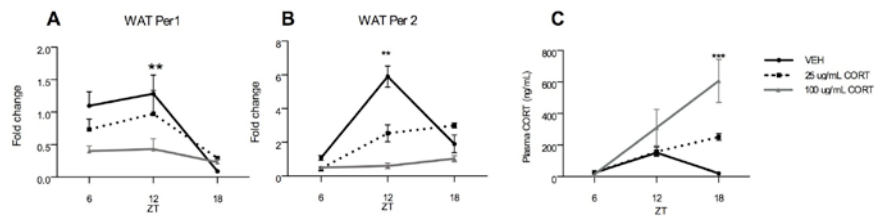


**Figure 4.2** Exogenous glucocorticoid (CORT) exposure result in decreased expression in clock genes under the light-dark cycle. White adipose tissue (WAT) from mice after 4 weeks of VEH, 25  $\mu\text{g}/\text{mL}$  or 100  $\mu\text{g}/\text{mL}$  CORT treatment was collected at 3 times periods across the light dark cycle and are shown here in zeitgeber time (ZT). Increasing doses of CORT resulted in greater reductions in the mRNA expression of (A) Per1 and (B) Per2. Results presented as fold changes and normalized to VEH ZT6. (C) Plasma CORT levels showed the typical diurnal rhythm with VEH and increased through the active dark period with both doses of CORT as they are exposed to the hormone through the day. \*\* indicates  $P<0.01$ , \*\*\*  $P<0.001$ .



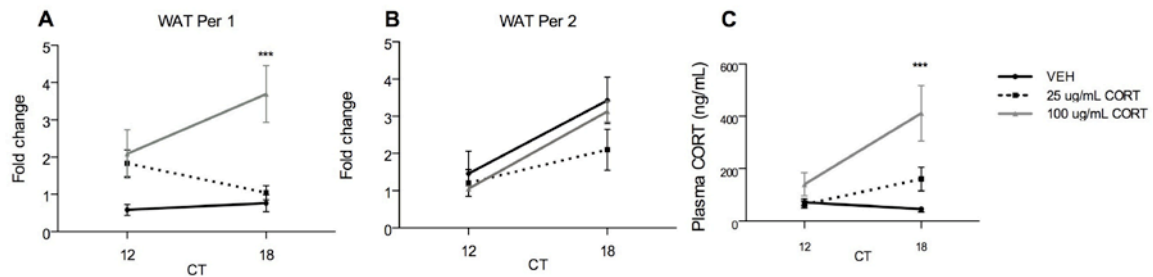


**Figure 4.3** Exogenous glucocorticoid (CORT) exposure result in differential expression in clock genes under constant darkness. White adipose tissue (WAT) from mice after 4 weeks of VEH, 25  $\mu\text{g}/\text{mL}$  or 100  $\mu\text{g}/\text{mL}$  CORT treatment were collected at the beginning or middle of their active period and are shown here in circadian time (CT). The 100  $\mu\text{g}/\text{mL}$  dose of CORT resulted in an increased expression of (A) Per1 through the active period while expression decreased in the 25  $\mu\text{g}/\text{mL}$  group and remained flat in VEH mice. (B) Per2 showed increased expression through the active period with little difference between groups. CORT results are presented as fold changes and normalized to VEH CT12. (C) While plasma CORT levels were increased in CORT treated mice due to exposure in the drinking water, levels in all groups were lower than under a light dark cycle. \*\*\* indicates  $P < 0.001$ .

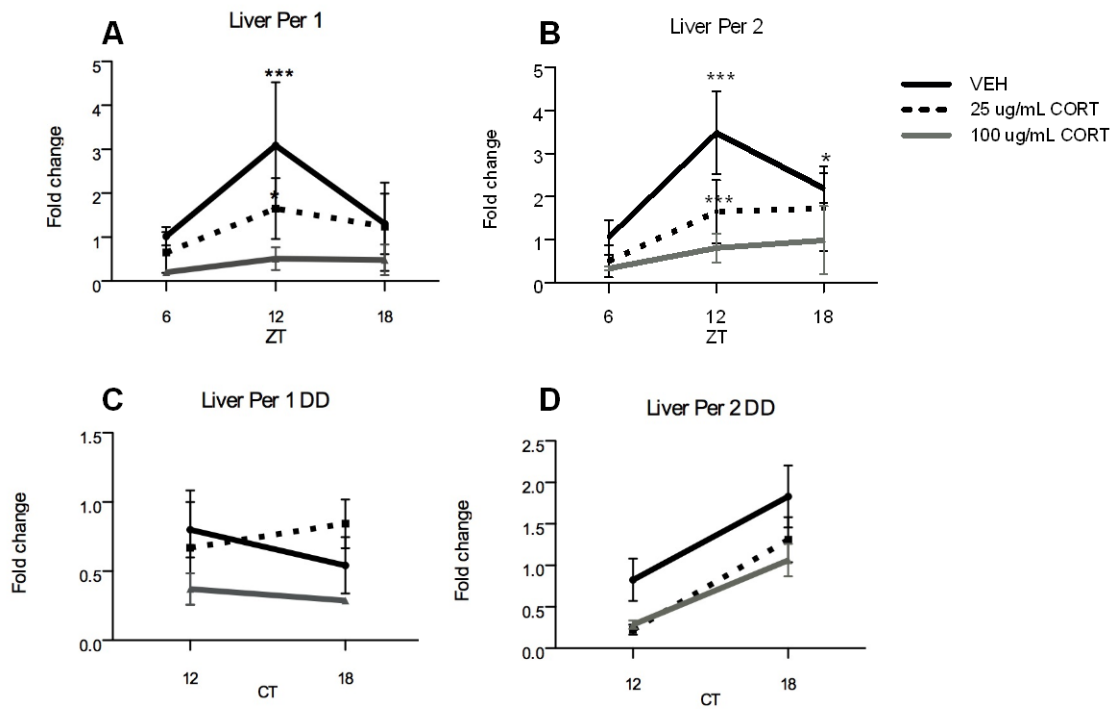


**Figure 4.4** *Exogenous corticosterone (CORT) exposure result in decreased expression of clock genes in both the light-dark cycle and under constant darkness.* Liver samples were collected following 4 weeks of VEH, 25  $\mu\text{g}/\text{mL}$  or 100  $\mu\text{g}/\text{mL}$  CORT treatment. For light-dark analysis, livers were collected at 3 time periods across the cycle and are shown here in zeitgeber time (ZT). For constant dark analysis samples were collected at the beginning or middle of their active period and are shown here in circadian time (CT). Under normal light conditions, increasing doses of CORT led to decreased and less rhythmic (A) Per1 and (B) Per2 expression. Under constant darkness levels of (C) Per1 and (D) Per2 showed a decrease

**Table 4.1** *Insulin signaling pathway-related gene expression in gonadal fat pads (white adipose tissue-WAT).* Values represent fold change ( $\pm$ SEM; n=4/group) in corticosterone treated mice compared to vehicle treated mice. Upregulation is noted in red, downregulation noted by blue. \*P<0.05.

Description	Gene Symbol	Fold Change vs. Control (Vehicle WT)
		CORT WT
Thymoma viral proto-oncogene 1	Akt1	-2.7435*
Thymoma viral proto-oncogene 2	Akt2	-2.6454*
Thymoma viral proto-oncogene 3	Akt3	-1.5594
FK506 binding protein 12-rapamycin associated protein 1	Mtor	-3.2344*
Glucose-6-phosphatase, catalytic	G6pc	-1.4525
Glucose-6-phosphatase, catalytic, 2	G6pc2	-1.6976
Growth factor receptor bound protein 2-associated protein 1	Gab1	-2.5865*
Glucokinase	Gck	-1.0112
Glycerol-3-phosphate dehydrogenase 1 (soluble)	Gpd1	-1.0147
Growth factor receptor bound protein 2	Grb2	-2.2245*
Glycogen synthase kinase 3 beta	Gsk3b	-1.9467
Hexokinase 2	Hk2	-2.4259*
Harvey rat sarcoma virus oncogene 1	Hras1	-1.6888*
Insulin-like growth factor I receptor	Igf1r	-5.5828
Insulin-like growth factor 2	Igf2	-4.1655
Insulin-like growth factor binding protein 1	Igfbp1	-1.2363
Insulin I	Ins1	-11.8433
Insulin-like 3	Insl3	-2.6272
Insulin receptor substrate 1	Irs1	-2.7721*
Insulin receptor substrate 2	Irs2	-3.6452
Jun oncogene	Jun	-2.5553
V-Ki-ras2 Kirsten rat sarcoma viral oncogene homolog	Kras	-1.8006*
Low density lipoprotein receptor	Ldlr	-1.1696
Leptin	Lep	1.6234
Mitogen-activated protein kinase kinase 1	Map2k1	2.7302
Mitogen-activated protein kinase 1	Mapk1	-1.6398
Nitric oxide synthase 2, inducible	Nos2	-2.4811
Neuropeptide Y	Npy	2.3522

**Table 4.1 Continued**

Phosphoenolpyruvate carboxykinase 2 (mitochondrial)	Pck2	-1.3319
3-phosphoinositide dependent protein kinase-1	Pdpk1	-2.145
Phosphatidylinositol 3-kinase, catalytic, alpha polypeptide	Pik3ca	-2.3925*
Phosphatidylinositol 3-kinase, catalytic, beta polypeptide	Pik3cb	-3.4366*
Phosphatidylinositol 3-kinase, regulatory subunit, polypeptide 1 (p85 alpha)	Pik3r1	-2.047
Phosphatidylinositol 3-kinase, regulatory subunit, polypeptide 2 (p85 beta)	Pik3r2	-2.5201*
Peroxisome proliferator activated receptor gamma	Pparg	-2.0049
Protein phosphatase 1, catalytic subunit, alpha isoform	Ppp1ca	-1.9979
Protein kinase C, gamma	Prkcc	-2.0118
Protein kinase C, iota	Prkci	-2.7625*
Protein kinase C, zeta	Prkcz	-3.3427*
Prolactin	Prl	-1.6976
Protein tyrosine phosphatase, non-receptor type 1	Ptpn1	-2.4683
Protein tyrosine phosphatase, receptor type, F	Ptprf	-3.4967
V-raf-leukemia viral oncogene 1	Raf1	-2.0223
Resistin	Retn	-2.0118
Ribosomal protein S6 kinase polypeptide 1	Rps6ka1	-1.4201
Harvey rat sarcoma oncogene, subgroup R	Rras	-1.7183
Src homology 2 domain-containing transforming protein C1	Shc1	-2.4133*
Solute carrier family 27 (fatty acid transporter), member 4	Slc27a4	-2.0973
Solute carrier family 2 (facilitated glucose transporter), member 1	Slc2a1	-2.2673*
Sorbin and SH3 domain containing 1	Sorbs1	-1.4959
Son of sevenless homolog 1 (Drosophila)	Sos1	-1.7124*
Sterol regulatory element binding transcription factor 1	Srebf1	-3.3601*

Values represent average fold change ( $\pm$ SEM; n=4/group) in response to corticosterone treatment (100  $\mu$ g/mL) mice compared to vehicle (1% ethanol) treated mice. Upregulation with a fold change greater than 2 is noted in red, downregulation with a fold change less than .5 noted by blue. All animals were euthanized at ZT6. \*P<0.05.

**Table 4.2** Obesity-related gene expression in gonadal fat pads (white adipose tissue-WAT).

Description	Gene Symbol	Fold Change vs Control-Vehicle WT
		CORT WT
Adenylate cyclase activating polypeptide 1	Adcyap1	0.6276
Adenylate cyclase activating polypeptide 1 receptor 1	Adcyap1r1	8.1004*
Adiponectin, C1Q and collagen domain containing	Adipoq	0.3271*
Adiponectin receptor 1	Adipor1	0.8959
Adiponectin receptor 2	Adipor2	0.3547*
Adrenergic receptor, alpha 2b	Adra2b	0.5205
Adrenergic receptor, beta 1	Adrb1	0.5502*
Agouti related protein	AgRP	0.4065*
Apolipoprotein A-IV	Apoa4	3.7877
Attractin	Atrn	0.698*
Brain derived neurotrophic factor	Bdnf	2.3316
Bombesin-like receptor 3	Brs3	0.8149
Complement component 3	C3	0.5657
Calcitonin/calcitonin-related polypeptide, alpha	Calca	0.7638
Calcitonin receptor	Calcr	0.6276
CART prepropeptide	Cartpt	0.6276
Cholecystokinin	Cck	1.3299
Cholecystokinin A receptor	Cckar	0.0891
Colipase, pancreatic	Clps	0.6276
Cannabinoid receptor 1 (brain)	Cnr1	0.4724*
Ciliary neurotrophic factor receptor	Cntfr	0.2591*
Carboxypeptidase D	Cpd	0.8244
Carboxypeptidase E	Cpe	0.5696
Corticotropin releasing hormone receptor 1	Crhr1	0.6276
Dopamine receptor D1A	Drd1a	0.3348
Dopamine receptor 2	Drd2	0.6276
Galanin	Gal	0.5979
Galanin receptor 1	Galr1	0.6276
Glucagon	Gcg	0.1014
Glucagon receptor	Gcgr	1.1132
Growth hormone	Gh	0.6276
Growth hormone receptor	Ghr	0.813
Ghrelin	Ghrl	0.6063*

**Table 4.2 Continued**

Growth hormone secretagogue receptor	Ghsr	0.6932
Glucagon-like peptide 1 receptor	Glp1r	0.6276
Melanin-concentrating hormone receptor 1	Mchr1	1.3896
Gastrin releasing peptide	Grp	0.6276
Gastrin releasing peptide receptor	Grpr	0.6276
Hypocretin	Hcrt	0.8301
Hypocretin (orexin) receptor 1	Hcrtr1	0.7327
Histamine receptor H1	Hrh1	0.8282
5-hydroxytryptamine (serotonin) receptor 2C	Htr2c	0.6276
Islet amyloid polypeptide	Iapp	0.6276
Interleukin 1 alpha	Il1a	0.6379
Interleukin 1 beta	Il1b	0.4868
Interleukin 1 receptor, type I	Il1r1	0.8594
Interleukin 6	Il6	0.4542
Interleukin 6 receptor, alpha	Il6ra	0.7603
Insulin I	Ins1	0.6276
Insulin II	Ins2	0.6996
Insulin receptor	Insr	0.5193*
Leptin	Lep	2.6172
Leptin receptor	Lepr	0.3197*
Melanocortin 3 receptor	Mc3r	0.6276
Neuromedin B	Nmb	0.3758*
Neuromedin B receptor	Nmbr	0.8093
Neuromedin U	Nmu	0.6483
Neuromedin U receptor 1	Nmur1	0.4959
Neuropeptide Y	Npy	1.6717
Neuropeptide Y receptor Y1	Npy1r	145.479
Nuclear receptor subfamily 3, group C, member 1	Nr3c1	0.4199*
Neurotrophic tyrosine kinase, receptor, type 2	Ntrk2	0.563*
Neurotensin	Nts	0.9189
Neurotensin receptor 1	Ntsr1	0.6276
Opioid receptor, kappa 1	Oprk1	0.6233
Opioid receptor, mu 1	Oprm1	0.3332*
Sigma non-opioid intracellular receptor 1	Sigmar1	1.2209
Pro-opiomelanocortin-alpha	Pomc	0.6948*
Peroxisome proliferator activated receptor alpha	Ppara	0.3131*
Peroxisome proliferator activated receptor gamma	Pparg	0.5592

**Table 4.2 Continued**

Peroxisome proliferative activated receptor, gamma, coactivator 1 alpha	Ppargc1a	0.3572*
Prolactin releasing hormone receptor	Prlhr	0.6276
Protein tyrosine phosphatase, non-receptor type 1	Ptpn1	0.7709
Peptide YY	Pyy	0.6276
Receptor (calcitonin) activity modifying protein 3	Ramp3	1.022
Sortilin 1	Sort1	0.6604
Somatostatin	Sst	0.6276
Somatostatin receptor 2	Sstr2	0.7029
Thyroid hormone receptor beta	Thrb	0.5169*
Tumor necrosis factor	Tnf	0.4627
Thyrotropin releasing hormone	Trh	0.7429
Urocortin	Ucn	0.6276
Uncoupling protein 1 (mitochondrial, proton carrier)	Ucp1	0.6276
Zinc finger protein 91	Zfp91	0.6742

Values represent average fold change ( $\pm$ SEM; n=4/group) in response to corticosterone treatment (100  $\mu$ g/mL) mice compared to vehicle (1% ethanol) treated mice. Upregulation with a fold change greater than 2 is noted in red, downregulation with a fold change less than .5 noted by blue. All animals were euthanized at ZT6. \*P<0.05.

**Table 4.3** Obesity related gene expression in in the hypothalamus of corticosterone (CORT) and vehicle treated mice.

Description	Gene Symbol	Fold Change vs 1% WT
		100 WT
Adenylate cyclase activating polypeptide 1	Adcyap1	1.1856
Adenylate cyclase activating polypeptide 1 receptor 1	Adcyap1r1	1.4132
Adiponectin receptor 1	Adipor1	-1.0938
Adiponectin receptor 2	Adipor2	1.4035
Adrenergic receptor, alpha 2b	Adra2b	<b>2.8992</b>
Adrenergic receptor, beta 1	Adrb1	-1.1014
Agouti related protein	Agrp	<b>13.823</b>
Apolipoprotein A-IV	Apoa4	<b>4.5757</b>
Brain derived neurotrophic factor	Bdnf	1.5881
Complement component 3	C3	1.4231
Calcitonin/calcitonin-related polypeptide, alpha	Calca	1.8886
CART prepropeptide	Cartpt	1.9084
Cholecystokinin	Cck	<b>2.4044</b>
Cholecystokinin A receptor	Cckar	-1.5397
Cannabinoid receptor 1 (brain)	Cnr1	-1.1629
Carboxypeptidase D	Cpd	-1.19
Galanin receptor 1	Galr1	-1.2666
Glucagon	Gcg	1.9894
Glucagon receptor	Gcgr	1.9894
Growth hormone	Gh	1.0393
Growth hormone receptor	Ghr	1.6215
Growth hormone secretagogue receptor	Ghsr	<b>2.6494</b>
Hypocretin	Hcrt	-1.3159
Hypocretin (orexin) receptor 1	Hcrtr1	1.1612
5-hydroxytryptamine (serotonin) receptor 2C	Htr2c	-1.4993**
Islet amyloid polypeptide	Iapp	-1.4006
Interleukin 1 beta	Il1b	<b>4.0065</b>
Interleukin 1 receptor, type I	Il1r1	<b>2.1347*</b>



**Table 4.3 Continued**

Insulin I	Ins1	1.9894
Insulin II	Ins2	1.9894
Leptin receptor	Lepr	2.3064*
Melanocortin 3 receptor	Mc3r	1.8777
Neuromedin B	Nmb	2.1845
Neuropeptide Y	Npy	2.3631
Neuropeptide Y receptor Y1	Npy1r	1.5699
Neurotrophic tyrosine kinase, receptor, type 2	Ntrk2	1.3494
Neurotensin	Nts	-2.0223*
Opioid receptor, mu 1	Oprm1	2.0739
Pro-opiomelanocortin-alpha	Pomc	7.5371
Peroxisome proliferator activated receptor alpha	Ppara	1.2275
Peroxisome proliferator activated receptor gamma	Pparg	2.0739
Peptide YY	Pyy	7.6954
Peroxisome proliferative activated receptor, gamma, coactivator 1 alpha	Ppargc1a	-1.4499*
Receptor (calcitonin) activity modifying protein 3	Ramp3	1.6309
Somatostatin	Sst	1.2475
Somatostatin receptor 2	Sstr2	1.1308
Thyrotropin releasing hormone	Trh	-1.4685
Urocortin	Ucn	1.9462
Uncoupling protein 1 (mitochondrial, proton carrier)	Ucp1	1.9894

Whole hypothalamus was collected by tissue punch from whole fresh frozen brain. Values represent average fold change ( $\pm$ SEM; n=4/group) in response to corticosterone treatment (100  $\mu$ g/mL) mice compared to vehicle (1% ethanol) treated mice. Upregulation with a fold change greater than 2 is noted in red, downregulation with a fold change less than .5 noted by blue. All animals were euthanized at ZT6. \*P<0.05 and \*\*P<0.01.

In order to determine how CORT treatment impact WAT metabolism, and if there was a circadian component, we analyzed several genes known to play active rolls in the development of obesity and insulin resistance in control and the 100  $\mu\text{g}/\text{mL}$  CORT treated mice, using SABiosciences RT<sup>2</sup>PCR pathway arrays, results described in Table 4.1 and 4.2. As an active metabolic organ with constant feedback to appetite and food intake regulation to the brain, we also used an array to study the impact in the hypothalamus (Table 4.3). Given a decrease in PPar $\alpha$  in the array (Table 2) and its known intersection with Per2, we analyzed PPar $\alpha$  to great detail across the light-dark cycle. As with Per2, CORT treatment resulted in decreased expression of PPar $\alpha$  most notably at ZT12 ( $F(2,16)=10.09$ ,  $p=0.0015$ ; Fig 4.5C), which coincided with the peak of Per2 expression in VEH mice. HNF4 $\alpha$  in the liver was also analyzed given its interaction with Per2. In CORT treated mice, there was also decreased expression at ZT18 ( $F(2, 12)=6.274$ ,  $p0.0136$ ; Fig 4.5F), which coincided with a significant decrease of Per2 expression in 100  $\mu\text{g}/\text{mL}$  CORT treated mice.

Although circulating levels of CORT are increased in treated mice, it is possible through actions of regulatory enzyme levels that the active level reaching receptors is not greatly varied. In WAT, 11 $\beta$ HSD1 is increased at ZT6 ( $p<0.001$ ) but decreased at ZT12 ( $p<0.01$ ), and ZT18 (not to significance) as determined by 2 way ANOVAs and Bonferroni posttest (time of day ( $F(2, 16)=67.95$ ,  $p<0.0001$ ; Fig 4.5A). There is a slight decrease of 11 $\beta$ HSD2 in WAT at ZT12 but not to significance (Fig 4.5B). In the liver, CORT treated mice show an increased in 11 $\beta$ HSD1 expression at the beginning of the dark cycle with decrease at ZT18, but not significantly greater than controls (Fig 4.5D). 11 $\beta$ HSD2 expression in the liver of VEH and control mice do not vary greatly at ZT6 or ZT12, but levels escalate greatly in VEH

mice at ZT18 ( $p < 0.01$ ; Fig 4.5E) as determined by Bonferroni after a main effect in treatment ( $F(1, 17) = 7.447$ ;  $p = 0.0143$ ).

Given that all studies were conducted in whole adipose tissue we stained WAT sections for F4/80, a membrane protein present in mature macrophages in mice. Staining revealed a large population of macrophages in 100  $\mu\text{g/mL}$  CORT treated mice (Supplemental Fig 4.2) compared to VEH mice.

In CORT treated mice, increased circulating leptin and increased mRNA expression (t test,  $p = 0.016$ ) of the leptin receptor in the hypothalamus in conjunction with abnormal activity would suggest irregular feeding patterns and food intake amounts that could account for their metabolic abnormalities. However, when CORT treated mice were pair fed (food intake was limited to that of control mice), they continued to gain a comparable amount of weight to CORT treated mice fed *ad lib*, both reaching a significantly greater weight change at week 4 compared to VEH *ad lib* fed mice ( $F(2,11) = 6.678$ ;  $p = 0.0167$ ; Fig 4.6), suggesting that the obese phenotype was independent of food intake.

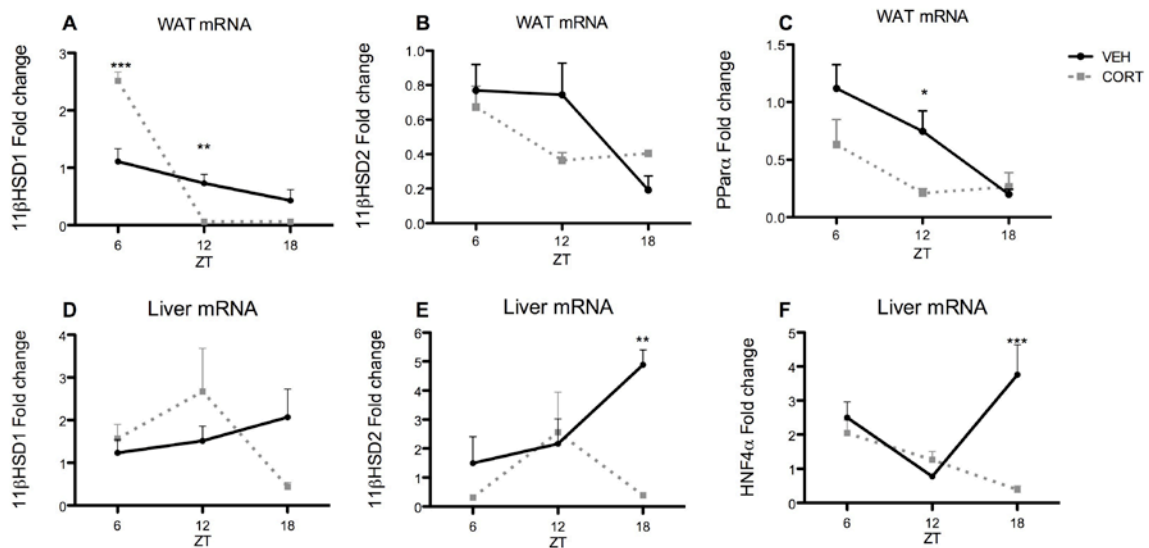


**Figure 4.5** Diurnal mRNA expression in white adipose tissue (WAT) and liver of control and 100 $\mu$ g/mL CORT treated mice. 4 weeks of chronic high doses of CORT treatment alters the pattern and degree of expression of (A) 11 $\beta$ HSD type 1 and (B) type 2 in the WAT, as well as in the liver (D-E, respectively). (C) PPar $\alpha$  expression in WAT is decreased at ZT6 and significantly so at ZT12 while HNF4 $\alpha$  decreased through the day to significance at ZT18 (n=3-4/group and time point). Fold changes of gene expression ( $\pm$ SEM) were determined by qRT-PCR. Values represent the level of normalized gene expression relative to the mean, overall normalized gene expression to ZT6. Significant peak levels of expression in VEH to 100 $\mu$ g/mL CORT \* P<0.05 and \*\*P<0.01, \*\*\*P<0.001, by two way ANOVA and Bonferroni posttest.

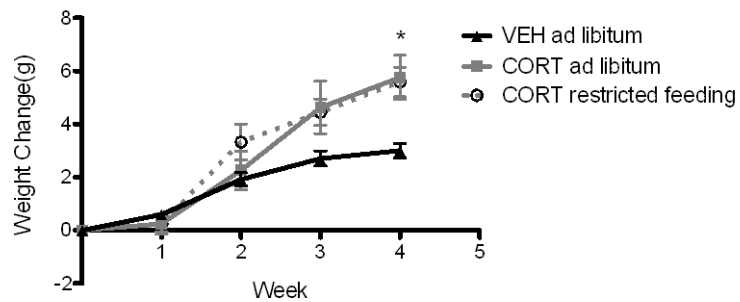
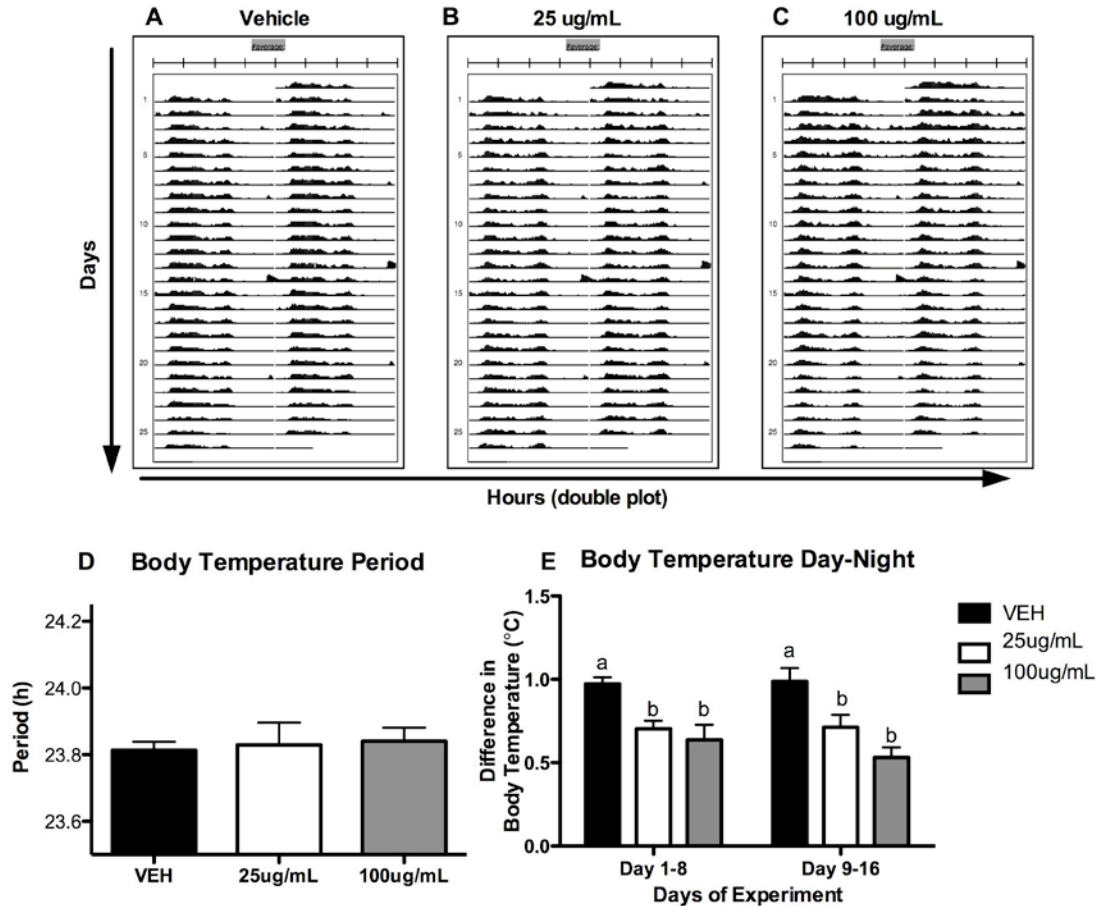
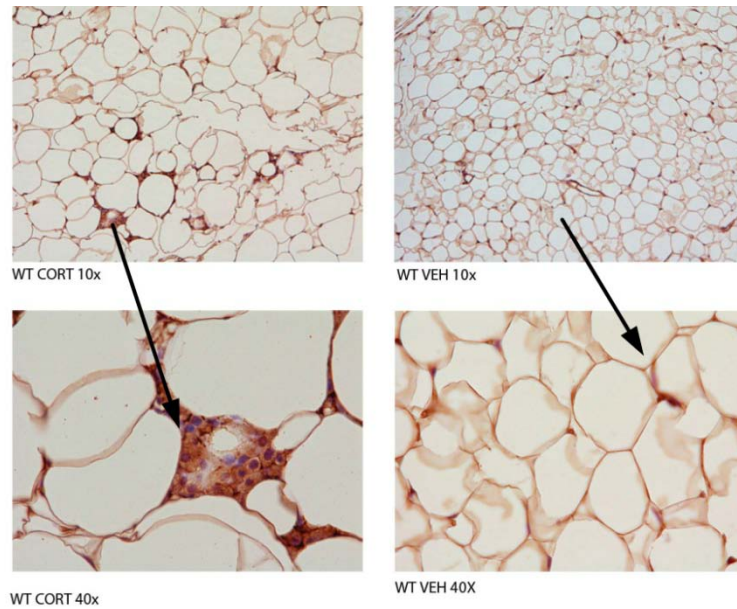


**Figure 4.6** *Clamped food intake in CORT treated mice does not prevent weight gain.* CORT treated mice were pair fed for the duration of treatment. Despite equivalent food intake to VEH mice (n=4/group) pair fed CORT mice (restricted feeding) continued to gain weight with comparable levels as CORT *ad lib* mice. \* P<0.05.



**Supplemental Figure 4.1** *Body temperature rhythms of vehicle and CORT treated mice.*

Body temperature was recorded in the light-dark cycle through the duration of the 4 week experiment with the use of surgically implanted MiniMitters. (A) Vehicle mice showed normal temperature rhythms in the light-day cycle while both (B) 25  $\mu\text{g}/\text{mL}$  and (C) 100  $\mu\text{g}/\text{mL}$  doses of CORT treatment resulted in slight biphasic rhythms. (E) “Day minus light” revealed a decreased body temperature amplitude in CORT treated mice emphasizing a flatter rhythm in 25  $\mu\text{g}/\text{mL}$  and 100  $\mu\text{g}/\text{mL}$  CORT mice. There was no difference in (D) body temperature period between groups as determined by free running behavior in constant darkness during the last 3 days of the experiment. Bars with the same letter are non statistically different from one another as determined by two-way ANOVA and plotted  $\pm\text{SEM}$ .



**Supplemental Figure 4.2** *Chronic CORT treatment results in macrophage infiltration.*

F4/80 stain of WAT reveals an inflammatory response and macrophage penetration after 4 weeks of chronic CORT treatment. Representative photos shown here from n=5 mice/group killed at ZT6. Top photos show at 10x, bottom photos at 40x.

## Discussion

In this set of studies we showed that chronic CORT treatment resulted in an altered pattern in daily activity with an increasingly biphasic pattern with one bout of activity at lights off, a bout of rest, and a final bout of activity before lights on. This separation in activity is clear in the 25  $\mu\text{g}/\text{mL}$  group, but more pronounced in 100  $\mu\text{g}/\text{mL}$  CORT treated mice. In addition, there was an obvious decrease in the amplitude of circadian rhythmicity in CORT treated animals, as measured by a smaller difference in day vs. night activity. When mice were placed in DD, they retained a free-running circadian activity rhythm similar to that of VEH mice. These changes in activity levels were accompanied by decreased clock gene expression in both white adipose tissue (WAT) and liver. This effect of expression was larger in 100  $\mu\text{g}/\text{mL}$  CORT treated mice compared to the 25  $\mu\text{g}/\text{mL}$  group. Constant darkness revealed a possible decoupling effect of CORT in that we observed an increase in Per1 mRNA expression in WAT despite the presence of light; this increase was not present in VEH mice. Per2 mRNA expression did not vary greatly between groups in WAT, but comparing expression levels with those in the light-dark cycle, we observed increased expression in CORT animals. Again, this pattern of results suggests that, in the absence of light cues, high circulating CORT can entrain clock gene rhythms in the WAT. Interestingly, this effect of CORT was not present in the liver, and indeed expression of both Per1 and Per2 mRNA were decreased in all groups. CORT levels, even in CORT treated mice that received CORT in their drinking water, showed decreased plasma CORT compared to the same time points under the light-dark cycle. This decrease in expression in untreated mice is to be expected given the decrease in rhythmic secretion from adrenals noted in constant dark conditions<sup>4</sup>, but it is unclear how the drinking rhythm may be altered in DD in treated mice.



Molecular studies have shown that occupied GC receptors bind to the glucocorticoid-responsive element (GRE) in the regulatory regions of many genes, thereby regulating target gene transcription.<sup>205</sup> A GRE is located in the promoter region of *Per1* and is reportedly involved in *Per1* expression, which allows GCs to directly interact with *Per1* as highlighted in an in vivo study showing *Per1* mRNA expression to be induced as the result of acute stress.<sup>206</sup> Therefore, upregulation of GCs induced by overactivation of the HPA axis might directly affect the circadian expressions of core clock genes in the periphery. Increases in circulating corticosterone levels and subsequent shifts in gene expression in mouse models of chronic mild stress<sup>203</sup> not only affirm the ability of GCs to entrain peripheral organs, but also in the case of the later study, also link these changes to metabolic irregularities.

Increased circulation of GCs in the way of persistent stimulation of the HPA axis by various stressors can cause metabolic disorders, such as insulin resistance, hypertension, and dyslipidemia.<sup>47,149,207</sup> These metabolic disturbances are also induced by dysregulation of the clock system as noted in Chapter 3, and by others.<sup>146,208</sup> It remains to be determined whether modulation of the HPA axis leads to metabolic problems through the disruption of the clock system, or if these systems influence the same metabolic pathways independently. Numerous molecules, such as the *PPar $\alpha$*  and *PPar $\gamma$* , *PGC-1 $\alpha$* , and *G6P*, play crucial roles as mediating metabolism and respond to modulations of both the core clock and GCs.<sup>146</sup>

Most studies exploring the interaction between the clock system and GC entrainment focus on metabolism on the level of the liver. Given the suggested decoupling effect of *CORT* during constant darkness as reported here, we explored in depth the mRNA expression of various genes known to be affected in pathways of obesity and insulin resistance, with attention given to *PPar $\alpha$*  as it has been shown to control proadipogenic

activity in WAT and modulated by Per2; we also made note of HNF-4 $\alpha$  in the liver as it is also modulated by Per2 and showed to be markedly affected by circadian disruption as observed in Chapter 3.<sup>182,209</sup> Analysis of PPar $\alpha$  across the light-dark system in CORT treated mice revealed a decrease consistent with decreased expression of Per2. This pattern was also the case for HNF-4 $\alpha$  expression in the liver, suggesting that altered expression of Per2 is required for CORT induced perturbations of metabolism-related gene expression to some degree in both the WAT and liver. In this way we show increased CORT acts together with the clock system, to perturb the WAT and liver leading to the onset of metabolic disturbances.

Since CORT levels can be varied on the tissue level through enzymatic regulation, we examined levels of 11 $\beta$ HSD type1 and type2 in the liver and WAT. Previously it was noted that CORT treatment resulted in increased protein expression of 11 $\beta$ HSD1 in the WAT but a decrease in liver, but that was only measured at ZT4-5. In the current study we looked at 3 different time points and saw changes in expression in both the liver and WAT across the day in both CORT and VEH treated mice. In WAT 11 $\beta$ HSD expression regulates CORT in a manner consistent with WAT Per clock gene expression. In CORT treated mice, 11 $\beta$ HSD1 increased expression at ZT6, and subsequently further increased presence of active CORT, resulted in the nadir of both Per1 and Per2 mRNA expression. Conversely, increased expression of 11 $\beta$ HSD2 in VEH mice at ZT12 corresponds to the peak of Per2 mRNA expression in WAT. Taken together 11 $\beta$ HSD and Per clock gene expression further suggest a CORT induced suppression of clock genes in this model. In that regard, GR expression needs to be measured to determine if levels in CORT treated mice are overall downregulated at this point of treatment and the subsequent downregulation could possibly result in the

decreased clock gene expression, which could be the case as suggested by a glucocorticoid receptor resistance (GCR) model.<sup>210</sup>

Several recent studies have emphasized that rhythmic abnormalities affect energy homeostasis, as well as glucose and lipid metabolism,<sup>179,211,212</sup> and in turn excess energy in the way of increased food intake through a high fat diet can also lead to rhythmic abnormalities<sup>16</sup>, perhaps also through increases in CORT.<sup>136,199</sup> While few studies have looked at GC induced shifts in clock gene expression in WAT, recent studies have shown that adipocyte-specific deletion of the core molecular clock component *Arntl* (also known as *Bmal1*) results in obesity in mice, with a shift in the diurnal rhythm of food intake, a result not seen in gene disruption in hepatocytes alone.<sup>196,121</sup> Additionally, it has been shown that circadian modulation of lipolysis rates regulate the availability of lipid-derived energy during the day, suggesting a role for WAT clocks in the regulation of energy homeostasis.<sup>181</sup> Taking these previous reports and our present results together, increased circulation of GCs through HPA axis activation under chronic stress<sup>4</sup> or in states of excess nutrition<sup>214</sup> may contribute to alterations in circadian clock gene expressions in the liver and WAT.

Beyond changes in clock genes and lipogenic factors, PCR array analysis in WAT also revealed marked decreases in many genes involved in the insulin-signaling pathway, a finding not surprising, given the increases in weight gain, adiposity, and increased levels of insulin, leptin and triglycerides in circulation.<sup>47</sup> Given that all analysis of WAT came from full tissue, rather than adipocyte culture, and the ability of macrophages to infiltrate adipose tissue and produce proinflammatory cytokines that alter organ function,<sup>215</sup> their presence should be kept in mind for future studies.

As an active metabolic organ, WAT plays a large role in the fast-fed cycle and is able to activate and deactivate anorectic and orexigenic neurons. For this reason we also ran a PCR array in hypothalamic tissue. However, apart from neurotensin, a peptide that targets anorexigenic neuropeptides, MSH and CART, we saw no significant changes in gene expression.<sup>216,217</sup> For this reason we ran a pair feeding study in order to clamp the food intake of CORT treated mice. After 4 weeks of equivalent food intake to VEH mice, CORT pair fed mice gained weight at a comparable level to CORT *ad lib* mice. This finding suggest that calories are not the final determinate in weight gain in CORT treated mice and could instead be the result of asynchrony of metabolic mediators.

In summary, to our knowledge, this is the first report to show chronic GCs exposure can alter clock gene expression in both the WAT and liver. Thus overactivation of the HPA-axis is likely to play an important role in the underlying mechanism of circadian induced obesity. The dysregulation of clock gene expression and subsequent loss of rhythmicity in genes regulating metabolism might trigger metabolic disturbances in states of increased GC exposure such as chronic stress.

## **Chapter 5: Cannabinoid CB<sub>1</sub> Receptor deficient mice are resistant to metabolic dysregulation following both circadian disruption and chronic glucocorticoid administration**

### **Abstract**

In mammals, including humans, disruptions in circadian (daily) rhythms are related to metabolic dysregulation, such as obesity and type II diabetes. The mechanisms by which circadian disruption modulates metabolic dysregulation are not well characterized; however, recent studies by our group suggest that consequences of glucocorticoid (GC) secretion and regulation may be involved. In the current set of studies we demonstrate that male mice exposed to a 10 h light: 10 h dark (LD10) circadian cycle or a constant high dose of corticosterone (CORT) in the drinking water, both of which create profound dysregulation of endogenous circadian processes including glucocorticoid regulation, and develop symptoms of metabolic syndrome, as evidenced by increased body weight gain, elevated triglyceride levels, hyperleptinemia and hyperinsulinemia. Interestingly, mice lacking the cannabinoid CB<sub>1</sub> receptor were protected against all of these changes in metabolic function, indicating that endocannabinoid signaling is required for circadian disruption to promote obesity and metabolic syndrome possibly through glucocorticoid regulation. These data build upon previous findings that indicate the endocannabinoid system is required for diet-induced obesity, but further suggest that this system plays a much broader role in the regulation of metabolic processes, as well as acting as a mediator of changes in metabolic function in response to an array of stimuli, and not just diet composition.

## **Rationale**

In mammals, circadian (daily) rhythms in physiology and behavior are driven by a brain clock located in the suprachiasmatic nucleus (SCN) of the hypothalamus, and synchronized to the environmental light/dark (LD) cycle.<sup>218</sup> It is important to note that the central clock regulates myriad “peripheral” oscillators in the rest of the brain, and periphery, including organs such as the heart, lungs, and liver, through glucocorticoids, among potential other entrainers as highlighted in Chapter 3 and 4. As such, it is thought the circadian clock regulates physiology and behavior both by the central clock, and through diffusible entraining signals that regulate local clocks in the periphery.

Our lab has modeled the metabolic effects associated with disruptions of the circadian system in a noninvasive manner as described in Chapter 3, by chronically housing male mice in 20-h light/dark (LD) cycles, incongruous with their endogenous ~24 hour circadian period. In terms of metabolic effects, it was demonstrated that chronic circadian disruption (CD) results in altered body temperature rhythms, increased weight gain, and elevated levels of plasma insulin and leptin.<sup>166</sup> These data are consistent with the increased rates of obesity and metabolic syndrome in individuals with disrupted circadian cycles.<sup>176</sup> Further in Chapters 3 and 4, disruption and subsequent metabolic dysfunction were found to occur in conjunction with blunted rhythms of clock genes in the liver and WAT and circulating levels of CORT. When CORT levels were increased, and plasma CORT rhythms altered, as shown in Chapter 4, mice continued to gain weight and showed clear changes in their circadian rhythms. In both cases, the mechanisms by which this shift in metabolic function that occurred following CD by light and chronic CORT, are not understood.

Recent work has led us to hypothesize that the endocannabinoid (eCB) system may play a role in CD and CORT induced metabolic dysregulation. The eCB system is a lipid signaling system primarily composed of the endocannabinoids, anandamide (AEA) and 2-arachidonylglycerol (2-AG), which exert their effects through activation of CB<sub>1</sub> and CB<sub>2</sub> cannabinoid receptors.<sup>219</sup> Activation of the CB<sub>1</sub> receptor results in increased appetite, insulin resistance, and increased hepatic lipogenesis, suggesting involvement of the endocannabinoid/CB<sub>1</sub> receptor system in obesity and its metabolic consequences.<sup>121,167</sup> These findings are consistent with the distribution of CB<sub>1</sub> receptors throughout neural feeding centers, and in peripheral tissues such as the liver, pancreas and adipose.<sup>121,167</sup> CB<sub>1</sub> receptor-deficient mice, or mice receiving treatment with CB<sub>1</sub> receptor antagonists, are resistant to diet-induced obesity and display improved metabolic measurements when subjected to high-fat feeding.<sup>121</sup> Similar findings have been reported in humans with the CB<sub>1</sub> receptor antagonist Rimonabant.<sup>150</sup> Although the role of the eCB system is established in models of diet-induced obesity, its role in other models of metabolic dysregulation has not been explored. Apart from its role in energy homeostasis, the eCB system was a promising choice since it has been shown to regulate the adaptive stress response, and eCBs are released upon glucocorticoid release.<sup>150,113</sup> Given that the eCB system within the periphery<sup>222</sup> and limbic and feeding centers in the brain<sup>223</sup> exhibits circadian fluctuations, the objective of the present study was to explore the role of eCB signaling in contributing to the metabolic profile of mice exposed to CD in the way of disruption of light cues, as well as through chronic exogenous CORT.

## **Experiment design**

### **Experiment 1**

This portion of the study involved several cohorts of animals. For the CD through shortened circadian day, 20 mice were initially studied, 5  $CB_1R^{-/-}$  mice placed under LD12 or LD10; and 5 WT mice places under LD12 or LD10 conditions (n=5/group). After 8 weeks of shift a few mice died leaving n=3-5/group.

### **Experiment 2**

The majority of studies in this chapter were run in the CORT drinking water model given its shorter duration, which resulted in the loss of few  $CB_1R^{-/-}$  mice through the duration of a protocol. In total 4 cohorts of mice (each ranging from 3-6/group and treatment) were run to explore the interaction between the endocannabinoid system and circulating levels of CORT on metabolism.

## **Results**

### **Experiment 1**

There was a significant interaction between circadian cycle and genotype on body weight [F (21, 91) = 2.91,  $p < 0.0005$ ; Fig. 5.1]. Post hoc analysis revealed wild-type mice exposed to CD exhibited significant increases in body weight relative to both wild-type mice and  $CB_1R^{-/-}$  mice on a 12:12 cycle at every week measured ( $p < 0.05$  for every week).  $CB_1R^{-/-}$  mice exposed to CD did not exhibit any increased weight gain, relative to 12:12 wild-type mice ( $p > 0.05$  for every week, except week 3). However, body weight of  $CB_1R^{-/-}$  mice



exposed to CD was also not significantly different than wild-type mice exposed to CD, indicating that a loss of CB<sub>1</sub> receptors only attenuated, but did not block, the effects of CD on weight gain. There was also no significant difference in body weight at any time point between wild-type and *CB1R*<sup>-/-</sup> mice on a 12:12 cycle.

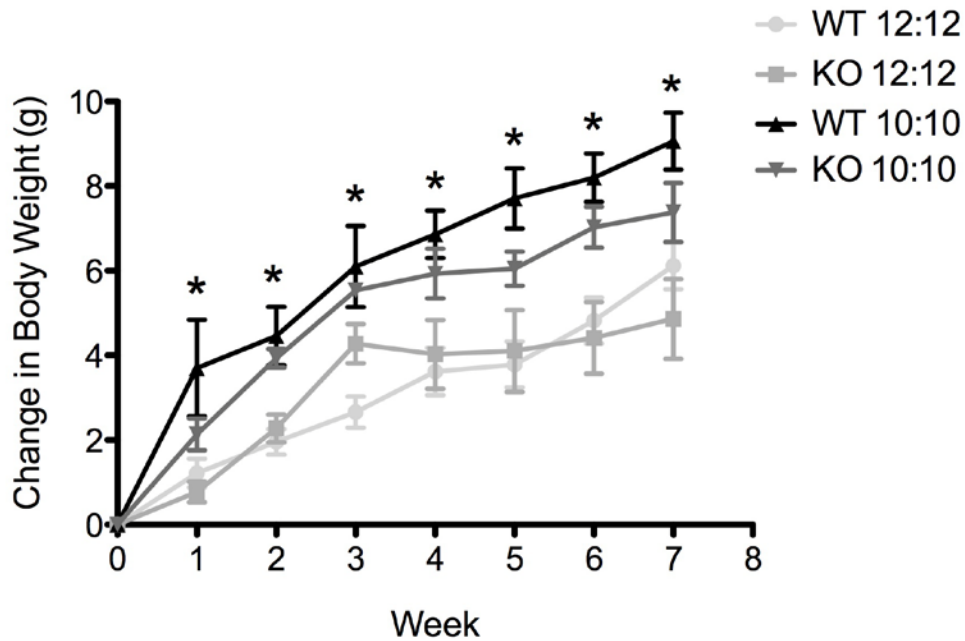


**Figure 5.1.** Circadian disruption causes an increase in body weight gain that is attenuated in CB<sub>1</sub> receptor deficient mice. Disruption of circadian cycles, through housing wild-type (WT) mice in a 10h:10h light/dark cycle (10:10) results in a progressive increase in weight gain, relative to WT mice housed in a standard 12h:12h light/dark cycle (12:12). CB<sub>1</sub> receptor knockout mice (KO) exhibit an attenuation in the weight gain induced by circadian disruption in a 10:10 light/dark cycle relative to WT mice undergoing circadian disruption. \* denotes a significant difference ( $p < 0.05$ ) in 10:10 WT mice relative to 12:12 WT and KO mice. 10:10 KO mice represented an intermediate phenotype as they were not significantly different from either the 10:10 WT mice or the 12:12 WT or KO mice at any time point (except at week 3 in which the 10:10 KO mice had significantly increased body weight relative to the 12:12 WT mice). Data are displayed as mean  $\pm$  SEM;  $n = 4-5$  / condition.

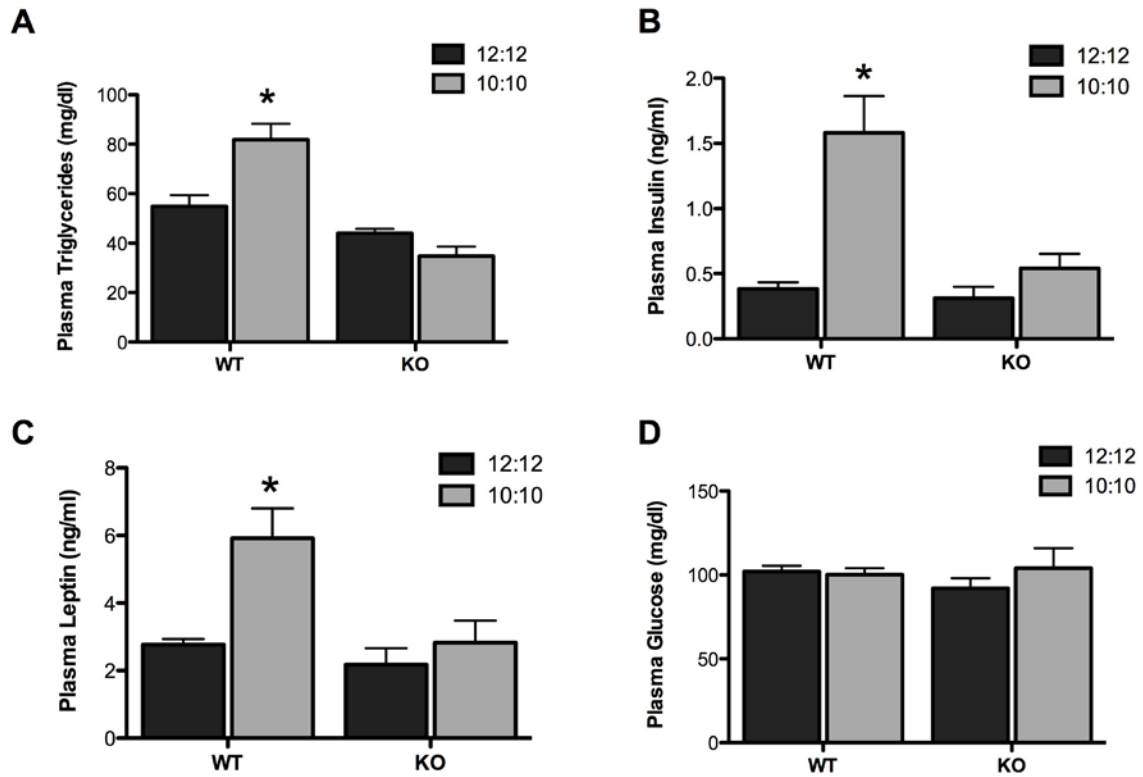


**Figure 5.2.** *Circadian disruption causes metabolic dysregulation, as evidenced by an increase in circulating triglycerides, insulin and leptin, which is blocked in  $CB_1$  receptor deficient mice.* Disruption of circadian cycles, through housing wild-type (WT) mice in a 10h:10h light/dark cycle (10:10) results in an increase in circulating levels of triglycerides (A), insulin (B) and leptin (C), but not glucose (D).  $CB_1$  receptor knockout mice (KO) housed in a 10:10 cycle did not exhibit any changes in metabolic markers in the circulation, indicating an integral role of the  $CB_1$  receptor in mediating metabolic dysregulation following circadian disruption. \* denotes significant differences between WT mice housed in a 10:10 cycle relative to both WT and KO mice housed in 12h:12h light/dark cycle (12:12) conditions and KO mice housed in 10:10 conditions. Data are displayed as mean  $\pm$  SEM; n = 4-5 / condition.

Analysis of metabolic markers in the blood, revealed a significant interaction between genotype and circadian cycle on triglycerides [F (1, 19) = 8.32,  $p < 0.01$ ; Fig. 5.2A] and insulin [F (1, 19) = 4.53,  $p < 0.05$ ; Fig. 5.2B] and a near significant interaction for these variables on leptin [F (1, 19) = 3.08,  $p = 0.09$ ; Fig. 5.2C]. A post-hoc Bonferroni analysis revealed that all of these markers were elevated in CD exposed wild-type mice relative to all other experimental conditions, including *CB1R*<sup>-/-</sup> mice exposed to CD ( $p < 0.05$  for all variables), indicating that *CB1R*<sup>-/-</sup> are resistant to CD induced changes in plasma metabolic markers. There was no effect of any experimental manipulation on basal glucose levels [F (1, 13) = 1.42,  $p > 0.05$ ; Fig. 5.2D].

## Experiment 2

There was a significant interaction between treatment and genotype on body weight [F (1, 16) = 14.08,  $p = 0.0017$ ; Fig. 5.3]. Post-hoc Bonferroni analysis revealed that weight was increased in CORT treated WT mice relative to all other experimental conditions, including *CB1R*<sup>-/-</sup> mice exposed to CORT. Body fat (F(1,16)=7.052;p=0.0173; Fig 5.3B) showed a similar interaction and liver weight showed a main effect of CORT (F(1,10)=6.363;p=0.03; Fig 5.3C) in WT mice (F(1,10)=8.05;  $p=0.018$ ).

WT CORT mice were found to eat more each week. Specifically, analysis revealed a main effect of CORT (F(3,12)=15.20;p=0.0002) with a significant difference at week 4 ( $p < 0.05$ , Fig 5.4A). Similarly WT CORT mice drank increasingly more each week (F(3,9)=9.014;  $p < 0.0045$ ) with a significant difference at week 4 ( $p < 0.05$ ; Fig 5.4B). This increase in feeding in WT CORT mice was accompanied by a decrease in activity across the day (Fig 5.5). This pattern of activity was also noted in circadian rhythm studies of VEH and

CORT treated WT mice where the activity was split between the start and the end of the active period. Focusing at activity across the plane and Z-axis (up and down movements; Fig 5.5A), this again seems to be the case. Total counts across the XY plane shows no difference during the light (inactive) period but an interaction ( $F(1,11)=5.092$ ,  $p=0.454$ ) and main effect of treatment ( $F(1,11)=13.05$ ,  $p=0.0041$ ) during the dark (active period; Fig 5.5B).

Combining activity through the day magnifies the interaction ( $F(1,11)=7.290$ ,  $p=0.0207$ ) and effect of CORT ( $F(1,11)=10.39$ ,  $p=0.0081$ ). The interaction between CB<sub>1</sub>R global knockout and CORT treatment is more clearly seen in Figure 5.5C where activity level was increased in CORT treated knockout mice compared to WT ( $t(6)=2.785$ ,  $p=0.0318$ ). This effect was maintained on the Z-Axis ( $t(6)=2.571$ ,  $p=0.05$ ). Given that VEH CB<sub>1</sub>R<sup>-/-</sup> mice exhibit less activity compared to WT mice, and with a minimal increase in activity in the former on CORT, activity likely plays a very small role in the overall weight change in mice.

In addition to weight gain and increased adiposity, a key component of the metabolic syndrome is insulin resistance, which manifested here in the form of hyperinsulinemia (Fig 5.6 B; main effect of CORT ( $F(1,16)=151.9$ ;  $p < 0.0001$ )) and hyperglycemia (Fig 5.7 A; interaction ( $F(1,10)=7.876$ ;  $p=0.0186$ ; posthoc analysis showed WT CORT exclusively to have increased basal glucose ( $P < 0.001$ )). In addition, we observed hyperleptinemia (Fig 5.6 A; main effect of CORT ( $F(1,16)=307$ ;  $p < 0.0001$ ), an indication of leptin resistance, whereas the plasma level of adiponectin, an adipokine that promotes fatty acid oxidation, was reduced as noted by 2 way ANOVA (Fig 5.6 C; main effect of CORT ( $F(1,11)=11.25$ ;  $p=0.0064$ )). Insulin and leptin parameters were significantly reduced in CB<sub>1</sub>R<sup>-/-</sup> (main effect of genotype ( $F(1,16)=39.47$ ;  $p < 0.0001$ , and ( $F(1,16)=32.95$ ;  $p < 0.0001$ ), insulin and leptin, respectively). While adiponectin levels were increased in CB<sub>1</sub>R<sup>-/-</sup> VEH treated mice as

revealed by Bonferroni posttests, there was no significant difference in CORT treated  $CB_1R^{-/-}$  mice. To investigate changes in the WAT, we measured adipocyte length using H&E stain in WAT. We found increased adipocyte length in WT CORT mice (Fig 5.6E-H), reflects the trend in plasma hormone levels. Analysis of adipocyte length (Fig 5.6D) reveals an interaction ( $F(1,145)=41.42$ ;  $p<0.0001$ ), a main effect of treatment ( $F(1,145)=282.2$ ;  $p<0.0001$ ), and a main effect of genotype ( $F(1,145)=34.72$ ;  $P<0.0001$ ). While these studies were conducted in males, females showed a similar trend (Supplementary Fig 5.1).

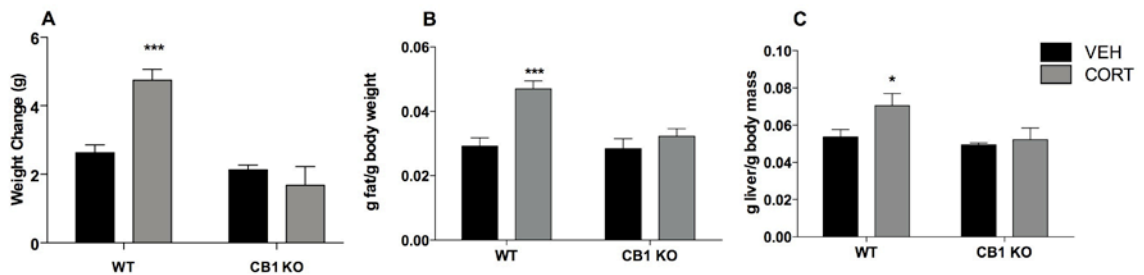


**Figure 5.3**  $CB_1^{-/-}$  mice are resistant to CORT induced weight gain.  $CB_1$  receptor global knockout prevents significant (A) weight gain, (B) increase in adiposity, and (C) increase in liver weight.  $N=4-5$ /group except liver weight  $N=3-5$ /group. Bars with the same letter do not significantly vary from one another. \* $P<0.05$ , \*\*\* $P<0.001$ .

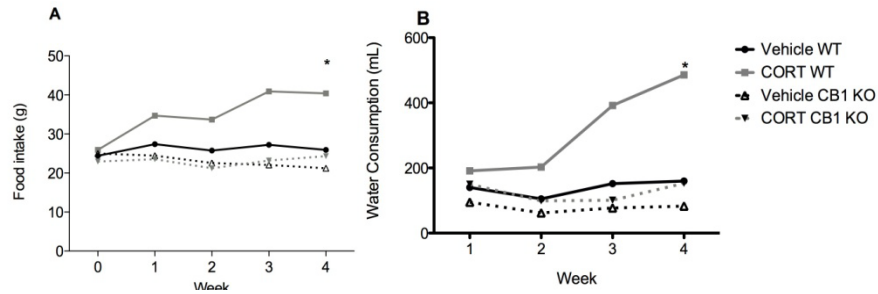


**Figure 5.4** *CORT treated CB1R<sup>-/-</sup> mice do not exhibit increased food and water intake.* CORT treated WT mice display hyperphagia (A) and increased water intake (B) not present in CORT treated CB1R<sup>-/-</sup> mice (n=5/group). \*P<0.05.

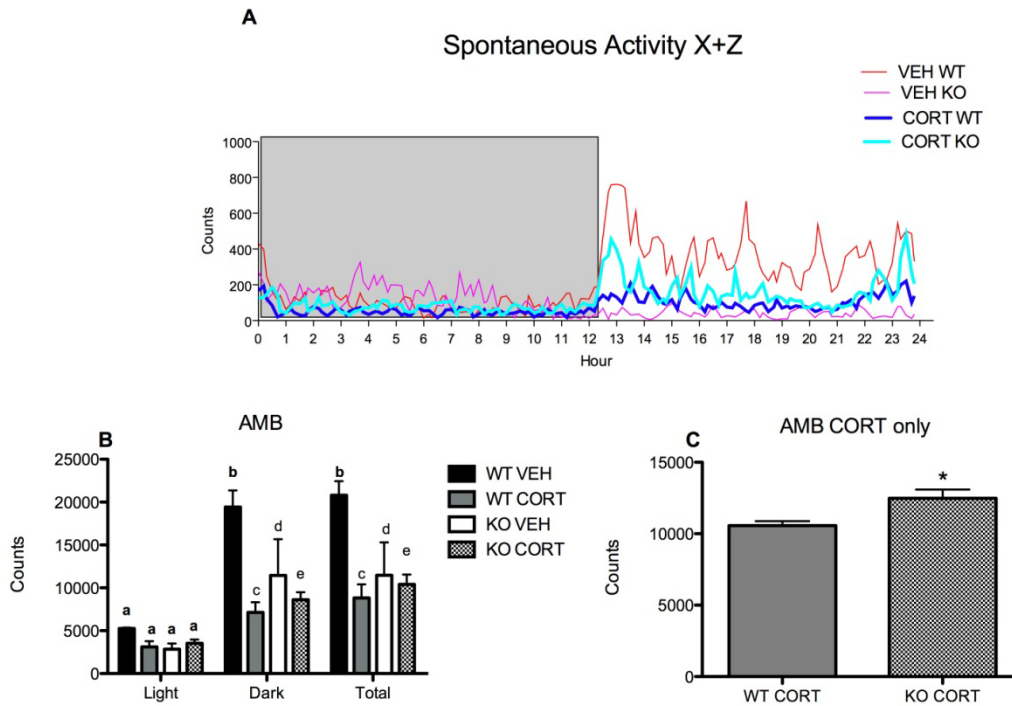


**Figure 5.5** *Spontaneous activity across the day.* Ambulatory movement was measured on the X and Z-Axis (movements up and down) for 4 days and averaged into 12 minute bins. (A) Shows this activity across the day (dark box indicates the inactive-light period) without SEM to make visualization easier. (B) Activity of X axis only split into light, dark and total. There is no difference in activity in the light phase but decreased activity noted during the dark in all groups compared to WT VEH. (C) Total activity of the X axis in groups treated with CORT is decreased in WT mice. N=4/group; \*p<0.5; bars with the same letter do not differ from one another.

Interestingly, there was no difference between groups in fasting glucose levels (Fig 5.7 B) and when insulin resistance and insulin sensitivity were measured through an insulin challenge,  $CB_1R^{-/-}$  mice were not able to prevent the decrease in insulin sensitivity induced by CORT treatment (Fig 5.7 C and Fig 5.7 D, main effect of CORT ( $F(1,12)=15.54$ ;  $P=0.002$ )). However, looking at the islet cells (Supplementary Fig 5.3A), we see largely intact cells in the case of the  $CB_1R^{-/-}$  animals and the breakdown of the cells in the case of CORT WT mice. The anatomy here in conjunction with high circulating levels of insulin and fasting glucose levels suggest an insulin resistance and the repository role of the islet cells to hypersecrete insulin. However, looking at the condition of the cells, it is reasonable to conjecture that the overnutrition state is “slowly” damaging cells and most likely, in future, they will unlikely be able to keep up with the demand, leading to impaired glucose tolerance with mild increase in postprandial glucose concentrations and then to diabetes with overt hyperglycemia.

$CB_1R^{-/-}$  also markedly lowered circulating TG levels in CORT treated mice as noted by 2 way ANOVA, which revealed an interaction between groups ( $F(1,16)=15.41$ ;  $p=0.0012$ ), a main effect of CORT ( $F(1,16)=73.65$ ;  $p<0.0001$ ), and a main effect of genotype ( $F(1,16)=18.32$ ;  $p=0.0006$ ; Fig 5.8A). Liver TG content was also lowered in  $CB_1R^{-/-}$  CORT mice in a similar fashion with an interaction between groups ( $F(1,12)=4.983$ ;  $p=0.045$ ) despite a main effect of CORT ( $F(1,12)=65.74$ ;  $p<0.001$ , Fig 5.11A). The decrease in liver TG in  $CB_1R^{-/-}$  CORT mice (Fig 5.7E) compared to WT CORT mice (Fig 5.8D) can also be noted by decreased presence of lipids by oil red o stain in liver tissue.

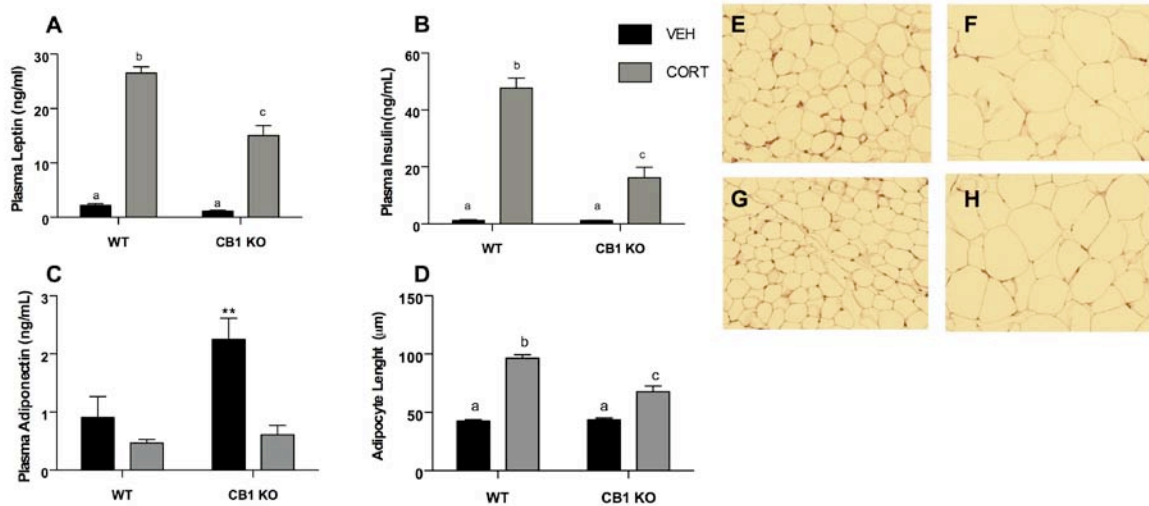


**Figure 5.6** *Metabolic effects of CB1R-/- in CORT treated mice.* Global knockout of the CB<sub>1</sub> receptor counteract CORT induced increases in plasma (A) leptin, (B) insulin, and to a lesser extent (C) adiponectin (n=3-5/group). (D) Adipocyte length as quantified by random selection of adipocytes (n=4-5/group). Representative H&E stain images of epididymal WAT tissue isolated from (E) WT VEH, (F) WT CORT, (G) CB<sub>1</sub>R-/- VEH, and (H) CB<sub>1</sub>R-/- CORT, images taken at 10x. Bars sharing the same letter are not statistically different from each other. \*\*P<0.01.



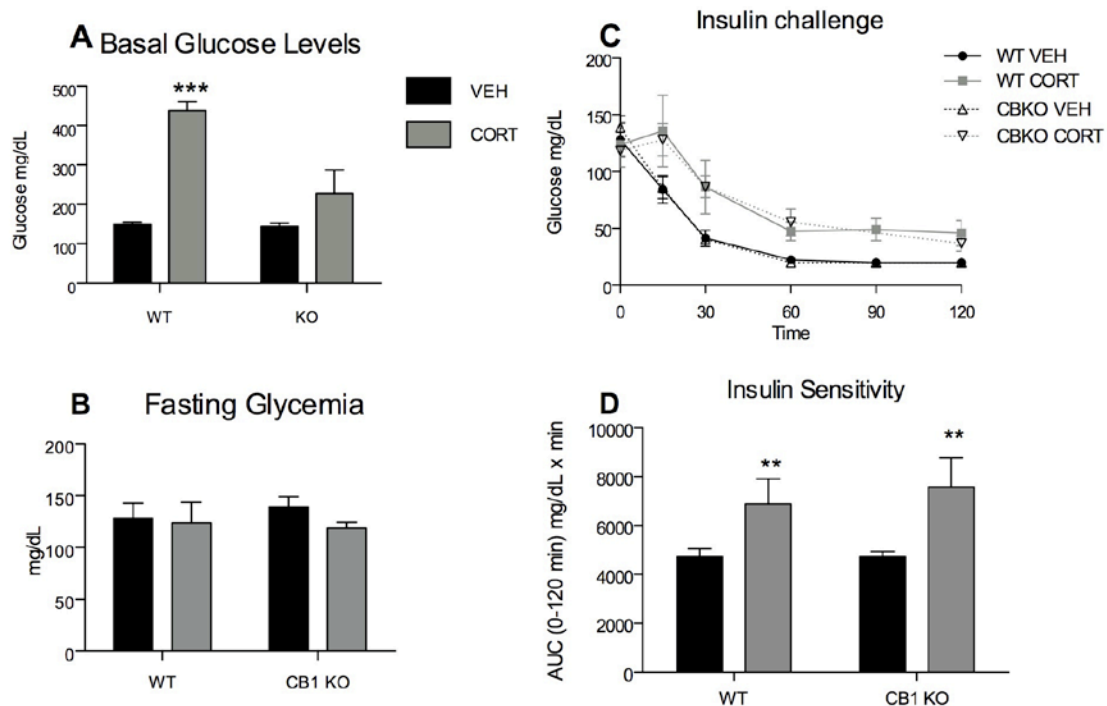


**Figure 5.7** Glucose levels and insulin sensitivity in CORT treated mice. While (A) basal glucose levels are reduced in CB<sub>1</sub>R<sup>-/-</sup> CORT treated mice, there is no difference in (B) fasting levels. (C) Glucose levels measured pre and post injection of an insulin bolus showed no effect of KO in CORT treated mice as measured over 120 minutes. (D) Area under the curve (AUC) again shows no difference in insulin sensitivity in WT and CB<sub>1</sub>R<sup>-/-</sup> CORT treated mice. N=3-5/group; \*\*P<0.01,\*\*\*P<0.001

CB<sub>1</sub>R<sup>-/-</sup> also reduced hepatocellular damage in CORT mice, as signified by a large reduction of plasma levels of alanine aminotransferase (ALT). There was a significant interaction between CORT treatment and genotype (F(1,11)=10.69; p=0.0075; Fig 5.9A) in circulating levels of ALT. Bonferroni posttests revealed an increase in this parameter in WT CORT mice compared to all other experimental conditions (P<0.001). Measurements of alkaline phosphatase (ALP), also a determinant of liver health or disease as a means of bile duct function, was found to have a main effect of genotype (F(1,11)=8.851; p=0.0126, Fig 5.9B). The extent of liver damage in CORT treated mice is further noted in H&E stained liver sections where full-blown steatosis is apparent (Supplementary Fig 5.3B).

Given the increased amounts of water the CORT mice were drinking, we also looked at parameters of kidney function as indicated by levels in blood plasma. Analysis showed no difference between groups in total protein in plasma (Fig 5.9C), but did show a decreased presence of phosphorus, in WT CORT mice compared to all other experimental groups as indicated by an interaction (F(1,11)=7.947; p=0.0167; Fig 5.9D) and subsequent Bonferroni posttests (p<0.001). TCO<sub>2</sub> also showed an interaction (F(1,12)=5.838; p=0.0325; Fig 5.9 E) with an increase in WT CORT mice compared to other experimental conditions (p<0.05).

Global knockout of CB<sub>1</sub> receptor decreased circulating cholesterol levels as noted by an interaction (F(1,10)=8.529; p=0.0153, Fig 5.9 F) and subsequent posttests showing an increase in WT CORT mice compared to the other experimental conditions (p<0.01). WT CORT mice have a slightly greater production and release of TG-rich VLDL, as measured by Pluronic-407 injections (hour 4 WT VEH vs. WT CORT p=0.089; Fig 5.10B).

The effect of CB<sub>1</sub>R<sup>-/-</sup> on substrate utilization was analyzed by indirect calorimetry. After 3 weeks of treatment, mice were moved into individually monitored metabolic chambers

where they were allowed to acclimate over the weekend and were then monitored for 4-5 days.  $CB_1R^{-/-}$  mice on CORT showed a reduction in respiratory quotient (RQ, Fig 5.11 B), resulting from an increase in fat oxidation (Fig 5.11 D) and decrease in carbohydrate oxidation (Fig 5.11F). Thus, the decrease in body weight and reduced adiposity was likely due to increased lipid oxidation.

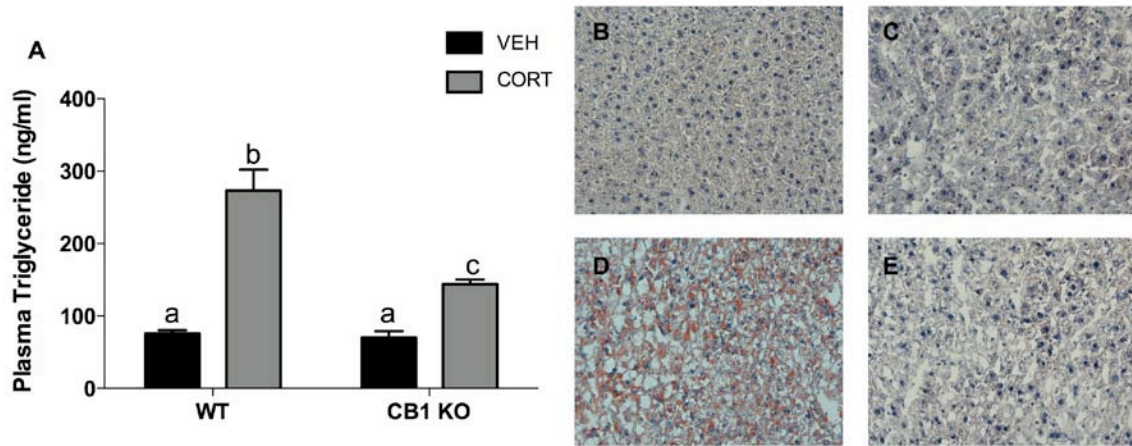


**Figure 5.8** Plasma triglycerides and liver lipid content are greatly reduced in CORT treated  $CB_1R^{-/-}$  mice. (A) Triglycerides measured in plasma isolated from mice showed a significant decrease in  $CB_1R^{-/-}$  mice, but not completely restored to the levels of VEH WT mice. Oil red O staining revealed the development of non-alcoholic fatty liver (NAFLD) in (D) CORT WT mice compared to the healthy livers of (B) VEH WT and (C) VEH KO. NAFLD was prevented in (E) CORT  $CB_1R$  mice. Representative liver stains shown at 10x. N=5/group. Bars with the same letter do not statistically differ from one another.

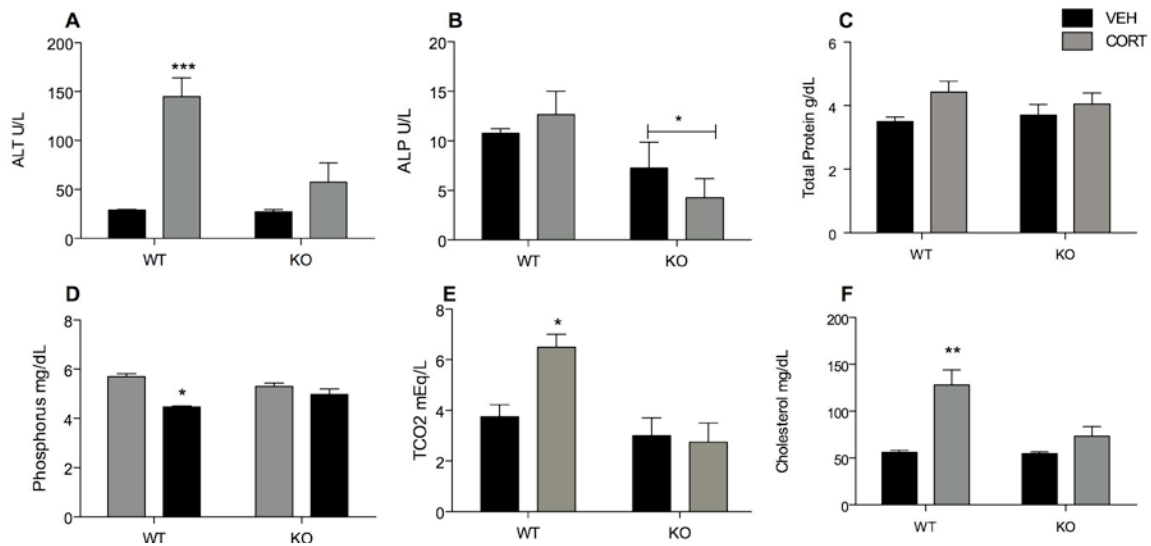


**Figure 5.9** Blood chemistry profile. (A) ALT and (B) ALP circulating levels, indicators of liver damage, are reduced in CORT treated  $CB_1R^{-/-}$  compared to other experimental conditions. Global knockout also prevents changes in (C) total protein, (D) phosphorus, and (E) TCO<sub>2</sub> indicators of kidney damage, and  $CB_1R^{-/-}$  significantly reduced CORT induced circulating cholesterol levels. N=4-5/group. \*P<0.05, \*\*P<0.01, \*\*\*P<0.0001.

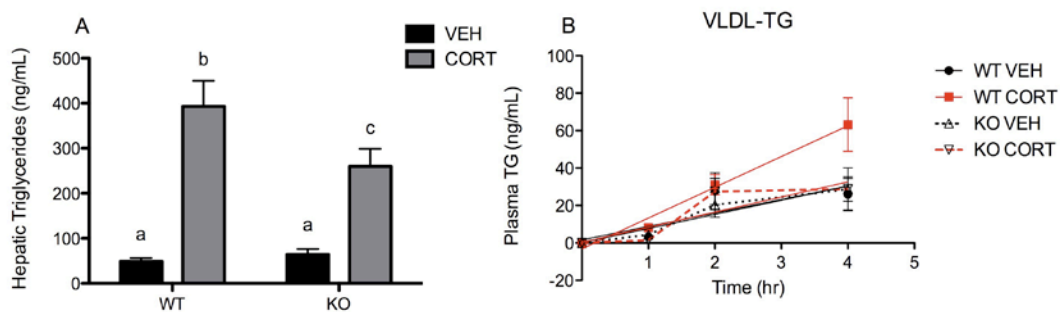


**Figure 5.10** Effect of  $CB_1R^{-/-}$  hepatic triglycerides and VLDL production. (A) Hepatic triglyceride content as determined by Folch (n=3-5/group), bars with the same letter are not significantly different from each other. (B) VLDL-TG production was determined over 4 hours after Pluronic-407 injection. Values are expressed as relative changes compared with respective controls. (n=3-4/group).

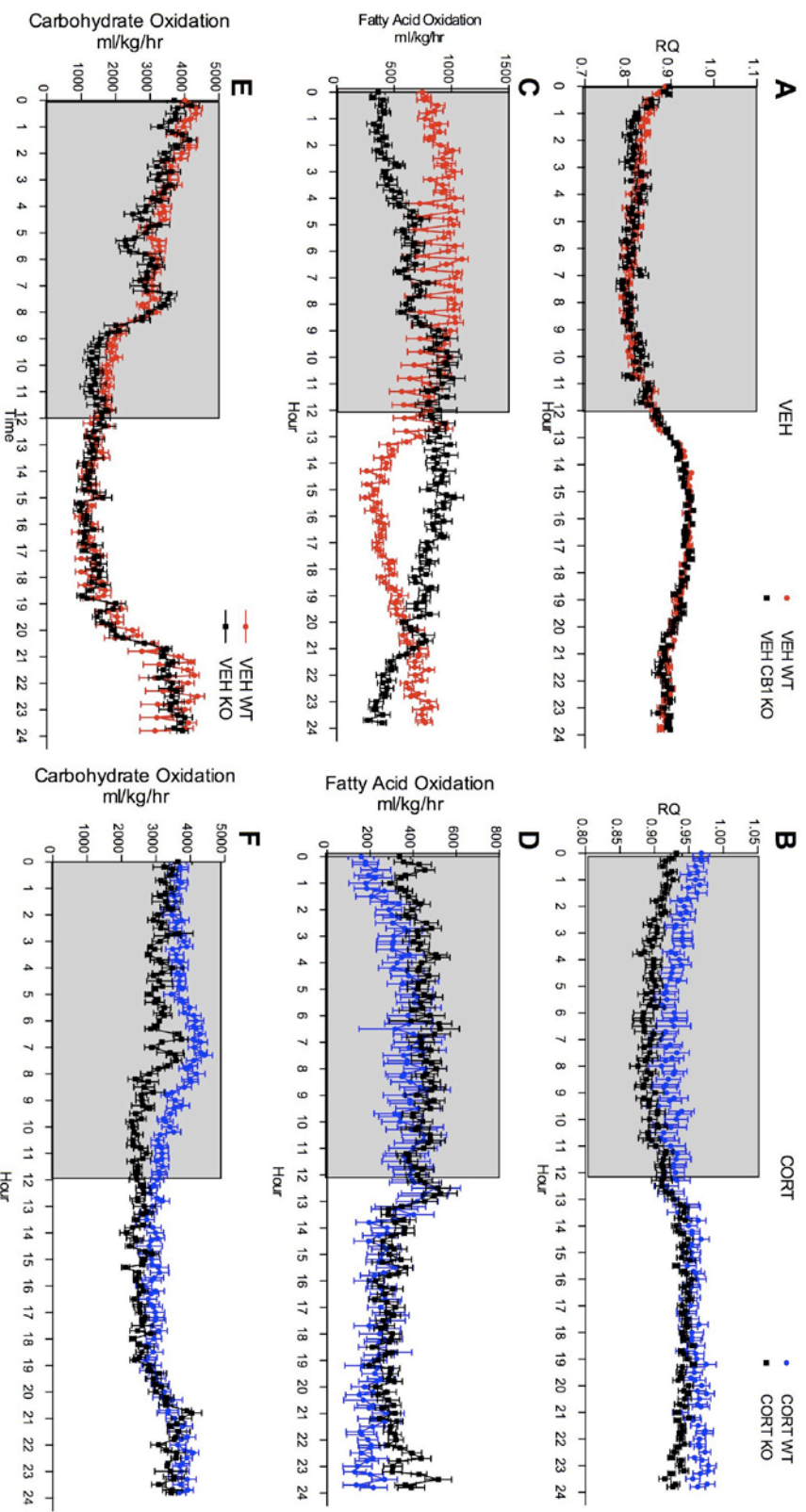


**Figure 5.11** *Substrate selection as measured by indirect calorimetry.* RQ in (A) VEH and (B) CORT treated WT and CB<sub>1</sub>R<sup>-/-</sup>

*/-* mice were assessed by a comprehensive animal metabolic monitoring system (CLAMS). Metabolic parameters were measured over a 4 day period, and equivalent time points, and were averaged together, presented in bins of 12 minutes. CB<sub>1</sub>R<sup>-/-</sup> induces reduction in RQ by decreasing (F) carbohydrate oxidation and increasing (D) fat oxidation in wild-type mice on CORT. The shaded area represents inactive period. The data are expressed as mean values  $\pm$  SEM, n=4/group.

**Table 5.1** Obesity related gene expression in gonadal fat pads (WAT).

Description	Gene Symbol	Fold Change vs. Control-Vehicle WT			vs. CORT WT	vs. Vehicle CBKO
		CORT WT	Vehicle CB KO	CORT CB KO	CORT CB KO	CORT CB KO
Adenylate cyclase activating polypeptide 1	Adcyap1	0.6276	1.1109	0.4325*	0.689	0.3893*
Adenylate cyclase activating polypeptide 1 receptor 1	Adcyap1r1	8.1004*	1.6161*	24.4879*	3.023	15.1527*
Adiponectin, C1Q and collagen domain containing	Adipoq	0.3271*	0.8207	0.2058*	0.6289	0.2507*
Adiponectin receptor 1	Adipor1	0.8959	2.558*	0.8302	0.9267	0.3245*
Adiponectin receptor 2	Adipor2	0.3547*	1.318	0.2769*	0.7806	0.2101*
Adrenergic receptor, alpha 2b	Adra2b	0.5205	3.3987*	0.672	1.291	0.1977*
Adrenergic receptor, beta 1	Adrb1	0.5502*	1.9308	0.6255	1.1369	0.324*
Agouti related protein	Agrp	0.4065*	4.4588	0.5816	1.4308	0.1304*
Apolipoprotein A-IV	Apoa4	3.7877	1.6663	0.5215	0.1377	0.3129
Attractin	Atrn	0.698*	1.3747	0.6498	0.931	0.4727*
Brain derived neurotrophic factor	Bdnf	2.3316	4.0116*	3.0592*	1.3121	0.7626
Bombesin-like receptor 3	Brs3	0.8149	1.2961	0.4325*	0.5307	0.3337*
Complement component 3	C3	0.5657	1.923	0.67	1.1845	0.3484*
Calcitonin/calcitonin-related polypeptide, alpha	Calca	0.7638	1.0625	0.5281*	0.6914	0.4971*
Calcitonin receptor	Calcr	0.6276	1.1109	0.4325*	0.689*	0.3893*
CART prepropeptide	Cartpt	0.6276	1.1109	0.4325*	0.689	0.3893*
Cholecystokinin	Cck	1.3299	1.1961	0.7194	0.5409	0.6014
Cholecystokinin A receptor	Cckar	0.0891	0.1577	0.0614	0.689	0.3893*
Colipase, pancreatic	Clps	0.6276	2.6651	1.2001	1.9121	0.4503
Cannabinoid receptor 1 (brain)	Cnr1	0.4724*	0.004*	0.0018*	0.0038*	0.3893*
Ciliary neurotrophic factor receptor	Cntfr	0.2591*	1.5157	0.3257*	1.2572	0.2149*
Carboxypeptidase D	Cpd	0.8244	1.8478	0.9427	1.1435	0.5102
Carboxypeptidase E	Cpe	0.5696	2.5024	0.4263	0.7484	0.1703*

**Table 5.1 Continued**

Corticotropin releasing hormone receptor 1	Crhr1	0.6276	2.1202	0.4325*	0.689	0.204
Dopamine receptor D1A	Drd1a	0.3348	1.1708	0.6259	1.8695*	0.5346
Dopamine receptor 2	Drd2	0.6276	2.2294	0.4325*	0.689	0.194
Galanin	Gal	0.5979	5.11	0.4948	0.8275	0.0968
Galanin receptor 1	Galr1	0.6276	1.1109	0.4325*	0.689	0.3893*
Glucagon	Gcg	0.1014	0.1588	0.1554	1.5326	0.9787
Glucagon receptor	Gcgr	1.1132	2.5713	1.0841	0.9739	0.4216*
Growth hormone	Gh	0.6276	1.9747	0.4325*	0.689	0.219
Growth hormone receptor	Ghr	0.813	1.3503	0.801	0.9852	0.5932
Ghrelin	Ghrl	0.6063*	5.5693	0.7679	1.2666	0.1379
Growth hormone secretagogue receptor	Ghsr	0.6932	1.1109	0.4857*	0.7007	0.4372*
Glucagon-like peptide 1 receptor	Glp1r	0.6276	1.6896	0.4362*	0.695	0.2582
Melanin-concentrating hormone receptor 1	Mchr1	1.3896	2.9862	7.0976	5.1077	2.3768
Gastrin releasing peptide	Grp	0.6276	1.1109	0.7608	1.2122	0.6849
Gastrin releasing peptide receptor	Grpr	0.6276	1.1947	0.4325*	0.689	0.362*
Hypocretin	Hcrt	0.8301	1.3051	0.4325*	0.521	0.3314*
Hypocretin (orexin) receptor 1	Hcrtr1	0.7327	1.6974	1.0791	1.4727	0.6357
Histamine receptor H1	Hrh1	0.8282	1.514*	0.3203*	0.3867	0.2115*
5-hydroxytryptamine (serotonin) receptor 2C	Htr2c	0.6276	5.0252	0.4325*	0.689*	0.0861
Islet amyloid polypeptide	Iapp	0.6276	2.1055	2.5152	4.0074	1.1946
Interleukin 1 alpha	Il1a	0.6379	4.446	0.8061	1.2637	0.1813
Interleukin 1 beta	Il1b	0.4868	1.2205	0.1767	0.3629	0.1447
Interleukin 1 receptor, type I	Il1r1	0.8594	1.2585	0.8197	0.9538	0.6513
Interleukin 6	Il6	0.4542	1.3771	0.7161	1.5766	0.52
Interleukin 6 receptor, alpha	Il6ra	0.7603	1.5052	0.9855	1.2962	0.6547
Insulin I	Ins1	0.6276	1.1109	0.4325*	0.689	0.3893*
Insulin II	Ins2	0.6996	1.9611	3.988	5.7002	2.0335
Insulin receptor	Insr	0.5193*	1.4109	0.6786	1.3068	0.481
Leptin	Lep	2.6172	0.9582	3.4878*	1.3327	3.6402*
Leptin receptor	Lepr	0.3197*	1.561*	0.4187*	1.3098	0.2682*
Melanocortin 3 receptor	Mc3r	0.6276	1.1109	0.4325*	0.689	0.3893*
Neuromedin B	Nmb	0.3758*	1.6472*	0.5994	1.5949	0.3639*
Neuromedin B receptor	Nmbr	0.8093	10.226	1.0816	1.3365	0.1058
Neuromedin U	Nmu	0.6483	1.6692	0.5736	0.8848	0.3436

**Table 5.1 Continued**

Neuromedin U receptor 1	Nmur1	0.4959	8.2582	0.2478*	0.4998	0.03
Neuropeptide Y	Npy	1.6717	6.7466	4.8255	2.8865	0.7152
Neuropeptide Y receptor Y1	Npy1r	145.479	1.5351	0.4697	0.0032	0.306*
Nuclear receptor subfamily 3, group C, member 1	Nr3c1	0.4199*	0.9532	0.2693*	0.6414	0.2825*
Neurotrophic tyrosine kinase, receptor, type 2	Ntrk2	0.563*	1.078	0.4352*	0.773	0.4037*
Neurotensin	Nts	0.9189	5.9759*	0.681	0.7411	0.114*
Neurotensin receptor 1	Ntsr1	0.6276	3.4145	0.4325*	0.689	0.1267
Opioid receptor, kappa 1	Oprk1	0.6233	1.1032	0.4295*	0.689	0.3893*
Opioid receptor, mu 1	Oprm1	0.3332*	3.6448	0.2069*	0.621	0.0568
Sigma non-opioid intracellular receptor 1	Sigmar1	1.2209	1.0087	1.3722*	1.1239	1.3604
Pro-opiomelanocortin-alpha	Pomc	0.6948*	1.8414	0.677	0.9745	0.3677
Peroxisome proliferator activated receptor alpha	Ppara	0.3131*	1.265	0.4555*	1.455*	0.3601
Peroxisome proliferator activated receptor gamma	Pparg	0.5592	1.1454	0.5424	0.97	0.4735*
Peroxisome proliferative activated receptor, gamma, coactivator 1 alpha	Ppargc1a	0.3572*	1.5837*	0.488*	1.3662	0.3081*
Prolactin releasing hormone receptor	Prhr	0.6276	1.1421	0.4377*	0.6975	0.3833*
Protein tyrosine phosphatase, non-receptor type 1	Ptpn1	0.7709	1.9634*	0.5966	0.7739	0.3039*
Peptide YY	Pyy	0.6276	1.7311	4.0718	6.4875	2.3522
Receptor (calcitonin) activity modifying protein 3	Ramp3	1.022	19.3599	4.3969	4.3025	0.2271
Sortilin 1	Sort1	0.6604	1.5157*	0.6897	1.0444	0.455*
Somatostatin	Sst	0.6276	1.2782	0.5836	0.9299	0.4566*
Somatostatin receptor 2	Sstr2	0.7029	2.8812	0.4774	0.6792	0.1657*
Thyroid hormone receptor beta	Thrb	0.5169*	1.4109	0.618*	1.1955	0.438*
Tumor necrosis factor	Tnf	0.4627	1.8628*	0.5411*	1.1696	0.2905*
Thyrotropin releasing hormone	Trh	0.7429	2.6193	0.4555*	0.6132	0.1739



**Table 5.1 Continued**

Urocortin	Ucn	0.6276	1.8489	0.4684*	0.7462	0.2533
Uncoupling protein 1 (mitochondrial, proton carrier)	Ucp1	0.6276	1.9108	0.4325*	0.689	0.2263
Zinc finger protein 91	Zfp91	0.6742	1.9782*	0.6137*	0.9102	0.3102*

Values represent average fold change ( $\pm$ SEM; n=4/group) in response to corticosterone treatment (100  $\mu$ g/mL) mice compared to vehicle (1% ethanol) treated WT or CB<sub>1</sub>R<sup>-/-</sup> mice. Upregulation with a fold change greater than 2 is noted in red, downregulation with a fold change less than .5 noted by blue. \*P<0.05.

**Table 5.2** *Insulin pathway related gene expression in gonadal fat pads (WAT).*

Description	Gene Symbol	Fold Regulation vs. Control (Vehicle WT)			vs. CORT WT	vs. Vehicle CBKO
		CORT WT	Vehicle CB KO	CORT CB KO	CORT CB KO	CORT CB KO
Thymoma viral proto-oncogene 1	Akt1	- 2.7435*	1.5828*	-1.4236	1.9272	-2.2532*
Thymoma viral proto-oncogene 2	Akt2	- 2.6454*	1.0425	-2.2299*	1.1863	-2.3246*
Thymoma viral proto-oncogene 3	Akt3	-1.5594	2.5359*	-1.0677	1.4605	-2.7076*
CAP, adenylate cyclase-associated protein 1 (yeast)	Cap1	-1.4325	2.0634*	-1.064	1.3463	-2.1954*
FK506 binding protein 12-rapamycin associated protein 1	Mtor	- 3.2344*	1.5052*	-1.1247	2.8759*	-1.6929*
Glucose-6-phosphatase, catalytic	G6pc	-1.4525	1.359	-5.9566*	-4.1011	-8.0948*
Glucose-6-phosphatase, catalytic, 2	G6pc2	-1.6976	-1.0534	-1.4738	1.1519	-1.3991
Growth factor receptor bound protein 2-associated protein 1	Gab1	- 2.5865*	1.6702	-1.4866	1.7399	-2.4829*
Glucokinase	Gck	-1.0112	2.3335	11.0847	11.2083	4.7502
Glycerol-3-phosphate dehydrogenase 1 (soluble)	Gpd1	-1.0147	1.633	2.2863	2.3198	1.4001
Growth factor receptor bound protein 2	Grb2	- 2.2245*	-1.0335	-2.0914*	1.0636	-2.0237*
Growth factor receptor bound protein 10	Grb10	1.1499	1.4768	1.1412	-1.0077	-1.2941
Glycogen synthase kinase 3 beta	Gsk3b	-1.9467	1.0371	-1.7165	1.1341	-1.7802
Hexokinase 2	Hk2	- 2.4259*	1.0389	-1.3585	1.7857*	-1.4113*
Harvey rat sarcoma virus oncogene 1	Hras1	1.6888*	-1.2058	-1.2222	1.3818	-1.0136
Insulin-like growth factor I receptor	Igf1r	-5.5828	1.5157	-2.4024	2.3238	-3.6414

**Table 5.2 Continued**

Insulin-like growth factor 2	Igf2	-4.1655	3.649*	-1.3305	3.1307	-4.8551*
Insulin-like growth factor binding protein 1	Igfbp1	-1.2363	2.2307	1.1531	1.4255	-1.9346
Insulin I	Ins1	11.8433	-2.5624	-17.7777	-1.5011	-6.9379
Insulin-like 3	Ins13	-2.6272	23.0229	-1.6071	1.6347	-37.0012
Insulin receptor substrate 1	Irs1	2.7721*	1.3241	-1.9786	1.401	-2.6199*
Insulin receptor substrate 2	Irs2	-3.6452	1.9119	-2.2377	1.629	-4.2782*
Jun oncogene	Jun	-2.5553	1.5289	-1.2286	2.0799	-1.8784*
V-Ki-ras2 Kirsten rat sarcoma viral oncogene homolog	Kras	1.8006*	1.1668	-1.6988*	1.06	-1.9821*
Low density lipoprotein receptor	Ldlr	-1.1696	-1.1038	-1.1603	1.008	-1.0512
Leptin	Lep	1.6234	1.3566	5.3629*	3.3035*	3.9531*
Mitogen-activated protein kinase kinase 1	Map2k1	2.7302	5.8058	4.3334	1.5872	-1.3398
Mitogen-activated protein kinase 1	Mapk1	-1.6398	1.268	-1.4285	1.1479	-1.8113*
Non-catalytic region of tyrosine kinase adaptor protein 1	Nck1	-1.403*	1.2016	-1.6812*	-1.1983	-2.0202*
Nitric oxide synthase 2, inducible	Nos2	-2.4811	3.0209	-1.2785	1.9406	-3.8624
Neuropeptide Y	Npy	2.3522	3.5925	4.3334	1.8423	1.2062
Phosphoenolpyruvate carboxykinase 2 (mitochondrial)	Pck2	-1.3319	1.9725*	1.1392	1.5173	-1.7315*
3-phosphoinositide dependent protein kinase-1	Pdpk1	-2.145	1.3827	-1.1888	1.8044*	-1.6438*
Phosphatidylinositol 3-kinase, catalytic, alpha polypeptide	Pik3ca	2.3925*	1.5395	-1.6016	1.4938*	-2.4657*
Phosphatidylinositol 3-kinase, catalytic, beta polypeptide	Pik3cb	3.4366*	1.1708	-2.3694*	1.4504	-2.7741*
Phosphatidylinositol 3-kinase, regulatory	Pik3r1	-2.047	2.0279	1.697	3.4738*	-1.195

**Vcdrg'70'Eqpvlpwgf "**

subunit, polypeptide 1 (p85 alpha)						
Phosphatidylinositol 3-kinase, regulatory subunit, polypeptide 2 (p85 beta)	Pik3r2	- 2.5201*	1.7291*	-1.1826	2.131	-2.0449*
Pyruvate kinase liver and red blood cell	Pklr	1.1301	2.8979	-1.3751	-1.554	-3.9848
Peroxisome proliferator activated receptor gamma	Pparg	-2.0049	1.3013	-1.113	1.8013	-1.4484
Protein phosphatase 1, catalytic subunit, alpha isoform	Ppp1ca	-1.9979	1.4093	-1.0977	1.8201*	-1.547
Protein kinase C, gamma	Prkcc	-2.0118	5.0543*	1.0338	2.0799	-4.8889*
Protein kinase C, iota	Prkci	- 2.7625*	1.2924	-1.5205	1.8169	-1.965*
Protein kinase C, zeta	Prkcz	- 3.3427*	1.7839	-1.6268	2.0548	-2.9019
Prolactin	Prl	-1.6976	-1.1607	-2.5482*	-1.5011	-2.1954
Protein tyrosine phosphatase, non-receptor type 1	Ptpn1	-2.4683	2.3054*	1.0446	2.5784	-2.2069*
Protein tyrosine phosphatase, receptor type, F	Ptprf	-3.4967	-1.1587	-4.4444	-1.271	-3.8357
V-raf-leukemia viral oncogene 1	Raf1	-2.0223	1.1447	-1.3054	1.5492	-1.4943*
Resistin	Retn	-2.0118	2.4158	2.0677	4.1598*	-1.1684
Ribosomal protein S6 kinase polypeptide 1	Rps6ka1	-1.4201	2.662	-1.8334	-1.291	-4.8804*
Harvey rat sarcoma oncogene, subgroup R	Rras	-1.7183	-1.2311	-1.7465	-1.0164	-1.4186
Related RAS viral (r-ras) oncogene homolog 2	Rras2	-1.0651	-1.1607	-1.1623	-1.0913	-1.0014
Serine (or cysteine) peptidase inhibitor, clade E, member 1	Serpine1	-1.4006	1.4923	1.0038	1.4059	-1.4866
Src homology 2 domain-containing transforming protein C1	Shc1	- 2.4133*	1.4794	-1.6958	1.4231	-2.5088*
Solute carrier family 27 (fatty acid	Slc27a4	-2.0973	1.2924	-1.1034	1.9007*	-1.426

**Vcdrg'704'Eqvlpwgf "**

transporter), member 4						
Solute carrier family 2 (facilitated glucose transporter), member 1	Slc2a1	- 2.2673*	1.3851	-1.2012	1.8875	-1.6638
Sorbin and SH3 domain containing 1	Sorbs1	-1.4959	-1.0534	-2.2611*	-1.5115	-2.1465*
Son of sevenless homolog 1 (Drosophila)	Sos1	- 1.7124*	1.3851	-1.5205	1.1262	-2.106*
Sterol regulatory element binding transcription factor 1	Srebf1	- 3.3601*	1.1871	-2.2493*	1.4938	-2.6703*

Values represent average fold change ( $\pm$ SEM; n=4/group) in response to corticosterone treatment (100  $\mu$ g/mL) mice compared to vehicle (1% ethanol) treated WT or CB<sub>1</sub>R<sup>-/-</sup> mice. Upregulation with a fold change greater than 2 is noted in red, downregulation with a fold change less than .5 noted by blue. \*P<0.05.

Analysis of mRNA expression in the liver and WAT further indicate a role of the CB<sub>1</sub>R in regulating lipid oxidation and gluconeogenesis. Analysis of numerous genes in WAT through the use of PCR arrays showed several subtle interactions between CORT treatment and genotype with the most prominent related to leptin and the leptin receptor, hexokinase 2 and likely GLUT4, although it was not included in this array mTOR, Slc27a4, among others regulating the insulin pathway (Table 5.1 and 5.2).

Analysis of Sterol regulatory element binding protein (SREBP)1c mRNA expression, a transcription factor involved in fatty acid metabolism and *de novo* lipogenesis, and mRNAs of lipogenic enzymes that are targets of SREBP-1c, fatty acid synthase (FAS) and acetyl-CoA carboxylase (ACC), show a similar pattern of interaction with a main effect of CORT (SREBP-1c  $F(1,14)=9.367$ ;  $p=0.0085$ ; Fig 5.12A), (FAS  $F(1,4)=8.272$ ;  $p=0.045$ ; Fig5.12B) and a main effect of treatment in ACC1  $F(1,11)=6.679$ ;  $p=0.0254$ ; Fig 5.12C). Posttests of the former two genes showed decreased expression significant in WT mice but not CB<sub>1</sub>R<sup>-/-</sup> mice ( $p<0.05$ ).

Other models which exhibit significant weight gain, such as diet induced obesity, show how increased expression of SREBP-1c and subsequent target genes. However, a decrease in SREBP-1c in WAT in WT CORT mice as noted in Table 5.1, suggest a shift in the deposition of triglycerides toward liver and muscle.<sup>242</sup> The shift in lipogenic burden from fat to liver coincides with a decrease in adipose tissue expression of SREBP-1c and an increase in liver expression. A similar trend was noted in a time course analysis of SREBP-1c where an increased expression of SREBP-1c is noted in WAT after 1 week of CORT treatment in WT mice, though this level did not reach significance (Supplementary Fig 5.2D). However, after 4 weeks of treatment, WT mice had significantly lower levels of SREBP-1c compared

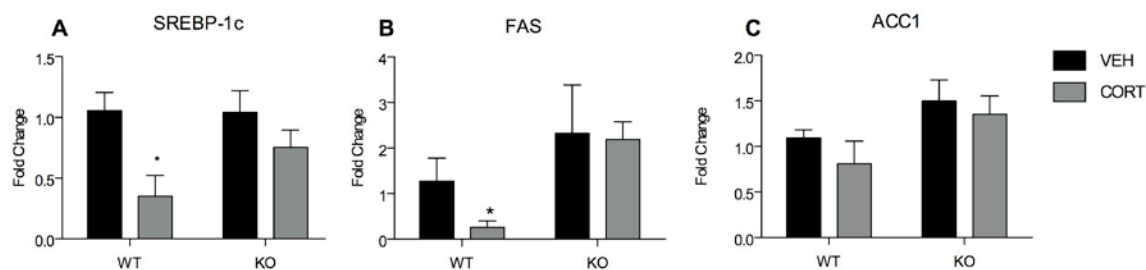


**Figure 5.12** Effect of global  $CB_1R$  knockout on liver mRNA expression of genes involved in lipid metabolism. CORT treatment results in decreased expression of (A) SREBP-1C, (B) FAS, and to a less degree ACC1. This reduction is not present in  $CB_1R^{-/-}$  CORT treated mice. N=3-5/group, \*P<0.05.

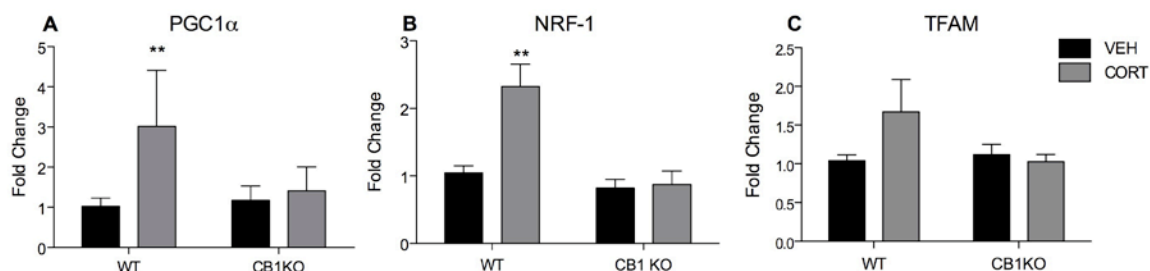
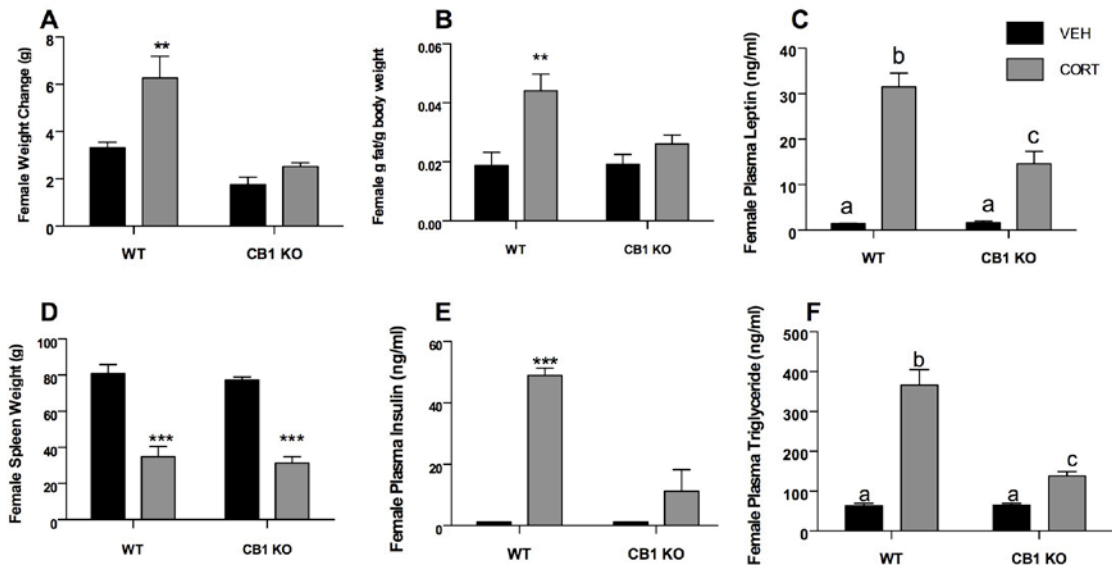


**Figure 5.13** Expression of genes responsible for energy homeostasis and respiration in the liver. Global knockout of the  $CB_1R$  decreases the expression of (A) PGC1α, (B) NRF-1, and (C) TFAM (n=4-5/group), \*\* P<0.01).

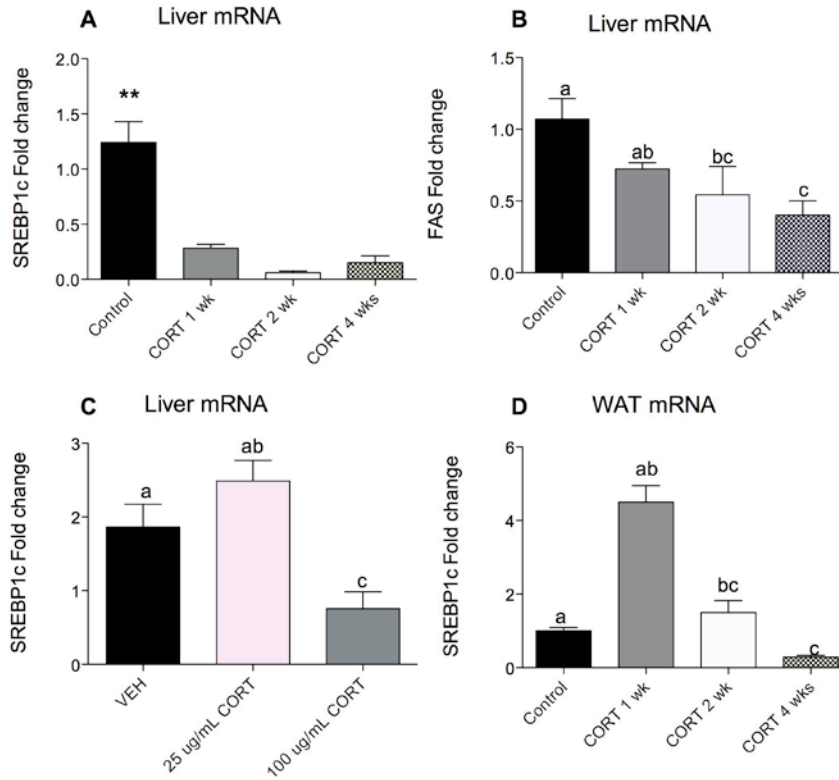
to 1 week treated mice ( $p < 0.05$ ) and controls ( $p < 0.01$ ). While the time point of increase of SREBP-1c was not noted in the liver (all time points of CORT treatment were significantly lower than in VEH mice,  $p < 0.01$ ), lower levels are noted after 2 and 4 weeks of treatment (Supplementary Fig 5.2A). A similar trend is noted in FAS expression in the liver (Supplementary Fig 5.2B). In a separate cohort of animals, an intermediate group of CORT treatment, 25  $\mu\text{g}/\text{mL}$ , mice showed increased expression of SREBP-1c after 4 weeks of treatment although the level did not reach significance compared to controls. Again, the 100  $\mu\text{g}/\text{mL}$  group showed decreased expression compared to both controls and the 25  $\mu\text{g}/\text{mL}$  groups ( $p < 0.05$ ; Supplementary Fig 5.2D).

Peroxisome proliferator-activated receptor gamma coactivator 1-alpha (PGC-1 $\alpha$ ) is a transcriptional coactivator that regulates genes involved in energy metabolism and mitochondrial biogenesis, such as Nuclear respiratory factor 1, NRF-1, another transcription factor that activates the expression of metabolic genes that regulate cellular growth, as well as genes required for mitochondrial respiration. Both PGC-1 $\alpha$  and NRF-1 showed interactions ( $F(1,14)=5.093$ ;  $p=0.0405$ ; Fig 5.13A; and  $F((1,14)=7.46$ ;  $p=0.0162$ ; Fig 5.13 B respectively). Bonferroni posttests revealed WT CORT treated mice to have increased levels compared to all other experimental conditions ( $p < 0.01$ ). Finally we looked at TFAM as another measure of mitochondrial function and number as an indication of respiration. TFAM showed a comparable pattern of expression in all groups but none significantly different from one another (Fig 5.13C).



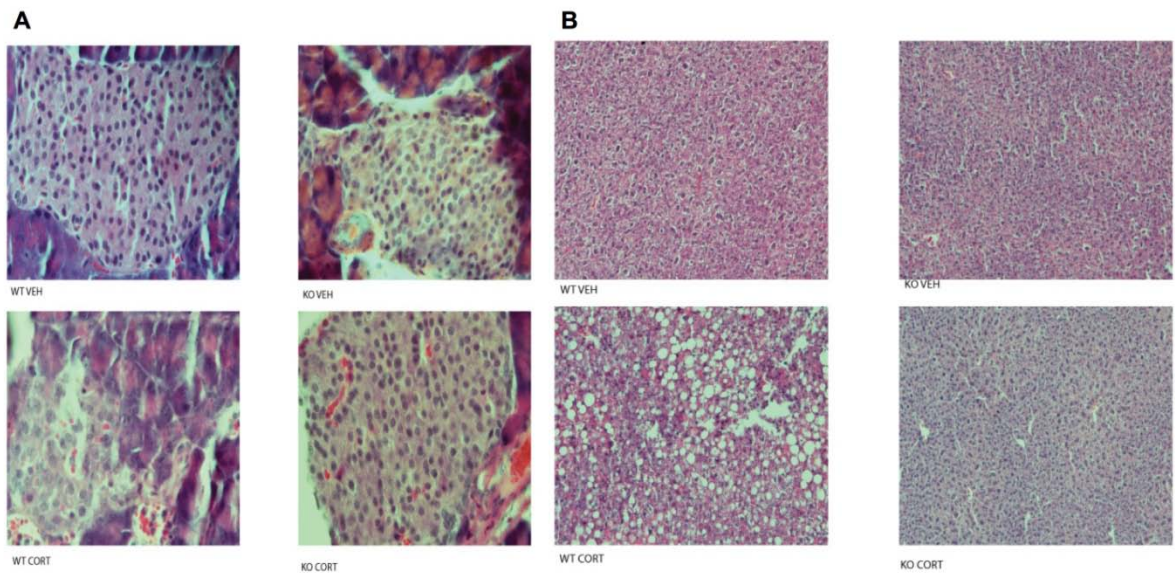


**Supplementary Figure 5.1** *Global knockout of the CB<sub>1</sub>R prevents the development of metabolic syndrome in CORT treated mice.* Female WT and CB<sub>1</sub>R<sup>-/-</sup> mice were placed on VEH or CORT for 4 weeks. CB<sub>1</sub>R<sup>-/-</sup> prevented the large (A) weight change, (B) increased adiposity, and elevated levels of (C) insulin, (E) leptin, and (F) triglycerides induced by CORT treatment. (D) Spleen weights are decreased in both groups of CORT treated mice showing a similar exposure to CORT. N=4-5/group, \*\*P<0.01, \*\*\*P<0.001, bars that share the same letter are not significantly different from one another.



### Supplementary Figure 5.2

**Supplementary Figure 5.2** Time and dose course of *SREBP1c* expression. Quantitative RT-PCR analysis of *SREBP1c* in (A) liver from 1-4 week 100  $\mu\text{g}/\text{mL}$  CORT treated mice, (C) liver from 25 and 100  $\mu\text{g}/\text{mL}$  CORT treated mice, and (D)WAT from 1-4 week 100  $\mu\text{g}/\text{mL}$  CORT treated mice. (B) FAS expression in liver from 1-4 week 100  $\mu\text{g}/\text{mL}$  CORT treated mice. All expressed as fold change ( $\pm\text{SEM}$ ) in relation to control group. Bars with the same letters are not scientifically different from one another. \*\* notes  $P < 0.01$  as determined by one way ANOVA.



**Supplementary Figure 5.3** *CB<sub>1</sub>R*<sup>-/-</sup> prevents CORT induced damage to the pancreas and liver. H&E staining reveals damage to the (A) islet cells in the pancreases of CORT WT mice, an effect not present in CORT *CB<sub>1</sub>R*<sup>-/-</sup> mice. Similarly CORT treated mice show signs of (B) liver steatosis while CORT *CB<sub>1</sub>R*<sup>-/-</sup> mice are spared damage. Pancreas images taken at 40x, liver at 10x, representative samples from n=5/group.

## Discussion

Both increased and decreased CORT signaling, as demonstrated in our models of altered light-dark cycle and CORT in the drinking water led to a disruption of circadian rhythms as noted by decreased mRNA expression of molecular clock genes and altered activity level as noted by tempograms and actograms, as noted in Chapter 4 and in previous publications.<sup>166</sup> Here we looked to find a common mechanism of CORT regulation that may lead to the obese phenotype in both mouse models.

The data generated herein provide insight into the potential mechanisms of CD-and CORT-induced metabolic dysregulation, revealing that mice lacking cannabinoid CB<sub>1</sub> receptors exhibited a blunted increase in body weight and a dramatic reduction of the elevations in circulating insulin and leptin, and triglycerides following 8 weeks of CD. These data are consistent with diet-based models of obesity and metabolic dysregulation, which show that disruption of CB<sub>1</sub> receptor signaling provides a significant degree of resistance to metabolic change.<sup>167,224</sup>

The mechanisms by which CD engage the eCB system to modulate metabolic processes, are still unknown. Endocannabinoid ligand content within feeding nuclei<sup>223</sup>, as well as the circulation,<sup>222</sup> are known to exhibit circadian fluctuations; however, the relationship of this regulation to the control of metabolic processes is not known. In humans, sleep deprivation results in an elevation in circulating levels of AEA,<sup>22</sup> and in rodents, sleep deprivation elevates central content of 2-AG.<sup>225</sup> While sleep deprivation and CD are different forms of circadian misalignment, these data provide evidence that disruption of normative circadian cycles can cause a resultant elevation in eCB signaling. Sustained CD may result in a similar tonic elevation in eCB signaling; however, this requires detailed analysis of normal circadian

rhythms of eCB content and how it is altered by CD. Furthermore, both central and peripheral CB<sub>1</sub> receptor signaling can modulate metabolic function,<sup>121</sup> thus determining if the current effects that are mediated by central or peripheral mechanisms are of great importance, particularly since peripherally restricted CB<sub>1</sub> receptor antagonists are being developed to treat and regulate obesity.<sup>226</sup>

In addition to these effects, a role for eCB signaling in the clock cannot be disregarded. For instance, it is known that SCN neurons are sensitive to the effects of eCBs.<sup>227</sup> As such, sustained CD may alter eCB signaling within the SCN, having broad ramifications for circadian regulation of many functions, including metabolic processes. Given that the effects of CD are wide ranging and not exclusive to metabolic processes,<sup>166</sup> it is essential to determine if modulation of CB<sub>1</sub> receptor function can alter all of the effects of CD, or if its role is specific to metabolic dysregulation.

In experiment 2, looking at chronic high levels of CORT, given the ability of glucocorticoids to rapidly mobilize eCB signaling, the eCB system seemed to be a plausible target to mediate these glucocorticoid effects. The data produced in these groups of experiments provide a detailed role of CB<sub>1</sub> receptor modulation of CORT-induced metabolic syndrome. In these studies, we revealed that mice lacking cannabinoid CB<sub>1</sub> receptors were resistant to CORT induced weight gain and gonadal fat pad and liver weights comparable to control mice, at least when grossly measured. mRNA expression of leptin in the WAT of treated mice showed an increase in CORT CB<sub>1</sub>R<sup>-/-</sup> mice compared to all other groups suggesting that the hormone is functioning properly in these and leads to decreased food intake compared to VEH CORT mice. Expression of several genes in the insulin pathway

also showed upregulation in CB<sub>1</sub>R<sup>-/-</sup> compared to VEH CORT mice and thus possibly improved insulin signaling.

Adiponectin levels were slightly increased in VEH WT mice and greatly increased in VEH CB<sub>1</sub>R<sup>-/-</sup> mice, knockout of the receptor did little to improve levels in CORT treated mice. mRNA expression of adiponectin again showed a decrease in both WT and CB<sub>1</sub>R<sup>-/-</sup> CORT treated mice. AdipoR1 and AdipoR2 serve as receptors for the adiponectin, and their reduction seems to be correlated with reduced adiponectin sensitivity; while AdipoR1 showed no change between control and CORT treated mice, with an elevation in VEH CB<sub>1</sub>R<sup>-/-</sup>. AdipoR2 followed the trend of its hormone with a decrease in both CORT treated groups compared to VEH mice. Differential expression here follows trends as seen by other groups where AdipoR1 regulates AMP-activated protein kinase (AMPK) activation and AdipoR2 activates peroxisome proliferator-activated receptor (PPAR)- $\alpha$  signaling pathways. Subsequently, we also observed decreased expression of the former in CORT treated mice.<sup>228</sup> This leads us to propose that CB<sub>1</sub>R activity here does not seem to involve adiponectin signaling.

Expression of resistin, like adiponectin, an adipose derived hormone, has been suggested to link adiposity to insulin resistance.<sup>229</sup> In this study mRNA expression of resistin in WAT was decreased in WT CORT treated mice while increased in CORT CB<sub>1</sub>R<sup>-/-</sup> mice. Resistin expression in WAT has been shown to be decreased in several mouse models of obesity while levels in circulation are higher in the obese phenotype and increases in circulation have been shown to play a vital role in the formation of insulin resistin,<sup>231,238</sup> suggesting that the increased expression of resistin in the WAT of CORT CB<sub>1</sub>R<sup>-/-</sup> should improve insulin sensitivity. However, an insulin challenge revealed decreased insulin sensitivity in both

CORT treated groups. To firmly evaluate the role of resistin in CORT mice, circulating levels of the hormone need to be taken into account.

In the present study, we also demonstrated that global  $CB_1R^{-/-}$  improves dyslipidemia, reverses hepatic damage and decreases cholesterol levels all induced by CORT treatments. These effects are in part driven by increased food intake, but as demonstrated in Chapter 4, an absence of increased caloric intake in CORT mice still resulted in weight gain comparable to weight gain in adlib CORT treated mice.  $CB_1R^{-/-}$  here was shown to increase activity levels in the otherwise inactive CORT mice, but in contrast to VEH treated mice these levels are still significantly decreased. Results here would suggest that global  $CB_1R^{-/-}$  is the combined result of centrally mediated decreases in caloric intake and a peripherally mediated increase in energy expenditure as hypothesized by others in cases of diet induced obesity.<sup>240,241</sup> Indeed the respiratory quotient was decreased in  $CB_1R^{-/-}$  CORT mice as the result of increased fatty acid oxidation and a decrease in carbohydrate oxidation.

In addition to eating more, WT CORT mice were also found to consume more water (polydipsia) and have increased urination (polyuria), both signs of overt diabetes. A concern here is that WT CORT mice might be exposed to more CORT over time, as it is in the drinking water, and thus the polydipsia provides a positive feed forward loop leading to larger effects not seen in  $CB_1^{-/-}$  mice since they were not drinking the same amounts of water. However, both groups of mice showed excess levels of circulating CORT and splenic atrophy, indicating that their exposure to CORT was very high, and likely equivalent.

Looking beyond adipocytes that appear to show an intermediate phenotype in CORT  $CB_1R^{-/-}$  mice, a likely target of CORT in regard to metabolic action is the liver.  $CB_1R^{-/-}$  reversed the CORT suppression of Srebp-1c and its target genes while simultaneously

reducing expression of PGC-1 $\alpha$  and its target genes. Results here point to a breakdown in the fasting-refeeding cycle as seen in Srebp-1c deleted mice,<sup>242</sup> where there is no longer an appropriate regulated expression of critical lipogenic genes such as FAS as shown in this study.<sup>235,236</sup> Here we see that increases in circulating levels are not sufficient to suppress gluconeogenesis as evident by increases in PGC-1 $\alpha$  and NRF-1,<sup>237</sup> suggesting that the liver is insulin resistant. When the liver becomes insulin resistant, it is still able to stimulate lipogenesis, creating a vicious cycle that aggravates insulin resistance and ultimately contributes to the onset of overt diabetes, as is the case in the CORT treated mice. The co-existence of hepatic insulin resistance (elevated gluconeogenesis) and sensitivity (elevated lipogenesis) at gene expression level has been observed in rodent diabetic models.<sup>27</sup> However, the mechanism of this co-existence of insulin sensitivity and resistance has not been revealed until now.<sup>239</sup>

In CORT treated mice, elevated levels of PGC-1 $\alpha$  indicate insulin resistance in the gluconeogenic pathways. In the initial week of CORT treatment, Srebp-1c remains insulin sensitive and thus fatty acid synthesis is accelerated and triglycerides accumulate in the liver. The excess in triglycerides is secreted in VLDL, raising plasma triglyceride levels. However, by week 4, we observed decreased expression of Srebp-1c, indicating a loss of insulin resistance in this pathway as well, and further noted by extensive non-alcoholic steatohepatitis (NASH). This decrease would suggest less fat accumulation, which we see if treatment of CORT goes beyond 5 weeks when mice actually begin to lose weight and often die. This decrease in Srebp-1c has recently been reported in the human condition of NASH.<sup>248</sup>



CB<sub>1</sub>R<sup>-/-</sup> mice remain insulin sensitive in both gluconeogenic and fatty synthesis pathways in the liver, despite a decrease in sensitivity in adipose tissue and in circulation. Looking at the level of the islet cell in the pancreas, the CB<sub>1</sub>R<sup>-/-</sup> prevents CORT induced damage or decrease in cell volume. Protection here was noted despite predominant expression of CB<sub>2</sub> receptor expression in the insulin secreting  $\beta$  cells. Both type 1 and type 2 receptors have been described in glucagon secreting  $\alpha$  cells.<sup>241</sup> Inhibition of  $\alpha$  cell signaling in CB<sub>1</sub>R<sup>-/-</sup> mice may aid in the maintained fast-fed cycles in CORT treated mice by stabilizing glucagon levels.

Collectively, these data compellingly suggest that the eCB system may be involved in the development of obesity from multiple etiologies, including diet, circadian dysregulation, and hormonal imbalance. Taken together, these data provide the first evidence that the eCB system is a contributor to metabolic dysregulation induced by disruption of circadian cycles and hormonal regulation, and suggest that future research should continue to investigate the wide-spanning role the eCB system may play in the genesis of multiple forms of metabolic disorders. However, it should be noted that the synthesis and production of CORT as induced by stress or in response to the rise and fall of the sun are independently controlled.<sup>18</sup> While the eCB system has been thoroughly characterized in the regulation of CORT under acute and chronic stress and acute and chronic glucocorticoid exposure,<sup>150</sup> its role in the diurnal release is unknown, making the results in that regard more difficult to interpret.

## **Chapter 6: Characterization of endocannabinoid system signaling in glucocorticoid treated mice**

### **Abstract**

Limbic and hypothalamic endocannabinoid (eCB) signaling is understood rather well in rodents under conditions of chronic stress; however, studies investigating the impact of prolonged exposure to glucocorticoid (GC) hormones have been limited by the concurrent exposure to the stress of daily injections. The present study was designed to examine the effects of a noninvasive approach to alter plasma corticosterone (CORT) on the eCB system not only, centrally in the amygdala, hippocampus, and hypothalamus, but also in the periphery in blood, liver, and white adipose tissue (WAT). More precisely, we explored the effects of a chronic, ie, 4-week exposure to CORT dissolved in the drinking water of mice (100 µg/ml) and measured cannabinoid CB<sub>1</sub> receptor binding, eCB content, activity of the eCB degrading enzyme fatty acid amide hydrolase (FAAH), and mRNA expression of both the CB<sub>1</sub> receptor and FAAH in both the hippocampus and amygdala. In the remaining tissue, we looked only at eCB content, and mRNA expression of CB<sub>1</sub> receptor, FAAH, N-acyl phosphatidylethanolamine phospholipase D (NAPE-PLD), monoacylglycerol lipase (MAGL), and diacylglycerol lipase, (DAGL). Our data demonstrate that protracted exposure to GCs reduce CB<sub>1</sub> receptor density and augmented anandamide (AEA) metabolism within limbic structures. Signaling in the limbic brain region could contribute to shifts in emotional behavior, especially increases in anxiety and depression-like behaviors, which occur following sustained CORT exposure. Results from the hypothalamus and periphery would suggest that the CORT induced metabolic drive is the result of increased synthesis and decreased degradation of AEA in the liver, which likely spills over to blood circulation. In conjunction with prior work, these findings suggest that increased AEA in the liver, and

possibly other sites through circulation, drives a shift in metabolic function that accelerates carbohydrate metabolism and compromises fatty acid metabolism, resulting in the development of fatty liver and fat stores in the adipose tissue.

## **Rationale**

Glucocorticoids (GC) are the final mediators of the hypothalamic pituitary adrenal (HPA) axis and play a crucial role in mounting the adaptive response to stress. Accumulating evidence has demonstrated that GCs induce endocannabinoid (eCB) signaling and, in turn, endocannabinoids regulate glucocorticoid secretion through both local and distal regulation of HPA-axis activity.<sup>113-115</sup> As described in the last chapter, the eCB system was originally characterized as the neuronal system to which the psychoactive constituent of cannabis  $\Delta^9$ -tetrahydrocannabinol (THC) interacted to exert its effects on physiology and behavior. The system comprises of two subtypes: the cannabinoid type 1 (CB<sub>1</sub>) and type 2 (CB<sub>2</sub>) signaling receptors.<sup>244,245</sup> The system also comprises the endogenous ligands of both receptors, anandamide (AEA) and 2-arachidonoylglycerol (2-AG), as well as the enzymes for ligand biosynthesis and degradation, such as the fatty acid amide hydrolase (FAAH).<sup>116,117,248</sup>

Interestingly, following conditions of chronic stress eCB signaling appears to breakdown, as chronic stress has been found to reduce both eCB content and receptor density (reviewed in Gorzalka et al., 2008).<sup>249</sup> However, the extent to which GCs contribute to the effects of chronic stress centrally, in limbic system and hypothalamic eCB signaling, and moreover in the periphery, is unclear. As such, the aim of the current study was to characterize the effects of our non-invasive corticosterone (CORT) drinking water model on the ability to modulate eCBs centrally in the hippocampus, amygdala, and hypothalamus and peripherally in the blood, WAT and liver.

## Experimental design

This study was carried out using 2 cohorts of vehicle (VEH) and CORT treated animals. In the first cohort n=7-8/group were euthanized and tissues were removed and processed for eCB parameters. In the second cohort n=4-5 were euthanized and tissue was removed and processed for mRNA expression.

## Results

Once again, chronic exposure to CORT in the drinking water in the present study, resulted in a significant increase in the concentration of plasma corticosterone measured in blood obtained following four weeks of sustained CORT exposure [ $t(8) = 6.705$ ,  $P < 0.01$ ; Supplementary Fig 6.1)]. These data were consistent with our previous report that demonstrates elevations in circulating CORT at all points of the circadian cycle with this dosage.<sup>15</sup> Additionally, mice which were exposed to CORT exhibited an increase in body weight relative to control animals [ $t(6) = 4.50$ ,  $P < 0.01$ ; Supplementary Fig. 6.1B), replicating our previous report that protracted exposure to CORT in the drinking water produces an obese phenotype.<sup>47</sup>

In the amygdala, chronic CORT treatment resulted in a decrease in the binding site density ( $B_{\max}$ ) [ $t(4) = 2.812$ ,  $P < .05$ ; Fig. 6.1A], but no significant difference in the dissociation constant ( $K_D$ ) [ $t(4) = 0.84$ ,  $P > .05$ ; Fig. 6.1B] for [ $^3\text{H}$ ]-CP 55,940 compared to those exposed to vehicle alone. Chronic exposure to CORT significantly decreased amygdalar content of the eCB AEA [ $t(7) = 3.641$ ,  $P < .01$ ; Fig 6.1C]; however, there was no change in concentration of 2-AG in mice treated with CORT compared to those receiving vehicle [ $t(7) = 0.3967$ ,  $P > .05$ ; Fig. 6.1D]. The fatty acid ethanolamides PEA [ $t(7) = 2.191$ ,  $P < .05$ ; Fig 6.1F] and OEA [ $t(7) = 2.198$ ,  $P < .05$ ; Fig 6.1E] were also decreased in the

amygdala of mice exposed to chronic CORT compared to vehicle. The  $V_{\max}$  for AEA hydrolysis by membranes isolated from the amygdala of mice exposed to chronic CORT was significantly increased compared to membranes from vehicle exposed mice [ $t(4) = 2.858$ ,  $P < .05$ ; Fig. 6.1G]. There was no significant difference in  $K_m$  for AEA hydrolysis between the two groups [ $t(4) = 0.6917$ ,  $P > .05$ ; Fig. 6.1H].

In the hippocampus, membranes isolated from mice treated with chronic CORT exhibited a significant decrease in [ $^3\text{H}$ ]-CP 55,940 binding site density [ $B_{\max}$   $t(5) = 2.336$ ,  $P < .05$ ; Fig. 6.2A], without a significant change in the  $K_D$  [ $t(5) = 2.031$ ,  $P > .05$ ; Fig. 6.2B] compared to the vehicle treated mice. Chronic CORT treatment resulted in a significant reduction in AEA content [ $t(10) = 3.534$ ,  $P < .05$ ; Fig. 6.2C], while there was a large increase in 2-AG content [ $t(10) = 4.979$ ,  $P < .0001$ ; Fig. 6.2D] in the hippocampus. As with AEA, PEA [ $t(10) = 3.264$ ,  $P < .05$ ; 6.2F] and OEA [ $t(10) = 6.611$ ,  $P < .0001$ ; 6.2E] also show significant decrease in the hippocampus as a result of chronic CORT treatment. Consistent with reductions in NAEs in the hippocampus, there was an increase in the  $V_{\max}$  for AEA hydrolysis in hippocampal membranes from CORT treated mice [ $t(4) = 3.902$ ,  $P < .05$ ; Fig. 6.2H] and no change in  $K_m$  [ $t(4) = 1.905$ ,  $P > .05$ ; Fig. 6.2G] compared to vehicle treated mice.

To quantify FAAH and  $\text{CB}_1$  receptor expression under conditions of chronic CORT, we used quantitative real time RT-PCR and mRNA extracted from the hippocampal and amygdalar brain regions from CORT and vehicle treated mice. Treatment with CORT resulted in no significant change compared to vehicle treated in mRNA for FAAH (hippocampus  $t(6) = 1.28$ ,  $p > 0.05$ ; amygdala  $t(5) = 0.278$ ,  $p > 0.05$ ) or the  $\text{CB}_1$  receptor (hippocampus  $t(6) = 0.783$ ,  $p > 0.05$ ; amygdala  $t(7) = 0.286$ ,  $p > 0.05$ ) (see Table 6.1).

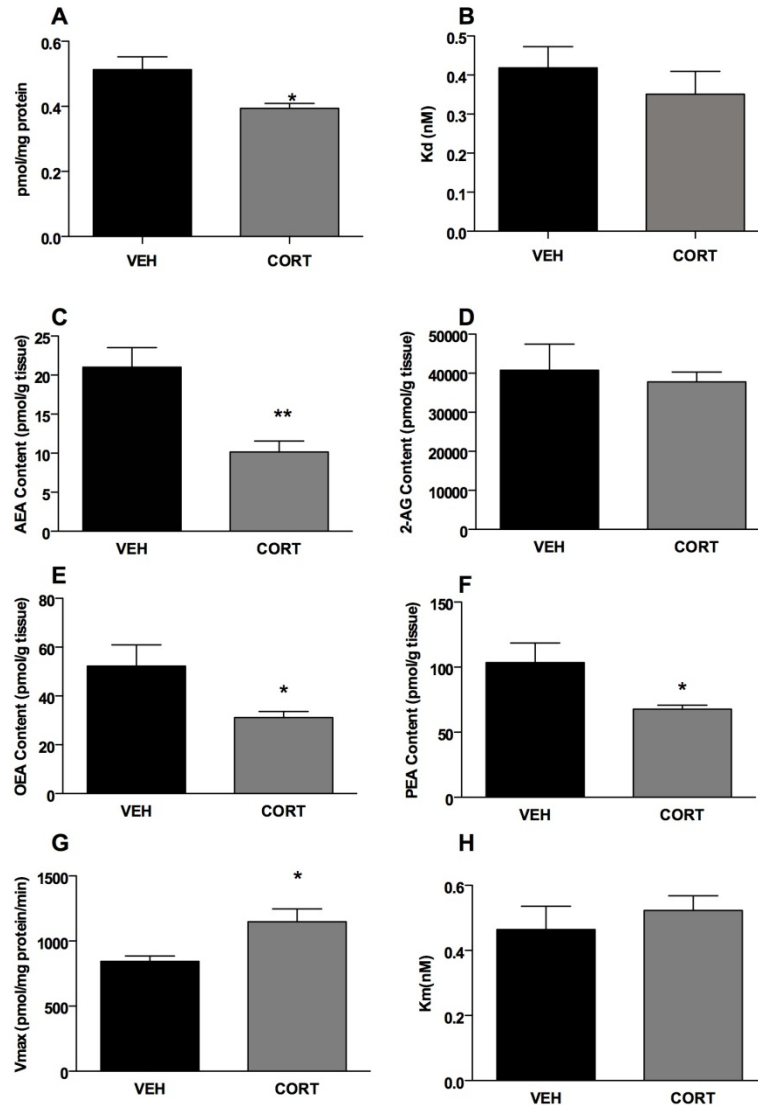


**Figure 6.1** Effect of chronic corticosterone (CORT; 100  $\mu\text{g}/\text{mL}$ ) on endocannabinoid parameters in the amygdala. (A) The binding site density ( $B_{max}$ ) of the CB<sub>1</sub> receptor was reduced by CORT treatment; (B) however there was no effect on the binding affinity ( $K_d$ ) of the CB<sub>1</sub> receptor. (C) CORT treatment reduced the tissue content of endocannabinoid anandamide (AEA), but (D) had no effect on the endocannabinoid 2-AG. (E) Consistent with the reduction in AEA content, CORT treatment increased the maximal hydrolytic activity ( $-V_{max}$ ) of the enzyme for AEA degradation fatty acid amide hydrolase (FAAH); (F) but had no effect on the binding affinity of AEA for FAAH. \*Significantly different from control ( $P < .05$ ), \*\*( $P = .0024$  and  $P = .008$ ), \*\*\*( $P = .0001$ ) ( $n = 7-8/\text{group}$  for endocannabinoid quantification;  $n = 4$  for CB<sub>1</sub> receptor binding parameters and enzyme activity).

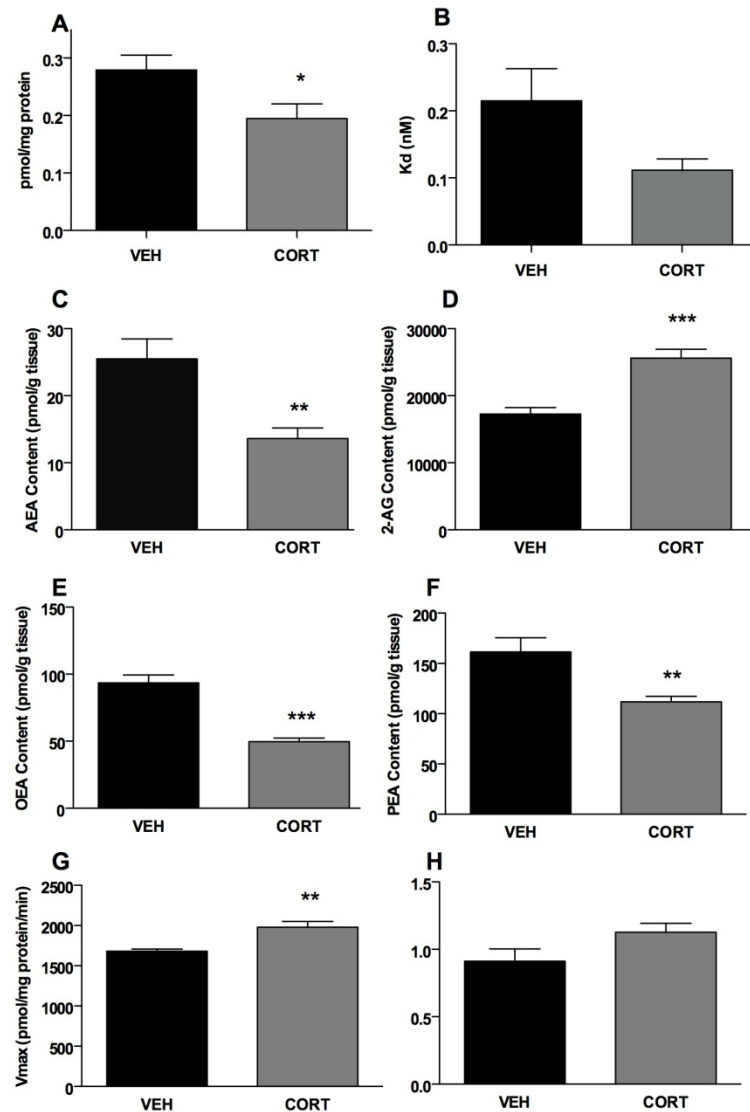


**Figure 6.2.** Effect of chronic corticosterone (CORT; 100  $\mu\text{g}/\text{mL}$ ) on endocannabinoid parameters in the hippocampus. (A) The binding site density ( $B_{\text{max}}$ ) of the CB<sub>1</sub> receptor was reduced by CORT treatment; (B) however there was no effect on the binding affinity ( $K_{\text{d}}$ ) of the CB<sub>1</sub> receptor. (C) CORT treatment reduced the tissue content of endocannabinoid anandamide (AEA), but (D) increased the content of the other endocannabinoid 2-AG. (E) Consistent with the reduction in AEA content, CORT treatment increased the maximal hydrolytic activity ( $V_{\text{max}}$ ) of the enzyme for AEA degradation fatty acid amide hydrolase (FAAH); (F) but had no effect on the binding affinity of AEA for FAAH. \*Significantly different from control ( $P < .05$ ), \*\* ( $P = .003$ ); ( $n = 9-10/\text{group}$  for endocannabinoid quantification,  $n = 4$  for CB<sub>1</sub> receptor binding parameters and enzyme activity).

**Table 6.1** The effects of chronic corticosterone administration on gene expression of the cannabinoid receptor and fatty acid amide hydrolase.

	Vehicle Treated	CORT
Amygdala		
CB <sub>1</sub> receptor	1.08±0.35	1.25±0.53
FAAH	1.10±0.18	1.19±0.25
Hippocampus		
CB <sub>1</sub> receptor	1.21±0.33	1.58±0.25
FAAH	1.22±0.19	1.86±0.59

Twenty-eight day administration of corticosterone (CORT) in the drinking water had no effect on the expression of mRNA for either the cannabinoid CB<sub>1</sub> receptor or fatty acid amide hydrolase (FAAH) within either the hippocampus or amygdala. Values denote means ±SEM and are expressed as fold changes of mRNA expression.



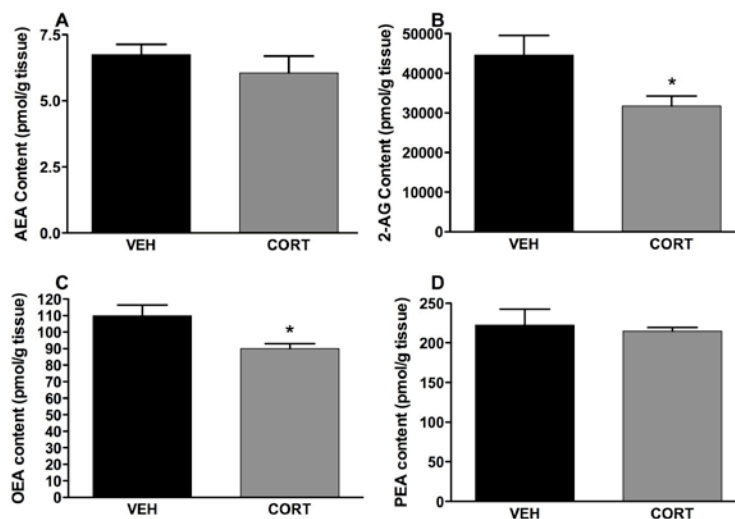


**Figure 6.3** Effect of chronic corticosterone (CORT; 100  $\mu\text{g}/\text{mL}$ ) on endocannabinoids in the hypothalamus. Chronic 4 week treatment of CORT compared to VEH mice, had no effect on (A) AEA or (D) PEA but decreased (B) 2-AG and (C) OEA. \* Notes significance of  $P < 0.05$ , \*\* $P < 0.01$ ,  $n = 4-6/\text{group}$ .

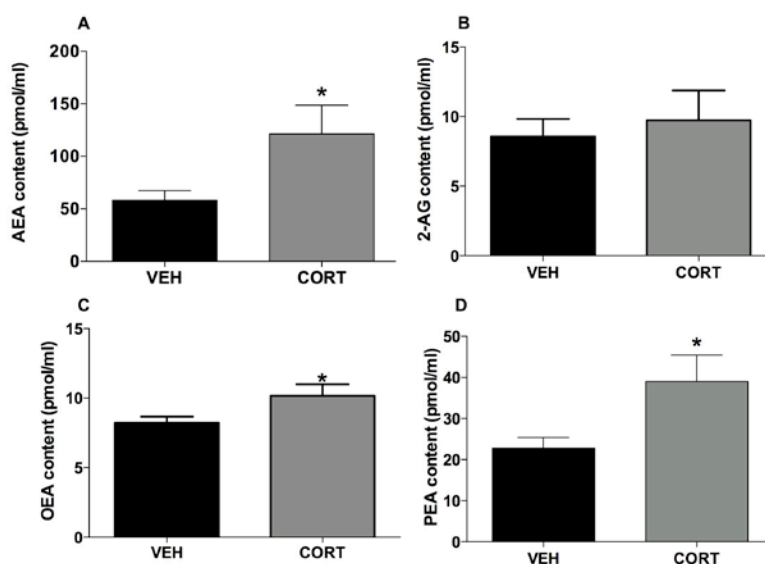


**Figure 6.4** Effect of chronic corticosterone (CORT; 100  $\mu\text{g}/\text{mL}$ ) on endocannabinoids in blood circulation. Chronic 4 week treatment of CORT compared to VEH mice, increased circulating levels of (A) AEA, (B) 2-AG, (C) OEA, and (D) PEA. \* Notes significance of  $P < 0.05$ ;  $n = 8-10/\text{gro}$

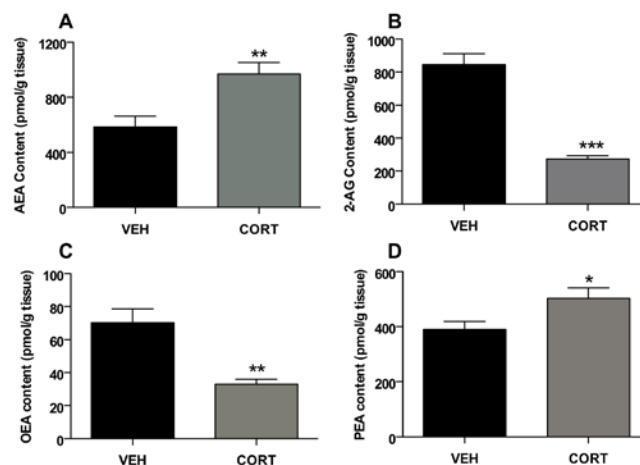


**Figure 6.5** Effect of chronic corticosterone (CORT; 100  $\mu\text{g}/\text{mL}$ ) on endocannabinoids in the liver. Chronic 4 week treatment of CORT compared to VEH treated mice, increased (A) AEA and (D) PEA content, but decreased content of (B) 2-AG, and (C) OEA. \*Notes significance of  $P < 0.05$ , \*\* $P < 0.01$ , \*\*\* $P < 0.001$ ;  $n = 8-10/\text{group}$ .

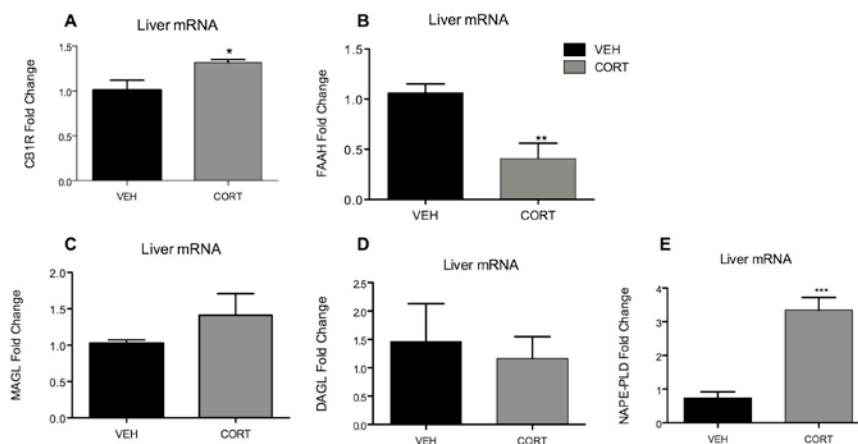


**Figure 6.6** Effect of chronic corticosterone (CORT) on mRNA expression of endocannabinoid parameters in liver. mRNA isolated from liver of VEH and CORT treated mice showed increased expression of (A)  $\text{CB}_1\text{R}$ , (C) MAGL, and (E) NAPE-PLD with decreases in (B) FAAH and (D) DAGL. \* Signifies  $P < 0.05$ , \*\* $P < 0.01$ , \*\*\* $P < 0.001$ ,  $n = 3-5/\text{group}$ .

In the hypothalamus we measured eCB levels. There was no significant difference between groups in AEA ( $t(6)=0.9194$ ,  $p=0.3933$ ) or PEA ( $t(6)=0.3870$ ,  $p=0.7121$ ) content. However, significant decreases were noted in 2-AG ( $t(7)=2.457$ ,  $p=0.0437$ ) and OEA levels ( $t(6)=2.796$ ,  $p=0.0313$ ).

Blood plasma isolated from mice treated with chronic CORT exhibited an increase in all parameters measured with significance in AEA content [ $t(15)=2.294$ ,  $P<0.05$ ; Fig. 6.4A], OEA [ $t(15)=2.159$ ,  $P<0.05$ ; 6.4C] and PEA [ $t(15)=2.458$ ,  $P<0.05$ ; 6.4D], 2-AG showed no significant difference [ $t(15)=0.4822$ ,  $P=0.6367$ ; Fig 6.4B].

Liver samples from CORT treated mice demonstrated an increase in AEA content [ $t(15)=3.267$ ,  $P<0.01$ ; Fig 6.5A] and PEA content [ $t(15)=2.422$ ,  $P<0.05$ ; Fig 6.5D]. These increases were accompanied by increased expression of the CB<sub>1</sub> receptor [ $t(5)=3.05$ ,  $P=0.0284$ ; Fig 6.6A] and decreased mRNA expression of the AEA degrading enzyme, FAAH [ $t(6)=3.756$ ,  $P<0.01$ ; Fig 6.6B] and a substantial increase in the biosynthetic AEA enzyme, NAPE-PLD [ $t(8)=5.711$ ,  $P<0.001$ ; Fig 6.6E]. Decreases were noted in 2-AG content [ $t(15)=7.019$ ,  $P<0.001$ ; Fig 6.5B] and OEA [ $t(15)=3.557$ ,  $P<0.01$ ; Fig 6.5C]. There were no significant changes in either MAGL or DAGL mRNA expression, the enzymes responsible for the degradation of 2-AG [ $t(5)=1.106$ ,  $P=.3192$ ; Fig 6.6C and  $t(6)=0.3895$ ,  $P=0.7103$ ; Fig 6.6D respectively].

WAT exhibited decreases in all eCB measures with significance in AEA content [ $t(16)=3.588$ ,  $P<0.01$ ; Fig 6.7A] The reductions in eCBs were met with decreased mRNA expression of the CB<sub>1</sub> receptor [ $t(5)=3.899$ ,  $P<0.05$ ; Fig 6.8A] and mRNA expression of FAAH [ $t(6)=2.523$ ,  $p<0.05$ ; Fig 6.8B]. Decreases were also noted in NAPE-PLD, MAGL, and DAGL, but none reached significance.

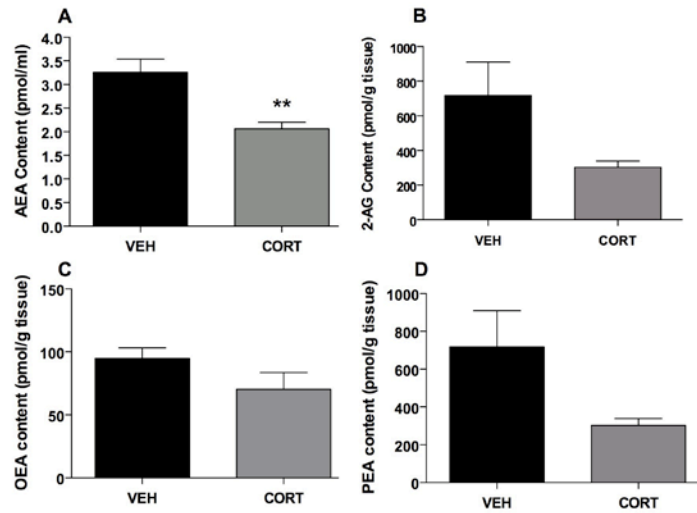


**Figure 6.7** Effect of chronic corticosterone (CORT; 100  $\mu\text{g}/\text{mL}$ ) on endocannabinoids in white adipose tissue (WAT). Chronic 4 week treatment of CORT compared to VEH treated mice, decreased WAT content of (A) AEA, (B) 2-AG, (C) OEA and (D) PEA. \*\*Notes significance of  $P < 0.01$ ;  $n = 8-1/\text{group}$ .

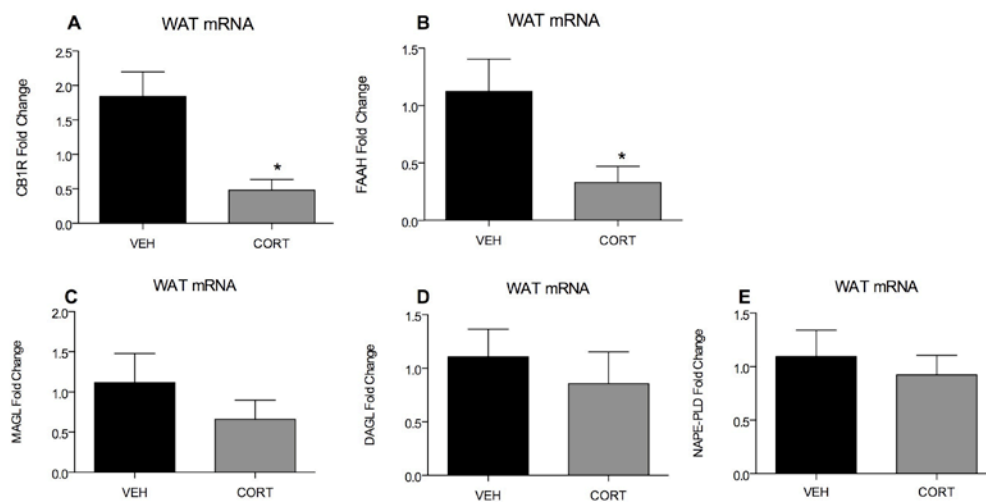
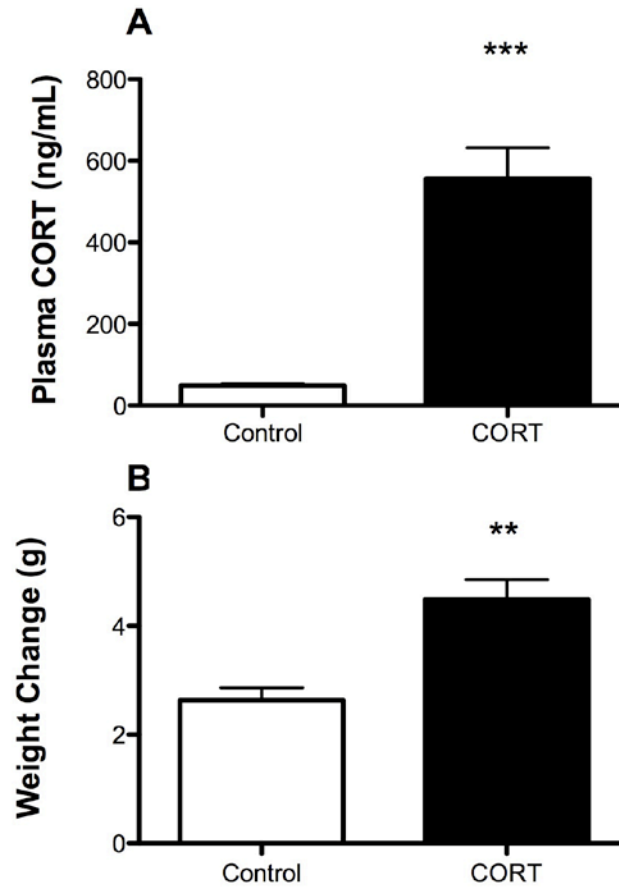


**Figure 6.8** Effect of chronic corticosterone (CORT; 100  $\mu\text{g}/\text{mL}$ ) on mRNA expression of endocannabinoid parameters in white adipose tissue (WAT). mRNA isolated from WAT of VEH and CORT treated mice showed decreased expression of (A)  $\text{CB}_1\text{R}$ , (B) FAAH, (C) MAGL, (D) DAGL, and (E) NAPE-PLD. \* Signifies  $P < 0.05$ ,  $n = 3-5/\text{group}$ .



**Supplementary Figure 6.1** *Basal levels in treated mice.* Chronic CORT treatment (100  $\mu\text{g/mL}$ ) results in (A) 10 fold elevation of plasma CORT (blood samples during light phase) and (B) a significant increase in weight gain across the 28 days of CORT exposure. \*\* Signifies  $P < .005$ .

## Discussion

In this study we demonstrated that chronic CORT delivered via the drinking water resulted in a significant decrease of CB<sub>1</sub> receptor binding in the hippocampus and amygdala, as well as a reduction of AEA within both of these limbic structures. The reduction of AEA was met by an increase in FAAH activity, suggesting that glucocorticoids likely reduce AEA through an increase in metabolic degradation as opposed to reductions in synthesis (although this wasn't directly tested and thus still remains a possibility). Additionally, chronic CORT increased 2-AG in the hippocampus, but not the amygdala.

Similar to the effects of chronic stress,<sup>250-252</sup> chronic CORT decreased CB<sub>1</sub> receptor density in the hippocampus. Chronic stress has not been found to affect CB<sub>1</sub> receptor binding in the amygdala of rats;<sup>253</sup> however it was reduced in the present study, suggesting that CB<sub>1</sub> receptor density in the amygdala is downregulated by CORT similarly to the effect in the hippocampus. It is possible that CB<sub>1</sub> receptor expression in the hippocampus is much more sensitive to CORT and as a result is downregulated by the increase in CORT secretion induced by chronic stress. This hypothesis is consistent with the fact that the hippocampus exhibits a higher level of glucocorticoid receptors than the amygdala.<sup>254</sup>

The increase in circulating CORT produced by the current regimen is equivalent to levels seen during exposure to stress (see (Karatsoreos et al., 2010)<sup>47</sup> for temporal and diurnal effects of this model on circulating levels of CORT); however, during exposure to stress the increased levels of CORT are pulsatile and transient, and not sustained at a high level as they are with the current CORT regimen. As a result, the described treatment unveiled a negative regulation of CB<sub>1</sub> receptor in the amygdala that was not seen following stress. This suggests that CB<sub>1</sub> receptor binding is negatively regulated in the amygdala, as well as the

hippocampus, but it would appear that CB<sub>1</sub> receptors within the hippocampus are more sensitive to CORT exposure than those in the amygdala.

It has been shown that the reduction in CB<sub>1</sub> receptor binding in the hippocampus following chronic stress or CORT treatment was met by a reduction in CB<sub>1</sub> receptor protein,<sup>251,253</sup> which is consistent with previous reports demonstrating that removal of CORT through ADX increases CB<sub>1</sub> mRNA in the striatum.<sup>256</sup> In the current study however, CORT did not downregulate CB<sub>1</sub> receptor mRNA suggesting that the reduction in CB<sub>1</sub> receptor binding may not be due to a downregulation of gene transcription of the CB<sub>1</sub> receptor by glucocorticoids. It is possible that the downregulation of CB<sub>1</sub> receptor mRNA may have happened at an earlier phase following glucocorticoid exposure and that by 4 weeks this effect has normalized as a compensatory response to the reductions in active receptor binding sites, but this hypothesis requires temporal studies to track CB<sub>1</sub> receptor mRNA across phases of CORT exposure.

Chronic CORT dramatically reduced AEA content within both the hippocampus and amygdala with an increase in AEA-mediated hydrolysis by FAAH, suggesting that CORT increases FAAH activity, which results in a reduction in AEA content. In support of this finding, two other fatty acid ethanolamides, which are substrates for FAAH, PEA and OEA, are also both reduced by chronic CORT. This reduction in AEA and increase in FAAH following chronic CORT directly mirrors the effects of chronic stress in both rats and mice,<sup>257-259</sup> suggesting that increases in CORT following chronic stress are likely the mediator of changes in FAAH activity and AEA content. Similar to the changes in the CB<sub>1</sub> receptor, this change in FAAH activity does not appear to be due to an upregulation of FAAH mRNA following CORT. This effect is not surprising given that glucocorticoids have been found to

exert negative regulation over FAAH transcription through activation of a glucocorticoid response element in the FAAH promoter, suggesting that glucocorticoid receptor activation would downregulate FAAH expression.<sup>261</sup> As such, a more parsimonious answer to this issue would be that chronic CORT modulates post-translational modification of FAAH in a manner that increases its hydrolytic activity. Ongoing research will seek to determine the mechanisms underlying the regulation of FAAH activity by glucocorticoids.

Chronic CORT was found to increase 2-AG in the hippocampus, but not amygdala. This finding is surprising as it is in direct contrast to the effects of CORT injections in the rat, where chronic CORT (by injection) had no effect on 2-AG in the hippocampus but increased it in the amygdala.<sup>253,261</sup> Moreover, chronic restraint stress in mice has reliably been found to increase 2-AG in both the amygdala and hippocampus where it has been hypothesized that 2-AG synthesis is increased upon repeated restraint application and that this change contributes to habituated HPA-axis response to repeated restraint stress.<sup>258,270</sup> In the rat chronic stress has been found to increase or have no effect on 2-AG in the amygdala (depending on the nature of the stress, e.g. chronic restraint vs. chronic unpredictable stress), and either reduce or have no effect on 2-AG in the hippocampus.<sup>250,251,257</sup> Thus, unlike AEA, FAAH or CB<sub>1</sub>, the regulation of 2-AG by glucocorticoids within limbic structures appears to be very complex, and likely is dependent upon the time of tissue collection following stress or glucocorticoid exposure as well as the fact that the bulk 2-AG measurements may not represent what is occurring at the synapse. As such, this aspect requires further investigation. However, given that 2-AG levels within the amygdala are reliably elevated by repeated exposure to a homotypic stressor,<sup>257-259,270</sup> it is likely that the difference in these effects from those seen following CORT injections<sup>261</sup> are due to the interactive nature of the injection



stress and the CORT levels.

These data demonstrate that chronic CORT suppresses limbic CB<sub>1</sub> receptor binding and AEA signaling, while having variable effects on 2-AG. Given the role of limbic eCB signaling in the regulation of emotional behavior,<sup>114,263</sup> these data would suggest that glucocorticoid-induced changes in limbic eCB signaling could contribute to shifts in emotional behavior, especially increases in anxiety and depression like behaviors which occur following sustained glucocorticoid exposure.<sup>264,265</sup> More interestingly in conjunction with our obese phenotype in these mice, alterations in limbic eCB signaling suggest possible changes in emotional behavior that are related to hormonally mediated obesity phenotypes. This could be particularly relevant for the growing rise of co-morbidity of mood and anxiety disorders with the increasing obesity epidemic.<sup>266-268</sup>

In the hypothalamus we note no significant changes in either mRNA expression of the CB<sub>1</sub> receptor nor in AEA levels; however, there was a decrease in 2-AG. Generally, feeding lowers, and fasting raises, hypothalamic, but not cerebellar, levels of 2-AG; however, it should be noted that these results are from rats.<sup>269</sup> Although measurements from the current study are taken at a basal state we see reduction in hypothalamic 2-AG, which occurs in response to satiation and is likely a homeostatic mechanism to prevent increases in food intake. In the CORT animals, this is probably on overdrive, that is the energy balance dysregulation is originating in the periphery and the observed changes in the hypothalamus are a compensatory response that is at least trying to keep feeding at bay to prevent unnecessary eating and facilitate the positive energy balance; however, as noted in previous chapters, regulation is not sufficient to cap food intake in CORT treated mice.

Turning to the periphery, we found differential effects in the blood, liver, and WAT.

In the liver we saw significant increases in AEA and PEA with decreases in 2-AG and OEA. Changes in CORT induced eCB levels in the liver were met by increases in mRNA expression of the CB<sub>1</sub> receptor and NAPE-PLD but decreases in FAAH. There were no changes in MAGL or DAGL. Results here would suggest an overabundance of AEA in the liver as a result of increased NAPE-PLD.<sup>270</sup> FAAH transcription is not at a sufficient level for AEA degradation. Furthermore, FAAH is not only necessary for the breakdown of AEA, but PEA and OEA as well, of which OEA levels are decreased in CORT treated mice perhaps due to its substrate competition for FAAH (although this needs to be directly tested).<sup>272,281</sup> Spill over from the liver is likely to result in increased presence in the blood of AEA, PEA, and OEA with no significant changes in 2-AG. Endocannabinoid parameters in WAT reveal a decrease in AEA, but no changes in PEA, OEA, or 2-AG. mRNA expression of FAAH was decreased as the expression of the CB<sub>1</sub> receptor, but again there were no changes in either MAGL or DAGL gene expression.

Endocannabinoid levels of WAT presented in this study from CORT treated mice vary from mouse diet induced studies and from visceral fat from obese patients, both of which show increases of 2-AG with no changes in AEA.<sup>281</sup> However, while the eCB system is rather well preserved evolutionarily,<sup>274</sup> there seems to be no clear pattern of activity in looking from mouse models or even among individuals. Circulating levels in obese females with type 2 diabetes showed increases in both AEA and 2-AG in the blood while mRNA expression in adipose tissue showed a reduction for both CB<sub>1</sub> receptor and FAAH,<sup>275</sup> but studies in men looking to link circulating eCBs and cardiometabolic risk in male obese subjects found a correlation between BMI and 2-AG, but not AEA<sup>276</sup> suggesting that several factors including hormonal cues can affect eCB dysregulation as noted by sex differences in

eCBs in the amygdala.<sup>277</sup> Perhaps these findings should come as no surprise given that sex and even racial differences can affect both fat distribution and eCB levels.<sup>278,279</sup> Findings in the current study showing decreases in AEA, and decreased expressions of FAAH and CB<sub>1</sub> receptor could shed light on cases of obesity induced by factors apart from food intake. A growing number of social science studies and even animal models of social stress are showing increases in weight gain as a result of a physiological stress.<sup>79-81</sup> Interactions between hormones and eCBs could offer insight into the obese phenotype in these models, which are easily translated into the human condition.

Endocannabinoid measurements in the liver have been more consistent across studies. Similar to CORT treated mice, liver of high-fat fed mice indicate that a high-fat diet increases hepatic anandamide owing to a major reduction in its degradation by FAAH; however, anandamide synthesis appears to be unchanged.<sup>287</sup> Because the membrane levels of the FAAH protein are not significantly altered, a high-fat diet may inhibit the activity rather than the expression of FAAH or as suggested in the CORT model; increase of AEA might also be accompanied by OEA resulting in a competition for FAAH deactivation as suggested in the CORT model. The upregulation of hepatic CB<sub>1</sub> receptor observed in mice on the high-fat diet is similar to the reported upregulation of CB<sub>1</sub> expression in CORT treated mice and could involve similar underlying mechanisms. Clinically, increased eCB tone has also been linked with the development of NAFLD.<sup>289</sup>

Induction of AEA is reported to decrease rather than increase fatty acid synthesis in rat hepatocytes through a noncannabinoid mechanism mediated by arachidonic acid, as indicated by the ability of the nonspecific FAAH inhibitor PMSF to block this effect.<sup>283</sup> Thus, four weeks of CORT treatment leads to increases in AEA, decreased mRNA expression of Srebp-

1c, and the development of NASH as noted in Chapter 5, suggesting that increased AEA decreases fatty acid synthesis in the liver. To confirm this hypothesis it would be ideal to look at AEA levels after a week of CORT treatment when fatty acid synthesis is more active. The lipogenic response to CB<sub>1</sub> receptor activation in isolated hepatocytes also argues strongly for a direct hepatic effect under in vivo conditions, although it does not rule out an additional, centrally mediated effect through neuronal or hormonal pathways. Inhibition of this lipogenic response in CB<sub>1</sub><sup>-/-</sup> mice both here and in case of high-fat diet, further confirm the lipogenic role of hepatic CB<sub>1</sub> receptor.<sup>287</sup> The overall story here suggests that increased CORT leads to increased NAPE-PLD in the liver, which then increases AEA synthesis. This mechanism likely contributes to the development of not only CORT induced obesity and subsequent increases in various metabolic parameters, but also fatty liver in control mice, as indicated by the absence of both changes in CB<sub>1</sub><sup>-/-</sup> mice on CORT.

In summary, we showed that chronic CORT treatment had differential effects on eCB parameters both centrally and peripherally. Results presented here differ from those presented by groups studying eCB regulation in cases of both chronic stress and from those studying regulation under a high fat diet, suggesting a unique and finely tuned role of the eCB system in regulating GC induced metabolic disturbances and the operation of multiple regulatory factors on the eCB system. Inferences of eCB regulation of GC action come most clearly from CB<sub>1</sub>R<sup>-/-</sup> mice as described in chapter 5 where the CORT induced metabolic syndrome phenotype was prevented by global knockout of CB<sub>1</sub> receptor; CB<sub>1</sub>R<sup>-/-</sup> mice also indicate that a lack of CB<sub>1</sub> receptor produces HPA-axis dysregulation.<sup>284</sup> However, analysis of regional concentrations of the eCB parameters sheds light into the central versus peripheral mediation of the eCB in GC mediated metabolic syndrome. In the next chapter we

make use of specific CB<sub>1</sub> receptor inhibitors and liver specific knockout of the CB<sub>1</sub> receptor in order to further elucidate central versus peripheral effects. eCB levels in mice with a normalized food

## **Chapter 7: Determination of central versus peripheral endocannabinoid regulation**

### **Abstract**

We previously reported through the use of cannabinoid CB<sub>1</sub> receptor deficient mice, the role of endocannabinoid (eCB) signaling as a mediator in glucocorticoid (GC) mediated metabolic syndrome. We have also shown that the detrimental metabolic effects of increased exposure to corticosterone (CORT) occur independently from food intake. It has recently been demonstrated that peripherally restricted CB<sub>1</sub> receptor antagonist, AM6545, is sufficient for weight-independent improvements in glucose homeostasis, fatty liver and plasma lipid profile in mice with genetic or diet-induced obesity. The aim of the current study was two-fold: first to replicate findings using pharmacological tools in the way of AM251, a global CB<sub>1</sub> receptor antagonist, and secondly to determine the role of eCB signaling in GC-mediated obesity and mouse model of the metabolic syndrome independent of central feeding effects by selectively targeting peripheral CB<sub>1</sub> receptors. With the exception of circulating triglyceride levels which were increased, AM251 treatment was able to prevent the negative metabolic actions of CORT. Subsequent CORT induced increase in total body weight, the weight of the abdominal/gonadal fat pads, and hyperphagia were substantially attenuated with the peripheral antagonist AM6545, indicating that peripheral CB<sub>1</sub> receptor activation contributes to hormonal and metabolic abnormalities and continues to regulate appetitive signals. In conjunction with prior studies, this data suggest that GC exposure produces an elevation of tonic eCB signaling which promotes the development of metabolic syndrome, through changes in feeding behavior in conjunction with peripheral metabolic processes.

## Rationale

In the previous chapters we have established a role for endocannabinoid (eCB) system signaling in alternative models of metabolic syndrome. In mouse models where circadian rhythms of clock genes and glucocorticoid (GC) signaling is blunted (Chapter 3) or in the case of increased corticosterone (CORT) exposure with blunted clock gene expression (Chapter 4), both were resistant to metabolic dysregulation by global knockout of the CB<sub>1</sub> receptor. Both models also led to variations in eCB signaling (Chapter 5 and Chapter 6). In conjunction with eCB system measurements, it appears that at least in the CORT water model, CORT increases NAPE-PLD in the liver resulting in increased AEA synthesis, which spills into the circulation. This increased AEA in the liver, and possibly other sites reached by the circulation, drives a shift in metabolic function that accelerates carbohydrate oxidation and compromises fat metabolism, resulting in the development of fatty liver and fat stores in the adipose tissue. These observations along with subtle changes in activity level in CORT CB<sub>1</sub>R<sup>-/-</sup> mice (Chapter 5) and the maintained weight gain in pair-fed CORT mice (Chapter 4), suggest that eCBs and CB<sub>1</sub> receptor regulate peripheral energy metabolism. While we are aware that the weight effect is in part due to central changes as noted by decreased food intake (Chapter 5) and CORT induced changes in eCB parameters in the limbic region (Chapter 6), the aim here was to parse central and peripheral endocannabinoid regulation to find the main site of interaction between GCs and the eCB system. In this way we first made use of the global CB<sub>1</sub> receptor antagonist, AM251 to replicate the effects of the global knockout and identify any side effects of daily injection. We next made use of the newly available and characterized peripheral specific CB<sub>1</sub> receptor antagonist, AM6545.<sup>251</sup>

Given the success of the peripheral antagonist, we moved to look at the effects in a

hepatocyte specific  $CB_1R^{-/-}$  mouse ( $LCB_1R^{-/-}$ ). While the CORT induced phenotype is blocked at every level in the  $CB_1R$  global knockout, the role of adipose tissue is minor compared with that of the liver.

## Experiment design

Three different cohorts of animals were used to carry the following studies. In the first group 26 mice were used in total, with 5 in both vehicle and CORT treated groups receiving saline injections and 8 in both vehicle and CORT treated groups receiving the global antagonist AM251. The second group receiving the peripheral antagonist AM6545 was run as the AM251 study. In the final study making use of  $LCB_1R^{-/-}$  mice, 28 mice in total were used, 6 WT on vehicle, 6  $LCB_1R^{-/-}$  on vehicle, 8 WT on CORT, and 8  $LCB_1R^{-/-}$  on CORT.

## Results

There was a significant interaction between CORT and treatment of both AM251 ( $F(1,15)=5.102$ ,  $p=0.0392$ ) and AM6545 ( $F(1,20)=4.745$ ,  $p=0.0416$ ; Fig 7.1A) on weight gain. Bonferroni posthoc revealed that the effect of CORT was only present in saline injected mice ( $p<0.05$ ). This weight loss can only partially be contributed to reduced adiposity as gross measures in WAT, while decreased (Fig 7.1 E, 7.2B-E, 7.3B-E), are not completely absent in mice treated with AM251 or AM6545. However, oil red o staining demonstrates decreased presence of lipids in the livers of CORT treated mice with injections of either AM251 (Fig 7.2 F-I) and AM6545 (Fig 7.3 F-I), suggesting that liver weights are also decreased as with  $CB_1R^{-/-}$  CORT treated mice in Chapter 5.



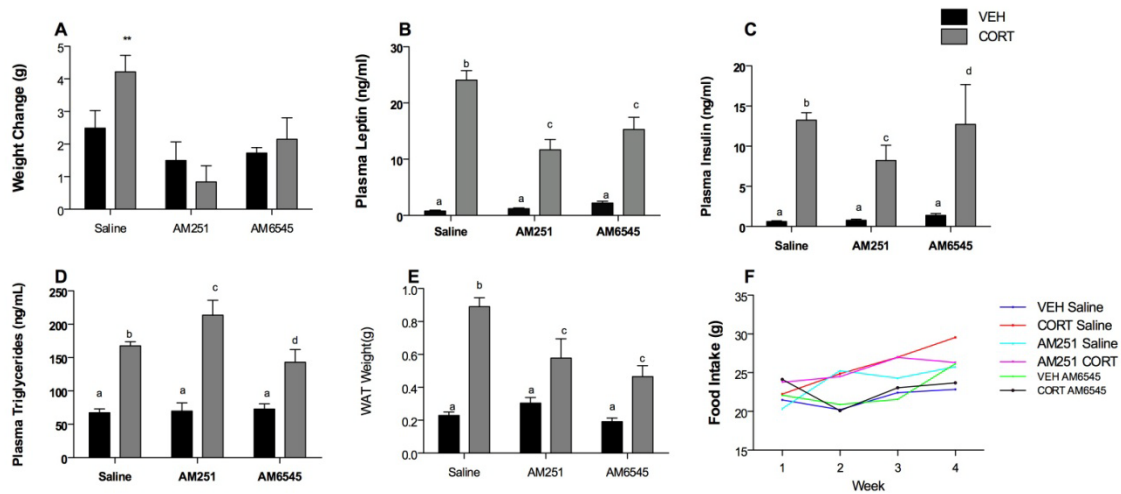


**Figure 7.1** Metabolic effects of chronic treatment with AM251 and AM6545 in CORT treated mice concurrently for 4 weeks. Both drugs delivered at 10/mg/kg/d, i.p, were able to reduce (A) weight change, (E) adiposity, and (B) plasma leptin. AM251 was able to reduce (C) plasma insulin while there was no change in mice treated with AM6545. Conversely, AM6545 was able to reduce circulating (D) triglyceride levels while levels seemed to be increased in AM251 treated mice. (F) Food intake was also decreased with both drugs but to a larger extent with AM6545. Bars with the same letter are not statistically different from one another. \*\*indicates  $P < 0.01$  as determined by two-way ANOVA and Bonferroni posthoc.

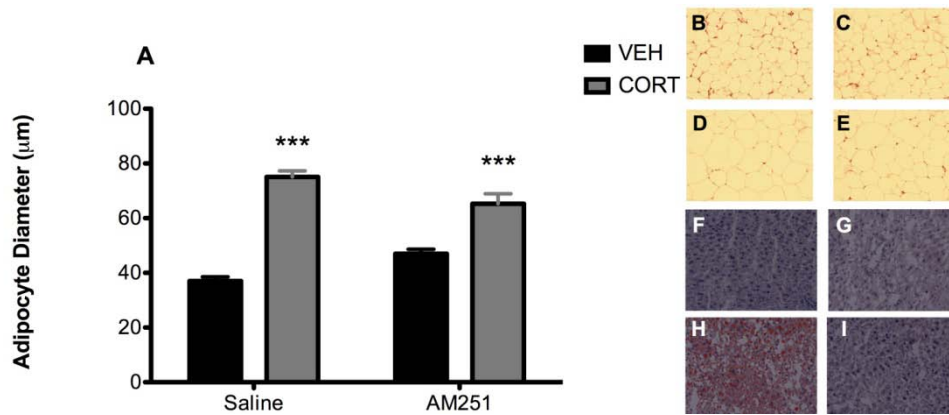


**Figure 7.2** *Histology of liver and WAT in AM251 treated mice.* (A) Adipocyte length as quantified by random selection of adipocytes (n=5-8/group). Representative images of H&E stain of WAT isolated from (B) Saline injected VEH, (C) AM251 injected VEH, (D) Saline CORT and (E) AM251 CORT, images taken at 10x. Oil red O staining demonstrated the ability of (I) AM251 to prevent the development of NAFLD as present in (H) saline injected CORT treated mice and resembled healthy livers of (F) saline VEH and (C) AM251 VEH mice. Representative liver stains shown at 10x. N=5-8/group. Bars with the same letter do not statistically differ from one another.

Patterns of circulating hormones exhibited intermediate effects in leptin and insulin in CORT treated mice with AM251 treatment compared to control mice. Interestingly, AM251 CORT mice showed increased levels of circulating triglycerides ( $F(1,15)=78.13$ ,  $p<0.001$ ), whereas this level was decreased with AM6545 injections ( $F(1,60)=8.170$ ,  $p=0.0114$ ). As with AM251, AM645 also showed intermediate levels of insulin and leptin.

Specific knockout of the CB<sub>1</sub> receptor in the liver (LCB<sub>1</sub>R<sup>-/-</sup>) was unable to either prevent weight gain in CORT treated mice, or improve overall adipose levels, and circulating leptin levels (Fig 7.4 A, B, and E respectively). Insulin levels in LCB<sub>1</sub>R<sup>-/-</sup> CORT treated mice were statistically greater than in WT CORT mice (interaction  $F(1, 21)=4.717$ ;  $p=0.0415$ , Fig 7.4F). Interestingly, despite no significant decrease in gross WAT weight, adipocyte size was decreased in these mice (Fig 7.5 A-E). LCB<sub>1</sub>R<sup>-/-</sup> mice also showed an overall decrease in liver weight, though not to the levels of control mice (interaction  $F(1,19)=4.755$ ,  $p=0.042$ , genotype  $F(1,19)=10.54$ ,  $p=0.0042$ ; Fig 7.4C). This data is consistent with the decreased lipid content in LCB<sub>1</sub>R<sup>-/-</sup> CORT treated mice as noted by oil red o stain (Fig 7.5 G-J), and decreased circulation of triglycerides (interaction  $F(1,23)=19.04$ ;  $p=0.0002$ ; genotype  $F(1,23)=10.65$ ,  $p=0.0034$ ; Fig 7.4D). Decreased ALT levels, an indicator of decreased liver damage in LCB<sub>1</sub>R<sup>-/-</sup> mice further validated the large effect of eCB signaling in the liver. ALT levels were noted by an interaction between groups ( $F(1,22)=13.23$ ;  $p=0.0015$ ) with posttest revealing that increased levels were present in WT CORT mice alone ( $p<0.01$ , Fig 7.5F)

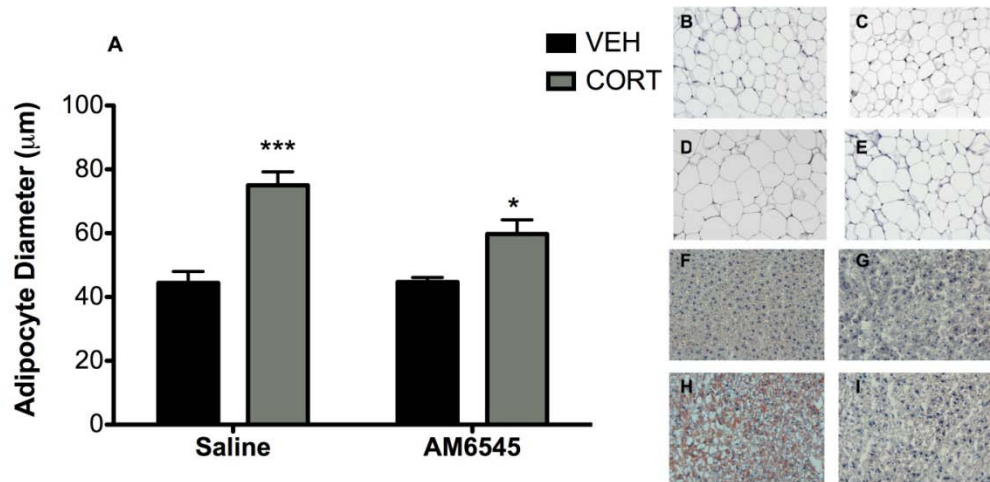


**Figure 7.3** *Histology of liver and WAT in AM6545 CORT treated mice.* (A) Adipocyte length as quantified by random selection of adipocytes (n=5-8/group). Representative images of H&E staining of WAT isolated from (B) Saline injected VEH, (C) AM6545 injected VEH, (D) Saline CORT and (E) AM6545 CORT, images taken at 10x. Oil red O staining demonstrated the ability of (I) AM6545 to prevent the development of NAFLD as present in (H) saline injected CORT treated mice and resembled healthy livers of (F) saline VEH and (G) AM6545 VEH mice. Representative liver stains shown at 10x. N=5-8/group. Bars with the same letter do not statistically differ from one another.

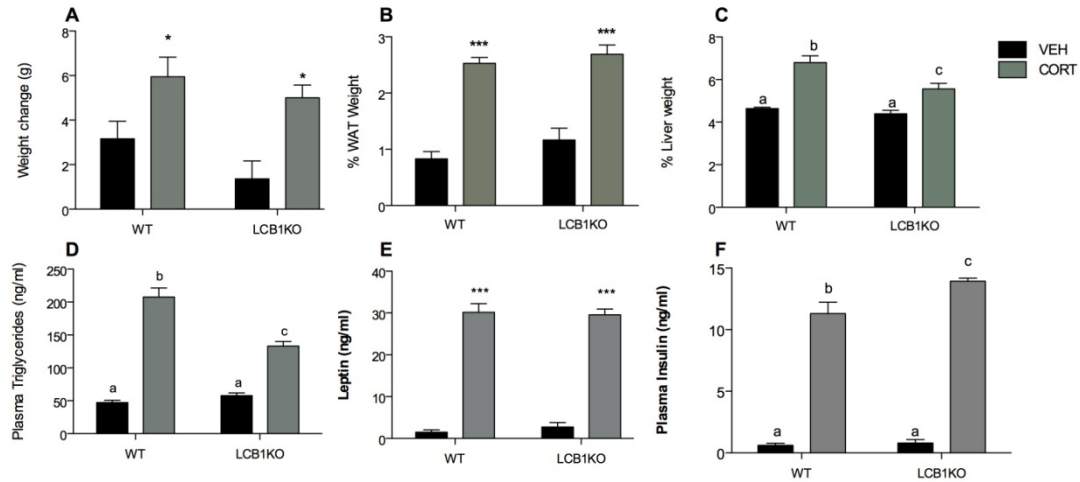


**Figure 7.4** *Metabolic effects of chronic CORT treatment in  $LCB_1R^{-/-}$  mice.* Specific knockout of the  $CB_1$  receptor in hepatic cells did not prevent CORT induced increases in (A) weight change, (B) adiposity, or (E) circulating leptin, and resulted in a slight increase of circulating (F) insulin. However, hepatic cell knockout in CORT treated mice was able to decrease overall (C) liver weight and circulating (D) triglycerides,  $n=6-8/\text{group}$ . Bars with the same letter are not statistically different from one another as determined by two-way ANOVA ( $\pm$ SEM). \* $P<0.05$ , \*\*\* $P<0.001$ .

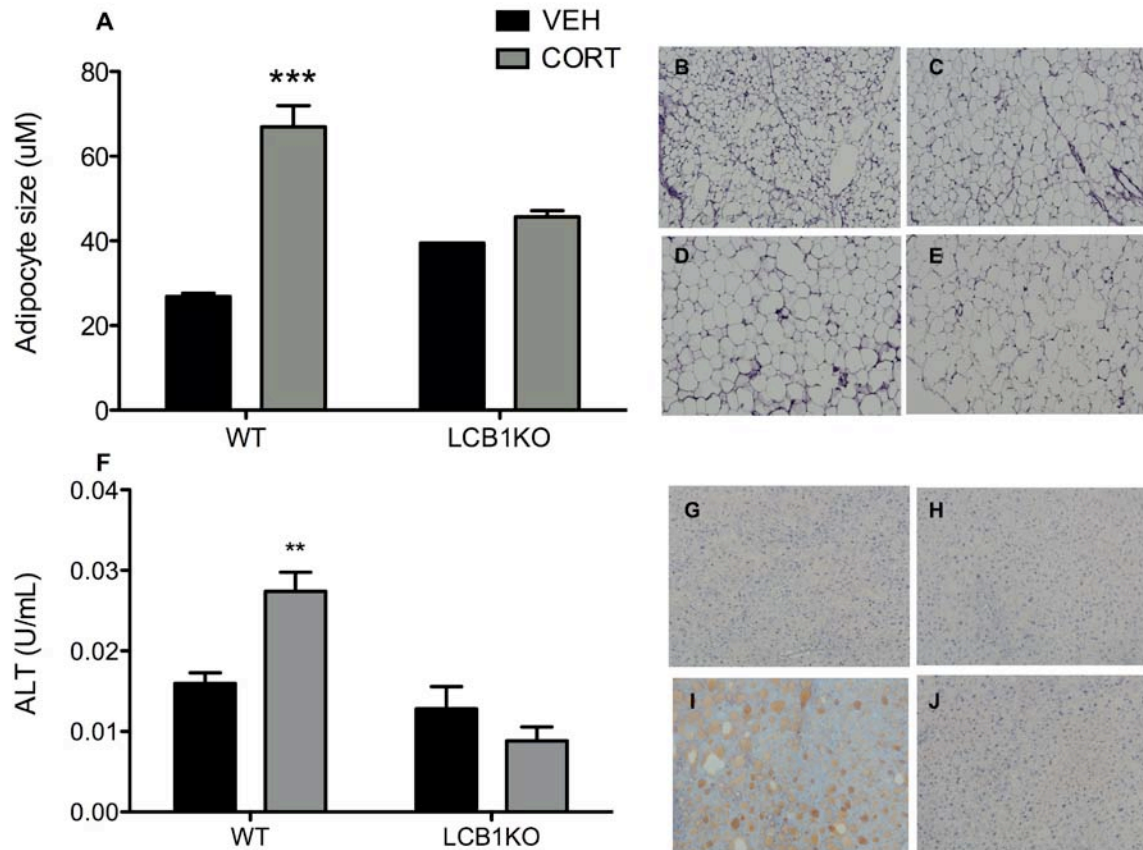


**Figure 7.5** Histology of liver and WAT in  $LCB_1R$  knockout *CORT* treated mice. (A) Adipocyte length as quantified by random selection of adipocytes ( $n=5-8$ /group), was decreased in liver specific ( $LCB_1KO$ ) mice. Representative images of H&E staining of WAT isolated from (B) WT VEH, (C)  $LCB_1KO$  VEH, (D) WT *CORT* and (E)  $LCB_1KO$  *CORT*, images taken at 10x. Oil red O staining demonstrated the ability of (J)  $LCB_1KO$  to prevent the development of NAFLD as present in (I) saline injected *CORT* treated mice and resembled healthy livers of (G) WT VEH and (H)  $LCB_1KO$  VEH mice. Representative liver stains shown at 10x.  $N=5-8$ /group. Bars with the same letter do not statistically differ from one another. (F) ALT, an indicator of liver damage is also reduced in  $LCB_1R$  KO mice.

## **Discussion:**

In this chapter, we confirmed findings in Chapter 5 that a global inhibition of eCB signaling through the CB<sub>1</sub> receptor prevents CORT induced metabolic anomalies with the global CB<sub>1</sub> receptor antagonist AM251 on all levels including weight gain, adiposity, circulating levels of leptin and insulin, as well as prevent the development of NAFLD. Additionally, AM251 resulted in an increase in circulating levels of triglycerides. It has been suggested by others that increases in circulating triglycerides are the result of an increase in clearance rate,<sup>286</sup> however, we would need to measure VLDL particle and TG transport rates to confidently say this was the case. Interestingly, concurrent treatment of AM251 and CORT did not result in decreased food intake until the final week of treatment, unlike the decreased intake that was noted in global knockout mice. It is also possible that food intake was impaired in the first few days of treatment but regained to levels of untreated animals as noted in studies of high fat diets, though the anorectic affect varies across studies.<sup>287,288</sup>

The primary aim of this paper was to separate the central and peripheral affects of CB<sub>1</sub>R blockade. As such, and having seen no clear negative side effects of daily chronic injections, we made use of the peripheral specific CB<sub>1</sub> receptor antagonist AM6545. Concurrent treatment with AM6545 and CORT resulted in an absence of weight gain and a decrease in adiposity, and circulating levels of leptin, insulin, and triglycerides, although the latter were not to the extent of levels in VEH mice. AM6545 also prevented the development of NAFLD. Despite lack of AM6545 penetration into the brain,<sup>251</sup> mice on the drug still showed decreased food intake possibly through responses to fast-fed hormonal cues coming from adipose tissue among other possible communication axes.<sup>289</sup> Studies have suggested that the orexigenic action of intestinal eCBs occurs via stimulation of CB<sub>1</sub> receptor located in

vagal afferent neurons, in particular, that CB1 receptors on afferent vagal neurons may be involved in the transmission and processing of gut food-stimulated signals important in the control of food intake and meal size.<sup>290,291</sup> However, a more recent study has demonstrated that neither vagal gut afferents, nor gut afferents traveling via the sympathetic nervous system, are required for Rimonabant to inhibit food intake.<sup>292</sup> If this is indeed the case, it will be important to determine the exact location of the eCB control of residual feeding.

In conjunction with results from previous chapters, the ability of AM6545 to prevent weight gain further suggested a strong role in liver eCB signaling as a large contributor to metabolic abnormalities noted in WT CORT mice. To confirm this hypothesis, we made use of hepatocyte specific knockout of the CB<sub>1</sub>R (LCB<sub>1</sub>R<sup>-/-</sup>). CORT treatment in LCB<sub>1</sub>R<sup>-/-</sup> mice revealed a unique role of liver endocannabinoid signaling, whereby liver knockout was not sufficient to prevent weight gain, adiposity or circulating leptin levels (results consistent with the remaining adipose levels); however, knockout here did result in decreased levels of circulating triglycerides and prevented the development of NAFLD. Unfortunately, we were unable to monitor food intake in these mice as they were a gift from collaborators at the NIH and had to remain in quarantine during the duration of the study.

In summary, using a peripherally-only active CB1 antagonist, we showed that the endocannabinoid system is a mediator of CORT induced metabolic syndrome primarily through peripheral mechanisms. Although findings strongly implicate hepatic CB<sub>1</sub> receptors in the development of hormonal induced obesity and related metabolic changes, they do not exclude the possibility that endocannabinoids acting on CB<sub>1</sub> receptors in the gut, adipose tissue, or vagus nerve, or communication between these organs, which may occur through neural pathways, may also exist. Further, residual weight and lipid clearance in the LCB<sub>1</sub>R-



/- mice could also be the result of CB<sub>1</sub>R in the stellate cells of the liver which have been shown to activate hepatic lipogenesis via paracrine system in mice chronically exposed to ethanol as may be the case here as CORT is dissolved in 1% ethanol.<sup>293</sup>

## **Chapter 8: Future Directions and Concluding Remarks**

### **Future Directions**

Studies presented in the previous chapters revealed that a disruption in external light cues on circadian (daily) rhythms resulted in altered hypothalamic pituitary adrenal (HPA) axis activity and a concurrent decrease in clock gene expression. Alternatively, an increase in circulating corticosterones (CORT) also resulted in altered clock gene expression. Both phenotypes altered metabolic regulation, resulting in increased weight gain, adiposity, developed NAFLD, and showed imbalances in hormones secretion. While clock gene expression likely plays a role in both mouse models through fluctuations of CORT, it is difficult to see where the pathways interact, rather than work independently. However, the endocannabinoid (eCB) system, which is well documented in the adaptive stress response and is itself regulated by glucocorticoid fluctuations and is further present in most peripheral organs where it regulates energy homeostasis, proved to be vital in the pathologies noted in our mouse models. Although analyzed in greater detail in the high CORT model, we observed the ability of endocannabinoid inhibition through the CB<sub>1</sub> receptor to prevent weight gain and high hormonal levels in both circadian shifted (low CORT) and exogenously delivered (high) CORT models.

In order to move forward with the circadian disrupted model, it would be ideal to determine the precise mechanism of action regarding the decreased GC circulation noted in the LD10 mice. Future experiments will seek to determine (1) if the noted down-regulation was preceded by an upregulation at an earlier time point as noted in other models of hypocortisolism,<sup>50,59</sup> (2) the down-regulation of specific receptors on different levels of the axis (hypothalamus, pituitary, adrenals, target cells), (3) reduced biosynthesis or depletion at

the various levels of the HPA axis yet to be measured (ACTH, adrenal corticosterone levels) and/or (4) increased negative feedback sensitivity to GCs. Given that low levels of GCs can lead to autoimmunity and inflammation as a result of compensatory hyperactivity of other mediators, it would also be interesting to fully study the impact of an immune challenge in this model of circadian disruption.

Additionally, we plan to look at the functional role of CORT in circadian shifted mice through CORT replacement. We hypothesize here that restoration in CORT levels will subsequently increase clock gene expression to the levels of control mice. As a preliminary study, we decided to continue with our CORT drinking model and from week one gave mice either water, VEH or CORT to drink while exposed to either a 24 hour day (12 hour light:12 hour dark) or a 20 hour day (10 hour light:10 hour dark).

Weekly measurements revealed a significant increase in weight change in CORT LD10 mice compared to VEH LD12 and water LD12 mice starting at week 3 as noted by two-way ANOVA and subsequent posthoc test ( $p < 0.05$ ; Fig 8.1A). Percentage of body fat showed a main effect of CORT treatment ( $F(1,50) = 42.03$ ,  $p < 0.0001$ ; Fig 8.1B). Unfortunately, VEH treatment seemed to have a negative effect on weight gain and prevented LD10 mice from gaining weight.

Metabolic parameters showed a similar additive effect when CORT treatment was paired with a LD10 cycle. Analysis of treatments across the day showed an increase in insulin levels at ZT12 in CORT LD12 mice compared to VEH LD12 and VEH LD10 mice ( $p < 0.01$ ; Fig 8.2A). CORT LD10 mice had greater levels at all measured time points. Leptin levels exhibited increased levels in CORT LD12 and CORT LD10 mice compared to both VEH

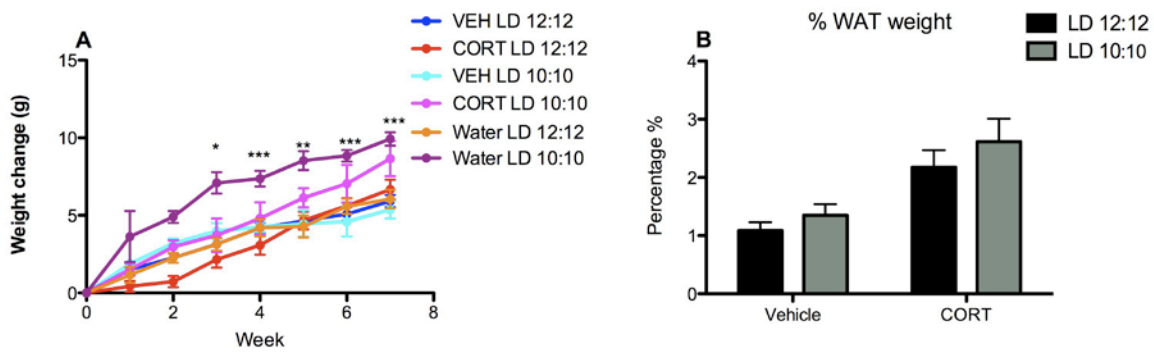


**Figure 8.1** Simultaneous CORT treatment and altered light cycle have an additive effect on weight gain and adiposity. Mice were given water, VEH (vehicle treatment of 1% ethanol in water), or 25  $\mu\text{g}/\text{mL}$  CORT (corticosterone dissolved in 1% ethanol) and placed on either a 12 hour light:12 hour dark or a 10 hour light: 10 hour dark light system. (A) Shifting alone on a water solution significantly increased weight compared to LD12 mice given water compared to VEH LD12 mice at every time point starting at week 3. (B) Overall adiposity was increased in CORT treated mice in both lighting conditions. \* $P < 0.05$ , \*\* $P < 0.01$ , \*\*\* $P < 0.001$ ;  $n = 13-15/\text{group}$ .

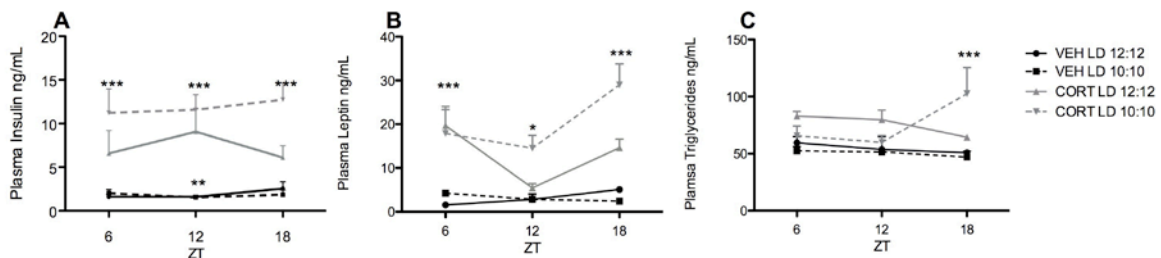


**Figure 8.2** Metabolic effect of simultaneous CORT treatment and altered light cycle. (A) Plasma insulin was significantly increased in CORT treated mice at all time points in CORT LD10 mice and at ZT 12 in CORT LD12 mice. (B) Plasma leptin was also increased in both CORT treatments at ZT 6 and at ZT12 and 18 in CORT LD10 mice compared to VEH mice. (C) Plasma triglycerides in CORT LD10 mice are at comparable levels of VEH mice at all time points but ZT 18 where they are significantly higher. \* $P < 0.05$ , \*\* $P < 0.01$ , \*\*\* $P < 0.001$ ,  $n = 4-5/\text{group}$  and time point.

groups at ZT6 and at ZT18 CORT LD10 mice had greater levels than all other experimental groups ( $p < 0.001$ ; Fig 8.2B). Interestingly, CORT LD10 mice had levels of triglycerides comparable to both VEH groups, and lower than CORT LD12 mice, at ZT 6 and ZT 12; but had significantly higher levels than all other experimental groups at ZT 18 ( $p < 0.001$ ; Fig 8.2C).

While CORT treatment was unable to reverse the physiological effects of a disrupted light cycle, treatment did appear to reestablish rhythmicity in clock gene expression. This trend was most clearly seen in *Per1* (Fig 8.3B) and *Per2* (Fig 8.3C) gene expression in WAT. *Per1* expression of both VEH LD12 mice ( $F(2,12)=5.291$ ;  $p=0.0271$ ) and CORT LD10 ( $F(2,12)=5.181$ ;  $p=0.0286$ ) exhibited rhythmicity while expression in VEH LD10 and CORT LD12 mice remained flat. This blunted expression in VEH LD10 and CORT LD12 resulted in decreased expression at ZT12 compared to both VEH LD12 and CORT LD10 ( $p < 0.01$ ). A similar trend was seen for *Per2* gene expression with rhythmicity in VEH LD12 ( $F(2,12)=22.36$ ;  $p < 0.001$ ; Fig 8.3C) and CORT LD10 ( $F(2,12)=5.35$ ,  $p=0.0365$ ). Rather than a flat expression, VEH LD10 mice and CORT LD12 mice exhibited a rhythmic pattern of *Per2* gene expression ( $F(2,12)=13.51$ ;  $p=0.0014$ ) and  $F(2,13)=54.67$ ;  $p < 0.0001$  respectively), but instead of increased expression at ZT12 VEH LD10 had their nadir while CORT LD12 mice had an intermediate expression as increased expression is not noted until ZT18. This differential expression between groups resulted in a difference in expression between VEH LD12 and VEH LD10 at ZT 6 ( $p < 0.05$ ). At ZT12 VEH LD10 and CORT LD12 had significantly lower expression ( $p < 0.001$ ) and higher expression at ZT18 ( $p < 0.05$ ) compared to VEH LD12 and CORT LD10. CORT LD10 mice showed an intermediate expression in mRNA expression of *Per1* in the liver showing no significant difference from either VEH

LD12 or VEH LD10. VEH LD12 was, however, greater at all time points and significantly so at ZT12 ( $p < 0.05$ ) compared to VEH LD10 mice. Expression patterns of Per2 mRNA in the liver are a bit more complicated and does not seem to follow the trends noted in WAT. Both VEH LD12 ( $F(2,10)=37.08$ ,  $p < 0.0001$ ) and VEH LD10 ( $F(2,12)=4.58$ ,  $p=0.0387$ ) showed a rhythmic expression of Per2 gene expression (Fig 8.3E) but seemed to be in the reverse of one another with increased expression in VEH LD12 at ZT18 and nadir at ZT6 while VEH LD10 had increased expression at ZT6 and a nadir at ZT12 with little increase at ZT18.

This CORT replacement study needs to be repeated using a means of CORT administration that does not require ethanol, but, preliminary results are promising with elevations in CORT in the shifting mice corresponding to increased clock gene expression to levels comparable to VEH non disrupted mice. How elevations in clock gene expression translate to possible metabolic, cognitive decline, or behaviour,<sup>166</sup> are yet to be fully determined, but Chapter 3 and 4 would suggest that a misalignment in the expression of enzyme and receptor systems could be to blame. Development of a means to keep these systems in sync could be vital in treating the metabolic syndrome.

Future studies also aim to characterize the possible unique role that the eCB system plays in the circadian disrupted mice. It could be the case here that chronic disruption acts like a chronic stressor. Prior studies have shown repeated activation of the HPA-axis by restraint stress also demonstrates habituation as measured by a progressive decrease in plasma corticosterone with increasing numbers of restraint episodes.<sup>150</sup> The eCB systems aid in this response through increases of 2-AG in the hypothalamus.<sup>150</sup> Given that we see no difference in food intake in disrupted mice, activation of the system on this level does not seem to affect

food intake, thus it remains to be determined how cross talk between the brain and the periphery leads to metabolic changes in these mice.

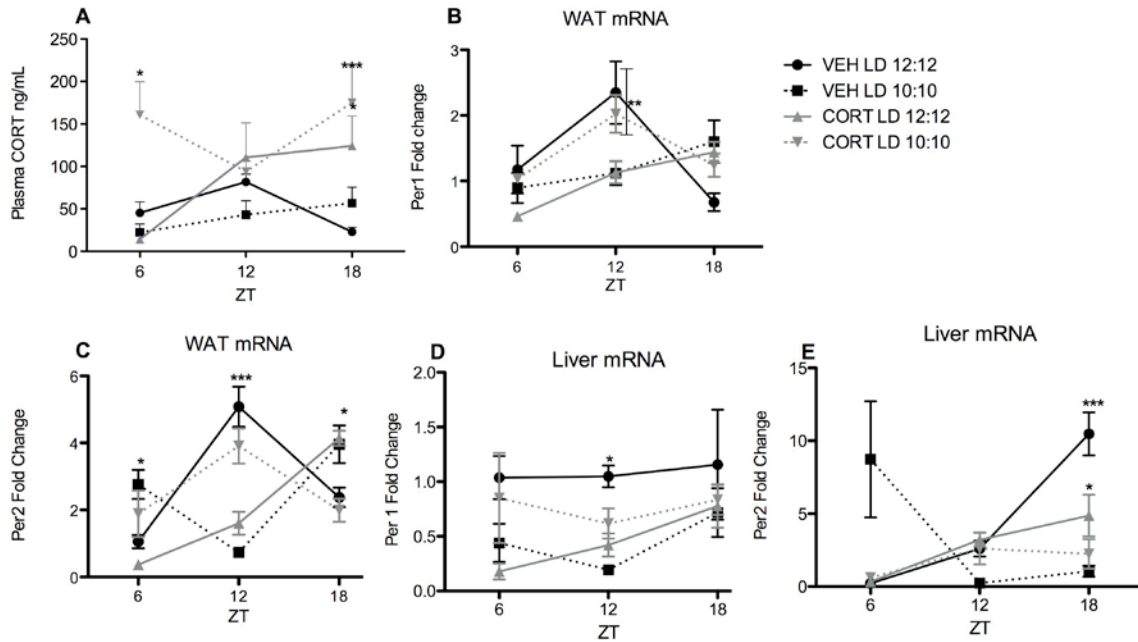


**Figure 8.3** Simultaneous CORT treatment and altered light cycle show a unique interaction in circulating CORT levels and clock gene expression. (A) Plasma CORT is decreased in VEH LD10 mice compared to VEH LD12 mice at all times points where as it is increased in CORT LD 12 mice. CORT LD10 mice have significantly greater levels at ZT 6 and ZT 18. In white adipose tissue (WAT), clock gene expression of (B) Per1 and (C) Per2 is decreased in VEH LD10 mice and CORT LD12 mice but CORT LD10 mice exhibit similar expression as VEH LD12 mice. A similar pattern of expression is noted in (D) Per1 mRNA in the liver with CORT LD10 demonstrating an intermediate expression. All groups had reduced (E) Per2 mRNA in the liver compared to VEH LD12 mice.

## **Concluding Remarks**

### **Environmental experience**

Since stressful experiences do not exist in a vacuum, it is important to study their existence in all environments and forms, as highlighted in this work though novel means to alter HPA-axis activity. Disturbances in environmental lighting cues and exogenous CORT in the drinking water disturbed endogenous CORT circulating levels and rhythm and led to the dysregulation of circadian rhythms and eCB signaling. This effect was especially noted in the periphery leading to impaired energy metabolism. CORT treatment did lead to decreases of CB<sub>1</sub>R binding site density in both the hippocampus and amygdala and also reduced AEA content and increased FAAH activity within both structures, suggesting that emotional state can also play a role in the CORT induced phenotype and as increased GC have been well linked to depression.<sup>8</sup> Since the social environment impacts the body in large part through the brain, future research should explore brain body crosstalk and how emotional state can affect the periphery, including metabolism. One possibility, as touched upon in previous sections, is the desynchronization between regulatory systems as the result of circadian disruption. Given the tightly and finely tuned regulation of the endocannabinoid system on stress and the stress response, circadian rhythm disruption could result in eCB signaling that acts to regulate CORT levels and prepare the system for mediating a response to an acute stressor, while simultaneously producing a maladaptive response elsewhere. For this reason, moving forward it is necessary to determine the precise mechanism of action regarding the decreased GC circulation in circadian disrupted mice and the level of eCB interaction.



With this mindset, researchers and policy makers are beginning to pay more attention to the “ecology of stress” because this concept is able to integrate both environmental and biological mechanisms to explain health disparities. Residential chronic stress is of particular interest because it is difficult or impossible to avoid; moreover, it is present on a regular basis, as the residential environment is part of daily living. Again, it is these everyday stressors- e.g. crowding, noise pollution, violence-that have been shown to have a greater effect on long-term well being than the less frequent, but major class of stressors generally referred to as life events.<sup>8</sup> Neighborhood stress is also interesting because it goes beyond the individual and can lead to the deterioration of the capacity of the population within a neighborhood to resist the pathological effects of ambient stress. Social structures, such as those found at the neighborhood level, determine at least in part, the exposure of individuals to stressors, as well as stress-buffering resources. Stressors presented in such an environment can include reduced or lack of access to opportunity or to the necessary means to achieve ends, as well as structural reduction in available alternatives or choices.<sup>294</sup>

Hypercortisolism has been linked to cognitive decline, immunosuppression, obesity and insulin resistance making it, theoretically, a key biological mechanism, linking disadvantage to poor health.<sup>21</sup> However, the experimental evidence linking chronic stress to elevated cortisol has been mixed.<sup>14</sup> Cortisol increases in response to acute stressors in laboratory settings have been well reported, but there is inconsistent evidence concerning the effects of long-term exposure to chronically stressful environments. Studies looking at individuals at varying degrees of employment and the impact of job-demand and job-control work stress on cortisol response on waking and throughout the day, found varying outcomes for males and females depending on job demands versus job control and depending, as well,

on levels of SES.<sup>295</sup> Mainly, low job control was associated with elevated cortisol throughout the day in men while job demands influenced cortisol over the day only in women. The greatest cortisol output was recorded from lower SES women who experienced high job demands. Low job control was more common in lower than higher SES men. Cortisol responses to waking were affected by job demands but not job control. The impact of high job demands varied with SES, leading to greater waking responses only in lower SES participants.<sup>9</sup> In contrast to these studies showing elevation in GC responses to stress, there is growing literature documenting decreased GC output (hypocortisolism). This occurrence was recently identified in the interaction between neighborhood social and physical characteristics and patterns of diurnal cortisol secretion.<sup>57</sup> In particular residents in neighborhoods with high levels of perceived and observed stressors or low levels of social support experience a flatter rate of cortisol decline throughout the day. Moreover, mean cortisol levels were found to be lower in higher stress, lower support neighborhoods.<sup>57</sup> This study adds to the growing evidence of hypocortisolism among chronically stressed adult populations and, further, challenges the current hypothesis that increased cortisol levels are the sole mechanism linking social disadvantage to poor health.<sup>21, 251,296,297</sup> The differences in study results between hypercortisolism and hypocortisolism, highlight the need for proper analyses of psychobiological pathways which must take into account variations in exposure to chronic stressors, as well as differences in responses to stressors.

Similar to the neighborhood environment, the workplace is an interesting setting to study chronic and repeated stressors. As with those in stress-producing neighborhoods, lower SES individuals who have less mobility and control in their jobs have less ability to avoid stressors; they also face continuing demands or health threats that can exacerbate the

effects of stress.<sup>298</sup> To date there has been a strong association between shift-work with an increased risk of hypertension, metabolic syndrome, dyslipidaemia, diabetes mellitus and vascular events.<sup>299-302</sup> These effects remain strong when adjusted for SES; however, shift workers, in general, are more likely to have worse SES than day workers. Alternatively stated those from lower SES are more likely to work jobs with unstable shift assignments. In this form of work, even a single overnight shift, is sufficient to alter health independent of health behaviors.<sup>303-309</sup>

One possible link to shift work and poor health could be the well reported findings on disruptions to circadian rhythms and impaired sleep and sleep quality as touched upon earlier in this review.<sup>310</sup> In order to study the impacts of sleep fragmentation on metabolic variables Baud et al. developed a 14-day model of instrumental sleep fragmentation in mice, and showed an impact on both brain-specific and general metabolism. Of particular interest the group demonstrated an increase of food intake without change in body weight, development of glucose intolerance, and perhaps most interesting an increase in the circadian peak of GCs which may account for the observed metabolic effects.<sup>311</sup> Such studies highlight the usefulness of proper animal models to explore and map out mechanisms of the human condition.

## **Final Summary**

Research on social stress has grown in recent years with both social and bench scientists considering its physiological and biochemical role in health outcomes. However, as the literature has grown, the story has become more complex with many arguing that decreased GC circulation in the case of chronic stress could be to blame rather than the widely held

dogma of hypercortisolism. In order to fully understand the role of GC mediated health issues, researchers must first clearly understand that there are varying levels of stress; and moreover, that the system does not act in isolation. Thinking in terms of allostasis and allostatic load, researchers can paint a broader picture that details a dynamic network of biomarkers, themselves influenced by an individuals genetic make-up, developmental history, and behavioral and psychological states.<sup>12</sup>

As detailed in the introduction chapter and work presented in this dissertation, advances in translational animal and human research has led to several advancements in the world of stress physiology and its role in the development of obesity and the metabolic syndrome. It is clear that human studies cannot fully control for all social environments encountered, especially those using retrospective analysis to measure risk factors over a lifetime. In addition, many risk factors are correlated, such as social class, material resources, neighborhood environment, and personal health behaviors and the potential for confounding, both measured and unmeasured variables, is quite high. When attempting to separate the effects of early life environment and later social status in human studies, researchers face the challenge of including study participants in all combinations of exposure categories and risk.<sup>8</sup> Using animal models in combination with human studies provides a novel opportunity to understand how social experiences become biologically embedded across the life course. Animal models provide a means to explore the questions raised by the epidemiologic work in humans and further allow manipulation of selected experimental variables for the investigation of psychosocial factors affecting vulnerability to stress exposure and HPA axis response.<sup>58,312-314</sup>

Prior animal and human studies on the role of endocannabinoid signaling on HPA axis activity laid the foundation for my studies. My work in rodents would suggest that GC-induced changes in limbic endocannabinoid signaling, in the presence of chronic GC exposure, could contribute to shifts in emotional behaviors, especially increases in anxiety and depression-like behaviors. Further work looking at the role of endocannabinoid signaling and the development of obesity and a metabolic syndrome phenotype, found the predominant mechanistic response for metabolic dysregulation was peripheral. Nevertheless, with the rise in co-morbidity of mood and anxiety disorders with the surge in the obesity, changes in limbic endocannabinoid signaling could impact behavior and hormonal shifts that result in an obese phenotype in an independent but meaningful way.<sup>124</sup> Additional work highlighted the role of endocannabinoid signaling in a mouse model of circadian disruption, a model developed based on the human experience of shifted or shortened days based on work shifts or inconsistent exposure to external light. While the precise mechanism of action is yet to be determined, preliminary experiments, and work presented here, would suggest it provides a compensatory response to moderate the blunted GC response in disrupted animals. It would be of interest to see how endocannabinoid signaling maps out in the human body for those experiencing circadian disruption as in shift workers or even those who have fragmented sleep. Data presented here was the first evidence that the endocannabinoid system may also be involved in the development of obesity from environmental manipulations. In addition to this novel evidence, these studies are also the first to provide a putative candidate system mediating the effects of circadian disruption on metabolic function. As peripherally restricted CB1 receptor antagonists are gaining steam as a novel

anti-obesity drug, these data suggest they may bear utility in treating metabolic syndrome and obesity from multiple causes.

A better understanding of the interplay between the environmental experience and an individual's stress behavioral and physiological response provides the tools to study stress on the level of the population, in the case of this review the role of the neighborhood and work environments. Stress and adversity among low SES neighborhoods come in many forms and varieties, including exposure to neighborhood violence, disorganized and dysfunctional schools, signs of deteriorations (e.g. vacant lots, litter, graffiti), gangs, inadequate services, discrimination, job insecurity, and lack of job control.<sup>315</sup> Future work in this regard will be focused upon unpacking these barriers, each of which can independently have numerous effectors, on not only GC secretion but its regulatory components as well.

## References:

1. Brock DW, Thomas O, Cowan CD, Allison DB, Gaesser GA, Hunter GR. (2009) Association between insufficiently physically active and the prevalence of obesity in the United States. *J Phys Act Health* 6(1): 1-5.
2. Rosenzweig JL, Ferrannini E, Grundy SM, Haffner SM, Heine RJ, Horton ES, Kawamori R (2008) Primary prevention of cardiovascular disease and type 2 diabetes in patients at metabolic risk: an endocrine society clinical practice guideline. *J Clin Endocrinol Metab* 93:3671-3689.
3. Grundy SM, Brewer HB, Jr., Cleeman JI, Smith SC, Jr., Lenfant C (2004) Definition of metabolic syndrome: Report of the National Heart, Lung, and Blood Institute/American Heart Association conference on scientific issues related to definition. *Circulation* 09:433-438.
4. Wilding JPH (2006) Treatment strategies for Obesity. *Obesity Reviews* 8:137-144.
5. Adler, N., Stewart, J., Cohen, S., Cullen, M., Roux, A.D., Dow, D., Evans, G., Kawachi, I., Marmot, M., Matthews, K., McEwen, B., Schwart, J., Seeman, T., Williams, (2007) *Reaching for a Healthier Life: Facts on Socioeconomic Status and Health in the U.S.* Chicago, IL: The John D. and Catherine T. MacArthur Foundation Research Network on Socioeconomic Status and Health.
6. Williams DR and Mohammed SA (2009) Discrimination and racial disparities in health: evidence and needed research *J Behav Med.* 32:20-47.
7. Seeman TE, Crimmins E, Huang MH, Singer B, Bucur A, Gruenewald T, et al. (2004) Cumulative biological risk and socio-economic differences in mortality: MacArthur studies of successful aging. *Social Science & Medicine* 58(10):1985–1997.
8. Matheson FI, Moineddin R, Dunn JR, et al. (2006) Urban neighborhoods, chronic stress, gender and depression. *Social Sci & Med* 63, 2604-2616.
9. Williams DR, Mohammed SA, Leavell J, et al. (2010) Race, socioeconomic status, and health: complexities, ongoing challenges, and research opportunities *Annals of the New York Acc of Sci* 1186:69-101.
10. McEwen BS. (2007) Physiology and Neurobiology of Stress and Adaptation: Central Role of the Brain *Physiol Rev* 87:873-904.
11. Fremont AM and Bird CE. (1999) Integrating sociological and biological models *J Health Soc Behav* 40(2):126-9.
12. McEwen BS. 2008. *Dialogues Clin Neurosci.* 8.
13. Sterling P and Eyer J (1988) Allostasis: a new paradigm to explain arousal pathology.

In: Fisher S, Reason J, eds. Handbook of Life Stress, Cognition and Health. 629-649.

14. Miller GE, Chen E, and Zhou ES (2007) If it goes up, must it come down? Chronic stress and the hypothalamic-pituitary-adrenocortical axis in humans. *Psychological Bulletin* 133:25-45.
15. Chrousos GP, Gold PW (1992) The concepts of stress and stress system disorders. Overview of physical and behavioral homeostasis. *JAMA* 267:1244-1252.
16. Chrousos GP (1998) Ultradian, circadian, and stress-related hypothalamic-pituitary-adrenal axis activity-a dynamic digital-to-analog modulation. *Endocrinology* 139:437-440.
17. Wang M (2005) The role of glucocorticoid action in the pathophysiology of the Metabolic Syndrome. *Nutr Metab* 2:3.
18. Jacobson L, Akana SF, Cascio CS, Shinsako J, Dallman MF (1988) Circadian variations in plasma corticosterone permit normal termination of adrenocorticotropin responses to stress. *Endocrinology* 122:1343-1348.
19. Herman JP, Ostrander MM, Mueller NK et al. (2005) Limbic system mechanisms of stress regulation: hypothalamo-pituitary-adrenocortical axis. *Prog Neuropsychopharmacol Bio Psychiatry* 29:1201-1213.
20. Pecoraro N, Dallman MF, Warne JP, Ginsberg AB, Laugero KD, la Fleur SE, Houshyar H, Gomez F, Akana SF, Bhargava A. (2006) From Malthus to motive: how the HPA axis engineers the phenotype, yoking needs to wants. *Prog Neurobiol* 79:247-340.
21. Sapolsky, R. M. (2005). The influence of social hierarchy on primate health. *Science* 308(5722):648-652.
22. Hruschka DJ, Kohrt BA & Worthman CM (2005). Estimating between- and within-individual variation in cortisol levels using multilevel models. *Psychoneuroendocrinology* 30, 698-714.
23. Dowd, JB, Simanek, AM, and Aiello, AE (2009). Socio-economic status, cortisol and allostatic load: a review of the literature. *International Journal of Epidemiology*, 38, 1297-1409.
24. Smyth JM, Ockenfels MC, Gorin AA et al. (1997) Individual differences in the diurnal cycle of cortisol. *Psychoneuroendocrinology* 22:89-105.
25. Stone AA, Schwartz JE, Smyth J et al. (2001) Individual differences in the diurnal cycle of salivary free cortisol: a replication of flattened cycles for some individuals. *Psychoneuroendocrinology*. 26(3):295-306.
26. Levine A, Zagoory-Sharon O, Feldman R, Lewis JG, Weller A. (2007) Measuring cortisol in human psychobiological studies. *Physiol Behav* 90:43-53.



27. Hellhammer DH, Ehlert U, Christine H. (2000) The potential role of hypocortisolism in the pathophysiology of stress-related bodily disorders. *Psychoneuroendocrinology* 25:1-35.
28. Dunkelman SS, Fairhurst B, Plager J, Waterhouse C. (1964) Cortisol metabolism in obesity. *J Clin Endocrinol* 24: 832–841
29. Fraser R, Ingram MC, Anderson NH, Morrison C, Davies E, Connell JM. (1999) Cortisol effects on body mass, blood pressure, and cholesterol in the general population. *Hypertension* 33:1364–1368
30. Berset M, Semmer NK, Elfering A, Jacobshagen N, Meier LL. (2011) Does stress at work make you gain weight? A two-year longitudinal study. *Environment & Health* 37(1): 45-53.
31. Bujalska IJ, Kumar S, Stewart PM. (1997) Does central obesity reflect “Cushing’s disease of the omentum”? *Lancet* 349:1210–1213
32. Stulnig TM and Waldhausl W. 11beta-Hydroxysteroid dehydrogenase Type 1 in obesity and Type 2 diabetes. (2004) *Diabetologia* 47(1)1-11.
33. Stewart PM, Krozowski ZS. (1999) 11 beta-Hydroxysteroid dehydrogenase. *Vitam Horm* 57:249–324
34. Walker BR, Campbell JC, Fraser R, Stewart PM, Edwards CR. (1992) Mineralocorticoid excess and inhibition of 11 beta-hydroxysteroid dehydrogenase in patients with ectopic ACTH syndrome. *Clin Endocrinol (Oxf)* 37:483–492 *Biol Chem* 275:30232-30239.
35. Sandeep TC, Walker BR. (2001) Pathophysiology of modulation of local glucocorticoid levels by 11beta-hydroxysteroid dehydrogenases. *Trends Endocrinol Metab* 12:446–453.
36. Kotelevtsev Y, Holmes MC, Burchell A et al. (1997) 11beta-Hydroxysteroid dehydrogenase type 1 knockout mice show attenuated glucocorticoid-inducible responses and resist hyperglycemia on obesity or stress. *Proc Natl Acad Sci USA* 94:14924–14929.
37. Stewart PM, Boulton A, Kumar S, Clark PM, Shackleton CH. (1999b) Cortisol metabolism in human obesity: impaired cortisone→cortisol conversion in subjects with central adiposity. *J Clin Endocrinol Metab* 84:1022–1027
38. Morton NM, Holmes MC, Fievet C et al. (2001) Improved lipid and lipoprotein profile, hepatic insulin sensitivity and glucose tolerance in 11{beta}-hydroxysteroid dehydrogenase type 1 null mice. *J Biol Chem* 276:41293–41300
39. Masuzaki H, Paterson J, Shinyama H, et al. (2001) A transgenic model of visceral obesity and the metabolic syndrome. *Science* 294:2166-70.

40. Paterson JM, Morton NM, Fievet C, et al. (2004) Metabolic syndrome without obesity: Hepatic overexpression of 11beta-hydroxysteroid dehydrogenase type 1 in transgenic mice. *Proc Natl Acad Sci U S A* 101:7088-93.
41. Vitaliano PP, Scanlan JM, Zhang J, Savage MV, Hirsch IB, Siegler IC. (2002) A path model of chronic stress, the metabolic syndrome, and coronary heart disease. *Psychosom Med.* 64:418–435.
42. van Eck M, Berkhof H, Nicolson N, Sulon J. (1996) The effects of perceived stress, traits, mood states, and stressful daily events on salivary cortisol. *Psychosom Med* 58:447–458.
43. Pruessner M, Hellhammer DH, Pruessner JC, Lupien SJ. (2003) Self-reported depressive symptoms and stress levels in healthy young men: associations with the cortisol response to awakening. *Psychosom Med* 65:92–99.
44. Holsboer F. (2001) Stress, hypercortisolism and corticosteroid receptors in depression: implications for therapy. *J Affect Disord.* 62:77–91.
45. Weber-Hamann B, Hentschel F, Kniest A, Deuschle M, Colla M, Lederbogen F, Heuser I. (2002) Hypercortisolemic depression is associated with increased intra-abdominal fat. *Psychosom Med.* 64:274–277.
46. Vogelzangs N, Suthers K, Ferrucci L, Simonsick EM, Ble A, Schragger M, Bandinelli S, Lauretani F, Giannelli SV, Penninx BW. (2007) Hypercortisolemic depression is associated with the metabolic syndrome in late-life. *Psychoneuroendocrinology* 32:151–159
47. Karatsoreos IN, Bhagat SM, Bowles NP, Weil ZM, Pfaff DW, McEwen BS. (2010) Endocrine and physiological changes in response to chronic corticosterone: a potential model of the metabolic syndrome in mouse. *Endocrinology* 151:2117-2127.
48. Nonogaki K, Nozue K, Oka Y. (2007) Social isolation affects the development of obesity and type 2 diabetes in mice. *Endocrinology* 148: 4658–66.
49. Shpilberg Y, Beaudry JL, D'Souza A, Campbell JE, Peckett A, Riddell MC. (2012) A rodent model of rapid-onset diabetes induced by glucocorticoids and high-fat feeding. *Dis Model Mech.* 5(5):671-80.
50. Fries E, Hesse J, Hellhammer J, Hellhammer D.H. (2005) A new view on hypocortisolism. *Psychoneuroendocrinol.* 30,1010-1016.
51. Friedman SB, Mason JW, Hanburg DA (1963) Urinary 17-hydroxycorticosteroid levels in parents of children with neoplastic disease: a study of chronic psychological stress. *Psychosom. Med.* 25:364 – 376.
52. Bourne PG, Rose RM, Mason JW. (1967) Urinary 17 OHCS levels. Data on seven

- helicopter ambulance medics in combat. *Arch. Gen. Psychiatry* 17:104 – 110.
53. Bourne PG, Rose RM, Mason JW. (1968) 17-OHCS levels in combat Special forces “A” team under threat of attack. *Arch. Gen. Psychiatry* 17:104-110.
54. Mason JW, Brady JV, Tolliver GA. (1968) Plasma and urinary 17-hydroxycorticosteroid responses to 72-hr. avoidance sessions in the monkey. *Psychosom. Med.* 30:608 – 630.
55. Juster RP, Sindi S, Marin MF, Perna A, Hashemi A, Pruessner JC, Lupien SJ. (2011) A clinical allostatic load index is associated with burnout symptoms and hypocortisolemic profiles in healthy workers. *Psychoneuroendo* 36:7977-805.
56. Trivison TG, O'Donnell AB, Araujo AB, Matsumoto AM, McKinlay JB. (2007) Cortisol levels and measures of body composition in middle. *Clin Endocrinol* 67(1):71-77.
57. Karb RA, Elliott MR, Dowd JB, and Morenoff J. (2012) Neighborhood-level stressors, social support, and diurnal patterns of cortisol: The Chicago Community Adult Health Study. *Social Science and Medicine* 1-10.
58. Bartolomucci A (2005) Resource loss and stress-related disease: is there a link? *Med Sci Monit* 11: RA147–154.
59. Houshyar H, Cooper ZD, Woods JH. (2001) Paradoxical effects of chronic morphine treatment on the temperature and pituitary-adrenal responses to acute restraint stress” a chronic stress paradigm. *J. Neuroendocrinol.* 13:862-874.
60. Houshyar H, Galigniana MD, Pratt WB, Woods JH. (2001) Differential responsivity of the hypothalamic-pituitary-adrenal axis to glucocorticoid negative-feedback and corticotropin releasing hormone in rats undergoing morphine withdrawal: possible mechanisms involved in facilitated and attenuated stress responses. *J Neuroendocrinol* 13:875–886
61. Houshyar H, Manalo S, Dallman MF. (2004) Time-dependent alterations in mRNA expression of brain neuropeptides regulating energy balance and hypothalamo-pituitary-adrenal activity after withdrawal from intermittent Morphine Treatment. *Journ Neurosci* 24(42):9414-9424.
62. Feng X, WangL , Yang S, Qin D et al. (2011) Maternal separation produced lasting changes in cortisol and behavior in rhesus monkeys. *PNAS* 108 (34):144312-14317.
63. Pecoraro N, Reyes F, Gomez F, Bhargava A, Dallman MF. (2004) Chronic stress promotes palatable feeding, which reduces signs of stress: feedforward and feedback effects of chronic stress. *Endocrinology* 145(8):3754-62.
64. Maniam J, Morris MJ. (2010) Palatable cafeteria diet ameliorates anxiety and depression-like symptoms following an adverse early environment.

Psychoneuroendocrinology 35 (5):717—728.

65. Laugero KD, Bell ME, Bhatnagar S, Soriano L, Dallman MF. (2001) Sucrose ingestion normalizes central expression of corticotropin-releasing-factor messenger ribonucleic acid and energy balance in adrenalectomized rats: a glucocorticoid—metabolic—brain axis? *Endocrinology* 142 (7):2796—2804.
66. Arce M, Michopoulos V, Shepard KN, Ha QC, Wilson ME. (2009) Diet choice, cortisol reactivity, and emotional feeding in socially housed rhesus monkeys. *Physiol. Behav.* 101 (4):446—455.
67. Tomiyama AJ, Dallman MF, Epel ES. (2011) Comfort food is comforting to those most stressed: evidence of the chronic stress response network in high stress women. *Psychoneuroendocrinology*. 36(10):1513-9.
68. Akana SF, Jacobson L, Cascio CS, Shinsako J, Dallman MF. (1988) Constant Corticosterone Replacement Normalizes Basal Adrenocorticotropin (ACTH) but Permits Sustained ACTH Hypersecretion After Stress in Adrenalectomized Rats. *Endocrinology* 122:1337-1342.
69. Van Cauter E, Leproult R, Kupfer DJ. (1996) Effects of gender and age on the levels and circadian rhythmicity of plasma cortisol. *J Clin Endocrinol Metab* 81:2468 –2473.
70. Lupien SJ, Gaudreau S, Tchiteya BM, Maheu F, Sharma S, Nair N PV Hauger RL, McEwen BS, Meaney MJ. (1997) Stress-induced declarative memory impairment healthy elderly subjects: relationship to cortisol reactivity. *J Clin Endocrinol Metab* 82:2070 –2075.
71. Adam, E. K., Hawkley, L. C., Kudielka, B. M., & Cacioppo, J. T. (2006) Day-to-day dynamics of experience-cortisol associations in a population-based sample of older adults. *Proceedings of the National Academy of Sciences*, 103:17058-17063.
72. Dallman MF (2010) Stress-induced obesity and the emotional nervous system. *Trends Endocrinol. Metab.* 21 (3):159—165.
73. McEwen BS (2008) Central effects of stress hormones in health and disease: understanding the protective and damaging effects of stress and stress mediators. *Eur. J. Pharmacol.* 583 (2—3):174—185.
74. Wardle J, Chida Y, Gibson EL, Whitaker KL, Steptoe A. (2010) Stress and adiposity: a meta-analysis of longitudinal studies. *Obesity* 19(4): 771-8.
75. Strelakova T, Spanagel R, Bartsch D, Henn FA, Gass P. (2004) Stress-Induced Anhedonia in Mice is Associated with Deficits in Forced Swimming and Exploration. *Neuropsychopharmacology* 29:2007 – 2017.
76. Rygula R, Abumaria N, Flugge G, Fuchs E, Ruther E, et al. (2005) Anhedonia and motivational deficits in rats: impact of chronic social stress. *Behav Brain Res* 162: 127–34.

77. Meerlo P, Overkamp GJ, Daan S, Van Den Hoofdakker RH, Koolhaas JM (1996) Changes in behaviour and body weight following a single or double social defeat in rats. *Stress* 1: 21–32.
78. Tamashiro KL, Hegeman MA, Nguyen MM, Melhorn SJ, Ma LY, et al. (2007) Dynamic body weight and body composition changes in response to subordination stress. *Physiol Behav* 91: 440–8.
79. Bartolomucci A, Pederzani T, Sacerdote P, Panerai AE, Parmigiani S, et al. (2004) Behavioral and physiological characterization of male mice under chronic psychosocial stress. *Psychoneuroendocrinology* 29: 899–910.
80. Foster MT, Solomon MB, Huhman KL, Bartness TJ (2006) Social defeat increases food intake, body mass, and adiposity in Syrian hamsters. *Am J Physiol Regul Integr Comp Physiol* 290: R1284–93.
81. Moles A, Bartolomucci A, Garbugino L, Conti R, Caprioli A, et al. (2006) Psychosocial stress affects energy balance in mice: modulation by social status. *Psychoneuroendocrinology* 31: 623–33.
82. Solomon MB, Foster MT, Bartness TJ, Huhman KL (2007) Social defeat and footshock increase body mass and adiposity in male Syrian hamsters. *Am J Physiol Regul Integr Comp Physiol* 292: R283–90.
83. Kuo LE, Kitlinska JB, Tilan JU, Li L, Baker SB, Johnson MD, Lee EW, Burnett MS, Fricke ST, Kvetnansky R, Herzog H, Zukowska Z. (2007) Neuropeptide Y acts directly in the periphery on fat tissue and mediates stress-induced obesity and metabolic syndrome. *Nat Med* 13:803–811.
84. Bartolomucci, A., Cabassi, A., Govoni, P., Ceresini, G., Cero, C., Berra, D., Dadomo, H., Franceschini, P., Dell’Omo, G., Parmigiani, S. et al (2009a) Metabolic consequences and vulnerability to diet-induced obesity in male mice under chronic social stress. *PLoS One* 4 (1) e4331.
85. Loizzo A, Loizzo S, Galietta G et al (2006) Overweight and metabolic and hormonal parameter disruption are induced in adult male mice by manipulations during lactation period. *Pediatr Res* 59:111–115.
86. Bjorntorp P, Rosmond R (2000) Neuroendocrine abnormalities in visceral obesity. *Int. J. Obes. Relat. Metab. Disord.* 24 (Suppl. 2):S80—85.
87. Dallman MF, Pecoraro NC, La Fleur SE (2005) Chronic stress and comfort foods: Self-medication and abdominal obesity. *Brain, Behavior, and Immunity* 19:275-280.
88. Adam TC, Epel ES (2007) Stress, eating and the reward system. *Physiol. Behav.* 91 (4):449—458. f
89. Torres SJ, Nowson CA (2007) Relationship between stress, eating behavior, and

obesity. *Nutrition* 23 (11—12):887—894.

90. Warne JP (2009) Shaping the stress response: interplay of palatable food choices, glucocorticoids, insulin and abdominal obesity. *Mol. Cell. Endocrinol.* 300 (1—2):137—146.

91. Epel E, Lapidus R, McEwn B, Brownell K. (2001) Stress may add bite to appetite in women: a laboratory study of stress-induced cortisol and eating behavior. *Psychoneuroendocrinology* 26: 37-49.

92. Gibson, LE (2006) Emotional influences on food choice: sensory, physiological and psychological pathways. *Physiol. Behav.* 89(1):53-61.

93. Mezuk B, Rafferty JA, Kershaw KN, Hudson D, Abdou CM, Lee H, Eaton WW, Jackson JS (2010) Reconsidering the role of social disadvantage in physical and mental health: stressful life events, health behaviors, race, and depression. *Am J Epidemiol*; 172(11):1238-49.

94. Heinrichs SC, Richard D. (1999) The role of corticotropin-releasing factor and urocortin in the modulation of ingestive behavior. *Neuropeptides* 33:350—359.

95. Heinrichs SC, Menzaghi F, Pich EM, Hauger RL, Koob GF. (1993) Corticotropin-releasing factor in the paraventricular nucleus modulates feeding induced by neuropeptide Y. *Brain Res* 611:18—24.

96. Currie PJ. (2003) Integration of hypothalamic feeding and metabolic signals: Focus on neuropeptide Y. *Appetite* 41:335—337.

97. Dallman MF, la Fleur SE, Pecoraro NC, Gomez F, Houshyar H, Akana SF.(2004) Minireview: Glucocorticoids—food intake, abdominal obesity, and wealthy nations in 2004. *Endocrinology*145:2633—2638.

98. Santana P, Akana SF, Hanson ES, Strack AM, Sebastian RJ, Dallman MF (1995) Aldosterone and dexamethasone both stimulate energy acquisition whereas only the glucocorticoid alters energy storage. *Endocrinology* 136:2214— 2222.

99. De Vriendt T, Moreno LA, De Henauw S (2009) Chronic stress and obesity in adolescents: Scientific evidence and methodological issues for epidemiological research. *Nutr Metab Cardiovasc Dis* 19:511—519.

100. Di Chiara G, Imperato A. (1988) Drugs abused by humans preferentially increase synaptic dopamine concentrations in the mesolimbic system of freely moving rats. *Proc Natl Acad Sci USA* 85:5274— 5278.

101. Koob GF, Le Moal M (2001) Drug addiction, dysregulation of reward, and allostasis. *Neuropsychopharmacology* 24:97—129.

102. Ito R, Robbins TW, Everitt BJ (2004) Differential control over cocaine-seeking

behavior by nucleus accumbens core and shell. *Nat Neurosci* 7:389–397.

103. Gosnell BA. (2000) Sucrose intake predicts rate of acquisition of cocaine self-administration. *Psychopharmacology Berl* 149: 286–292.

104. Divertie GD, Jensen MD, Miles JM. (1991) Stimulation of lipolysis in humans by physiological hypercortisolemia. *Diabetes* 40: 1228–1232.

105. Slavin BG, Ong JM, Kern PA (1994) Hormonal regulation of hormone-sensitive lipase activity and mRNA levels in isolated rat adipocytes. *J Lipid Res.* 35(9):1535-41.

106. Arner P (2002) Insulin resistance in type 2 diabetes: Role of fatty acids. *Diabetes Metab Res Rev* 18(Suppl 2):S5–S9.

107. Bjorntorp P (1996) The regulation of adipose tissue distribution in humans. *Int J Obes Relat Metab Disord* 20:291–302.

108. Bjorntorp P (2001) Do stress reactions cause abdominal obesity and comorbidities? *Obes Rev* 2:73–86.

109. Hauner H, Schmid P, Pfeiffer EF (1987) Glucocorticoids and insulin promote the differentiation of human adipocyte precursor cells into fat cells. *J Clin Endocrinol Metab* 64:832–835.

110. Tomlinson JW, Stewart PM (2002) The functional consequences of 11beta-hydroxysteroid dehydrogenase expression in adipose tissue. *Horm Metab Res* 34:746–751.

111. Kuo LE, Czarnecka M, Kitlinska JB, Tilan JU, Kvetnansky R, Zukowska Z. (2008) Chronic stress, combined with a high-fat/high-sugar diet, shifts sympathetic signaling toward neuropeptide Y and leads to obesity and the metabolic syndrome. *Ann N Y Acad Sci* 1148:232–237.

112. Erhuma A, McMullen S, Langley-Evans SC, Bennett AJ (2009) Feeding pregnant rats a low-protein diet alters the hepatic expression of SREBP-1c in their offspring via a glucocorticoid-related mechanism. *Endocrine* 36: 333-338.

113. Hill MN, McEwen BS (2010) Involvement of the endocannabinoid system in the neurobehavioural effects of stress and glucocorticoids. *Prog Neuropsychopharmacol Biol Psychiatry* 34:791-797.

114. Hill MN, Patel S, Campolongo P, Tasker JG, Wotjak CT, Bains JS (2010) Functional interactions between stress and the endocannabinoid system: from synaptic signaling to behavioral output. *J Neurosci* 30:14980-14986.

115. Steiner MA, Wotjak CT (2008) Role of the endocannabinoid system in regulation of the hypothalamic-pituitary-adrenocortical axis. *Prog Brain Res* 170:397-432.

116. Devan WA, Hanus L, Breuer A, Pertwee RC, Stevenson LA, Griffin G, et al. Isolation

and structure of a brain constituent that binds to the cannabinoid receptor. *Science* 1992; 258:1946-9.

117. Sugiura T, Kondo S, Sukagawa A, Nakane S, Shinoda A, Itoh K, Yamashita A, Waku K (1995) 2-Arachidonoylglycerol: a possible endogenous cannabinoid receptor ligand in brain. *Biochem Biophys Res Commun* 215:89-97.

118. Deutsch DG, Ueda N, Yamamoto S. The fatty acid amide hydrolase (FAAH). *Prostaglandins Leukot Essent Fatty Acids* 2002; 66:201-10.

119. Howlett AC. (2002) The cannabinoid receptors. *Prostaglandins Other Lipid Mediat* 68-69:619-31.

120. Hill MN, McEwen B. (2010) Involvement of the endocannabinoid system in the neurobehavioural effects of stress and glucocorticoids. *Prog Neuropsychopharmacol Biol Psychiatry*. 34(5):791-797

121. Quarta C, Mazza R, Obici S, Pasquali R, Pagotto U (2011). Energy balance regulation by endocannabinoids at central and peripheral levels. *Trends Mol Med* 17:518–26.

122. Valenzuela C, Castillo V, Aguirre C, Ronco AM, Llanos M (2011) The CB1 receptor antagonist SR141716A reverses adult male mice overweight and metabolic alterations induced by early stress. *Obesity* 19:29–35.

123. Davidson T, Kanoski SE, Schier LA, Clegg DJ, Benoit SC (2007) A potential role for the hippocampus in energy intake and body weight regulation. *Current Opinion in Pharmacology* 7:613–616.

124. Bowles N, Hill MN, Bhagat SM, Karatsoreos IN, Hillard CJ, McEwen BS (2011) Chronic, noninvasive glucocorticoid administration suppresses limbic endocannabinoid signaling in mice *Neuroscience* 204:83-89.

125. Harmer SL, Panda S, and Kay SA (2001). Molecular bases of circadian rhythms. *Annu. Rev. Cell Dev. Biol.* 17, 215–253.

126. Hastings MH (1997) Circadian rhythms. *Curr. Biol.* 7:670.

127. Rusak B and Zucker I (1979) Neural regulation of circadian rhythms. *Physiol. Rev.* 59:449.

128. Schibler U, Ripperger J, and Brown SA. (2003) Peripheral circadian oscillators in mammals: time and food. *J. Biol. Rhythms* 18: 250–260.

129. Perreau-Lenz, Pevet P, Buijs RM, Kalsbeek A (2004) The biological clock: the bodyguard of temporal homeostasis. *Chronobiol Int.* 21(1):1-25.

130. Storch KF (2002) Extensive and divergent circadian gene expression in liver and heart.



Nature 417(6884):78-83.

131. Panda S (2002). Coordinated transcription of key pathways in the mouse by the circadian clock. *Cell* 109(3):307-320.

132. Reppert SM, Weaver DR. (2002) Coordination of circadian timing in mammals. *Nature* 418:935-941.

133. Preitner N, Damiola F, Lopez-Molina L, Zakany J, Duboule D, Albrecht U, Schibler U. (2002) The orphan nuclear receptor REV-ERBa controls circadian transcription within the positive limb of the mammalian circadian oscillator. *Cell* 110: 251-260.

134. Sato TK, Panda S, Miraglia LJ, Reyes TM, Rudic RD, McNamara P, Naik, KA FitzGerald, GA, Kay SA, Hogenesch, JB (2004) A functional genomics strategy reveals Rora as a component of the mammalian circadian clock. *Neuron* 43:527–537

135. Canaple L, Rambaud J, Dkhissi-Benyahya O, Rayet B, Tan NS, Michalik L, Delaunay F, Wahli W, and Laudet V. (2006) Reciprocal regulation of brain and muscle Arnt-like protein 1 and peroxisome proliferator-activated receptor  $\alpha$  defines a novel positive feedback loop in the rodent liver circadian clock. *Mol. Endocrinol.* 20:1715–1727.

136. Kohsaka, Laposky AD, Ramsey KM, Estrada C, Joshu C, Kobayashi Y, Turek FW, Bass J (2007) High-fat diet disrupts behavioral and molecular circadian rhythms in mice. *Cell Metab.* 6:414–421

137. Hsieh MC, Yang SC, Tseng HL, Hwang LL, Chen CT, Shieh KR (2010) Abnormal expressions of circadian-clock and circadian clock-controlled genes in the livers and kidneys of long-term, high-fat-diet-treated mice. *Int J Obes* 34:227–239.

138. Turek FW, Joshu C, Kohsaka A, Lin E, Ivanova G, McDearmon E, Laposky A, Losee-Olson S, Easton A, Jensen DR, Eckel RH, Takahashi JS, and Bass J. (2005) Obesity and metabolic syndrome in circadian Clock mutant mice. *Science* 308, 1043-1045.

139. P. McNamara, Curtis AM, Boston RC, Panda S, Hogenesch JB, Fitzgerald GA (2004) BMAL1 and CLOCK, two essential components of the circadian clock, are involved in glucose homeostasis. *PLoS Biol.* 2: e377

140. Marcheva B, Ramsey KM, Buhr ED, Kobayashi Y, Su H, Ko CH, Ivanova G, Omura C, Mo S, Vitaterna MH, Lopez JP, Philipson LH, Bradfield CA, Crosby SD, JeBailey L, Wang X, Takahashi JS, and Bass J (2010) Disruption of the clock components CLOCK and BMAL1 leads to hypoinsulinaemia and diabetes. *Nature* 466: 627–631.

141. Stow LR, Richards J, Cheng KY, Lynch IJ, Jeffers LA, Greenlee MM, Cain BD, Wingo CS, Gumz ML (2012) The Circadian Protein Period 1 Contributes to Blood Pressure Control and Coordinately Regulates Renal Sodium Transport Genes Hypertension 59: 1151-1156

142. Dallmann, R., and Weaver, D. R. (2010) Altered body mass regulation in male

mPeriod mutant mice on high-fat diet. *Chronobiol. Int.* 27, 1317–1328.

143. Tronche, F., Kellendonk, C., Reichardt, H.M., and Schütz, G. (1998) Genetic dissection of glucocorticoid receptor function in mice. *Current Opinion in Genetics and Development* 8, 532-538.

144. Rosenfeld P, Van Eekelen JAM, Levine S, De Kloet ER. (1988) Ontogeny of the Type 2 glucocorticoid receptor in discrete rat brain regions: an immunocytochemical study. *Developmental Brain Res.* 42: 119-127.

145. Balsalobre A, Brown SA, Marcacci L, Tronche F, Kellendonk C, Reichardt HM, Schutz G, Schibler U (2000) Resetting of circadian time in peripheral tissues by glucocorticoid signaling. *Science* 289(5488):2344–2347.

146. Bass J, Takahashi JS (2010) Circadian integration of metabolism and energetics. *Science* 330: 1349–1354.

147. Kaneko K, Yamada T, Tsukita S, Takahashi K, Ishigaki Y, Oka Y, Katagiri H (2009) Obesity alters circadian expressions of molecular clock genes in the brainstem. *Brain Res* 1263: 58–68.

148. Chung S, Son GH, Kim K (2011) Circadian rhythm of adrenal glucocorticoid: its regulation and clinical implications. *Biochim Biophys Acta* 1812: 581–591.

149. Nader N, Chrousos GP, Kino T (2010). Interactions of the circadian CLOCK system and the HPA axis. *Trends Endocrinol Metab* 21: 277–286.

150. Patel S, Roelke CT, Rademacher DJ, Cullinan WE, Hillard CJ (2004) Endocannabinoid signaling negatively modulates stress-induced activation of the hypothalamic-pituitary-adrenal axis. *Endocrinology* 145:5431–5438.

151. Oster H, Damerow S, Kiessling S, Jakubcaková V, Abraham D, Tian J, Hoffmann MW, Eichele G (2006) The circadian rhythm of glucocorticoids is regulated by a gating mechanism residing in the adrenal cortical clock. *Cell Metab.* 4(2):163–173.

152. Oishi K, Amagai N, Shirai H, Kadota K, Ohkura N, and Ishida N (2005) Genome-wide expression analysis reveals 100 adrenal gland-dependent circadian genes in the mouse liver. *DNA Res.* 12:191–202.

153. Nicholson WE, Levine JH, Orth DN (1976) Hormonal regulation of renal ornithine decarboxylase activity in the rat. *Endocrinology* 98, 123–128.

154. Casanueva FF, Dieguez C (1999) Neuroendocrine regulation and actions of leptin. *Front. Neuroendocrinol.* 20:317–363.

155. Barnea M, Madar Z, Froy O (2009) High-fat diet delays and fasting advances the circadian expression of adiponectin signaling components in mouse liver. *Endocrinology*

150:161–168 37.

156. Barnea M, Madar Z, and Froy O. (2010) High-fat diet followed by fasting disrupts circadian expression of adiponectin signaling pathway in muscle and adipose tissue. *Obesity (Silver Spring)* 18:230–238.

157. Cano P, Cardinali DP, Rios-Lugo MJ, Fernandez-Mateos MP, Reyes Toso CF, and Esquifino AI (2009) Effect of a high-fat diet on 24-hour pattern of circulating adipocytokines in rats. *Obesity* 17: 1866–1871

158. Cha MC, Chou CJ and Boozer CN(2000) High-fat diet feeding reduces the diurnal variation of plasma leptin concentration in rats. *Metabolism* 49:503–507

159. Havel PJ, Townsend R, Chaump L, and Teff K. (1999) High-fat meals reduce 24-h circulating leptin concentrations in women. *Diabetes* 48: 334–341.

160. Damiola F, Le Minh N, Preitner N, Kornmann B, Fleury-Olela F, and Schibler U. (2000) Restricted feeding uncouples circadian oscillators in peripheral tissues from the central pacemaker in the suprachiasmatic nucleus. *Genes Dev* 14:2950–2961

161. Sherman H, Frumin I, Gutman R, Chapnik N, Lorentz A, Meylan J, le Coutre J, and Froy O. (2011) Long-term restricted feeding alters circadian expression and reduces the level of inflammatory and disease markers. *J. Cell. Mol. Med.* 15, 2745–2759 metabolism. *Cell* 134:728–742

162. Sherman H, Genzer Y, Cohen R, Chapnik N, Madar Z, and Froy O (2012). Timed high-fat diet resets circadian metabolism and prevents obesity. *The FASEB Journal* 8:3493-502

163. Sage D, Ganem J, Guillaumond F, Laforge-Anglade G, Francois-Bellan AM, Bosler O, Becquet D (2004) Influence of the corticosterone rhythm on photic entrainment of locomotor activity in rats. *J Biol Rhythms.* 19(2):144–156.

164. Kiessling S, Eichele G, Oster H (2010) Adrenal glucocorticoids have a key role in circadian resynchronization in a mouse model of jet lag. *JCI.* 120 (7):2600-2609.

165. Cho K, Ennaceur A, Cole JC, Suh CK (2011) Chronic jet lag produces cognitive deficits. *J Neurosci.* 20:1–5.

166. Karatsoreos IN, Bhagat S, Bloss EB, Morrison JH, McEwen BS (2011). Disruption of circadian clocks has ramifications for metabolism, brain, and behavior. *Proc Natl Acad Sci USA*108:1657–62.

167. Osei-Hyiaman D, Liu J, Zhou L, Godlewski G, Harvey-White J, Jeong W-il, et al (2008) Hepatic CB1 receptor is required for development of diet-induced steatosis, dyslipidemia, and insulin and leptin resistance in mice. *J Clin Invest* 118:3160–9.

168. Postic C, Shiota M, Niswender KD, Jetton TL, et al (1999) Dual roles for glucokinase

- in glucose homeostasis as determined by liver and pancreatic beta cell-specific gene knock-outs using Cre recombinase *J Biol Chem* 274(1):305-15.
169. Moverare-Skrtric S, et al (2006) Dihydrotestosterone treatment results in obesity and altered lipid metabolism in orchidectomized mice. *Obesity* 14(4):662-672.
170. Hillard CJ, Wilkison DM, Edgemon WS, Campbell WB (1995) Characterization of the kinetics and distribution of N-arachidonylethanolamine (anandamide) hydrolysis by rat brain. *Biochim Biophys Acta* 1257:249-256.
171. Patel S, Carrier EJ, Ho WS, Rademacher DJ, Cunningham S, Reddy DS, Falck JR, Cravatt BF, Hillard CJ (2005) The postmortal accumulation of brain N-arachidonylethanolamine (anandamide) is dependent upon fatty acid amide hydrolase activity. *J Lipid Res* 46:342-349.
172. Omeir RL, Chin S, Hong Y, Ahern DG, Deutsch DG (1995) Arachidonoyl ethanolamide-[1,2-<sup>14</sup>C] as a substrate for anandamide amidase. *Life Sci* 56:1999-2005.
173. Hill MN, Karatsoreos IN, Hillard CJ, McEwen BS. (2010) Rapid elevations in limbic endocannabinoid content by glucocorticoid hormones in vivo. *Psychoneuroendocrinology* 35: 1333-1338.
174. Williams J, Wood J, Pandarinathan L, Karanian DA, Bahr BA, Vouros P, Makriyannis A (2007). *Anal. Chem.* 79:5582-5593.
175. Karatsoreos IN (2012) Effects of circadian disruption on mental and physical health. *Curr Neurol Neurosci Rep.* 12:218–25.
176. Suwazono Y, Dochi M, Sakata K, Okubo Y, Oishi M, Tanaka K, et al. (2008) A longitudinal study on the effect of shift work on weight gain in male Japanese workers. *Obesity* 16:1887–93.
177. Scheer FAJL, Hilton MF, Mantzoros CS, Shea SA. (2009) Adverse metabolic and cardiovascular consequences of circadian misalignment. *Proc Natl Acad Sci USA* 106:4453–8
178. Niedhammer I, Lert F, Marne MJ. (1996) Prevalence of overweight and weight gain in relation to night work in a nurses' cohort. *Int J Obesity* 20:625–33.
179. Turek FW, Joshu C, Kohsaka A, Lin E, Ivanova G, McDearmon E, Laposky A, Losee-Olson S, Easton A, Jensen DR, Eckel RH, Takahashi JS, Bass J (2005) Obesity and metabolic syndrome in circadian Clock mutant mice. *Science* 308: 1043–1045.
180. Paschos GK, Ibrahim S, Song WL, Kunieda T, Grant G, Reyes TM, Bradfield CA, Vaughan CH, Eiden M, Masoodi M, Griffin JL, Wang F, Lawson JA, FitzGerald GA. (2012). Obesity in mice with adipocyte-specific deletion of clock component Arntl. *Nature Medicine* 18(12) 1768-1779.

181. Shostak A, Meyer-Kovac J, Oster H (2013). Circadian regulation of lipid mobilization in white adipose tissues. *Diabetes* in press
182. Grimaldi B, Bellet MM, Katada S, Astarita G, Hirayama J, Amin RH, Granneman JG, Piomelli D, Leff T, Sassone-Corsi P (2010). Per2 Controls Lipid Metabolism by Direct Regulation of PPAR $\gamma$ . *Cell Metabolism* 12(4):509-520.
183. Brun RP, Tontonoz P, Forman BM, Ellis R, Chen J, Evans RM, Spiegelman BM (1996) Differential activation of adipogenesis by multiple PPARA isoforms. *Genes and Development* 10:974-984.
184. Waddington Lamont E, Robinson B, Stewart J, Amir S (2005) The central and basolateral nuclei of the amygdala exhibit opposite diurnal rhythms of expression of the clock protein Period2. *Nrc Natl Acad Sci USA* 102:4180-4184.
185. Kwak SP, Young EA, Morano I, Watson SJ, Akil H (1992) Diurnal corticotropin-releasing hormone mRNA variation in the hypothalamus exhibits a rhythm distinct from that of plasma corticosterone. *Neuroendocrinology*. 55(1):74-83.
186. Hammond GL (1995) Potential functions of plasma steroid-binding proteins. *TEM* 6: 298-304.
187. Mendel CM (1989) The free hormone hypothesis a physiologically based mathematical model. *Endocrine Reviews* 10: 232-274
188. Breuner CW, Orchinik M (2002) Beyond carrier proteins plasma binding proteins as mediators of corticosteroid action in vertebrates. *J Endocrinology* 175:99-112.
189. Tinnikov AA, Oskina IN (1994) Seasonal variations in corticosterone and corticosterone-binding globulin levels in white laboratory and Norway rats. *Hormone and Metabolic Research* 26:559–560.
190. Tinnikov AA (1999) Responses of serum corticosterone and corticosteroid-binding globulin to acute and prolonged stress in the rat. *Endocrine* 11:145–150.
191. Spencer, RL, Miller AH, Moday H, McEwen BS, Blanchard, RJ, Blanchard DC, Sakai RR, (1996) Chronic social stress produces reductions in available splenic type II corticosteroid receptor binding and plasma corticosteroid binding globulin levels. *Psychoneuroendocrinology* 21, 95–109.
192. Fleshner M, Deak T, Spencer RL, Laudenslager ML, Watkins LR, Maier SF (1995) A long term increase in basal levels of corticosterone and a decrease in corticosteroid-binding globulin after acute stressor exposure. *Endocrinology* 136, 5336–5342.
193. Deak T, Nguyen KT, Cotter CS, Fleshner M, Watkins L, Maier SF, Spencer RL (1999) Long-term changes in mineralocorticoid and glucocorticoid receptor occupancy following exposure to an acute stressor. *Brain Research* 847, 211–220.

194. Frairia R, Agrimonti F, Fortunati N, Fazzari A, Gennari P, Berta L (1988) Influence of naturally occurring and synthetic glucocorticoids on corticosteroid-binding globulin-steroid interaction in human peripheral plasma. *Ann N Y Acad Sci.* 538:287-303.
195. Hsu BR and Kuhn RW (1988) The role of the adrenal in generating the diurnal variation in circulating levels of corticosteroid-binding globulin in the rat. *Endocrinology* 122(2):421-6.
196. Schmutz I, Ripperger JA, Baeriswyl-Aebischer S, and Albrecht U (2010) The mammalian clock component PERIOD2 coordinates circadian output by interaction with nuclear receptors. *Genes and Dev.* 24:345-357.
197. Braissant O, Fougère F, Scotto C, Dauca M, Wahli W (1996) Differential expression of peroxisome proliferator-activated receptors (PPARs): tissue distribution of PPAR- $\alpha$ , - $\beta$ , and - $\gamma$  in the adult rat. *Endocrinology* 137:354–366.
198. Hatori M, Vollmers C, Zarrinpar A, DiTacchio L, Bushong EA, Gill S, Leblanc M, Chaix A, Joens M, Fitzpatrick J, Ellisman MH, and Panda S (2012) Time-Restricted Feeding without Reducing Caloric Intake Prevents Metabolic Diseases in Mice Fed a High-Fat Diet. *Cell Metabolism* 15:848-860.
199. Sherman H, Genzer Y, Cohen R, Chapnik N, Mada Z, Froy O (2012). Timed high-fat diet resets circadian metabolites and prevents obesity. *FASEB J* 26(8):3493-502.
200. Eckel-Mahan-Eckel KL, Patel VR, Mohny RP, Vignola KS, Baldi P, Sassone-Corsi P (2012) Coordination of the transcriptome and metabolome by the circadian clock. *PNAS* 109, 14:5541-5546
201. Oishi K, Itoh N (2013). Disrupted daily light-cycle induces the expression of hepatic gluconeogenic regulatory genes and hyperglycemia with glucose intolerance in mice. *Biochemical and Biophysical Research communication*. In press
202. Palumbo ML, Canzobre MC, Pascuan CG, Rios H, Wald M, Genaro AM (2010) Stress induced cognitive deficit is differentially modulated in BALB/c and C57Bl/6 mice: correlation with Th1/Th2 balance after stress exposure. *J Neuroimmunol* 218: 12–20.
203. Takahashi K, Yamada T, Tsukita S, Kaneko K, Shirai Y, Munakata Y, Ishigaki Y, Imai J, Uno K, Hasegawa Y, Sawada S, Oka Y, Katagiri H (2013). Chronic mild stress alters circadian expressions of molecular clock genes in the liver *Am J Physiol Endocrinol Metab* 304:E301-E309.
204. Hernandez-Morante JJ, Gomez-Santos C, Milagro F, Campion J, Martinez JA, Zamora S, Garaulet M (2009) Expression of cortisol metabolism-related genes shows circadian rhythmic patterns in human adipose tissue. *Int J Obes* 33(4):473-80.
205. So AY, Bernal TU, Pillsbury ML, Yamamoto KR, Feldman BJ (2009) Glucocorticoid regulation of the circadian clock modulates glucose homeostasis. *Proc Natl Acad Sci USA*

106: 17582–17587.

206. Yamamoto T, Nakahata Y, Tanaka M, Yoshida M, Soma H, Shinohara K, Yasuda A, Mamime T, Takumi T (2005) Acute physical stress elevates mouse period1 mRNA expression in mouse peripheral tissues via a glucocorticoid-responsive element. *Journal of Biological Chemistry* 280: 42036–42043.

207. Cagampang FR, Poore KR, Hanson MA (2011). Developmental origins of the metabolic syndrome: body clocks and stress responses. *Brain Behav Immun* 25: 214–220.

208. Froy O (2010) Metabolism and circadian rhythms—implications for obesity. *Endocr Rev* 31: 1–24.

209. Kalsbeek A, Meroz M, Roenneberg T and Foster RG (2012) *Progress in Brain Research*, Vol. 199:233-245

210. Cohen S, Janicki-Deverts D, Doyle WJ, Miller GE, Frank E, Rabin BS, Turner RB (2012) Chronic stress, glucocorticoid receptor resistance, inflammation, and disease risk *PNAS* 109(16):5995-5999.

211. Prasai MJ, George JT, Scott EM (2008) Molecular clocks, type 2 diabetes and cardiovascular disease. *Diab Vasc Dis Res* 5: 89–95.

212. Rudic RD, McNamara P, Curtis AM, Boston RC, Panda S, Hogenesch JB, Fitzgerald GA (2004). BMAL1 and CLOCK, two essential components of the circadian clock, are involved in glucose homeostasis. *PLoS Biol* 2: e377.

213. Alberts P, Ronquist-Nii Y, Larsson C, Klingstrom G, Engblom L, Edling N, Lidell V, Berg I, Edlund PO, Ashkzari M, Sahaf N, Norling S, Berggren V, Bergdahl K, Forsgren M, Abrahmsen L (2005). Effect of high-fat diet on KKAY and ob/ob mouse liver and adipose tissue corticosterone and 11-dehydrocorticosterone concentrations. *Horm Metab Res* 37: 402–407.

214. Tannenbaum BM, Brindley DN, Tannenbaum GS, Dallman MF, McArthur MD, Meaney MJ (1997) High-fat feeding alters both basal and stress-induced hypothalamic-pituitary-adrenal activity in the rat. *Am J Physiol Endocrinol Metab* 273: E1168–E117.

215. Pitt, H. (2007) Hepato-pancreato-biliary fat: the good, the bad and the ugly. *HPB* 9(2):92-97.

216. Elias CF, Lee CE, Kelly JF, Ahima RS, Kuhar M, Saper CB, Elmquist JK (2001) Characterization of CART neurons in the rat human hypothalamus. *Jour of Comp Neuro* 432 (1):1-19.

217. Tritos NA, Vicent D, Gillette J, Ludwig DS, Flier ES and Maratos-Flier E (1998). Functional interactions between melanin-concentrating hormone, neuropeptides Y, and anorectic neuropeptides in the rat hypothalamus. *Diabetes* 47(11):1687-1682.

218. Hastings MH, Reddy AB, Maywood ES (2003) A clockwork web: circadian timing in brain and periphery, in health and disease. *Nat Rev Neurosci* 4: 649–61.
219. Freund TF, Katona I, Piomelli D (2003). Role of endogenous cannabinoids in synaptic signaling. *Physiol Rev* 83:1017–66.
220. Silvestri C, Ligresti A, Di Marzo V (2011) Peripheral effects of the endocannabinoid system in energy homeostasis: adipose tissue, liver and skeletal muscle. *Rev Endocrine Metab Dis* 12:153–62.
221. Van Gaal LF, Rissanen AM, Scheen AJ, Ziegler O, Rössner S (2005). Effects of the cannabinoid-1 receptor blocker rimonabant on weight reduction and cardiovascular risk factors in overweight patients: 1-year experience from the RIO-Europe study. *Lancet* 365:1389–97.
222. Vaughn LK, Denning G, Stuhr KL, de Wit H, Hill MN, Hillard CJ (2010). Endocannabinoid signalling: has it got rhythm? *Br J Pharmacol* 160:530–43.
223. Valenti M, Viganò D, Casico MG, Rubino T, Steardo L, Parolaro D, et al (2004) Differential diurnal variations of anandamide and 2-arachidonoyl-glycerol levels in rat brain. *Cell Mol Life Sci* 61:945–50.
224. Ravinet Trillou C, Delgorge C, Menet C, Arnone M, Soubrié P (2004) CB1 cannabinoid receptor knockout in mice leads to leanness, resistance to diet-induced obesity and enhanced leptin sensitivity. *Int J Obesity* 28:640–8.
225. Chen C, Bazan NG. Lipid signaling: sleep, synaptic plasticity, and neuroprotection (2005) *Prostaglandins Other Lipid Mediat* 77:65–76.
226. Kunos G, Tam J. The case for peripheral CB<sub>1</sub> receptor blockade in the treatment of visceral obesity and its cardiometabolic complications (2011) *Br J Pharmacol* 163:1423–31.
227. Acuna-Goycolea C, Obrietan K, van den Pol AN (2010). Cannabinoids excite circadian clock neurons. *J Neurosci* 30:10061–6.
228. Yamauchi T, Nio Y, Maki T, Kobayashi M, Takazawa T, Iwabu M, et al (2007) Targeted disruption of AdipoR1 and AdipoR2 causes abrogation of adiponectin binding and metabolic actions. *Nat Med.* 13:332–9.
229. Steppan CM, Bailey ST, Bhat S, Brown EJ, Banerjee RR, Wright CM, Patel HR, Ahima RS, Lazar MA (2001). The hormone resistin links obesity to diabetes. *Nature* 409:307-12.
230. Way, J.M., Gorgun, C.Z., Tong, Q., Uysal, K.T., Brown, K.K., Harrington, W.W., Oliver, W.R., Jr., Willson, T.M., Kliewer, S.A., and Hotamisligil, G.S. (2001). Adipose tissue resistin expression is severely suppressed in obesity and stimulated by peroxisome



proliferator activated receptor gamma agonists. *J. Biol. Chem.* 276: 25651– 25653.

231. McTerman, PG, McTernan CL, Chetty R, Jenner K, Fisher M, Lauer MN, Crocker J, Barnett AH, Kumar S (2002). Increased resistin gene and protein expression in human abdominal adipose tissue. *J. Clin. Endocrinol. Metab* 87:2407-2413.

232. Addy C, Wright H, Van Laere K, Gantz I, Erondu N, Musser BJ, Lu K, Yuan J, Sanabria-Bohorquez, et al (2008) The acyclic cb1 r inverse agonist taranabant mediates weight loss by increasing energy expenditure and decreasing caloric intake. *Cell Metab* 7(1):68-78.

233. Jbilo O, Ravinet-Trillou C, Arnone M, Buisson I, Bribes E, Peleraux G, Soubrie P, Le Fur G, Galieggue S, Casellas P (2005) The CB1 receptor antagonist rimonabant reverses the diet-induced obesity phenotype the regulation of lipolysis and energy balance. *FASEB J.* 19(11):1567-1569.

234. Liang G, Yang J, Horton JD, Hammer RE, Goldstein JL, et al. (2002) Diminished Hepatic Response to Fasting/Refeeding and Liver X Receptor Agonists in Mice with Selective Deficiency of Sterol Regulatory Element-binding Protein-1c. *J Biol Chem* 277: 9520–9528.

235. Flowers MT, Ntambi JM (2009) Stearoyl-CoA desaturase and its relation to high-carbohydrate diets and obesity. *Biochimica et Biophysica Acta (BBA) - Molecular and Cell Biology of Lipids* 1791: 85–91.

236. Horton JD (2008) *PHYSIOLOGY: Unfolding Lipid Metabolism.* *Science* 320: 1433–1434.

237. Wu Z, Puigserver P, Andersson U, Zhang C, Adelmant G, Mootha V, Troy A, Cinti S, Lowell BB, Scarpulla RC, Spiegelman BM (1999) Mechanisms controlling mitochondrial biogenesis and respiration through the thermogenic coactivator PGC-1. *Cell* 98:115–124

238. Shimomura I, Matsuda M, Hammer RE, Bashmakov Y, Brown MS, et al. (2000) Decreased IRS-2 and Increased SREBP-1c Lead to Mixed Insulin Resistance and Sensitivity in Livers of Lipodystrophic and ob/ob Mice. *Molecular Cell* 6: 77–86.

239. Brown MS, Goldstein JL (2008) Selective versus Total Insulin Resistance: A Pathogenic Paradox. *Cell Metabolism* 7: 95–96.

240. Nagaya T, Tanaka N, Suzuki T, San K, Horiuchi A, Komatsu M, Nakajima T, Nishizawa T, Joshita S, Umemura T, Ichijo T, Matsumoto A, Yoshizawa K, Nakayama J, Tanaka E, Aoyama T. (2010) Down-regulation of SREBP-1c is associated with the development of burned-out NASH. *Journal of Hepatology* 53:724-731.

241. Starowicz KM, Cristino L, Matias I, Capasso R, Racioppi A, Izzo AA, Di Marzo V (2008) Endocannabinoid dysregulation in the pancreas and adipose tissue of mice fed with a high-fat diet. *Obesity (Silver Spring)* 16: 553–565.

242. Nadler ST, Attie AD (2001) Please pass the chips: genomic insights into obesity and diabetes. *J Nut* 131(8): 2078-2081.
243. Hill MN, Patel S, Campolongo P, Tasker JG, Wotjak CT, Bains JS (2010c) Functional interactions between stress and the endocannabinoid system: from synaptic signaling to behavioral output. *J Neurosci* 30:14980-14986.
244. Matsuda LA, Lolait SJ, Brownstein MJ, Young AC, Bonner TI (1990) Structure of a cannabinoid receptor and functional expression of the cloned cDNA. *Nature* 346:561-564.
245. Munro S, Thomas KL, Abu-Shaar M (1993) Molecular characterization of a peripheral receptor for cannabinoids. *Nature* 365:61-65.
246. Devane WA, Hanus L, Breuer A, Pertwee RG, Stevenson LA, Griffin G, Gibson D, Mandelbaum A, Etinger A, Mechoulam R (1992) Isolation and structure of a brain constituent that binds to the cannabinoid receptor. *Science* 258:1946-1949.
247. Sugiura T, Kondo S, Sukagawa A, Nakane S, Shinoda A, Itoh K, Yamashita A, Waku K (1995) 2-Arachidonoylglycerol: a possible endogenous cannabinoid receptor ligand in brain. *Biochem Biophys Res Commun* 215:89-97.
248. Deutsch DG, Ueda N, Yamamoto S (2002) The fatty acid amide hydrolase (FAAH). *Prostaglandins Leukot Essent Fatty Acids* 66:201-210.
249. Gorzalka BB, Hill MN, Hillard CJ (2008) Regulation of endocannabinoid signaling by stress: implications for stress-related affective disorders. *Neurosci Biobehav Rev* 32:1152-1160.
250. Hill MN, Patel S, Carrier EJ, Rademacher DJ, Ormerod BK, Hillard CJ, Gorzalka BB (2005b) Downregulation of endocannabinoid signaling in the hippocampus following chronic unpredictable stress. *Neuropsychopharmacology* 30:508-515.
251. Hill MN, Carrier EJ, McLaughlin RJ, Morrish AC, Meier SE, Hillard CJ, Gorzalka BB (2008b) Regional alterations in the endocannabinoid system in an animal model of depression: effects of concurrent antidepressant treatment. *J Neurochem* 106:2322-2336.
252. Reich CG, Taylor ME, McCarthy MM (2009) Differential effects of chronic unpredictable stress on hippocampal CB1 receptors in male and female rats. *Behav Brain Res* 203:264-269.
253. Hill MN, Carrier EJ, Ho WS, Shi L, Patel S, Gorzalka BB, Hillard CJ (2008a) Prolonged glucocorticoid treatment decreases cannabinoid CB1 receptor density in the hippocampus. *Hippocampus* 18:221-226.
254. Ahima RS, Harlan RE (1990) Charting of type II glucocorticoid receptor-like immunoreactivity in the rat central nervous system. *Neuroscience* 39:579-604.
255. Karatsoreos IN, Bhagat SM, Bowles NP, Weil ZM, Pfaff DW, McEwen BS (2010)

Endocrine and physiological changes in response to chronic corticosterone: a potential model of the metabolic syndrome in mouse. *Endocrinology* 151:2117-2127.

256. Mailleux P, Vanderhaeghen JJ (1993) Glucocorticoid regulation of cannabinoid receptor messenger RNA levels in the rat caudate-putamen. An in situ hybridization study. *Neurosci Lett* 156:51-53.

257. Hill MN, McLaughlin RJ, Bingham B, Shrestha L, Lee TT, Gray JM, Hillard CJ, Gorzalka BB, Viau V (2010b) Endogenous cannabinoid signaling is essential for stress adaptation. *Proc Natl Acad Sci U S A* 107:9406-9411.

258. Patel S, Roelke CT, Rademacher DJ, Hillard CJ (2005b) Inhibition of restraint stress-induced neural and behavioural activation by endogenous cannabinoid signalling. *Eur J Neurosci* 21:1057-1069.

259. Rademacher DJ, Meier SE, Shi L, Ho WS, Jarrahian A, Hillard CJ (2008) Effects of acute and repeated restraint stress on endocannabinoid content in the amygdala, ventral striatum, and medial prefrontal cortex in mice. *Neuropharmacology* 54:108-116.

260. Waleh NS, Cravatt BF, Apte-Deshpande A, Terao A, Kilduff TS (2002) Transcriptional regulation of the mouse fatty acid amide hydrolase gene. *Gene* 291:203-210.

261. Hill MN, Ho WS, Meier SE, Gorzalka BB, Hillard CJ (2005a) Chronic corticosterone treatment increases the endocannabinoid 2-arachidonoylglycerol in the rat amygdala. *Eur J Pharmacol* 528:99-102.

262. Patel S, Kingsley PJ, Mackie K, Marnett LJ, Winder DG (2009) Repeated homotypic stress elevates 2-arachidonoylglycerol levels and enhances short-term endocannabinoid signaling at inhibitory synapses in basolateral amygdala. *Neuropsychopharmacology* 34:2699-2709.

263. Lutz B (2009) Endocannabinoid signals in the control of emotion. *Curr Opin Pharmacol* 9:46-52.

264. Sterner EY, Kalynchuk LE (2010) Behavioral and neurobiological consequences of prolonged glucocorticoid exposure in rats: relevance to depression. *Prog Neuropsychopharmacol Biol Psychiatry* 34:777-790.

265. Schulkin J (2006) Angst and the amygdala. *Dialogues Clin Neurosci* 8:407-416.

266. Dunbar JA, Reddy P, Davis-Lameloise N, Philpot B, Laatikainen T, Kilkkinen A, Bunker SJ, Best JD, Vartiainen E, Kai Lo S, Janus ED (2008) Depression: an important comorbidity with metabolic syndrome in a general population. *Diabetes Care* 31:2368-2373.

267. Chrousos GP, Kino T (2009) Glucocorticoid signaling in the cell. Expanding clinical implications to complex human behavioral and somatic disorders. *Ann N Y Acad Sci*

1179:153-166.

268. Takeuchi T, Nakao M, Nomura K, Yano E (2009) Association of metabolic syndrome with depression and anxiety in Japanese men. *Diabetes Metab* 35:32-36.

269. Kirkham TC, Williams CM, Fezza Filomena, DiMarzo V. (2002) Endocannabinoid levels in rat limbic forebrain and hypothalamus in relation to fasting, feeding, and satiation: stimulation of eating by 2-arachidonoyl glycerol. *Br J Pharmacol.* June; 136(4): 550–557.

270. Okamoto Y, Morishita J, Tsuboi K, Tonai T, Ueda N (2004) Molecular characterization of a phospholipase D generating anandamide and its congeners. *J Biol Chem* 279:5298–5305.

271. Maurelli S, Bisogno T, DePetrocellis L, Di Luccia A, Marino G, Di Marzo V. (1995) Two novel classes of neuroactive fatty acid amides are substrates for mouse neuroblastoma 'anandamide amidohydrolase. *FEBS Lett.* 377:82–86.

272. Jonsson KO, Vandevoorde S, Lambert DM, Tiger G, Fowler CJ. (2001) Effects of homologues and analogues of palmitoylethanolamide upon the inactivation of the endocannabinoid anandamide. *Br J Pharmacol.* 133:1263–1275.

273. Matias I, Gonthier M-P, Orlando P, Martiadis V, De Petrocellis L, Cervino C, Petrosino S, Hoareau L, Festy F, Pasquali R, et al. (2006) Regulation, function and dysregulation of endocannabinoids in obesity and hyperglycemia. *J Clin Endocr Metab* 91 (8) 3171-3180.

274. McPartland JM, Matias I, Di Marzo V, Glass M. (2006) Evolutionary origins of the endocannabinoid system. *Gene* 370:64-74.

275. Engeli S, Janke J, Gorzelniak K, Bohnke J, Ghose N, Lindschau C, Luft FC, Sharma AM (2005) Activation of the peripheral endocannabinoid system in human obesity. *Diabetes* 54:2838–2843

276. Cote M, Matias I, Lemieux I, Petrosino S, Almeras N, Despres JP, Di M V (2007) Circulating endocannabinoid levels, abdominal adiposity and related cardiometabolic risk factors in obese men. *Int J Obes (Lond)* 31: 692–699.

277. Krebs-Kraft D. L., Hill M. N., Hillard C. J., McCarthy M. M. (2010). Sex difference in cell proliferation in developing rat amygdala mediated by endocannabinoids has implications for social behavior. *Proc. Natl. Acad. Sci. U.S.A.* 107, 20535–20540.

278. He Q, Horlick M, Thronton J, Wang J, Pierson RN, Heshka S, Gallagher D. (2002) Sex and Race Differences in Fat Distribution among Asian, African-American, and Caucasian Prepubertal Children. *The Journal of Clinical Endocrinology & Metabolism* 87:2164-70.

279. Jumpertz R, Guijarro A, Pratley RE, Piomelli D, Krakoff J. (2010) Central and Peripheral Endocannabinoids and Cognate Acylethanolamides in Humans: Association

with Race, Adiposity, and Energy Expenditure. *J of Clin Endo & Meta* 96 (3):787-791.

280. Osei-Hyiaman D, DePetrillo M, Pacher P, Liu J, Radaeva S, Batkai S, Harvey-White J, Mackie K, Offertaler L, Wang L, Kunos G (2005) Endocannabinoid activation at hepatic CB1 receptors stimulates fatty acid synthesis and contributes to diet-induced obesity. *J Clin Invest* 115:1298–1305

281. Bensaid, M, et al. (2003) The cannabinoid CB<sub>1</sub> receptor antagonist SR141716 increases Acrp30 mRNA expression in adipose tissue of obese *fa/fa* rats and in cultured adipocyte cells. *Mol. Pharmacol.* **63**:908-914.

282. Hezode C, Zafrani ES, Roudot-Thoraval F, Costentin C, Hessami A, Bouvier-Alias M, Medkour F, Pawlotsky JM, Lotersztajn S, Mallat A. (2008) *Daily cannabis use, a novel risk factor of steatosis severity in patients with chronic hepatitis C.* *Gastroenterology* 134(2):432-9.

283. Guzman, M, Fernandez-Ruiz, JJ, Sanchez, C, Velasco, G, Ramos, JA. (1999) Effects of anandamide on hepatic fatty acid metabolism. *Biochem. Pharmacol.* **50**:885-888.

284. Zoppi S, Nievas BG, Madrigal JL, Manzanares J, Leza JC, Garcia-Bueno B. (2001) Regulatory role of cannabinoid receptor 1 in stress-induced excitotoxicity and neuroinflammation. *Neuropsychopharmacology* 36(4):805-18.

285. Tam J, Vemuri VK, Liu J, Batkai S, Mukhopadhyay B, Godlewski G, Osei-Hyiaman DO, Ohnuma S, Ambudkar SV, Pickel J, Makriyannis A, Kunos G (2010) Peripheral CB1 cannabinoids receptor blockade improves cardiometabolic risk in mouse models of obesity *J Clin Invest* 120(8):2953-2966.A285

286. Parks EJ, Krauss RM, Christiansen MP, Neese RA, and Hellerstein MK (1999) Effects of a low-fat, high carbohydrate diet on VLDL-triglyceride assembly, production and clearance. *J Clin Invest.* 104(8):1087-1096.

287. Hildebrant AL, Kelly-Sullivan DM, Black SC (2003) Antiobesity effects of chronic cannabinoid CB1 receptor antagonist treatment in diet-induced obese mice. *Eur J Pharmacol* 462:125-32.

288. Chambers AP, Sharkey KA, Koopmans HS (2004) Cannabinoid (CB)<sub>1</sub> receptor antagonist, AM251, causes a sustained reduction of daily food intake in the rat. *Physiology & Behavior* 82:863-869.

289. Holmes E, Li JV, Marchesi JR, Nicholson JK (2012) Gut Microbiota Composition and Activity in Relation to Host Metabolic Phenotype and Disease Risk. *Cell Metabolism* 16:559-564.

290. Burdyga G, Lal S, Varro A, Dimaline R, Thompson DG, Dockray GJ (2004) Expression of cannabinoid CB1 receptors by vagal afferent neurons is inhibited by cholecystokinin. *J. Neurosci.* 24:2708–2715

291. Gomez R, Navarro M, Ferrer B, Trigo JM, Bilbao A, Del Arco I, Cippitelli A, Nava F, Piomelli D, Rodriguez de Fonseca F (2002) A peripheral mechanism for CB1 cannabinoid receptor-dependent modulation of feeding. *J. Neurosci.*, 22:9612–9617
292. Madsen AN, Jelsing J, van de Wall E, Vrang N, Larsen PJ, Schwartz GJ (2009) Rimonabant induced anorexia in rodents is not mediated by vagal or sympathetic gut afferents. *Neuroscience letters* 449 (1):20-23.
293. Teixeira-Clerc F, Julien B, Grenard P, Tran Van Nhieu J, Deveaux V, Li L, Serriere-Lanneau V, Ledent C, Mallat A, Lotersztajn S (2006) CB1 cannabinoid receptor antagonism: a new strategy for the treatment of liver fibrosis. *Nat Med* 12: 671–676.
294. Wheaton, B. (1999). *The nature of stressors. A handbook for the study of mental health: Social contexts, theories, and systems* 176–197.
295. Kunz-Ebrecht SR, Kirschbaum C, Steptoe A (2004) Work stress, socioeconomic status and neuroendocrine activation over the working day. *Social Science & Media* 58:1523-1530.
296. Dowd JB, Ranjil N, Do D, Young EA, House JS, and Kaplan GA (2011). Education and levels of salivary cortisol over the day in US adults. *Annals of Behavioral Medicine*, 41 (1):13-20.
297. Gunnar MR, and Vazquez DM. (2001). Low cortisol and flattening of expected daytime rhythm: potential indices of risk in human development. *Development and Psychopathology*, 13: 515-538.
298. Dohrenwend BP (2006) Inventorying stressful life events as risk factors for psychopathology: Toward resolution of the problem of intracategory variability. *Psychol Bull.* 132(3):477-95.
299. Pan A, Schernhammer ES, Sun Q, Hu FB (2011) Rotating night shift work and risk of type 2 diabetes: two prospective cohort studies in women. *PLoS Med* 8:e1001141.
300. Lieu SJ, Curhan GC, Schernhammer ES, Forman JP (2012) Rotating night shift work and disparate hypertension risk in African-Americans. *J Hypertens* 30:61-6.
301. Uetani M, Sakata K, Oishi M, Tanaka K, Nakada S, Nogawa K, et al. (2011) The influence of being overweight on the relationship between shift work and increased total cholesterol level. *Ann Epidemiol* 21:327-35.
302. Vyas MV, Garg AX, Iansavichus AV, Costella J, Donner A, Laugsand LE, Janszky I, Mrkobrada M, Parraga G, Hackam DG (2012) Shift work and vascular events: systematic review and meta-analysis. *BMJ* 345
303. Lo SH, Lin LY, Hwang JS, Chang YY, Liau CS, Wang JD (2010) Working the night shift causes increased vascular stress and delayed recovery in young women. *Chronobiol*

Int 27:1454-68.

304. Brown DL, Feskanich D, Sánchez BN, Rexrode KM, Schernhammer ES, Lisabeth LD (2009) Cardiovascular symptoms in an effort to forestall or avert the rotating night shift work and the risk of ischemic stroke. *Am J Epidemiol* 169:1370-7.

305. Fujino Y, Iso H, Tamakoshi A, Inaba Y, Koizumi A, Kubo T, et al (2006). A prospective cohort study of shift work and risk of ischemic heart disease in Japanese male workers. *Am J Epidemiol* 164:128-35.

306. Haupt CM, Alte D, Dörr M, Robinson DM, Felix SB, John U, et al (2008) The relation of exposure to shift work with atherosclerosis and myocardial infarction in a general population. *Atherosclerosis* 201:205-11.

307. Kawachi I, Colditz GA, Stampfer MJ, Willett WC, Manson JE, Speizer FE, et al (2011) Prospective study of shift work and risk of coronary heart disease in women. *Circulation* 124:3178-82.

308. Laugsand LE, Vatten LJ, Platou C, Janszky I (2011) Insomnia and the risk of acute myocardial infarction. *Circulation* 124:2073-81.

309. Tuschsen F, Hannerz H, Burr H (2006) A 12 year prospective study of circulatory disease among Danish shift workers. *Occup Environ Med* 63:451-5.

310. Fynn P. The Effects of Shift Work on the Lives of Employees. In *Monthly Labor Review* 104(10):31-35.

311. Baud MO, Magistretti PJ, Petit JM (2013) Sustained sleep fragmentation affects brain temperature, food intake and glucose tolerance in mice. *J Sleep Res.* 22(1):3-12.

312. Coccorello R, D'Amato FR, Moles A (2008) Chronic social stress, hedonism and vulnerability to obesity: Lessons from Rodents. *2009 Neurosci Biobehav* 33(4):537-550.

313. Huhman KL (2006) Social conflict models: can they inform us about human psychopathology? *Horm Behav* 50: 640–6.

314. Bartolomucci A, Palanza P, Sacerdote P, Panerai AE, Sgoifo A, et al (2005) Social factors and individual vulnerability to chronic stress exposure *Neurosci & Biobehav Reviews* 29(1):67-81.

315. Israel BA, Schulz AJ, Estrada-Martinez L, Zenk SN, Viruell-Fuentes E, Villarruel AM, et al (2006) Engaging urban residents in assessing neighborhood environments and their implications for health. *Journal of Urban Health*, 83(3), 523-539.